

Advancing immunotherapy for HPV-related cancers: Improving therapeutic vaccination approaches and understanding the immunosuppressive role of myeloid cells

THÈSE N° 8697 (2018)

PRÉSENTÉE LE 7 SEPTEMBRE 2018

À LA FACULTÉ DES SCIENCES DE LA VIE

PROGRAMME DOCTORAL EN BIOTECHNOLOGIE ET GÉNIE BIOLOGIQUE

ÉCOLE POLYTECHNIQUE FÉDÉRALE DE LAUSANNE

POUR L'OBTENTION DU GRADE DE DOCTEUR ÈS SCIENCES

PAR

Gabriele GALLIVERTI

acceptée sur proposition du jury:

Prof. B. E. Ferreira De Sousa Correia, président du jury

Prof. M. Swartz, D. Hanahan, directeurs de thèse

Prof. P. Romero, rapporteur

Prof. C. Löwik, rapporteur

Prof. J. Huelsken, rapporteur



ÉCOLE POLYTECHNIQUE
FÉDÉRALE DE LAUSANNE

Suisse
2018

Acknowledgments

First of all I would like to thank my two supervisors Prof. Melody Swartz and Prof. Douglas Hanahan for allowing me to work in their amazing labs. Thank you for your guidance, for the always insightful comments and suggestions, and for giving me the freedom of pursuing my own ideas and interests.

I would also like to thank the president Prof. Bruno Correia and the other members of the committee Prof. Joerg Huelsken, Prof. C.W.G.M. Lowik and Prof. Pedro Romero for accepting my invitation and for reviewing my (quite long) thesis.

A huge thanks goes to Stephan Wullschleger and Bruno Torchia for the invaluable help with experiment and for the support they have given me, working on this projects would have been much harder without them.

Thanks to Melanie Tichet for the also invaluable help and support.

Thanks to all the members of the Swartz and Hanahan labs for the help, advices and good moments shared. A special thanks to Maria, Manuel, Sylvie, Marcela, Shann, Sachiko, Lambert and Ehud.

Thanks to all my friends back home in Italy for always staying the same despite the distance. To me you are a second family.

Thanks to my aunt Miriam, I cherish the time we hangout together.

Thanks to Chiara for her always kind support and encouragement during this adventure, for her patience and for all the good times and travels around the world that we shared.

Finally, I would like to thank my amazing parents for their unconditional and extraordinary support that they keep on giving me (and for all the food they brought me throughout these 5 years). I feel like the luckiest person in the world having you.

Abstract

Human Papilloma Viruses (HPVs) are the most common sexually transmitted agents worldwide, and chronic infection with oncogenic HPVs can lead to the development of lesions in the cervix, the vulva, and the head and neck region. In some patients, these lesions will eventually progress to squamous cell carcinomas that have the potential to spread to distant sites.

Cervical cancer is by far the most common type of HPV-related malignancy, and at the early stages can be treated quite effectively. However, for patients in the later stages of tumor progression traditional therapeutic approaches like chemotherapy are poorly effective, and the development of novel strategies based on immunotherapy is undergoing.

Clinical trials using HPV E6/E7-derived synthetic long peptides (SLPs) vaccines have shown promising results. However, these vaccines are only leading to significant responses in a low percentage of patients bearing pre-malignant lesions, whereas they seem to be completely ineffective in patients with advanced tumors, suggesting the presence of immune-escape mechanisms.

Here I describe an improved therapeutic vaccination approach based on conjugation of E7-derived SLPs to solid-phase ultra-small (30 nm in diameter) nanoparticles (NPs). The NP-conjugated formulation (NP-E7LP) was able to significantly enhance both the systemic and local anti-tumor immune responses, leading to higher CD8 T cell infiltrates in the tumor microenvironment (TME) resulting in a significant reduction in tumor burden and overall increased survival in mice bearing transplantable HPV+ TC1 and SC1 tumors.

Next, I demonstrate that a transgenic mouse model for HPV-related cancers expressing the HPV16 early region under the keratin 14 promoter bears striking similarities to cervical cancer patients regarding the alteration of the immune system provoked by HPVs. By taking advantage of the K14HPV16 H2b model, I show that the use of a nanoparticle-conjugated vaccine is required to elicit an immune response, but that, similarly to cervical cancer patients, therapeutic vaccination alone is not sufficient to elicit efficacious anti-tumor immunity. I also illustrate that combinatorial trials involving several different therapeutic antibodies are not sufficient to significantly boost the anti-tumor immune response. Finally, I identify a substantial increase in immunosuppressive myeloid cells (MDSCs) as the mechanism likely responsible for the observed impairment of the immune response, a feature that seems to be shared by cervical cancer patients. Interestingly,

although the attention of most of the researchers in the field is usually focused on the TME, I provide evidence that this myeloid cell-dependent mechanism is acting upstream in the lymphoid organs where it inhibits the very first steps in the generation of the anti-tumor immune response. My data suggest that this mechanism could potentially put an early stop to the cancer-immunity cycle, thereby contributing to the ineffectiveness of immunotherapies in cervical cancer patients. In summary, this thesis provides new knowledge that will contribute to the improvement of immunotherapy-based approaches against cervical cancer and other HPV-related diseases with the potential for applicability to other types of cancer.

Keywords:

Human papillomavirus, cervical cancer, immunotherapy, therapeutic vaccination, nanoparticles, immunosuppressive myeloid cells, MDSCs.

Sommario

I virus del papilloma umano (HPV) sono gli agenti patogeni trasmissibili sessualmente più diffusi al mondo. Un'infezione cronica con un HPV oncogenico può portare allo sviluppo di lesioni pre-maligne nella cervice, nella vulva o nelle regioni della testa e del collo, portando in alcuni casi allo sviluppo di carcinomi squamocellulari. Il cancro alla cervice è il più comune tra quelli causati da HPV e le terapie classiche come la chemioterapia sono scarsamente efficaci, specialmente in pazienti con tumore in stadio avanzato e, per far fronte al problema, è in corso lo sviluppo di nuovi approcci basati sull'immunoterapia.

Studi clinici condotti usando vaccini basati su peptidi sintetici derivati dalle proteine virali E6 ed E7 hanno mostrato risultati incoraggianti. Questi vaccini hanno portato a risposte significative in una percentuale di pazienti con lesioni pre-maligne mentre, al contrario, sembrano completamente inefficaci in pazienti con forme avanzate di tumore, suggerendo che in questi ultimi siano attivi dei meccanismi che permettono al tumore di sfuggire alla risposta immunitaria.

In questa tesi, viene descritto un approccio di vaccinazione terapeutica basato sulla coniugazione di peptidi sintetici derivati da E7 (E7LP), a delle nano-particelle (NP) sintetiche microscopiche (di 30 nm di diametro). L'uso del vaccino a nano-particelle (NP-E7LP) ha incrementato significativamente la potenza della risposta immunitaria sia a livello sistemico che a livello del tumore, provocando una significativa riduzione della massa tumorale ed un generale aumento della sopravvivenza dei topi portatori di tumori.

Successivamente ho dimostrato che un modello di topo transgenico, esprime la regione precoce del genoma di HPV sotto il controllo del promotore della cheratina 14, presenta delle caratteristiche simili ai pazienti per quanto riguarda le alterazioni del sistema immunitario causate da HPV. Sfruttando questo modello, chiamato K14HPV16 H2b, ho constatato che l'uso di un vaccino basato sulle NP è assolutamente necessario per generare una risposta immunitaria. Tuttavia, la sola vaccinazione non è sufficiente ed un trattamento combinato con anticorpi terapeutici non è in grado di migliorare la risposta immunitaria. Ho dimostrato che l'aumento delle cellule mieloidi immunosoppressive è un possibile meccanismo responsabile del blocco delle risposte immunitarie osservata in questo modello, una caratteristica che sembra essere presente anche in pazienti con cancro alla cervice.

E' interessante notare che, nonostante la maggior parte dei ricercatori indirizzi la propria attenzione al tumore e ai tessuti circostanti, I dati presentati in questa tesi dimostrano che questo meccanismo di immunosoppressione sia attivo già a monte negli organi linfoidi, dove va ad inibire le prime fasi della risposta immunitaria. Ciò porta ad un arresto prematuro della risposta anti-tumorale che, di conseguenza, non può essere stimolata dai trattamenti immunoterapici.

In conclusione, credo che questa tesi contenga una serie di osservazioni che aiuteranno a promuovere il miglioramento degli approcci basati sull'immunoterapia del cancro alla cervice e di altri tipi di tumore causati da HPV e che, inoltre, posseggano il potenziale di essere estese anche a molti altri tipi di cancro.

Parole chiave:

Virus del papilloma umano, cancro alla cervice, immunoterapia, vaccino terapeutico, nanoparticelle, cellule mieloidi immunosoppressive, MDSCs.

Table of contents

Acknowledgments	3
Abstract	5
Sommario	7
Chapter 1	13
1.1 Introduction	13
1.1.1 Background	13
1.1.2 Human Papillomaviruses	14
1.1.3 HPV infections and cancer prevalence	17
1.1.4 From infection to cervical cancer	17
1.1.5 Cervical cancer prevention	19
1.1.6 Screening.....	20
1.1.7 Treatment	21
1.1.8 Immunotherapy.....	21
1.1.9 HPV and cervical cancer escape from the immune response	29
1.1.10 Mouse models of HPV+ cancers.....	34
1.2 General considerations and scope of the thesis.....	36
Chapter 2	39
Nanoparticle conjugation of human papillomavirus 16 E7-long peptides enhances therapeutic vaccination efficacy against well-established solid tumors in mice	39
2.1 Introduction	39
2.2 Results	41
2.2.1 Immunization with NP-conjugated E7LP generates systemic immune responses that prolong survival of TC-1 tumor-bearing mice.....	41
2.2.2 Tumors from NP-E7LP treated mice have increased tumor-specific CD8 T cells infiltrates.	46
2.2.3 NP-E7LP vaccination does not cause an increase in intra-tumoral regulatory T cells and improves the CD8/Treg ratio.	48
2.2.4 Nanoparticle-conjugation improves the effectiveness of long peptide vaccination against orthotopic cervico-vaginal tumors, experimental lung metastases, and subcutaneous HPV+ squamous cell carcinomas.	50
2.2.5 Efficacy-associated changes in the tumor microenvironment are progressively lost upon disease stabilization and relapse.	54
2.2.6 NP-E7LP synergizes with agonistic anti-41BB/CD137 to further boost tumor rejection.	57
2.3 Discussion	59

2.4 Materials and methods	62
2.5 Important notes	67
2.6 Supplementary information	69
Chapter 3	81
Immunosuppressive myeloid cells impair immunotherapy in a transgenic mouse model of HPV-related cancer	81
3.1 Introduction	81
3.2 Results	83
3.2.1 Characterization of the MHC haplotype expression and changes in the tumor microenvironment in K14HPV16 H2b mice.....	83
3.2.2 NP-conjugation of E7 is required to elicit an immune response in K14HPV16 H2b (HPV+) mice upon vaccination.	86
3.2.3 NP-vaccination caused only minor changes in CD8 T cell infiltrates in the tumor microenvironment that were not accompanied by a reduction in cervical tumor size.	89
3.2.4 Assessing local barriers in the TME that might impair CD8 T cells infiltration and functions.	93
3.2.5 The E7-specific immune response is impaired in HPV+ mice.	95
3.2.6 Local barriers do not prevent tumor infiltration by CD8 T cells and shrinking of FVB H2b transplanted SC-1 tumors.....	99
3.2.7 HPV+ mice show impaired CD8 responses against OVA and LCMV-derived peptides. .	102
3.2.8 CD8 T cells activation and proliferation is not intrinsically defective in HPV+ mice.....	103
3.2.9 Lymphoid organs of HPV+ mice are characterized by the presence of phenotypically different regulatory T cells and show a general increase in all the major myeloid cell populations.	104
3.2.10 The lymph nodes of HPV+ mice are bathed in immunosuppressive factors.....	108
3.2.11 APC activity is suppressed in HPV+ mice.	109
3.2.12 Activation of DCs derived from HPV+ mice is not intrinsically defective.....	111
3.2.13 E7LP-loaded DC-vaccines are also poorly effective in HPV+ mice, and activation of adoptively-transferred DCs is suppressed in the lymph nodes and spleen of HPV+ mice.	112
3.2.14 Testing combinatorial strategies aimed to directly boost the immune response and increase tumor infiltration	115
3.2.15 Combination of vaccination with anti-PD1 and anti-CTLA4 does not boost the generation of E7-specific CD8 T cells and does not elicit changes in the TME	116
3.2.16 Targeting APCs with anti-CD40 agonistic antibody does not boost the anti-E7 immune response following vaccination.	121
3.2.17 Investigating the role of Tregs as potential immunosuppressive cells in HPV+ mice..	122
3.2.18 Metronomic cyclophosphamide treatment depletes Tregs at the tumor site but kills the vaccine-elicited E7 specific CD8 T cells.	123

3.2.19 Combinatorial strategies to target Tregs employing anti-CD25, anti-CD4 and anti-CTLA4 show poor depleting activity and fail to significantly boost immune responses.	125
3.2.20 In-vitro co-culture of Tregs with CD8 T cells and DCs does not increase in the suppressive activity of HPV+ mice-derived Tregs over the HPV- counterparts.	133
3.2.21 Myeloid cells from HPV+ mice suppress CD8 T cells proliferation and cytokine production and impair DCs activation.....	136
3.2.22 Myeloid cells in HPV+ mice are a source of immunosuppressive factors and produce increased reactive oxygen species.....	139
3.2.23 In-vitro blocking of IL-10 does not rescue the immunosuppression by MDSCs.	142
3.2.24 In-vitro treatment with IDO inhibitors do not rescue CD8 T cell proliferation but causes a generalized improvement in BMDC activation.....	144
3.2.25 Inhibition of Arg1, iNOS or reactive oxygen species does not rescue CD8 T cells proliferation in vitro.	145
3.2.26 HPV+ mouse derived neutrophils show distinctive gene expression profiles.....	146
3.2.27 Monocytes/macrophages suppress CD8 T cells proliferation in-vitro.....	151
3.2.28 Testing alternative approaches for targeting myeloid cells	152
3.2.29 Antibiotic treatment does not affect myeloid cells nor ameliorate the response to the vaccine	153
3.2.30 Targeting myeloid cells with depleting antibodies is poorly effective in HPV+ mice ..	154
3.2.31 Strategies targeting monocytes/macrophages are also poorly effective in HPV+ mice	162
3.2.32 Chemotherapy aimed to eliminate myeloid cells are only transiently effective.....	166
3.2.33 Blocking IL-10 or IDO does not relieve the systemic immunosuppression	170
3.2.34 Sildenafil does not abrogate the suppressive activity of myeloid cells.....	171
3.2.35 Increased levels of G-CSF and GM-CSF in HPV+ mice could explain the increase in myeloid cells.	172
3.2.36 Blocking growth factors to reduce myeloid cells number seems feasible but requires additional testing	173
3.2.37 Investigating mechanisms behind expansion of the myeloid cell compartment and the production of G-CSF and GM-CSF	177
3.2.38 HPV+ mice have systemic inflammation as indicated by an increase in several factors related to inflammatory conditions	178
3.2.39 GM-CSF is produced locally in the skin.....	179
3.2.40 B lymphocyte depletion causes a reduction in the number of circulating macrophages but does not alter the local immune infiltrates in the ear skin.....	183
3.2.41 Aspirin treatment further suppress the anti-E7 immune response.....	187
3.2.42 Prednisolone treatment shuts down the immune system of HPV+ mice and could represent an attractive future component of combinatorial regimens	189

3.3 Discussion	196
3.4 Materials and methods	201
3.5 Acknowledgments.....	210
3.6 Specific contribution to experiments	210
Chapter 4	211
Concluding remarks	211
4.1 Summary and general discussion.....	211
4.2 Future directions	219
Appendix	225
Abbreviations.....	225
Gating strategies	227
Bibliography.....	239
Curriculum Vitae	253

Chapter 1

1.1 Introduction

1.1.1 Background

Cancer is a group of extremely complex and diverse diseases that currently affect millions of people worldwide (WHO). Although thanks to research, huge improvements have been made and we now have extensive knowledge of many of the mechanisms regulating the growth and survival of cancer cells (1, 2), we are still far from fully understanding these diseases and how to cure them.

The simplistic view of cancer dictates that it originates from a rogue cell that has accumulated genetic alterations, causing it to lose control of its cellular processes and leading to uncontrolled division and multiplication. In truth, this is only a small part of what happens during cancer development; in fact, although a tumor is largely made of cancer cells that are constantly proliferating, tumor development usually involves a multiplicity of cell types interacting with one another in profound and complex ways (1, 2). These interactions can be indispensable for tumor growth, and they often play a role in protection and resistance to therapies, further adding to the extreme complexity of these diseases (1–4).

For some types of cancers, the initial insult that triggers the malignant transformation is caused by infection with an oncogenic virus (5). Observations of these viruses in animals date back to more than 100 years and were only confirmed in humans in 1964, with the discovery of the link between Burkitt-lymphoma and the Epstein-Barr Virus (6). In the following years, several viruses have been found to be causally linked with cancer development. In 1983, Harald zur Hausen isolated Human papillomavirus 16 (HPV16), and later HPV18, from cancer biopsies of the cervix (7, 8), and since then it has been demonstrated that HPVs are collectively responsible for virtually all the cases of cervical cancer (9). Additionally, HPVs have also been reported as the cause of a significant portion of head and neck, penile, anal, vaginal and vulvar cancers (10, 11).

According to the latest reports from the HPV information center, despite the development of prophylactic vaccines, millions of people worldwide are currently infected or at risk of infection from HPVs, making them potential future oncologic patients and highlighting the need for developing effective treatments for this type of cancer.

This introduction will mainly rely on findings and observations related to cervical cancer, as this is by far the most common and the most studied HPV-related type of cancer.

1.1.2 Human Papillomaviruses

HPVs are a group of more than 200 double-stranded DNA viruses that infect keratinocytes of the skin and of mucosal surfaces (12). Viral transmission happens through contact with infected skin, most frequently as a consequence of sexual intercourse (13). According to the CDC website, HPVs are so common that almost every individual has come in contact or will come in contact with one or more HPV types during their lifetime. Based on their ability to induce malignant transformation, HPVs can be divided into two groups, high-risk HPVs and low-risk HPVs. Among the high risk ones, HPV16 and HPV18 are responsible for the vast majority of cancers with the former accounting for more than 60% of them alone (14, 15).

The HPV genome encodes for 8 proteins. 6 early proteins (E1, E2, E4, E5, E6 and E7) are necessary for the viral functions, for the viral life cycle and for triggering the malignant transformation of infected cells. The 2 late proteins instead, form the viral capsid (L1 and L2) (16).

The viral life cycle (Fig. 1) start with infection of the basal keratinocytes, usually via small lesion in the epithelium that allows the viral particles to penetrate and reach the basal layer (17). In these cells, production of the early protein is kept at low levels thanks to the transcriptional repression regulated by E2 on the other HPV genes (16); the late proteins are not being produced yet. As the infected keratinocytes divide and move towards the upper layer of the epithelium, the viral protein production increases, capsid protein start to be transcribed, and new viral particles are formed and spread to neighboring cells (18). Unlike many other viruses, the life cycle of HPV is intraepithelial, and the release of new viral particles does not involve the lysis of the cell, helping the virus remaining hidden from the immune system (19, 20).

Malignant transformation of the infected cells is caused by the combined action of the viral proteins E6 and E7 which have been found to interact with and alter the function of a plethora of cellular proteins and genes. Some of the known functions of E6 include the promotion of proteasomal degradation of p53 (21), that results in a compromised integrity of the cell's genome (22), prevention of apoptosis by inhibiting *Bax* gene expression and promotion of the Bax protein degradation (23), the immortalization of the cells by preventing the shortening of telomeres (24) and a general de-regulation of PDZ domain-containing proteins (25), that favor cellular

transformation due to the loss of cell-cell contact and cell polarity (26). E7 can instead bind and inactivate the retinoblastoma protein (pRb) causing the loss of cell cycle control and leading to uncontrolled proliferation (27, 28). E7 can also interact with histone deacetylases (HDACs) (29), de-regulating gene expression and further promoting proliferation and it can contribute to the evasion from the immune system by inactivating several factors involved in the anti-viral response (30, 31). Inhibiting E6 and E7 expression blocks malignant progression in cervical cancer cells and, although they are able to promote carcinogenesis independently from one another, the efficiency of the process is enhanced when they are co-expressed due to complementary and synergistic effects (18).

Although it is not found in all the tumors, integration of the HPV genome happens very frequently and contributes to the transformation process through the loss of E2 expression (32). In this situation, E2 can no longer restrain the expression of E6 and E7, leading to an increase in their production that ultimately push towards malignant transformation (33). Thanks to the action of these proteins, the infected keratinocytes will start proliferating, accumulating mutations and gradually lose their normal phenotype and, at the same time, the infection will spread to neighboring cells. This process, if left unchecked by the immune system, will lead to the formation of a pre-cancerous lesion and, eventually, invasive cancer (13, 18) (Fig. 1).

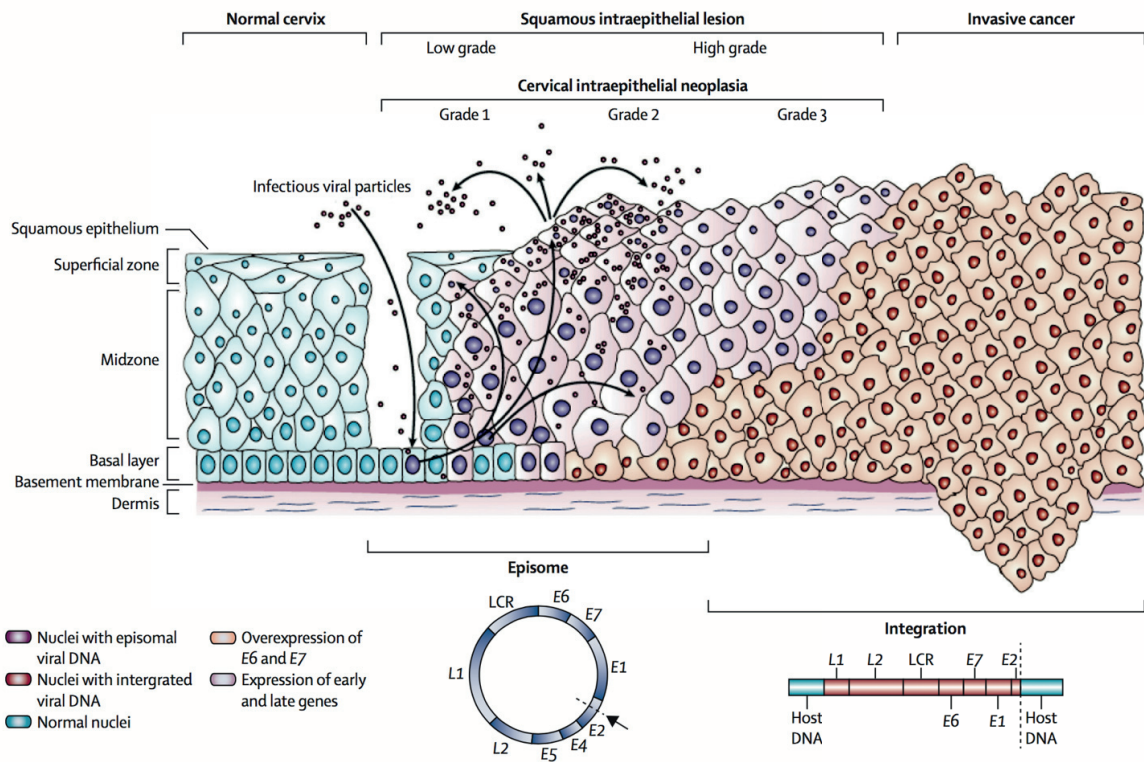


Figure 1: Human papillomavirus lifecycle and organization of its genome. Human papillomavirus is thought to access the basal cells through microabrasions in the cervical epithelium. After infection, the early human papillomavirus genes E1, E2, E4, E5, E6, and E7 are expressed, and the viral DNA replicates. In the upper layers of epithelium (the midzone and superficial zone) the viral genome is replicated further, and the late genes L1 and L2, and E4 are expressed. L1 and L2 encapsidate the viral genomes to form progeny virions in the nucleus. The shed virus can then initiate a new infection. Low-grade intraepithelial lesions support productive viral replication. Certain high-risk human papillomavirus infections progress to high-grade cervical intraepithelial neoplasias. The progression of untreated lesions to invasive cancer is associated with the integration of the human papillomavirus genome into the host chromosomes (red nuclei), with associated loss or disruption of E2, and subsequent upregulation of E6 and E7 oncogene expression. LCR=long control region. Image and image description taken and adapted from (13).

1.1.3 HPV infections and cancer prevalence

The latest estimates of the global prevalence of HPV infections is around 11.7% (34), meaning that more than 500 million people might currently be infected with at least one HPV type. Studies have shown that only a minority of the HPV infections will progress all the way to invasive cancer since normally, 90% of the people will spontaneously clear the virus thanks to the intervention of the immune system (34).

Despite this, given the huge number of infected individuals, 4.5% of the total new cancer cases worldwide was attributed to these viruses in a 2012 study (35). Namely, 640.000 new cancer cases were caused by HPV, with 570.000 cases being in women, in which cervical cancer accounts for more than 80% of the total (more than 450.000 cases) (36). Cervical cancer is the second most common cause of cancer-related death worldwide in women aged 15-44 years (34) and its incidence peaks in relatively young women with less than 25 years (37). The fact that this cancer is affecting mostly women early in their life poses a serious need for efficacious therapeutic approaches. HPVs can cause both squamous cell carcinoma (SCC, 80% of the cases) or adenocarcinoma (20%) of the cervix (38). For yet unclear reasons, cervical cancer usually develops in the so-called transformation zone, a specific region of the cervix where the epithelium changes from stratified to columnar (39).

In high-income countries, thanks to screening programs, the incidence of cervical cancer is decreasing but in less developed areas HPV infections remain still largely uncontrolled and unmonitored (40). Prophylactic vaccines against the most common high-risk viruses are now available, and they will hopefully contribute to the eventual disappearance of the disease (41, 42). However, at the moment, there is still a huge number of individuals that will not get vaccinated or that are already infected with the virus (and for which prophylactic vaccination cannot bring any benefit) (42, 43). For this reason, it is estimated that, for at least another 50 years, the burden of HPV-related cancers will remain relevant (34).

1.1.4 From infection to cervical cancer

As already mentioned, most HPV infections are usually spontaneously cleared by the host in 6-24 months from the first diagnosis (44, 45) (Fig. 2). It is now well accepted that the immune system plays a role in viral clearance (19, 46, 47). In fact, infections in immunocompromised patients have an increased incidence and a longer persistence than in healthy individuals (11), and

spontaneous regression of pre-cancerous lesions is often associated with a humoral and cellular immune response against the viral antigens (48). However, this is not always the case, and even in some immunocompetent patients the virus will persist and, in approximately 10% of the infected, will lead to the development of cancer (11). Several studies suggest that genetic predisposition might play a role in determining the fate of the HPV infection, but the underlining mechanisms tilting the balance towards clearance or persistence remains largely unclear (18). The quality and magnitude of the initial immune response to the virus likely play a fundamental role in determining the evolution of the disease (11). A strong cell-mediated immunity early on, might lead to the eradication of the infection while a weak and delayed response might be linked to persistence of the virus.

It can take several years, typically 5-10 and in some cases up to 20, for an HPV infection to evolve and reach the stage of invasive squamous cell carcinoma (49, 50). The disease course is characterized by a well-defined multistep progression that, as already mentioned, starts with infection of the basal keratinocytes in the cervix (17). At this stage, if the infection is not cleared, it will persist, leading to the formation of pre-cancerous lesions. These lesions, termed CIN for cervical intraepithelial neoplasia, will go through 3 stages of progression (51). CIN1 indicates mild changes in the epithelium and most of these lesions will spontaneously disappear, not leading to cancer. CIN2 indicates moderate changes, while CIN3 presents more severe changes and it is often referred to as carcinoma in situ (50). CIN3 lesions require treatments as soon as possible to reduce the chances of further progression to a more severe condition (49, 50). Although the likelihood of progression to invasive malignancy increases with every step, all CIN lesions can still spontaneously regress (50).

Finally, the last step in the disease is the progression from the high-grade CIN3 to invasive SCC, squamous cell carcinoma that, if left untreated, will eventually metastasize to distant organs ultimately leading to the patient's death (52). As for other types of cancer, the probability of successful treatment depends on the stage at which the disease is identified (according to data from the American cancer society). Early stage cervical cancer is usually completely curable while patients in the later stages, especially when the disease has spread outside of the pelvis, usually have a very poor prognosis (52–54).

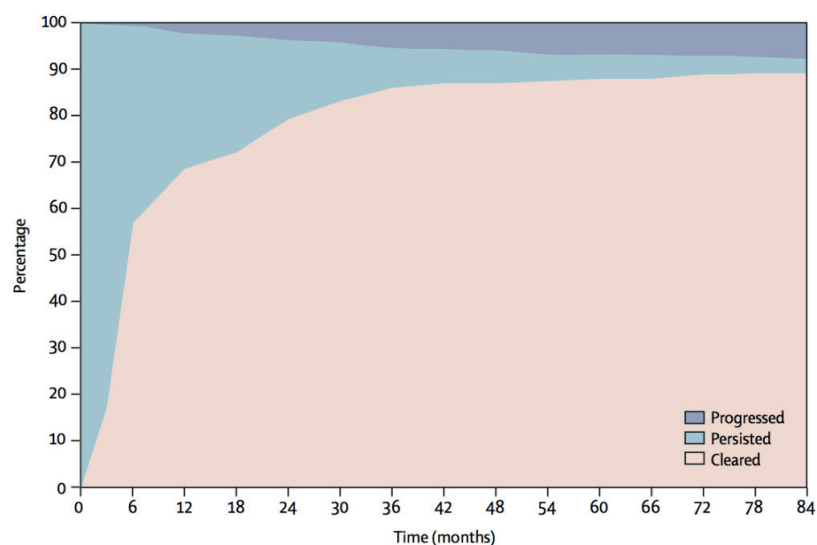


Figure 2: Average clearance, persistence, and progression of carcinogenic HPV infections. Carcinogenic HPV infections detected by DNA testing tend to resolve quickly within a year of detection. Details vary by population, cytological status, and age, but this diagram of infections illustrates a typical pattern. Over time, the risk of a pre-cancer diagnosis rises while the probability of eventual clearance among the still-persistent infections falls. Image and image description taken and adapted from (50).

1.1.5 Cervical cancer prevention

As these cancers are caused by a viral infection, the primary mean of prevention is represented by vaccination against high-risk HPVs (34). Up to date, three prophylactic vaccines have been approved and commercialized: Cervarix, Gardasil-4 and recently, Gardasil-9 (41, 42). Cervarix confers protection against high-risk HPV16 and 18, Gardasil-4 against HPV 16 and 18 and the low-risk HPV6 and 11, while Gardasil-9 additionally includes the high risk 31, 33, 45, 52 and 58 to the list. Based on similarities between the viruses it has been suggested that Cervarix and Gardasil-4 vaccines could offer cross-protection against HPV31, 33 and 45 (42).

These vaccines are all based on virus-like particles (VLPs) that are entirely made of the viral protein L1. When produced in eukaryotic cells, this protein self-organizes to form a complete viral capsid against which protective antibodies will be directed upon immunization. Antibody responses elicited by prophylactic vaccination have been found to be significantly stronger than those elicited by natural HPV infection and, studies conducted on vaccinated patients showed promising

results in terms of seropositivity rates and protection (42). Limitations of this prophylactic formulations include that they confer protection only to a limited number of HPV types. Being directed against the viral capsid proteins, they are unable to elicit cell-mediated immune responses capable of directly attacking infected cells, and it is therefore unlikely that they will offer advantages to patients already bearing the virus (42, 43).

Although these vaccines seem to be very effective at eliciting protective responses, coverage in high-income countries is still far from being complete, and their price remains prohibitive for lower-income countries. To reach an optimal situation, efficient vaccination programs will need to be established along with new production methods that allow for a drastic price reduction (42).

1.1.6 Screening

Screening remains, to date, the most efficient practice to prevent the development of cervical cancer. In high-income countries, screening is part of a well-defined program that also includes guided biopsy in case of abnormal results, the decision on whether to treat or not the identified lesion, treatment and finally follow-up (50).

Screening is usually performed starting 5-10 years after the first sexual intercourse, in this timeframe the possibility of testing positive for an HPV infection is high, but the risk of cervical cancer is still low (50). Screening procedures are cytology-based, e.g., with the Papanicolaou (PAP) test, which involves the scrubbing of the cervical mucosa and the following analyses of cellular abnormalities in the smear. The goal of the screening is to identify potentially dangerous pre-cancerous lesions to either treat them immediately to prevent further progression, or to keep them monitored and eventually intervene in case of progression (50). Historically, the clinical standard to diagnose pre-cancer and determine its stage has been colposcopically-directed biopsy. This technique can be helpful not only to classify the lesion but also to determine its extension and location, information that are useful for the eventual treatment (50).

Testing for HPV DNA could also be added to the screening procedure as it is very sensitive and can provide information on the HPV type and consequently on the risk of malignant progression (55).

1.1.7 Treatment

At present, the standard treatment that follows the diagnosis of an equivocal CIN2 or a defined CIN3 lesion is to remove the entire transformation zone. However, in many countries, such interventions are no longer acceptable, and other treatments that could spare the fertility of the patients are utilized in place of radical hysterectomy (the removal of the entire uterus) like cone-shaped excision and cryotherapy (50, 53, 54). If the pre-cancerous lesion is identified and removed at an early stage, the treatment is usually curative (53, 54).

Surgery is also the primary treatment in case of the presence of localized cervical cancer that, in its early stages is considered to be curable in almost 100% of the cases. However, when the tumor is at an advanced stage of progression, especially if it has spread outside of the pelvis, the treatments are considered to be only palliative and rely on the use of chemo and/or radiotherapy (56). In these cases, although it is often possible to prolong the patient's life and ameliorate the symptoms, it is unlikely to achieve remission, highlighting the need for better therapeutic options (56). Standard of care treatment for advanced cervical cancer is chemotherapy with paclitaxel and cisplatin (57).

Recently, the so-called immunotherapy has quickly become one of the most promising approaches for the treatment of cancer. These therapies have quickly shown the potential of outperforming classical therapies at prolonging the patient's life, and a rapidly growing number of studies are continuously improving the knowledge in the field (58, 59).

Of note, topical application of imiquimod, a TLR-7 agonist that acts by generating inflammation and activating the immune system locally, is already in clinical use for HPV-related lesions and has shown promising results mainly in the treatment of vulvar intraepithelial neoplasia (60, 61).

1.1.8 Immunotherapy

The notion of immunotherapy, that consists in using components of the immune system, like cytokines or antibodies, or in taking advantage of patient's own immune system to attack cancer has been around for many years however, it is only in the last few decades that this approach started to show impressive results even in patients with late-stage cancer (58, 59, 62). Thanks to these advances, the use of immunotherapy became a concrete clinical reality, in theory, applicable to many different types of cancers. This led to many clinical trials and prompted an

expansion of immuno-oncology research, leading to the development of many different approaches (58, 59).

These therapies come in different flavors, ranging from therapeutic antibodies, capable of directly targeting cancer cells or altering key regulatory mechanism of immune cells to make them more active against the disease, to therapeutic vaccines capable of triggering the generation of an anti-tumor responses, to direct transfer of tumor-specific killer cells into the bloodstream of a patient. A prominent example are the ones involving the use of immune checkpoint blockade antibodies that are starting to receive approval for the use in patients and that are widely being tested against many types of cancer leading, in some cases, to remarkably long-term responses even in terminally ill patients. These checkpoint blocking antibodies have been shown to be effective in a significant percentage of patients in greatly prolonging their lifespan or, although only in a few individuals, leading to complete tumor eradication (58).

HPV-related cancers and immunotherapy

Cervical cancer, and in general all HPV-related ones, represent ideal models to study these approaches because, unlike many other tumor types, the HPV-associated proteins are de-facto tumor-associated (neo)-antigens (TAAs) that can potentially be targeted by the immune system (48, 63). Knowing which TAAs to target makes it possible to monitor the anti-tumor immune response in patients assessing the abundance and functionality of tumor-specific cells and to design vaccines capable of eliciting a response against these targets. For this reason, the most widely studied immunotherapeutic approach for the treatment of HPV-related cancer has been therapeutic vaccination (48, 63).

From epidemiological studies and from analyses of the HPV-specific immune response in patients, it is clear that the immune system possesses the capability to eradicate the infection and to spontaneously regress pre-cancerous lesions, suggesting that a therapeutic approach aimed at directing the immune system against the viral antigens could, in principle, be effective (11).

At the moment, several clinical trials involving patients with cervical cancer are testing different immunotherapies like therapeutic vaccines of different kinds, checkpoint inhibitors against PD1, PD-L1, PD-L2 and CTLA4, or adoptive immunotherapy using patient-derived tumor infiltrating lymphocytes (TILs), but definitive results from all these studies are not available yet (56, 64).

The following paragraphs will give an overview of the different immunotherapeutic approaches that have been developed and are currently being investigated for cancer treatment.

Therapeutic vaccines

Therapeutic vaccines are very different from the “classical” prophylactic vaccines. The goal of the latter is to prevent the disease from infecting and causing damage to the host and consequently to prevent it from spreading. On the other hand, therapeutic vaccines are designed for the treatment of patients that are already ill and, their goal is to elicit an immune response capable of fighting against the disease (42).

Many types of therapeutic vaccines are currently available. They usually involve the delivery of an antigen (the target of the immune response) in the form of a protein or peptide (65) or in the form of a DNA sequence encoding for the antigen (66). These vaccines, as they are not very immunogenic compared to live/attenuated pathogen-based vaccines, are usually coupled with an adjuvant, a compound that activates antigen presenting cells thereby allowing them to mature and prepare to elicit the immune response against the delivered antigen (42, 67).

One of the most promising therapeutic vaccination formulation for the treatment of HPV+ lesions is based on synthetic long peptides. These peptides are usually around 30aa of length and they are delivered as a mixture of peptides designed to cover the entire length of the target protein (usually E7 and/or E6 in this case) (65). As therapeutic vaccination with SLPs will be the main focus of Chapter 2 of this thesis, a more detailed description of their features and limitations will be provided later on and they will not be further discussed here.

DNA-based anticancer vaccines rely instead on the delivery of a molecule coding for TAAs. The delivery can be of naked DNA or DNA inserted into a vector (virus, viral particles or bacteria). Once injected, the construct is picked up by DCs (or often by muscle cells) that starts expressing it and, in the presence of an adjuvant, this will lead to the generation of an immune response (66).

Another approach to therapeutic vaccination relies on the direct administration of donor- or patient-derived dendritic cells that, after isolation, have been expanded ex-vivo, activated and loaded with the desired TAAs before re-infusion. Although this approach is more complex than the aforementioned ones, it offers a few advantages like the possibility of genetically modify the DCs to make them more active or resistant to tumor-related immunosuppression or even to avoid the

concomitant administration of adjuvants, which could result in inflammation-related side effects. DCs can be loaded with TAA using peptides, mRNAs, viral vectors or bulk cancer cell lysate (68, 69). The antigens in a therapeutic vaccine can also be provided by directly delivering tumor cells, this approach ensures, in theory, that all the TAA are present in the vaccine. Tumor cells can either derive from the patient or they can be derived from cell lines. The latter case is exemplified by GVAX, a vaccine containing 2 prostate cancer cell lines (70). However, after early promising results, GVAX failed the phase III trial likely due to the poor immunogenicity of this class of vaccines or on the limitations linked to the use of cancer cell lines as the source of TAA, which might not exactly match the antigen spectrum of the patients.

Therapeutic vaccine formulations can also be based on live-attenuated TAA-expressing bacteria like *Listeria monocytogenes* (Lm). A recently developed Lm-HPV16-E7 based vaccine has shown promising results leading to robust immune responses and antitumor activity (71, 72).

In the case of HPV, therapeutic vaccination is the most common type of immunotherapy under investigation, and many different therapeutic vaccination approaches are currently being tested in the clinic, usually employed in patients with pre-malignant lesions or cancer (73). Unfortunately up to date, although some formulations have shown remarkable results against pre-cancerous lesions, their efficacy is still far from optimal, and they still can't provide significant benefits in patients with advanced cervical cancer as single treatments (74, 75). This suggests that there is still room for improving these vaccines and that successful therapeutic vaccination approaches in patients with an advanced malignancy will likely require the additional layering of combinatorial therapies aimed at removing the immunosuppressive barriers build by cancer cells.

Tumor-targeting antibodies

This group of therapies includes all the antibodies that are directly targeted towards tumor cells or to components secreted by the tumor-associated stroma that act on tumor cells. Many of these antibodies exist, and can have very different mechanisms of action: they can bind to receptors that are selectively expressed or overexpressed on tumor cells blocking their signaling functions (76) (EGFR- (77) and CD20- (78) targeting antibodies are only a few of the already approved ones and additionally, it is worth mentioning anti-FasL antibodies (79), a target that has been reported to be expressed on cervical cancer cells and that can lead to CD8 T cells killing (80)). These antibodies can also act by blocking tumor- or stromal- secreted factors that are involved in tumor

growth and neutralize their action (e.g. the anti-VEGFA bevacizumab, an antibody that has also been approved for the treatment of cervical cancer in combination with standard of care chemotherapy) (81), they can trigger the death of cancer cells when conjugated with a toxin or a radionuclide (82) , they can opsonize tumor cells leading to activation of antibody driven cell cytotoxicity (83) or, in the case of bi-specific antibodies, they can both bind tumor cells and concomitantly activate T cells for enhanced killing (84).

Checkpoint inhibitors and agonistic antibodies

Right now, most of the attention of the immunotherapy field is probably directed to this class of therapeutic antibodies, where an ever-growing number of new and ongoing clinical trials are currently testing their application against a wide variety of cancers (85). Unlike the previous one, this class of antibodies is targeted against receptors that play a role in the immune response.

Checkpoint inhibitors bind to inhibitory receptors or ligands whose normal function is to suppress or keep under control the adaptive immune response, thereby “releasing the breaks” and enhancing the function and activation of T cells (86). Checkpoint mechanisms have evolved to prevent the excessive activation of the immune system in order to prevent unwanted damage to the host caused by an uncontrolled immune response (87). Their blockade in tumor patients has been shown to be capable of triggering novel antitumor-immune responses or to re-invigorate existing ones (88). At the moment, antibodies against two targets, PD-1 and CTLA4, have been approved for the use in humans where they are showing robust and durable responses in a cohort of patients with different types of solid tumors and many more are currently being widely tested (59).

Agonistic antibodies act differently than checkpoint inhibitors, rather than blocking inhibitory signals, their goal is to bind to and activate co-stimulatory molecules on the cell surface leading to enhanced activation of the target population, usually T cells (89) or APCs (90). Particularly, agonistic antibodies against CD40, 41BB, and OX40 have shown promising results in animal models of cancer (91).

The drawbacks associated with these therapies are linked to the potential over-stimulation of the immune system caused by these antibodies, that could lead to severe to lethal adverse events in a subset of patients (59).

Other immunomodulatory antibodies

Antibodies can also be utilized to block secreted immunosuppressive factors or cytokines that are often involved in the neutralization of the anti-tumor response. These factors could come directly from the tumor cells or the tumor-associated stroma and act on all arms of the immune system. Examples of such targets is TGF β 1 (92) that can negatively impact both the antitumor T cell response and the antigen presenting cells (93).

Immuno-stimulating cytokines

Cytokines play a key role in regulating almost every aspect of immune responses (94). However, although the delivery of these factors has been tested many times trying to boost anti-tumor immunity, cytokines as monotherapies have shown very little clinical activity (59, 95).

Generally, immune-stimulatory cytokines are given to cancer patients in combination with other agents as adjuvant therapy, as it happens with GM-CSF, often used to boost the efficacy of therapeutic peptide vaccines (96). A few exceptions exist, in fact, IL-2 and IFN- α 2 are approved for the use in melanoma patients and against hairy cell leukemia respectively (59).

Importantly, therapies based on cytokines have to be carefully monitored and evaluated. The risk of a cytokine cascade that leads to severe and potentially lethal effects needs to be taken into serious consideration for these therapeutics (59).

Adoptive cell transfer (ACT)

ACT refers to the re-administration to the patients of lymphocytes (generally CD8 T cells, but this has also been tested with other cell types) that have been previously isolated from the bloodstream or the tumor and then expanded and eventually modified ex-vivo to enhance their effector functions (59).

This therapy differs from other approaches involving the re-infusion of patients derived cells (like the previously mentioned DC vaccines) in fact, ACT involves the delivery of a population that is enriched in tumor-reactive immune cells that can directly recognize and kill the patient's cancer cells (97, 98). The advantage of this approach is that it is, in theory, possible to transfer a high amount of tumor-specific T cells thereby bypassing the need for eliciting a robust enough antitumor-response in the patient, e.g., by therapeutic vaccination, that is not always easily achievable due to the often established tolerance towards TAAs (99).

Moreover, the isolated lymphocytes can also be modified prior to re-infusion to provide them with a tumor-specific T cell receptor or with a so-called chimeric antigen receptor (CAR) (100) and/or they can be provided with the optimal factors to ensure the proper activation (101). To promote the survival and functions of the transferred cells, the administration to the patient is often supplemented with the addition of exogenous cytokines like IL-15 (102).

Radio and chemotherapy

It is becoming increasingly evident that many of the conventional therapies can affect immune cells. In some cases, their efficacy relies, at least in part, on the changes that are exerted on the antitumor immune response (103). Certain chemo- and radiotherapies can induce the so-called immunogenic cell death (ICD) of cancer cells (104, 105). This consists in the release of TAA and danger associated molecular patterns (DAMPs). These molecules can be taken up by APCs leading to their activation and maturation, that will ultimately result in the generation or in the boost of the anti-tumor immune response (106). At the moment, a few of the FDA-approved drugs have been shown to be bonafide ICD inducers (59).

Chemotherapy has also been reported to be able to selectively eliminate suppressive cell populations like Tregs and MDSCs. Metronomic doses of cyclophosphamide can lead to the selective elimination of Tregs at the tumor site (107) leading to an improvement of the overall CD8/Treg cell ratio that can be a prognostic factor for certain types of cancers (108). Various studies show that 5-fluorouracil (109), gemcitabine (110) and a combination of carboplatin/paclitaxel (111) have the ability of selectively eliminate myeloid-derived suppressor cells (MDSCs) in mouse models and/or in cancer patients, potentially leading to an overall improvement of the anti-tumor immune response and in the response to therapeutic vaccination. Additionally, it has been shown that radiotherapy can promote the re-programming of tumor-promoting M2-like macrophages to a more anti-tumor M1-like phenotype in the TME (112).

Blocking suppressive mechanisms or depleting suppressive cells

In cancer patients, several immunosuppressive factors can be produced by tumor cells, the tumor-associated stroma or by suppressive immune populations, like MDSCs, which could be present in the TME, collectively blocking the anti-tumor immune response (113, 114).

Small molecule inhibitors can be used to block or reduce the activity of an immunosuppressive factor. An example is IDO, an enzyme that catalyzes a reaction in the conversion of the amino acid tryptophan to kynurenine that has immunosuppressive activity on both CD8 T cells and DCs. Additionally, this reaction also depletes tryptophan that is an essential element for T cells (115, 116). IDO has been negatively associated with survival of cervical cancer patients, and currently, IDO inhibitors are undergoing testing in clinical trials (117, 118).

Strategies to deplete the suppressive populations, different than the above-mentioned chemotherapy regimens, are under development. A fusion between IL-2 and the diphtheria toxin can enhance the efficacy of immunotherapy by eliminating Tregs (119), and alternative approaches to target MDSCs are also being studied (120, 121).

Similarly to what radiotherapy can do, several agents exert their anti-tumor activity by changing the phenotype and/or alter the recruitment of pro-tumoral M2-like macrophages to the TME. In this group, we mainly find inhibitors of chemokines and their receptors and agents that interfere with the activity of colony stimulating factor 1 (CSF1) and CSF1 receptor (CSF1R) (122).

Others

The long list of approaches that target or take advantage of the immune system continues to expand and some additional strategies worth mentioning include the use of oncolytic viruses, non-pathogenic viral strains that specifically infect and cause the death of cancer cells (123), and the administration of pattern recognition receptors agonists, molecules that act as adjuvants, activating several immune cell population and causing the release of pro-inflammatory molecules that ultimately boost the anti-tumor immune response (124).

Regarding cervical cancer treatment, although not yet tested in clinical studies, it is pertinent to mention that intracellular antibodies are also being studied. The rationale of using this so-called intrabodies relies on the need for cancer cells to continuously express E6 and E7. Blocking the oncogenic proteins with an antibody directly inside the cell might impede cancer growth. This approach has shown promising results in in-vitro cervical cancer cell lines and the possibility of delivering the therapy topically makes it an attractive strategy for HPV-related cancers (125).

1.1.9 HPV and cervical cancer escape from the immune response

HPVs are the most common sexually transmitted viruses and, as already mentioned, millions of people are currently infected, undoubtedly making HPV a very successful virus. Such a widespread diffusion is made possible by the evolutionary adaptation of the virus, that has developed an impressive amount of mechanisms to remain hidden and manipulate the host immune response to its advantage (32, 126). The identification and characterization of these mechanisms, both at the infection phase and later when cancer appears, are fundamental and critical steps for the design of effective immunotherapy strategies against HPV and HPV-related cancers.

During the initial phases of the infection, the viral life cycle allows HPV to remain hidden. Viral proteins are kept at low levels and are not secreted, and the release of new viral particles happens only in the outer layers of the epithelium, where the surveillance of the immune system is scarce. The virus is also not causing viremia nor inflammation (46, 127). All these elements are by themselves already dampening the chances of being detected by the immune system. However, the strategies at the viruses' disposal are much broader and have proven to be very effective. Immune-escape mechanisms can be divided into intracellular and extracellular and are aimed not only at hiding the virus but also at actively inhibiting antiviral immune responses, especially antigen presentation by dendritic cells (DCs) and cytotoxic CD8 T cell responses (32).

Unfortunately, many of these mechanisms are likely to remain active and play an important role in the infected cells even after malignant transformation. Moreover, while it has been shown that in the first phases of the infection the generation of a pro-inflammatory response is inhibited to allow the virus to remain hidden, upon cancer development there is a formation of a chronically inflamed tumor microenvironment that promotes tumor progression (11, 128). Additionally, as many years can pass between the initial infection and the subsequent formation of a tumor, the development of tolerance towards the viral antigens is also playing a major role in the immune-escape of the virus and of the tumor (126).

Intracellular immune-evasion strategies

Keratinocytes form the first barrier against invading pathogens in the skin of the host (129). They act both as a physical obstacle and as sentinels for the immune system, capable of releasing cytokines and chemokines required to attract other immune cells and to start an immune

response against potential threats that have breached the skin (130). Because of the central role of these cells in regulating immunity, HPVs had to evolve mechanisms to dampen the immune-related functions of keratinocytes.

In addition to the strategies mentioned above that are closely linked to the viral life cycle, HPVs have been found to alter gene expression in the host cells. This process influences the production of chemokines, adhesion molecules and viral-sensing receptors in the infected keratinocytes. HPV E7 associates with and activates DNA methyltransferase 1 leading to changes in the methylation status of several genes (131). E7-dependent hyper-methylation of the CXCL14 promoter leads to transcriptional downregulation of this chemokine, that is responsible for attracting multiple lymphocytes like NK cells, Langerhans cells and dendritic cells (132). Additionally, the same mechanism has been found to lower the production of E-cadherin, an adhesion molecule that is important for Langerhans cells movement and homing in the epithelium (133). Langerhans cells normally reside in the skin, where they continuously monitor the environment in search of pathogens and danger signals and, upon recognition of those, undergo maturation and migration to the draining lymph node where they can orchestrate the appropriate immune response. Human Langerhans cells can prime naïve-CD8 T cells that are known to be critical for the antiviral immune response to HPV (134, 135). Loss of CXCL14 and E-cadherin impairs the ability of Langerhans cells to accumulate at the site of HPV infection leading to a defective delivery and presentation of the HPV antigens to the lymph node (133).

HPV E7 can also interfere with histone modifications causing trimethylation in histone 3 in the TLR9 promoter region, leading to downregulation of this receptor (136). As the role of TLR9 is to recognize viral DNA (137), it is not surprising that HPVs have evolved mechanisms to abrogate its function. Lack of this TLR on the infected keratinocytes impairs their capacity to recognize the viral genome, therefore preventing the generation of an inflammatory response. TLR9 is not the only viral-sensing mechanism that is blocked by HPVs; it has been reported that the STING pathway, another DNA recognition mechanism, is also negatively affected by E7 (138).

A key antiviral mechanism involves signaling from different types of interferons (IFNs) that cause changes in the infected cells and its neighbors, that impair viral replication, favor antigen presentation and generally promote antiviral and inflammatory responses (139). IFN signaling pathways have been found to be severely dysregulated in HPV infected cells by a mechanism that involves the binding of viral oncoproteins, both E6 and E7, to interferon response factors (IRFs)

(11). IRFs are transcription factors that regulate the expression of genes induced by interferons, and their blockade causes the loss of a major arm of the antiviral immunity in the infected cells (31, 140).

Changes to intracellular processes are not limited to chemokines and receptors. Antigen presentation is a key requirement for cell-mediated immunity to kill an infected cell. HPV infection has been associated with alteration in multiple components of the antigen presentation machinery (32). Infected keratinocytes have been found to have decreased expression of the immunoproteasome IFN γ -inducible subunits PSMB8 and PSMB9, two enzymes required for the processing of antigens (141). Expression of TAP1 and 2 is also repressed by HPVs, impairing the transport of HPV-derived peptides into the ER for loading on MHCI molecules (141, 142). Additionally, it has also been observed that expression of ERAP1, an aminopeptidase capable of epitope editing, can also be increased leading to alterations in the antigenic HPV peptides that can no longer be recognized by the adaptive immune system (143). Finally, expression of MHC class-I (MHCI) in mice and HLA-A and -B in humans, can be impaired by the HPV proteins (144).

Interestingly, changes in intracellular pathways that regulate inflammatory responses can also be utilized by the virus at the advanced stages of the disease to generate tumor-promoting inflammation. In fact, NF- κ B levels have found to be elevated in cervical cancers, and this is thought to favor the establishment of a chronically inflamed tumor microenvironment that can foster tumor growth (11).

Overall, these changes lead to a decreased capacity of sensing the viral infection and of initiating the generation an antiviral immune response, they render the infected cells resistant to CD8 T cell-mediated killing and, upon progression to cancer, they can also provide aid to the malignant cells.

Extracellular immune-evasion strategies

HPV is also capable of altering the function of numerous immune cell population that have a key role in its eradication, primarily by inhibiting the generation of optimal T cell responses and promoting the production and recruitment of immature and suppressive myeloid cells. Many of the effects that will be described in the following paragraph are playing a major role at the advanced stages of infection when pre-cancerous lesions, and later invasive cancer, are formed, thereby helping tumor growth, dissemination, and escape from the anti-tumoral immune response (32). Keratinocytes carrying the HPV genome show minimal production of pro-

inflammatory cytokines like IL-1 β (73) and other chemokines like CCL20, a feature that can contribute to preventing the generation of an early local inflammatory response (126).

It has been reported that HPV+ cancer patients have a reduced number of DCs in the blood and a higher frequency of immature DCs (126, 145, 146). This effect has been linked to HPV, and it not only leads to a reduced number antigen presenting cells that are capable of mediating the initiation of an anti-tumor response, but the presence of non-fully mature APCs could lead to the generation of regulatory T cells that can further inhibit the immune response (126, 147). Inhibiting DCs maturation can ultimately impair the generation of a strong CD8 T cell response and instead promote the establishment of tolerance and hypo-responsiveness towards the viral antigens.

HPV can also directly affect T cell responses. A robust Th1-polarized immune response is usually generated against intracellular pathogens and its needed to efficiently eliminate HPV infection (73). Th2 responses on the other hand, are involved in allergic reactions and are usually poorly pro-inflammatory (148). It has been observed that HPV can interfere with the correct Th1/Th2 polarization of the antiviral response favoring the outcome towards the latter (149). Th2-associated cytokines like IL-10 and IL-6 are often detected in HPV+ lesions with very limited amounts of Th1-associated cytokines (11, 149, 150). IL-10 can have a direct inhibitory effect on CD8 T cells (151) and DCs (152), while IL-6 has been shown to be important for promoting the suppressive functions of MDSCs (153). This shift to Th2 may favor the generation of a sub-optimal response that facilitates persistence rather than regression (154).

It is now evident that during cancer progression there are changes in the mechanisms orchestrated by HPVs, perhaps reflecting the additional presence of novel mutations in the cell genome, that act to promote the development of a chronically inflamed TME with abundant recruitment of tumor-promoting cells that can protect the tumor from the assault of the immune system.

In order to create such microenvironment, HPV-driven tumors cause expansion and infiltration of several immunosuppressive populations like Tregs, TAMs, and MDSCs for which there are extensive reports that show how these cells can suppress antitumor immune responses and promote tumor growth (126, 155, 155–157). The mechanisms responsible for this, involve the aforementioned blockade of APC maturation (that can lead to Tregs generation) and the

production of growth factors (such as G-CSF and M-CSF) and cytokines (like IL-6) that can promote myeloid cell expansion and suppressive functions (147, 158–161).

Cervical cancer patients often have an increase in myeloid cells not only in the TME but also in the circulation, which has been linked with the presence of higher levels of G-CSF (158). Direct production of this growth factor has been found in more than 80% of cervical tumor samples, and it has been associated with a decreased survival and a worse response rate to standard of care chemotherapy (158). Direct G-CSF production from cervical cancer cell lines has been shown in mouse models to promote an increase of MDSCs that are responsible for promoting tumor growth and resistance to radiotherapy (162). In patients, elevated plasma levels of G-CSF are linked to an increase in neutrophils and tolerogenic monocytes-derived dendritic cells that are inversely correlated to T cells numbers and activity (163). Other studies have shown that MDSCs depletion can ameliorate the antitumor-immune response in mouse models of HPV+ cancers and it can improve the response to therapeutic vaccination in patients (111).

Macrophages seem to also play a role in tumor progression, in fact, their recruitment and polarization towards the “M2” phenotype has also been described to happen in the cervical cancer TME (156), and it has been shown in mouse models that it can promote tumor growth and resistance to chemotherapy (164).

T cells could also be involved in directly fostering cancer development. Interestingly, IL-6 mediated CCL20 induction in cancer-associated fibroblasts can lead to Th17 cells recruitment, a subtype of T cells that is often associated with chronic inflammatory diseases of the skin and that could further promote the pro-tumorigenic inflammatory environment (165).

The increased numbers and the highly immunosuppressive nature of all these cell types suggest that they could be playing a role in suppressing immune responses even outside of the TME, possibly providing further explanation to the poor responsiveness of many HPV+ cancer patients to therapeutic vaccination (166).

Finally, cervical cancer cells have also been found to express the immunosuppressive PDL1 and IL10 (155), and in some patients, the expression of FasL (80, 167, 168) could be implicated in the direct killing of tumor-specific CD8 T cells (80). IDO production by HPV+ cancer cells has also been documented, and its activity has been linked to a worse survival (117). Although it is unclear whether the production of these factors depend on the HPV proteins or if they are exclusively

linked to cancer development, they certainly represent additional barriers to an efficient antitumor response.

1.1.10 Mouse models of HPV+ cancers

Mouse models have been instrumental for the study of cervical cancer and in general of all HPV-related cancers. HPVs cannot infect mice, so these models are mainly based on transplantable cancer cells that have been engineered to express selected HPV proteins, generally E6 and E7, or on genetically engineered mouse models (GEMMs). HPV GEMMs can carry in their genome from only 1 of the two oncogenic protein to the whole early region of HPV16 usually under the control of a keratinocyte-specific promoter like the one of keratin 14 (169). Notably, humanized mouse models also exist and they have been used to elucidate the functions of HPV proteins (170).

By far, the most common mouse model of HPV+ cancer relies on the subcutaneous implantation of TC-1 cells. These are lungs epithelial cells that have been engineered to express HPV16 E6 and E7 together with an oncogenic Kras mutant (171). Once implanted, and if left untreated, they rapidly expand, and the immune system cannot control tumor growth on its own. This model has been mainly used to test different therapeutic vaccination approaches, favored by the fact that TC-1 cells usually respond to immunization and, like other subcutaneous models, by the ease of following both tumor size and mice survival (111, 172). A variant of this model involves the orthotopic implantation of TC-1 cells in the cervico-vaginal tract of the mouse to study the tumor in a more physiological microenvironment (173, 174). Studies in these models led to the development of the different therapeutic vaccination approaches that are currently being tested in the clinic (75, 111).

However, treatments in TC-1 transplanted mice usually work quite well and, although these are good models to compare the potency of different immunization approaches, they do not mimic the disease very well. It has proven to be hard to reproduce the same efficacy in humans, highlighting the need of sophisticated models to better recapitulate all the complex features of HPV-related malignancies (74, 166).

Here is where GEMMs come in, these mouse models are usually more complex and harder to treat than transplantable cells-derived tumors and, although they are far from being perfect models,

usually provide a setting that more closely resembles the situation in patients. Since HPV-related tumor growth in humans is driven by E6 and E7, it is relatively easy to mimic the disease in mice (169). Studies in GEMM have been useful to understand and manipulate the mechanisms promoting tumor growth. Several transgenic mouse models have been developed during the last 30 years differing in the site of expression and the numbers of HPV proteins expressed. The most relevant models restrict transcription of the HPV genes in the keratinocytes by putting them under the transcriptional control of the K14 promoter (169). The K14-HPVE5/E6/E7 only expresses 1 of the listed HPV proteins, this models allowed the study of the functions of the oncogenic proteins and particularly of the less studied E5, revealing that the importance of the latter might be underappreciated in human cancers (175–177).

Several studies relied instead on the K14-HPV16 mouse model that expresses the entire HPV16 early region under the K14 promoter. These mice were usually supplemented with estradiol, required to induce the formation of cervical cancer in this model. The disease progression seen in patients is well recapitulated in this transgenic mouse, where it is characterized by multistep progression accompanied by an increase in VEGF expression and angiogenesis along with enhanced local inflammation. These close similarities make this model very attractive for the study of HPV-related cancers and their treatment (178–180). However, since tumor development in these mice is only permissive in the FVB/n background, investigation on the adaptive E7-specific antitumor-immune response is limited by the incapability of displaying the HPV E7-derived CD8 peptide on MHC I molecules, allowing only the study of the CD4 response (181). Recently, to overcome this limitation, the K14-HPV16 FVB/n mouse was crossed to C57BL/6 mice to obtain the H2b locus thereby providing the capability of presenting the CD8 peptide of E7 to the immune system (182). Thanks to this addition, the new K14-HPV16 H2b model seems to be well suited for studying immunotherapies against HPV-related cancers. Data presented in Chapter 3 of this thesis have been generated using this mouse model.

Recently, the delivery of oncogenic plasmids carrying the HPV proteins has been used to induce tumors in the oral cavity that were capable of spreading to the local draining lymph-node. Although some caveats like the immunogenicity of the reporter genes exists, this and other similar models could be of particular interest, in that they could represent the perfect compromise between transplantable and transgenic mouse models, recapitulating the spontaneous tumor formation and, at the same time, avoiding potential problems related to immunological tolerance

that could arise in GEMMs. However, further studies will need to be conducted to assess how closely they can effectively recapitulate the human disease (183).

Of note, a recent report describes an HPV-cancer model that involves the infection of immunocompromised mice with a murine papillomavirus leading to the development of cervical, anal and tongue lesions. Although unfortunately, the results were not reproducible in commonly used immunocompetent mice, this could still represent an interesting model in which to mimic and study the mechanisms of the disease in immunocompromised individuals like the ones affected by HIV, a population with increased susceptibility to HPV infection (170).

1.2 General considerations and scope of the thesis

As discussed above, the burden of HPV-related cancer is still relevant and will remain so for at least several decades. Moreover, HPV+ cancer can serve as an ideal model in which to study immunotherapeutic approaches both because targetable TAAs are known and also because of the presence of several barriers to immunotherapy that can be relevant for many other tumor types and that encourage the testing of complex approaches.

Collectively, the evidence discussed so far shows how HPV have evolved numerous strategies to evade the immune response. Moreover, not only can the virus and the tumor utilize numerous immunosuppressive strategies to begin with, but it is also likely that the time that passes between initial infection and the development of cervical cancer is significantly contributing to the establishment of at least a certain degree of immunological tolerance or non-responsiveness towards the viral proteins, not to mention the additional barriers and mutations that could arise during cancer progression. Tolerance and multiple mechanisms of HPV-dependent immunosuppression will likely need to be overcome in order to achieve therapeutic responses in patients.

Given the complexity of the situation, it is not surprising that approaches based on therapeutic vaccination alone have only shown extremely poor efficacy against the advanced form of cervical cancer. Future development of immunotherapeutic strategies for the treatment of this cancer will have to be focused on implementing multi-targeted approaches in combination with potent therapeutic vaccines. These approaches need to aim at restoring the ability of the host to mount potent anti-tumoral T cell responses by boosting pre-existing or generate de-novo CD8 T cell

responses. Additionally, future therapies will need to be able to break tolerance while at the same time eliminate most of the suppressive barriers both in the periphery and in the TME.

The scope of this thesis is precisely to illustrate ways to enhance the efficacy of currently clinically available therapeutic vaccination approaches and, by using a genetically engineered mouse model of spontaneous cancer, to investigate mechanisms impairing the efficacy of immunotherapeutic interventions for HPV+ cancers and to test combinatorial strategies aimed to improve the success of future therapeutic approaches based on immunotherapy.

Chapter 2

Nanoparticle conjugation of human papillomavirus 16 E7-long peptides enhances therapeutic vaccination efficacy against well-established solid tumors in mice

This chapter of the thesis will illustrate a promising strategy based on ultra-small (30 nm diameter) nanoparticles to drastically improve the efficacy of synthetic long peptides based therapeutic vaccines using several mouse models of HPV+ cancers.

2.1 Introduction

In contrast to many types of cancer, where finding a suitable antigen for therapeutic vaccines might require complex analyses of the tumor and prediction of neo-antigen binding to MHC (184, 185), HPV+ malignancies can be targeted by using the viral oncoproteins (48, 75). In fact, clinical trials using HPV oncoprotein-derived synthetic long peptide (SLPs) vaccines to treat patients with early-stage vulvar intra-epithelial neoplastic (VIN) and cervical intra-epithelial neoplastic (CIN) lesions has shown promising results, in some cases leading to complete responses (74, 75, 186). However, SLP vaccines have demonstrated poor efficacy in a percentage of these patients and in the treatment of more advanced disease (74, 166), indicating that improvements are needed for therapeutic vaccines to become a tractable strategy. It has been reported that clinical responses to SLP vaccines are dependent on the efficient delivery to dendritic cells (DCs), which need to process SLPs into short peptides for presentation on MHC molecules (69, 187, 188) so as to elicit robust CD8 T cell responses (74, 186). In fact, CD8 responses are typically hard to detect in patients treated with HPV vaccines, and, moreover, although SLPs can elicit a robust CD4 Th1 response, the induced CD8 counterpart is usually weaker (74, 75, 186, 189). In addition to the magnitude of the CD8 response, the CD8/Treg ratio is a prognostic marker for HPV+ cancers (190). Therapeutic vaccination of HPV+ cancer patients typically leads to an increased abundance of Tregs (191) and, interestingly, larger pre-malignant lesions show a greater increase in intra-tumoral Tregs compared to smaller ones (74). The stimulation of Treg infiltration consequent to therapeutic vaccination may contribute to the poor efficacy of this approach (192, 193). As such, identifying means to enhance SLP vaccine potency while avoiding the prolific induction of Tregs

might serve as a more-robust baseline treatment upon which to build combinatorial trials against primary and recurrent cervical and other HPV+ malignancies.

Bioengineering approaches have emerged as important technologies to improve immunotherapies, including lymph-node targeting vaccines (194–198). Previously, it has been shown that protein-conjugation to one such ultra-small polymeric nanoparticle (NP) formulation can boost the generation of immune responses to model tumor antigens (194, 195). The chemical structure of this 30 nm-diameter NP, with disulfide bonds on the surface, makes it possible to load them with thiol-bearing antigenic payload molecules (199). Their small size enables these NPs to rapidly reach draining lymph nodes after subcutaneous and intradermal administration, where they can be efficiently taken up by dendritic cells (DCs) (199, 200). Once internalized by DCs, the disulfide bonds that bind the antigen payload to the surface of the NPs are broken, and the released antigen is preferentially directed towards processing and loading on MHC I molecules leading to a strong CD8 T cell response (194, 195, 199–201).

We hypothesized that NP-conjugation of SLPs derived from the HPV protein E7 (E7LP) could boost immune responses against E7-expressing neoplasias, in particular well-established solid tumors at different anatomical locations. To test this hypothesis, the E7₄₃₋₇₇ SLP (E7LP) GQAEPDRAHYNIVTFCKCDSTLRLCVQSTHVDIR (172) was conjugated to NPs, and compared to the non NP-conjugated free (liquid) E7LP in several mouse models of HPV+ cancers. As a foundation, we used HPV16 E6/7-transformed TC-1 cells, which have been widely used in mice to test therapeutic strategies against HPV+ cancers (111, 171–174) and a skin squamous cell carcinoma cell line (termed SC1) derived from HPV16 transgenic mice (178, 182). We comparatively evaluated the two vaccine formulations in mice bearing subcutaneous TC-1 and SC1 tumors, orthotopic TC-1 tumors at the cervico-vaginal tract (174) and experimental TC-1 lung metastases (202). The results presented below reveal how conjugating SLPs, that are currently being evaluated in clinical trials (74, 166, 186, 186, 203), to a solid-phase platform bring clear benefits for therapeutic vaccine delivery strategy compared to a conventional free/liquid vaccine.

2.2 Results

2.2.1 Immunization with NP-conjugated E7LP generates systemic immune responses that prolong survival of TC-1 tumor-bearing mice.

Classical (free-peptide/liquid) therapeutic vaccine formulations against HPV16-driven cervical cancers have had equivocal therapeutic responses against established carcinomas, motivating efforts to improve immunization strategies. Thus, we first sought to determine whether therapeutic vaccination with the NP-conjugated E7LP could be more effective than the free E7LP formulation at eliciting systemic E7-specific CD8 T cell responses in mice with well-established solid tumors, and to comparatively assess effects of the two vaccines on overall survival. C57Bl/6 mice were subcutaneously implanted with 0.5×10^6 E7- and E6-expressing TC-1 cells. When the mean size of the palpable solid tumors was approximately 100 mm³, we administered either NP-E7LP+CpG or free E7LP+CpG, or PBS as control (Fig. 1A).

Since clinical responses to therapeutic vaccination have been correlated with the induction of a systemic E7 tumor antigen-specific CD8 T cell response (73), we began by comparatively evaluating the systemic adaptive immune response. Tumor-bearing mice were sacrificed 9 days after immunization and E7-specific CD8 T cells in the spleen were quantitated by flow cytometry analyses (Fig. 1B and C). Mice that received NP-E7LP showed a 3- to 16-fold increase in the number of E7-specific CD8 T cells compared to mice that were immunized with the free E7LP. Notably, E7-specific CD8 T cells were undetectable in PBS treated mice, suggesting the absence of a spontaneous CTL immune response against TC-1 tumors (Fig. 1B and C).

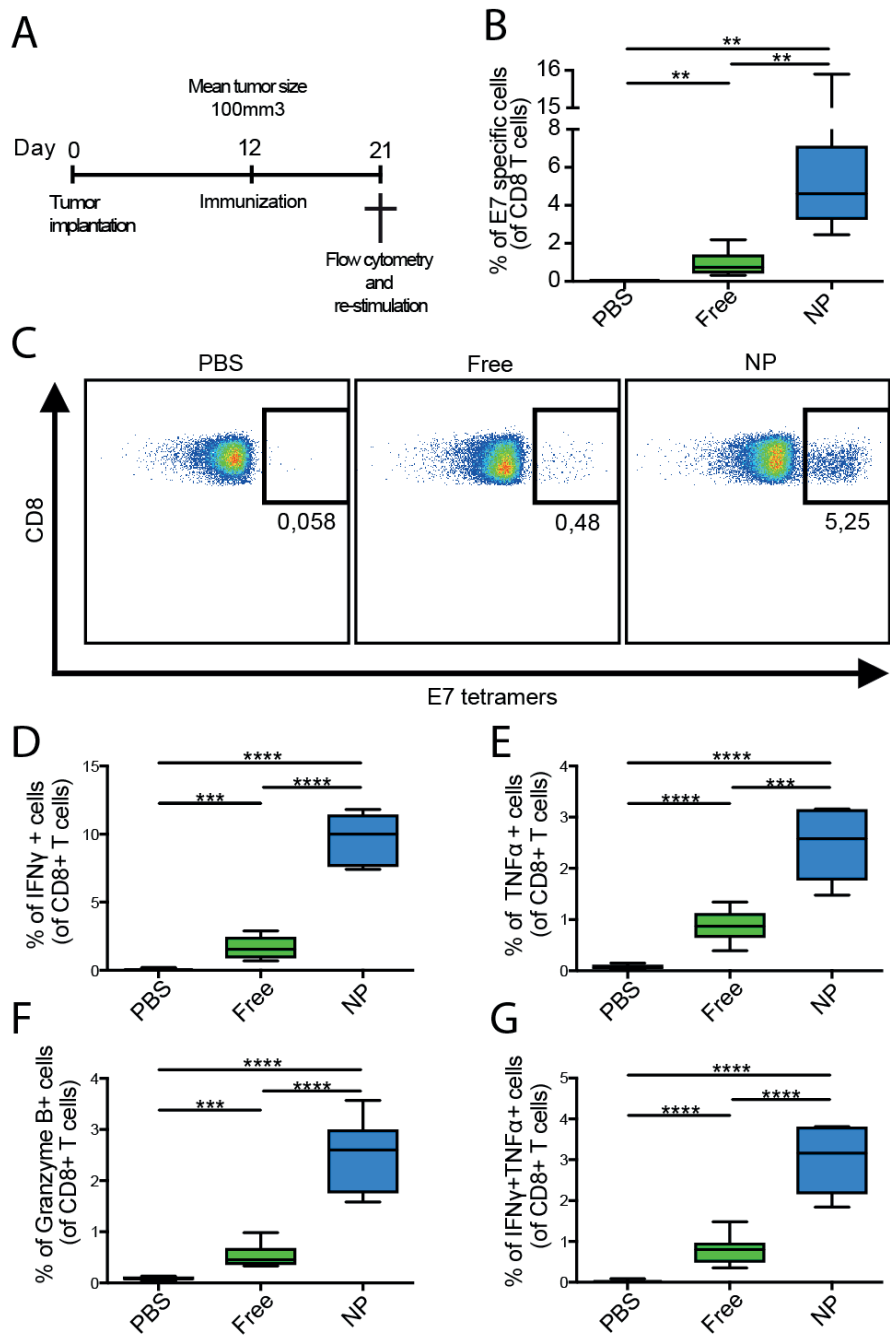
To comparatively evaluate the functionality of the E7-specific CD8 T cells elicited by the two vaccine formulations, splenocytes harvested 9 days after immunization were re-stimulated in-vitro with the class I MHC restricted E7 peptide RAHYNIVTF (171). NP-E7LP treated mice showed a significant increase in cells expressing IFN γ (Fig. 1D and S1), TNF α (Fig. 1E and S1) and Granzyme B (GZB) (Fig. 1F and S1) compared to mice that were immunized with free E7LP. An increase in TNF α and IFN γ double-positive cells was also detected in the NP-E7LP immunized mice, indicating that poly-functional CD8 T cells were being generated in higher numbers (Fig. 1G and S1). As expected, no cytokine or GZB production was detected in PBS-treated animals (Fig. 1D, E, F and S1).

consistent with the observed absence of E7-specific CD8 T cells (Fig. 1B and C). These results show that the NP-E7LP vaccine formulation is superior to the free E7LP vaccine at inducing a strong systemic CD8 T cell response, which is characterized by a larger pool of E7 specific cells and a more robust production of pro-inflammatory cytokines and GZB required for the killing of target cells.

Congruent with the enhanced immune response elicited by the NP-vaccine, mice that received the NP-conjugated E7LP formulation survived significantly longer than those who received the free form of E7LP, while all the PBS treated control mice rapidly reached the defined end point (tumor volume > 1cm³) starting at day 20 post-implantation (Fig. 1H). Although overall survival was improved in both vaccinated groups, 5/9 tumors in mice treated with free E7LP did not respond to vaccination and kept growing, and these mice had to be euthanized around day 20, similarly to PBS-treated mice (Fig. 1H and I). In marked contrast, 9/9 NP-E7LP treated mice showed tumor regression after immunization; moreover, in the NP treated group, tumor shrinkage was faster and tumor size remained stable (below 250mm³) for a longer period than in the 4/9 transitory responders to the free-E7LP (Fig. 1I). Among the NP-E7LP treated mice, 3/9 showed a complete response with the disappearance of a palpable mass, and 1/9 was still tumor free at day 137 post-implantation (Fig. 1H and I). No mouse showed a complete response in the free E7LP treated group (Fig. 1I).

To determine whether CD8 and/or CD4 T cells play roles in the effects of nanoparticle vaccination, the NP-E7LP immunization of TC-1 tumor-bearing mice was combined with anti-CD4 or anti-CD8 depleting antibody treatment (or a combination of the two). CD4 depletion did not affect the efficacy of the vaccine, revealing that CD4 T cell help is not required for the enhanced effect of the NP formulation (Fig. S2). On the other hand, CD8 T cell depletion completely abolished the effect of the vaccine, demonstrating that the antitumor immune response elicited with NP-E7LP is dependent on CD8 T cells (Fig. S2). Combined depletion of CD8 and CD4 T cells was similar to CD8 depletion alone, further highlighting the fact that CD4 T cells do not play a role in the antitumor immune response in this context (Fig. S2). Although the E7LP we used contains both a CD4 and a CD8 epitope, in light of the dispensability of the CD4 response for the antitumor effects, we decided to focus our attention solely on CD8 T cell responses.

Our initial experiments were designed to treat well-established solid tumors. Next we vaccinated TC-1 tumor-bearing mice at an earlier time-point, of incipient neoplasia, similarly to what has been reported in a previous study (204), namely day 7 after implantation, when the mean tumor volume was $\sim 22\text{mm}^3$ and 32% of the mice lacked a palpable mass. In this setting both formulations led to some prolonged responses, although the NP vaccine appears slightly superior (Fig S3A and B). As such, immunization of mice with incipient neoplasia may not be fully informative about the effects of therapies aimed at well-established solid tumors, where the relative benefits of the NP formulation is evident.



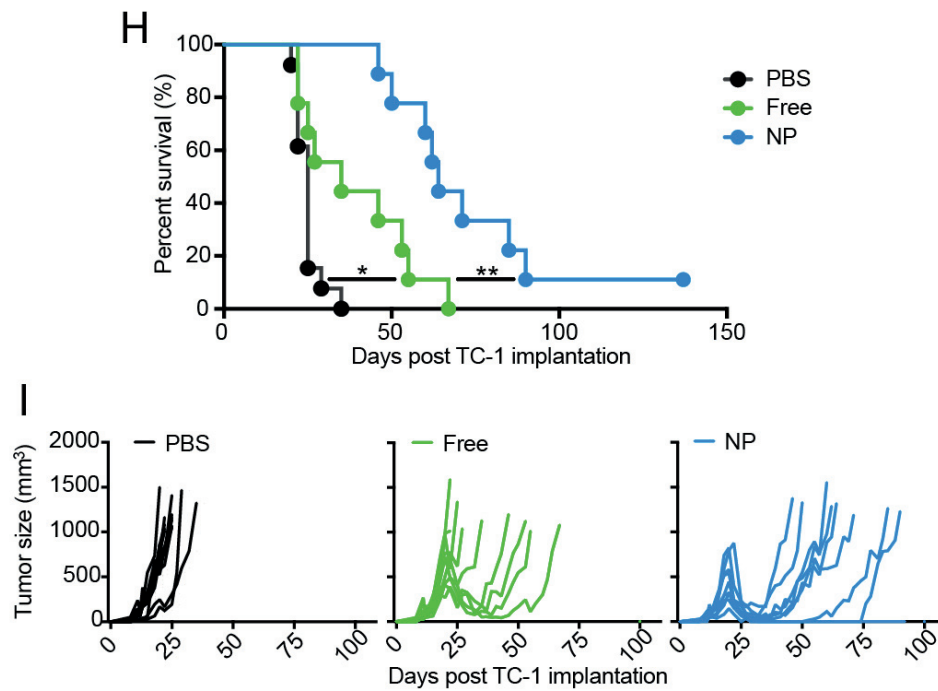


Figure 1. NP-E7LP immunization increases the abundance of systemic E7-specific CD8 T cells producing activation-associated cytokines, and improves survival of tumor-bearing mice. Mice were subcutaneously implanted with TC-1 cells, immunized when mean tumor volume was 100mm³ and sacrificed 9 days later for analyses. (A) Schematic of the experimental layout. (B) Flow cytometry analyses of E7-specific CD8 T cells in the spleen using tetramers recognizing the HPV16 E7 CD8 peptide RAHYNIVTF presented on H2Db. Gating strategy for this population can be found in the Appendix Fig. 1. (C) Representative flow cytometry plots of tetramer staining for E7-specific CD8 T cells gated on single cell live B220-CD3+CD8+ lymphocytes. (D, E, F, G) Flow cytometry analyses of IFN γ , TNF α and GZB production by CD8 T cells after in-vitro re-stimulation with the HPV16 E7 CD8 peptide RAHYNIVTF. Gating strategy for these populations can be found in the Appendix Fig. 3. (H) Survival of subcutaneous TC-1 tumor-bearing mice. (I) Individual TC-1 tumor growth curves. Groups: PBS (B-G n=8, H-I n=13), Free E7LP (B-G n=8, H-I n=9) and NP-E7LP (B-G n=8, H-I n=9). Statistics: * $p < 0.05$; ** $p < 0.01$; *** $p < 0.001$; **** $p < 0.0001$; n.s. = not significant.

2.2.2 Tumors from NP-E7LP treated mice have increased tumor-specific CD8 T cells infiltrates.

We next assessed the abundance of E7 specific CD8 T cells inside the TC-1-derived tumors, and characterized associated effects on the tumor microenvironment, comparing the NP-E7LP with the free E7LP vaccine. Again, using the previously described protocol (Fig 1A), TC-1 tumor-bearing mice were sacrificed 9 days after vaccination. Flow cytometry analyses of the tumors revealed a CD8 T cell response that reflected the systemic responses described above in the spleen. Thus, tumors harvested from mice treated with the NP-E7LP vaccine had significantly higher CD8 T cell infiltrates compared to tumors from free E7LP treated mice as revealed by FACS, while control mice treated with PBS did not have appreciable CD8 T cell infiltrates (Fig. 2A). The fraction of E7-specific CD8 T cells determined by tetramer staining followed the same trend, with NP-E7LP treated mice having significantly more tumor-infiltrating antigen-specific cells than free E7LP treated mice (Fig. 2B). Consistent with these results, immuno-staining of tumor tissue sections from NP-E7LP treated mice with anti-CD8 showed massive infiltrates of CD8 T cells that were distributed throughout the lesion. In contrast, tumors from the free E7LP-treated group contained only scattered CD8 T cell infiltrates, while CD8 T cells were virtually absent in the PBS-treated control groups (Fig. 2C and S5A). To assess the functionality of the tumor-infiltrating E7-specific cells, we performed a re-stimulation assay using disaggregated cells from whole tumors. Intracellular staining for IFN γ , TNF α and GZB revealed that cytokine production by CD8 T cells was barely detectable in tumors derived from PBS and free E7LP-treated mice (Fig. 2D, E and F), whereas mice that received NP-E7LP showed significant production of IFN γ (Fig. 2D), TNF α (Fig. 2E) and GZB (Fig. 2F), underscoring the increased immune activity of the NP-vaccine over the free vaccine formulation.

We next analyzed innate immune cell infiltrates in treated TC-1 tumors 9 days post vaccination. Irrespective of the formulation, vaccination caused a significant increase in intra-tumoral CD11b⁺F4/80⁺ macrophages compared to control PBS treatment (Fig. S4A). Notably, despite the general increase, the subpopulation of “M2-like” CD206⁺ (MRC1⁺) macrophages was significantly lower in both immunized groups (Fig. S4B). Vaccination was also associated with an increase in CD11b⁺HiLy6C⁺Ly6G⁻ monocytes (Fig S4C); there was, however, no significant change in CD11b⁺HiLy6C⁻Ly6G⁺ neutrophils, which were rare in infiltrating TC-1 tumors (Fig. S4D). Although more abundant in treated mice, no significant differences in F4/80-CD11b⁺CD11c⁺ and F4/80-

CD11b-CD11c+ dendritic cells (DCs) were detected between cohorts that received the two vaccines, although the F4/80-CD11b-CD11c+ DCs were significantly increased in the NP-treated group compared to PBS-treated controls (Fig. S4E and F). Thus the NP-E7LP formulation behaved similarly to the free E7LP form in regard to eliciting innate immune infiltration, suggesting that the enhanced efficacy of the NP-E7LP vaccine is predominantly due to a larger influx of tumor-specific and cytokine producing CD8 T cells rather than to specific changes in innate immune cell populations.

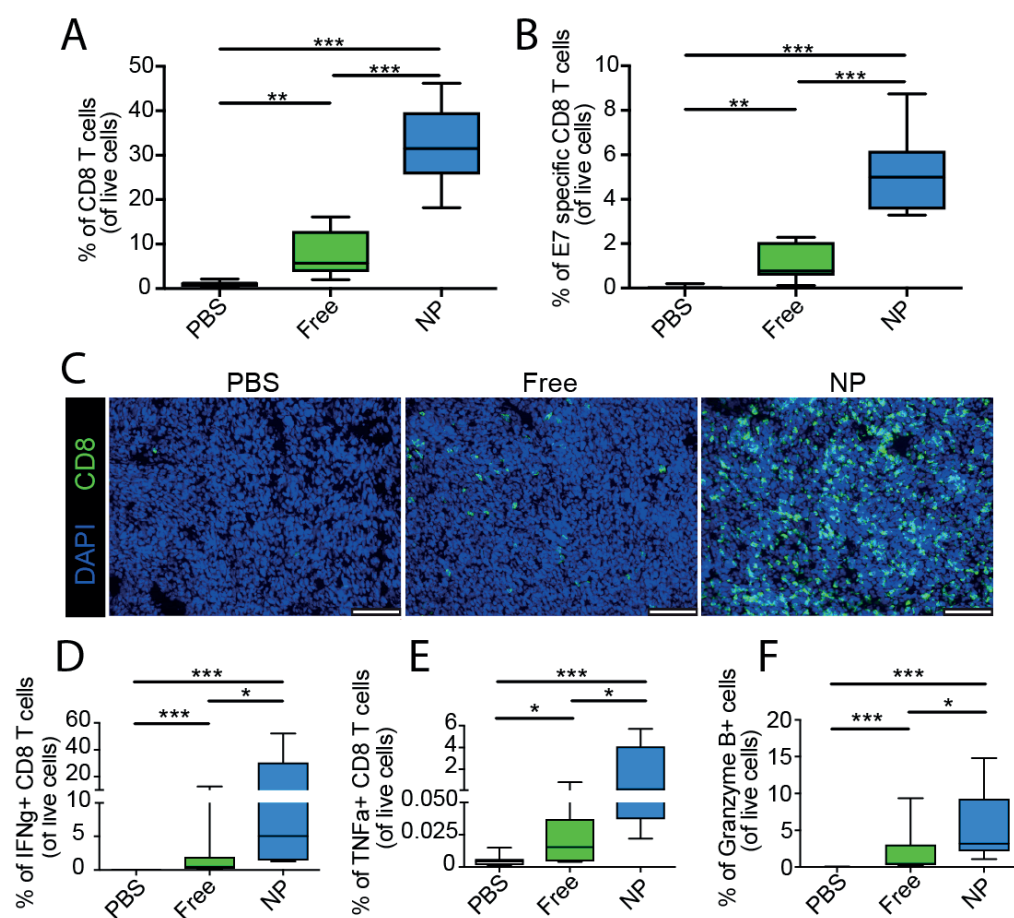


Figure 2. NP-E7LP immunization leads to increased CD8 T cell infiltration and cytokine production in the tumor microenvironment. Mice were subcutaneously implanted with TC-1 cells, immunized when mean tumor volume was 100mm³ and sacrificed 9 days later for flow cytometry analyses (n=8 per group) or embedded in OCT and fresh frozen for sectioning (n=4 per group). Flow cytometry analyses of intra-tumoral (A) CD8 T cells. (Gating strategy for this population can be

*found in the Appendix Fig. 1) and (B) E7-specific CD8 T cells using tetramers recognizing the HPV16 E7 CD8 peptide RAHYNIVTF. (C) Immuno-fluorescent staining for CD8 (green) and nuclei (blue) on 10um sections derived from frozen OCT-embedded tumors, 4 samples per group were stained, analyzed and a representative field of the tissue is shown. Scale bars are 100µm. (D, E, F) Flow cytometry analyses of IFN γ , TNF α and GZB production from CD8 T cells after in-vitro re-stimulation with the HPV16 E7 CD8 peptide RAHYNIVTF. Groups: PBS (n=12), Free E7LP (n=12), NP-E7LP (n=12). Statistics: * $p < 0.05$; ** $p < 0.01$; *** $p < 0.001$; **** $p < 0.0001$; n.s. = not significant.*

2.2.3 NP-E7LP vaccination does not cause an increase in intra-tumoral regulatory T cells and improves the CD8/Treg ratio.

It has been observed that vaccination with SLPs is associated with an increase in regulatory T cells (Tregs) (191, 204) that is even more pronounced in patients bearing larger pre-malignant lesions and typically associated with poorer responses (74). Thus Tregs are suspected to be an obstacle to the achievement of a potent anti-tumor responses (192, 193), and the intra-tumoral CD8/Treg ratio is, in fact, a prognostic factor for HPV+ cancers (190). Given the previously reported ability of nanoparticles to direct antigens towards the intracellular pathway that leads to peptide cross-presentation and loading on MHCI molecules, resulting in strong CD8 responses (199, 201), we reasoned that the use of NP-conjugated vaccines could lead to a relative increase in peptide loading on MHCI molecules that could impact the intra-tumoral CD8/Treg ratio. Therefore, we analyzed Treg cells infiltrating TC-1 tumors by flow cytometry 9 days after immunization of tumor-bearing mice. Vaccination with free E7LP led to a significantly increased abundance in intra-tumoral Tregs compared to the NP-E7LP treated group (Fig. 3A). Tregs were present in NP-E7 vaccinated mice at similar frequencies to the PBS treated control mice (Fig. 3A). In contrast to a previous study performed with TC-1 tumors, where Tregs were reportedly abundant in untreated tumors (205), we detected relatively few Tregs. Consequently, the CD8 to Treg ratio was considerably improved in NP-E7LP treated tumors compared to the free E7LP group (Fig. 3B). Total CD4 T cell infiltrates were unchanged upon vaccination with both formulations and similar to those in PBS treated tumors (Fig. 3C).

These results suggest that vaccination using nanoparticle-bound antigen limited the generation and consequent intra-tumoral accumulation of regulatory T cells following therapeutic vaccination. This effect is likely due to the ability of nanoparticles to direct the delivery of antigens towards the intracellular processing pathway responsible for peptide cross-presentation on MHC class I molecules (199, 201) ultimately favoring a higher intra-tumoral CD8/Treg ratio.

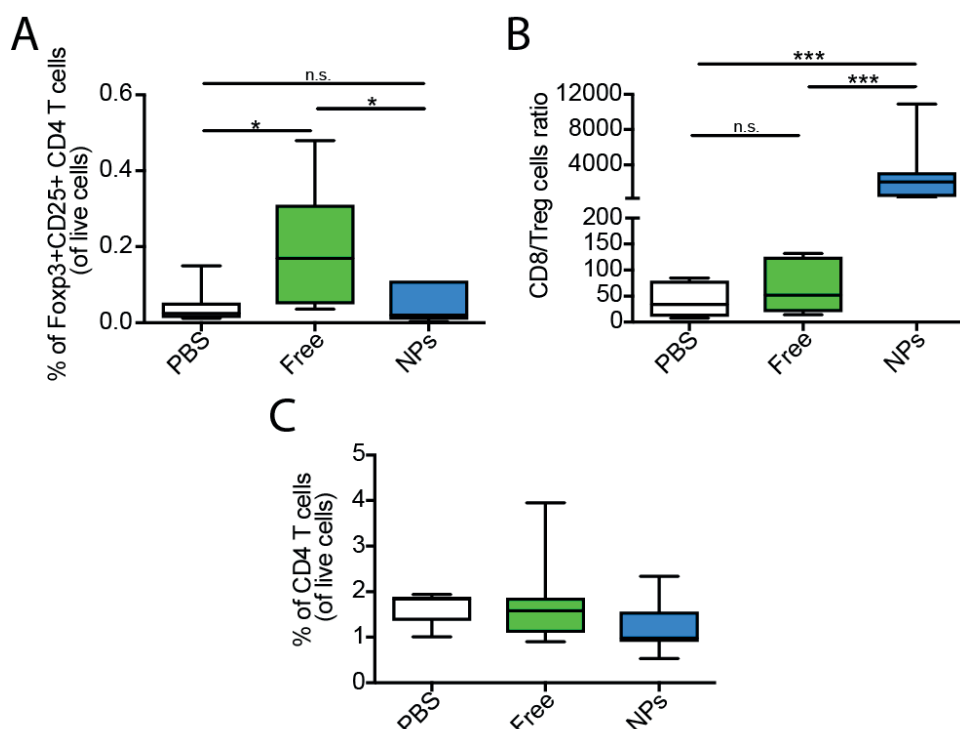


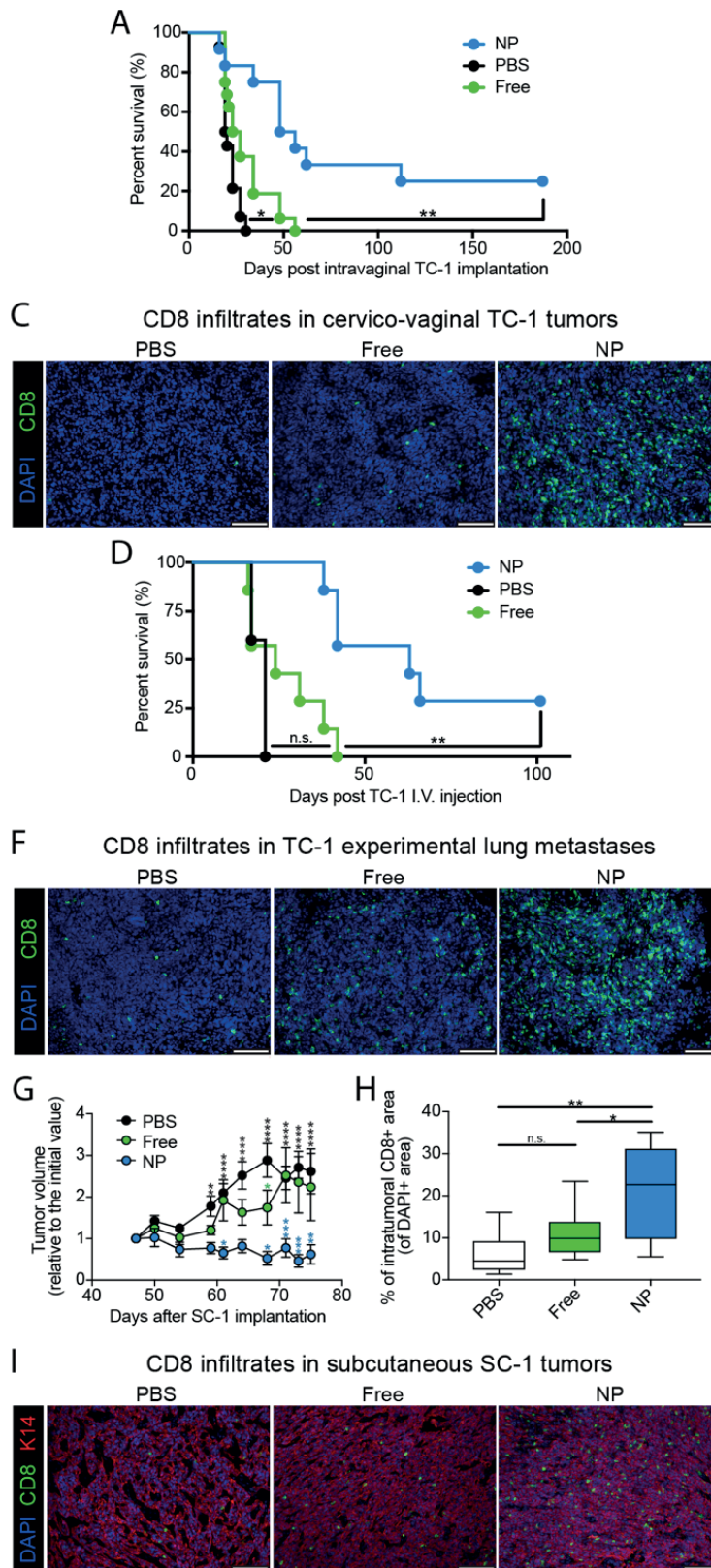
Figure 3. NP conjugation of E7LP prevents the accumulation of intra-tumoral regulatory T cells upon vaccination. Mice were subcutaneously implanted with TC-1 cells, immunized when mean tumor volume was 100mm³ and sacrificed 9 days later for analyses. For flow cytometry analyses, all the cells were gated on single, live cells. (A) Flow cytometry analyses of CD4+Foxp3+CD25+ regulatory T cells in the tumor. Gating strategy for this population can be found in the Appendix Fig. 2. (B) The ratio of CD8+ T cells to CD4+Foxp3+CD25+ regulatory T cells in TC-1 tumors calculated from flow cytometry data. (C) Flow cytometry analyses of total CD4 T cells in the tumor. Gating strategy for this population can be found in the Appendix Fig. 2. Groups: PBS (n=7), Free E7LP (n=7), NP-E7LP (n=7). Statistics: *p < 0.05; **p < 0.01; ***p < 0.001; ****p < 0.0001; n.s. = not significant.

2.2.4 Nanoparticle-conjugation improves the effectiveness of long peptide vaccination against orthotopic cervico-vaginal tumors, experimental lung metastases, and subcutaneous HPV+ squamous cell carcinomas.

Although HPVs can infect skin and mucosal keratinocytes, HPV+ tumors are most frequently found in the cervix (50, 73, 206–209) and, as for many other types of cancers, late stage disease is characterized by metastatic dissemination that typically presents in the lungs (210, 211). Thus, we sought to compare the NP formulation with the classical free long peptide vaccine against TC-1 tumors arising in the cervico-vaginal tract and in lung metastases. Similarly to the subcutaneous tumor model, in order to compare the vaccines in an advanced disease setting, cervico-vaginal TC-1 tumor-bearing mice were immunized at day 14 after implantation, when tumors were well established (Fig 4B). The NP-E7LP vaccination significantly improved the survival of mice bearing orthotopic cervico-vaginal TC-1 tumors compared to the free E7LP with 25% of the mice surviving for more than 150 days (Fig 4A and B). Similarly, when mice bearing well-established TC-1 lung metastases (at day 9 post i.v. inoculation) were treated, (Fig 4D and E), efficacy was improved over the free vaccine, with 28.5% of the mice surviving for more than 100 days after implantation. As expected from the improved survival, tumors and lung metastases collected from NP-E7LP immunized mice 9 days after vaccination showed a marked increase in CD8 T cell infiltrates compared to the Free-E7LP group while PBS treated control showed almost no CD8 infiltrates in either setting (Fig. 4C, F and S5B, C).

The specific cancer type most frequently caused by HPV infection is squamous cell carcinoma (13, 63). Although TC-1 cells are widely used as a model for HPV+ cancer (28–32) it is notable that this cell line was generated by engineering lung epithelial cells to express the E6 and E7 oncogenes and the human c-Ha-Ras oncogene (212). Therefore, to test the efficacy of NP-E7LP immunization in a more representative setting, we employed skin tumor-derived squamous cell carcinoma cells (SC1) that were generated from K14HPV16 H2b transgenic mice that express the HPV16 early genes under the transcriptional control of the keratin 14 promoter (178, 182). SC1 cells were implanted subcutaneously and mice were immunized when mean tumor volume was 100mm³. Vaccination with nanoparticle-bound E7LP led to tumor regression/stabilization while tumors from mice that received either Free-E7LP or PBS kept growing (Fig. 4G). As expected from this observation, NP-E7LP treatment led to a significant increase in intra-tumoral CD8 T cells compared to the other

groups (Fig. 4H and I). These results underscore the superior efficacy of NP-E7LP over the free vaccine in a physiologically relevant disease settings.



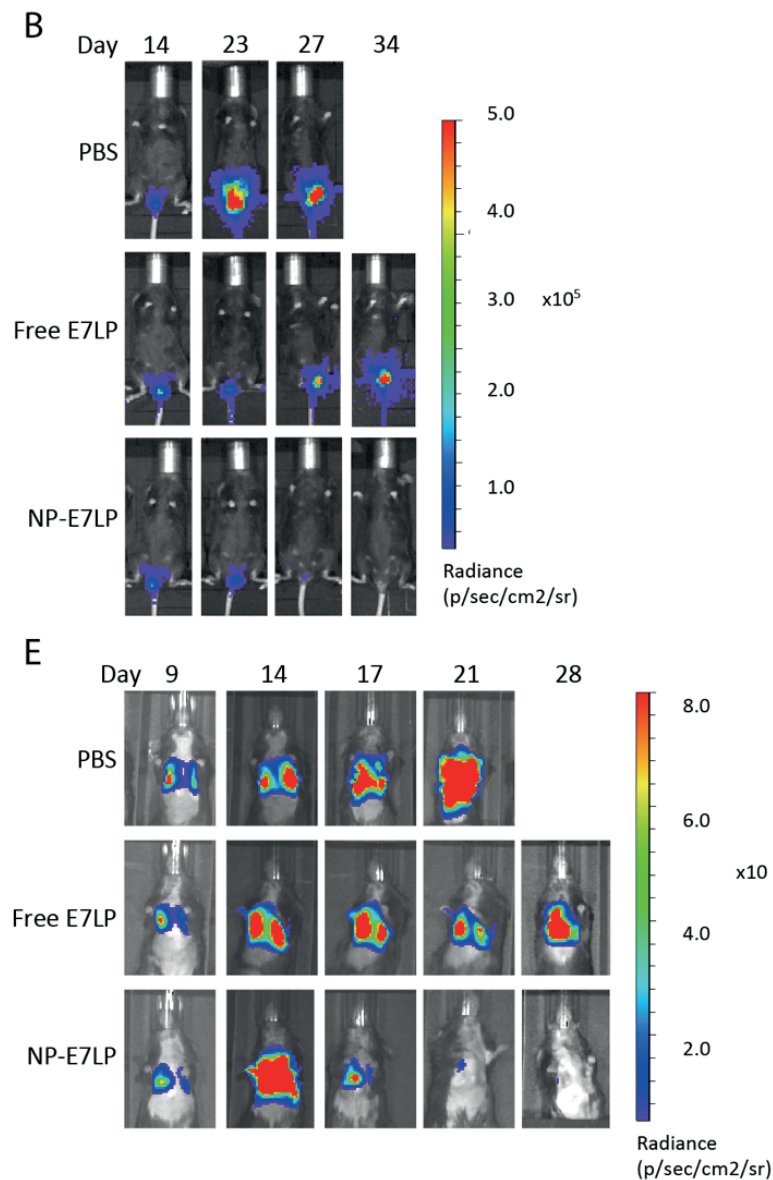


Figure 4. Nanoparticle conjugation improves survival and CD8 T cell infiltration in mice with cervico-vaginal tumors, or lung metastases, or squamous cell carcinomas. (A) Survival of cervico-vaginal TC-1 tumor-bearing mice. (B) Representative bioluminescence images of cervico-vaginal TC-1 tumor-bearing mice at the indicated time-points after cell implantation, with Day14 representing the starting day of the treatment. (C) Immuno-fluorescent staining for CD8 (green) and nuclei (blue) on 10um sections derived from frozen OCT-embedded cervico-vaginal tumors harvested 9 days after immunization, 3 (PBS and NP) or 4 (Free) samples were stained, analyzed and a representative field of the tissue is shown. Scale bars are 100 μ m. (D) Survival of TC-1 lung

metastasis-bearing mice. (E) Representative bioluminescence images of TC-1 lung metastases-bearing mice at the indicated time-points after cell implantation, with Day9 representing the starting day of the treatment. (F) Immuno-fluorescent staining for CD8 (green) and nuclei (blue) of lung metastases derived from 10µm sections of frozen OCT-embedded lungs harvested 9 days after immunization, 4 (PBS) or 8 (Free and NP) samples were stained, analyzed and a representative field of the tissue is shown. Scale bars are 100µm. (G) SC1 tumor growth normalized to the initial size at the time treatment commenced. Black stars refer to PBS vs NP, Green stars refer to Free vs PBS and blue stars refer to NP vs Free. (H) Quantification of intra-tumoral CD8 T cells performed on histological sections. The values are calculated as the percentage of DAPI+ CD8 T cell nuclei area to the total DAPI+ nuclei area inside the keratin 14+ tumor area. (I) Immunofluorescence staining for CD8 (green), keratin 14 (K14, red) and nuclei (blue) on 10µm sections derived from frozen OCT-embedded tumors. Scale bars are 100µm. Cervico-vaginal TC-1 tumors groups: PBS (n=14 + 3 for histology), Free E7LP (n=16 + 4 for histology), NP-E7LP (n=12 + 3 for histology). TC-1 lung metastases groups: PBS (n= 10 + 5 for histology), Free E7LP (n= 7 + 8 for histology), NP-E7LP (n= 7 + 8 for histology). SC1 tumors groups: PBS (n=9), Free E7LP (n=9), NP-E7LP (n=9). Statistics: * $p < 0.05$; ** $p < 0.01$; *** $p < 0.001$; **** $p < 0.0001$; n.s. = not significant.

2.2.5 Efficacy-associated changes in the tumor microenvironment are progressively lost upon disease stabilization and relapse.

Despite the increase in systemic and local immune responses obtainable using NP-E7LP, most of the subcutaneous TC-1 tumors eventually relapsed to progressive tumor growth after an initial phase of tumor shrinkage (response) that was followed by an intermediate phase where the tumor size remained relatively stable for a period ranging from 10 to 50 days, (Fig. 1I). These phases are reminiscent of the three phases in anti-tumor immunity described in a series of landmark publications by Schreiber and colleagues (213). In light of this observation, we sought to characterize the changes in the TME that are associated with these three phases (Fig S6B) in mice that received the NP-E7LP vaccine.

We first analyzed expression of the E7 oncogene, potential mutation of the E7-derived CD8 peptide, and expression of several components of the antigen processing and presentation

machinery, comparing responding tumors to relapsed ones. We found no significant change that could explain a loss of response towards the tumor cells (Fig. S6A).

We then examined the T cells in the tumor microenvironment, and found that CD8 T cell infiltration progressively decreased after the response phase (Fig 5 and S7A). CD8 T cell activity, as indicated by ICOS staining, was high in the response phases but was already lost in the stable disease phase (Fig 5 and S7B). Interestingly, there was no increase in the expression of the exhaustion markers PD-1, Lag3 and Tim3 in the relapse phase compared to the response phase (data not shown). The data suggest that tumor relapse might be consequent to a loss of CD8 T cell activity, as suggested by the loss of ICOS staining in the TME, and not by exhaustion of CD8 T cells.

Macrophages were present in the TME at all stages, although the expression of F4/80 appeared to be upregulated in responding and stable tumors (Fig. 5, S7C and S8). The DC- and M1-macrophage marker CD11c (214) was absent in PBS treated tumor sections but present throughout sections of response-phase tumors, and then progressively lost during progression to stable disease and then relapse phase tumors (Fig. 5 , S7D and S8). Staining for the M2 macrophage marker MRC1 (CD206) (214) was conversely increased in untreated and relapsed tumors (Fig. 5, S7E and S8). These data indicate that the abundance of DCs and the abundance and phenotype of macrophage changes concordant with CD8 T cell activity. Notably it has previously been reported that macrophages are modulated by the activity of CD8 T cells and required for the antitumor response against TC-1 tumors elicited by vaccination (172). As such, it seems likely that the DC and macrophage dynamics in the stable disease and relapse phases are consequent to the loss of CD8 T cells and their activity.

Immune escape has previously been linked to increased PD-L1 expression in the tumor microenvironment that serves to suppress antitumor T cell responses (215, 216). In marked contrast, our analysis revealed that PD-L1 was upregulated in the response phase where activated CTLs are abundant, likely induced by CD8 T cell-secreted IFN γ , whereas it was virtually absent in untreated tumors and in the stable disease and relapse phase tumors (Fig. 5 and S7F), seemingly ruling it out PD-L1 expression as a primary mechanism responsible for the progressive loss of CD8 T cells. Interestingly, PD-L1 was prominently expressed in vascular structures while remaining comparatively low on other cells in the tumor microenvironment.

Consistent with results obtained by others showing that checkpoint inhibitors have poor efficacy in this model (204), the addition to the NP-E7LP vaccine of a combination of anti-PD1, anti-Tim3 and anti-Lag3 had no benefit on tumor growth and mice survival (data not shown).

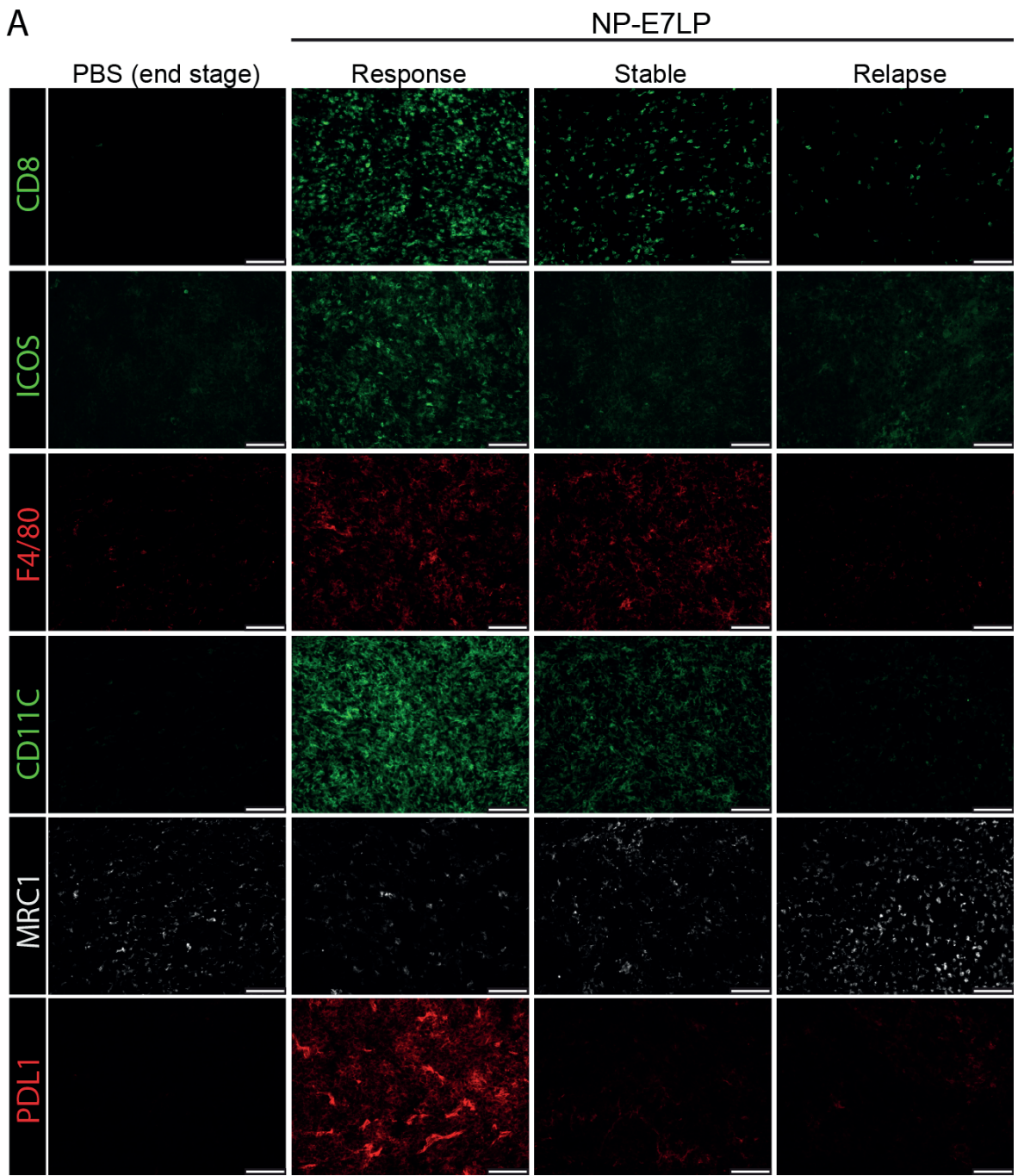


Figure 5. Analyses of the tumor microenvironment at different stages of disease progression. Immuno-fluorescent staining for CD8, ICOS, F4/80, CD11c, MRC1 and PDL1 on 10um sections derived from frozen OCT-embedded tumors collected at the indicated time-points as in Fig S6B. PBS treated tumors were collected at the same time after TC-1 cells implantation as tumors in the response phase; at this timepoint, PBS treated tumor were already at the endpoint. Scale bars are 100µm. Groups: PBS (n=2), NP-E7LP response (n=4), NP-E7LP stable (n=4) and NP-E7LP relapse (n=4).

2.2.6 NP-E7LP synergizes with agonistic anti-41BB/CD137 to further boost tumor rejection.

It has been previously reported that early immunization with a traditional free long peptide vaccine of mice bearing incipient TC-1 tumors led to remarkable responses when given in combination with an agonistic anti-41BB antibody that activates the CD137 co-stimulatory receptor on T cells (204). In light of this result and the evident loss of CD8 T cell activity in the stable disease and relapse phases (Fig. 5 and S7B), we sought to comparatively evaluate the effects of anti-41BB in the context of both vaccines. To better evaluate the potential benefit of this agonistic antibody we pushed the model further, by treating larger later-stage tumors that are poorly responsive to immunization with free-E7LP alone. Thus, we subcutaneously inoculated 0.5×10^6 TC-1 cells and immunized TC-1 tumor-bearing mice when mean the tumor volume was around 170mm³. Mice treated with free-E7LP reached the end point within 3 weeks after implantation TC-1 cells, while, as in previous experiments, all the mice treated with the NP-E7LP formulation survived significantly longer (Fig. 6A and B). Anti-41BB significantly improved survival in combination with both vaccine formulations (Fig. 6A and B). Notably, the efficacy of free-E7LP+anti-41BB was comparable to that of NP-E7LP alone, to which the inclusion of anti-41BB also added benefit, further improving therapeutic efficacy.

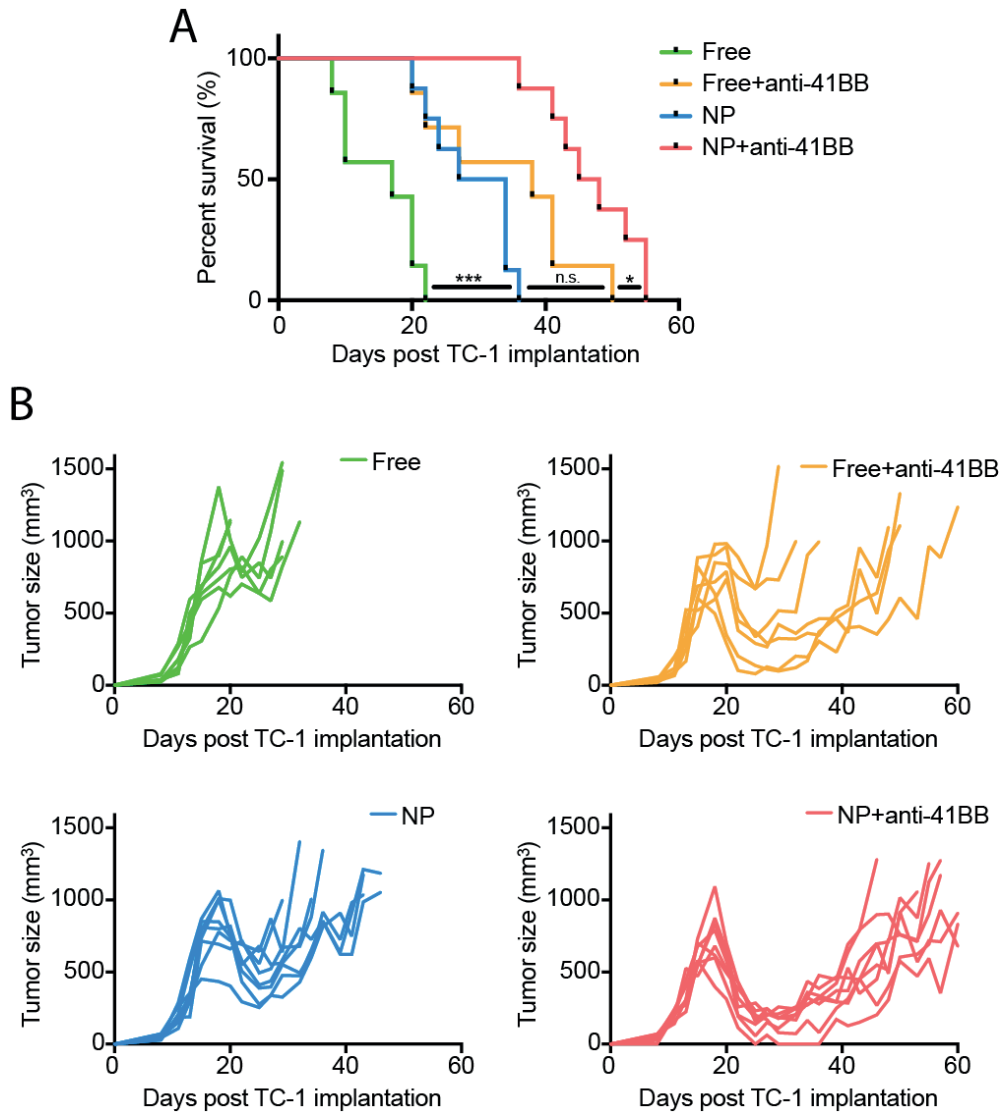


Figure 6. Therapeutic vaccination in combination with the agonistic antibody anti-41BB. 0.5×10^6 TC-1 cells were implanted into the flank of the mice at day 0. Mice were immunized when mean tumor volume was 170 mm^3 and monitored for survival and tumor growth. Selected groups also received 3 doses of anti-41BB I.P. every 3 days starting the day of immunization. (A) Survival of subcutaneous TC-1 tumor-bearing mice; NP vs Free $p=0.0007$, NP vs Free+41BB $p=0.0855$, NP vs NP+41BB $p=0.0001$, NP+41BB vs Free+41BB $p=0.0260$, Free vs Free+41BB $p=0.0016$. (B) Individual TC-1 tumor growth curves. Groups: Free E7LP ($n=7$), NP-E7LP ($n=8$), Free E7LP+anti-41BB ($n=7$) and NP-E7LP+anti41BB ($n=8$).

Statistics: * $p < 0.05$; ** $p < 0.01$; *** $p < 0.001$; **** $p < 0.0001$; n.s. = not significant.

2.3 Discussion

Recognizing the recent success of immunotherapies using immune checkpoint-blocking antibodies, therapeutic vaccination remains an attractive strategy to direct the immune system against specific cancer-associated antigens in solid tumors. Anti-cancer vaccines can be used to provide a further boost of the patient's own antitumor immune response or to wake up the immune system in those patients that do not show a spontaneous antitumor response. CD8 T cells play a fundamental role in tumor rejection, and thus generation of a strong CD8 response is the primary goal of therapeutic vaccines. Cervical cancer and other HPV-induced malignancies should be prototypes for immunotherapy in general and therapeutic vaccines in particular, given that the viral oncogenes encode neo-antigenic oncoproteins that drive the disease. In patients with HPV+ tumors, however, generating therapeutically efficacious CTL responses has proven difficult to achieve in the majority of patients with classical vaccination strategies involving peptide/protein vaccines (67), including recent studies utilizing HPV E7-derived synthetic long peptides. SLP vaccine formulations have typically elicited a robust Th1 CD4 response, whereas the CD8 response was usually weak (74, 75, 186, 189). Notably, E7 SLPs have proven to be effective in a fraction of patients bearing early pre-malignant HPV+ lesions (intra-epithelial neoplasias), whereas efficacy against bona fide malignancies has been very limited (74, 166), underlining the need for better therapeutic approaches.

Herein we show that by conjugating an E7-derived SLP to synthetic ultra-small (30 nm) nanoparticles, it is possible to significantly boost the CD8 T cell response following immunization (3-16 -fold), consistent with the previously reported (194, 195, 199–201) ability of NPs to enhance MHC-I antigen-presentation by efficient delivery of their antigenic payload to cross-presenting DCs. The NP-E7LP vaccine formulation was capable, in comparison to the non-NP-conjugated free-E7LP, of eliciting a stronger systemic immune response characterized by a larger pool of E7-specific CD8 T cells producing activation-associated cytokines and GZB, as measured in the spleen of tumor-bearing mice after immunization.

The NP-E7LP vaccine induced greater infiltration of tumors by CD8 T cells in both subcutaneous and cervico-vaginal TC-1 tumors as well as in TC-1 derived lung metastases, in comparison to the

free E7LP. The results highlight the ability of the NP-generated CD8 T cells to efficiently reach different anatomical locations and perform their effector function. Therapeutic vaccination with NP-E7LP in TC-1 tumor-bearing mice bearing well-established solid tumors led to tumor shrinkage in 100% of the treated animals and was able to significantly increase their lifespan. In contrast, in this disease setting, free-E7LP produced a response only in about 50% of the mice. Notably, the NP-vaccine was able to provide long-term survival in 25% and 28.5% of the mice with orthotopic TC-1 tumors or experimental lung metastases respectively, while all of the mice treated with the free E7 long peptide rapidly succumbed to the disease. Similar results were observed in mice bearing subcutaneous HPV16+ squamous cell carcinomas, extending the comparative benefits to the histologic tumor type caused by HPV infection. Thus, in SC1 tumor-bearing mice, NP-E7LP immunization led to higher intra-tumoral CD8 T cell infiltrates compared to the classical free E7LP, resulting in tumor regression/stabilization in contrast to the free E7LP vaccine, which was completely ineffective in this setting.

These data clearly demonstrate that NP-conjugation can markedly improve upon the capability of SLPs to induce tumor-antigen-specific CD8 T cells in sufficient quantity and activity to produce substantive regressions of well-established solid tumors, leading in some cases to appreciable survival benefit.

Promising results have also been reported for other distinct vaccines delivery platforms based on larger particles (217, 218) and lymph node targeting vaccines, either alone (196) or in complex combinatorial strategies (219). Interestingly, compared to elaborate therapeutic combinations (219), we showed that a relatively simple approach, solely based on conjugation of the antigenic SLPs to a nanoparticle-based delivery system and administration of a single dose of NP vaccine, is enough to prompt significant benefits in terms of magnitude of the antitumor response, leading to therapeutic benefits in mouse models that were not achievable with a traditional “liquid” unconjugated formulation.

Collectively, the results from the present study and other reports clearly demonstrate that a variety of solid-phase and lymph-node targeting systems have considerable potential to improve the generation of immune responses following therapeutic vaccination. It will be auspicious in

future studies to compare these distinctive antigen delivery systems head-to-head in the same experimental setting, in order to rigorously assess their relative benefits.

We have in particular confirmed the results of a previous study describing the potential of combining therapeutic vaccination with anti-41BB (204), strengthening the proof of concept for a synergistic effect between agonistic antibodies and lymph-node targeting solid-phase delivery systems. Data obtained in patients (111) and data generated in our lab using a transgenic HPV16 mouse model (data not shown) suggest that successful treatment of advanced HPV+ cancers will require complex combinatorial approaches aimed at both eliciting strong CD8 T cell responses and at eliminating HPV-related immunosuppressive barriers. As a first step, we suggest that combinations of novel antigen-delivery platforms, such as the NPs described herein, with agonistic antibodies, such as the aforementioned anti-41BB, could represent a solid basis on which to build future treatment strategies for HPV+ cancer patients.

Interestingly, the beneficial effects of conjugation to our NP platform seem to extend beyond more efficient generation of CD8 T cells. A recognized limitation of therapeutic vaccines based on SLPs is the concomitant generation of regulatory T cells (Tregs) in response to the immunization (191, 204), an undesirable response that has also been observed in HPV+ cancer patients treated with therapeutic SLP vaccines, particularly those with larger/advanced lesions (74). Consistent with this observation, we observed that immunization of mice bearing well-established tumors with free-E7LP was associated with an increase in tumor-infiltrating Tregs that resulted in a low CD8/Treg ratio. In notable contrast, immunization with the NP-E7LP did not cause changes in intra-tumoral Treg infiltrates, resulting in a much higher CD8/Treg ratio. These observations suggest that, by means of NP conjugation, it may be possible to restrict the generation of Tregs and thereby helping circumvent one of the limitations of SLP vaccines.

Despite the substantial increase in both systemic and local anti-tumor immune responses achievable with the NP-vaccine in the various models studied herein, we observed that most tumors eventually relapsed. Tumor shrinkage was followed by a relatively long stable-disease phase that lasted up to 50 days in subcutaneously transplanted mice, followed by relapse to progressive tumor growth. Our data indicate that the relapse is not due to a loss of antigen

presentation by tumor cells, but it is associated with a reduction of intra-tumoral CD8 T cells and possibly a loss of their activity. These changes are evidently not caused by the presence of immunosuppressive M2 macrophages or by expression of the inhibitory molecule PD-L1. Future studies will be focused on understanding the mechanism underlying the loss of CD8 T cells that evidently leads to tumor relapse, knowledge which may present new combinatorial strategies for sustaining tumor immunity and preventing relapse. Importantly, we envisage that the treatment regimen with NP-bound SLP described herein could be used as a model in which to study changes associated with immunoediting (213) as well as strategies to re-activate the immune response during the stable disease/equilibrium phase, which could be relevant for cancer patients treated with immunotherapies.

In conclusion, our data illustrate the potential for this and generally for other nanoparticle-based lymph-node targeting platforms (196, 217–220) or, in general, for solid-phase vaccines (221) to serve as effective delivery vehicles to boost the efficacy of neo-antigen-based therapeutic vaccines in patients, most obviously to target HPV+ cancers with the well-validated E7LPs, but potentially also other cancers for which stimulatory neo-antigens have been identified (222). It can be envisaged that the use of antigenic peptides coupled with such systems will enhance many immunotherapeutic vaccine strategies for solid tumors - single or combinatorial - involving SLPs.

2.4 Materials and methods

Immunization. Mice were immunized with a total amount of 15 µg of E7LP as free peptide or in the NP-bound formulation, and 20 µg (subcutaneous TC-1 tumors experiment) or 40µg (intravaginal tumors, lung metastases and SC1 experiments) of CpG was used as adjuvant. For the free E7LP vaccine, the long peptide was first dissolved in DMSO and then diluted in PBS prior to immunization. Control mice were treated with PBS. Groups were assigned by randomizing the mice according to the tumor volume or to the bioluminescence signal to ensure a similar size distribution. All the mice from one experiment were immunized together on the same day. All tumor-bearing mice were immunized once. Subcutaneous (s.c.) immunizations of mice were performed in the four limbs using the Hock method (223). S.c. TC-1 tumor-bearing mice were

immunized when mean tumor size was around 100 mm³ (usually at day 10-12 after implantation) unless otherwise stated. Cervico-vaginal tumor-bearing mice were immunized s.c. in the back near the tail. S.c. SC1 tumor-bearing FVB H2b mice were immunized once, 3 weeks after tumor implantation when the mean tumor size reached 100 mm³.

Mice, Tumor Cells and Antibody Treatments. For all TC-1 implantation experiments, C57BL/6NCrl mice were used. C57BL/6NCrl mice (aged 6-8 weeks) were purchased from Charles River and kept under pathogen-free conditions at the animal facility of Ecole Polytechnique Fédérale de Lausanne (or at the animal facility of the Centre Hospitalier Universitaire Vaudois for the cervico-vaginal experiment). All experiments were performed in accordance with Swiss law and with approval of the Cantonal Veterinary Office of Canton de Vaud, Switzerland.

For the subcutaneous (s.c.) model, TC-1 cells (kindly provided by Prof TC Wu, Johns Hopkins University) were cultured in DMEM medium (Gibco), 10% FBS (Gibco), P/S (100Units/ml penicillin, 100 µg/ml streptomycin; Gibco), and were implanted subcutaneously on the flank of C57BL/6NCrl mice with inoculations of 500'000 cells in 100 µl HBBS. Tumor growth was measured with a caliper using the formula $V = W^2 L \pi / 6$ and mice were sacrificed when tumor size reached 1000 mm³.

For the cervico-vaginal tumor model, tumors were induced as described in (174). Briefly anesthetized diestrus-synchronized female mice were pre-treated with 4% nonoxynol-9 (Abcam) for 6h, and were then intra-vaginally implanted with 50'000 TC-1 cells engineered to express a luciferase reporter gene (TC-1-Luc). Tumor growth was monitored by bio-luminescence index (BLI) using the Xenogen imaging system after intraperitoneal injection of 50 mg/kg D-luciferin (PerkinElmer) in PBS. Mice were sacrificed when interruption criteria defined in the animal license were reached.

For the lung metastasis model, 500'000 TC-1-Luc were re-suspended in 100 µl of PBS and injected into the tail vein of female mice. Lung metastases were monitored by BLI after intraperitoneal injection of 50 mg/kg D-luciferin (PerkinElmer) in PBS. Images were acquired using a Photon Imager (IVIS Spectrum) system and data analyzed with the provided software (IVIS). Mice were imaged twice a week, and were sacrificed when interruption criteria defined in the animal license were reached.

SC1 cells were generated from a squamous cell carcinoma of the skin of a K14HPV16/H2b mouse (182). The K14HPV16/H2b line was generated by crossing K14HPV16/FVB/n (H2q) mice (179, 180,

224) with C57BL/6 (H2b) mice to introduce the H2b locus. F1 mice were backcrossed for 11 generations to FVB/n, selecting for the H2b locus in every generation. This genetic configuration allows K14HPV16/H2b mice to present E7-derived peptides on MHCI molecules whilst maintaining the FVB/n background that is permissive for squamous carcinogenesis. SC1 cells were cultured in DMEM medium (Gibco), 10% FBS (Gibco), P/S (100 Units/ml penicillin, 100 µg/ml streptomycin; Gibco), and 1'000'000 SC1 cells resuspended in 100 µl HBBS/matrigel (1:1 solution) were implanted s.c. on the flank of FVB H2b mice. Tumor growth was measured with a caliper using the formula $V = W^2L\pi/6$.

For CD4 and CD8 T cell depletion, TC-1 tumor-bearing mice received intra-peritoneal (i.p.) injections every 4 days of 10 mg/kg aCD4 (clone GK1.5, BioXcell) and/or 10 mg/kg aCD8 antibody (clone 53-6.7, BioXcell). Antibody treatment started 3 days before vaccination and was continued for 3 weeks. CD4 and CD8 T cell depletion was monitored weekly by flow cytometry analyses on the blood. Mice with less than 95% depletion were excluded from the analyses.

For the anti-41BB treatment, mice received 3 doses of 350 µg of anti-41BB (clone LOB12.3, BioXcell) I.P. every 3 days starting at day 12 together with the vaccine. No toxicity was detected based on mortality and body weight.

Reagents. CpG-B 1826 oligonucleotide (5'-TCCATGAGCTTCCTGACGTT-3' as phosphorothioated DNA bases) was purchased from Microsynth and used as adjuvant in both vaccine formulations. HPV16 E7 long peptide (aa 43-77, purity>90%) was purchased from Think Peptides and the Protein and Peptide Chemistry Facility, UNIL and used for NP conjugation and immunization. HPV16 E7 CD8 peptide RAHYNIVTF was purchased from Think Peptides and used for re-stimulation.

Nanoparticle (NP) synthesis and Conjugation. NPs were synthesized, functionalized and characterized as previously described (199, 201, 225). For antigen conjugation, HPV16 E7 long peptide was dissolved in DMSO and incubated for 12h in endotoxin-free water in the presence of NPs and guanidine hydrochloride (AppliChem) at room temperature. NP-E7LP was purified by size-exclusion chromatography using CL-6B matrix (Sigma-Aldrich), eluted and stored in PBS at room temperature. The size of NP before and after conjugation was determined by dynamic light scattering and remained around 30 nm. E7LP loading on the nanoparticles was measured by BCA

assay (Thermo Fisher Scientific). NPs alone have been shown to have no adjuvant activity (226, 227).

Cell preparation for flow cytometry and antigen-specific in-vitro re-stimulation. Spleens were harvested and gently disrupted through a 40- μ m filter (Fisher Scientific). Red blood cells were lysed using ACK lysis buffer, and cells were filtered again through a 40- μ m filter before use. Tumors were harvested and minced using a scalpel and digested for 45 min using collagenase A (0.33 U/ml, Roche), dispase (0.85 U/ml, Roche), DNaseI (144 U/ml, Roche) in RPMI medium with intermittent shaking at 37°C. For CD8 T cell antigen-specific re-stimulation, cell suspensions from either spleen or tumor were cultured at 37°C for 6h in a 96 well plate in the presence of 1 μ g/ml of the HPV16 CD8 peptide RAHYNIVTF. After the first 3h of culture, brefeldin A (Sigma-Aldrich) was added to a final concentration of 5 μ g/ml. All the cells were cultured in IMDM medium (Gibco) supplemented with 10% FBS (Gibco) and 1x penicillin/streptomycin (100 Units/ml penicillin, 100 μ g/ml streptomycin; Gibco).

Flow cytometry. For surface staining and blocking, cells were incubated for 15min on ice with the antibodies diluted in PBS 2% FBS. Before tetramer and antibody staining, all cell suspensions from tumor or spleen were blocked with anti CD16/32 (BioLegend). Cells were then labeled with fixable live/dead cell viability reagent (Invitrogen) diluted in PBS for 15 min on ice. Staining with a tetramer recognizing HPV16 E7 peptide 49-57 presented by H2Db (University of Lausanne, UNIL) was performed before antibody staining for 30 min at room temperature. If no intracellular staining was performed after surface staining, cells were fixed with 2% PFA in PBS for 15 min on ice. For intracellular staining, cells were permeabilized and fixed with the Foxp3/Transcription Factor Staining Buffer Set Kit (eBioscience) following the manufacturer instructions and then incubated overnight with the antibodies diluted in 1x Permeabilization buffer provided with the aforementioned kit. After staining, cells were washed and re-suspended in PBS 2% FBS for analyses. Samples were acquired on a Gallios analyzer (Beckman Coulter) and data were analyzed using FlowJo software (Tree Star Inc.). Antibodies used for flow cytometry: CD3 (clone 145-2C11, ThermoFisher), CD4 (clone RM4-5, BioLegend), CD8a (clone 5H10, ThermoFisher), B220 (clone RA3-6B2, ThermoFisher), IFN γ (clone XMG1.2, BioLegend), TNF α (clone MP6-XT22, ThermoFisher), GZB (clone NGZB, ThermoFisher), Foxp3 (clone FJK-16s, ThermoFisher), CD25 (clone PC61.5,

ThermoFisher), CD45 (30-F11, ThermoFisher), CD11b (clone M1/70, ThermoFisher), CD11c (clone N418, BioLegend), Ly6G (clone 1A8, BioLegend), Ly6C (clone HK1.4, ThermoFisher), CD206 (clone C068C2, BioLegend), MHCII (clone M5/114.15.2, BioLegend).

Immunofluorescence staining. Tumors were harvested, embedded in OCT (Sakura) and fresh frozen on dry ice. 10µm thick sections were cut from OCT-embedded tumors using a cryostat and collected on Superfrost Plus glass slides (Thermo Scientific). Tissue sections and OCT embedded tumors were stored at -80°C. For immunofluorescence staining, sections were fixed in ice-cold methanol (Fisher Scientific) for 10min before proceeding. Slides were washed with PBS to remove the remaining OCT and then blocked for 45min at room temperature with PBS + 5% BSA + 2.5% FBS and then stained with primary antibodies diluted in PBS + 1% BSA overnight at 4° in a humidified chamber. On the following day, slides were washed with PBS and stained with secondary antibodies diluted in PBS + 1% BSA for 1h at room temperature. Before mounting, slides were washed again in PBS and then covered with mounting media (Dako) containing DAPI (Roche, 5µg/ml). Coverslips (Menzel Glaser) were applied to the slides and sealed using nail polish. Images were acquired using a Leica DM5500B and processed using Fiji (ImageJ). Antibodies used for immunofluorescence staining: CD8 (clone 53-6.7, eBioscience), keratin 14 (clone poly19053, BioLegend), ICOS (clone 7E.17G9, BD Biosciences), F4/80-PE (clone BM8, eBioscience), CD11c-FITC (clone N418, BioLegend), MRC1-Alexa fluor 647 (clone C068C2, BioLegend), PD-L1-PE (MIH5, eBioscience).

RNA extraction and real time PCR. RNA from tumor tissue was isolated with the miRNeasy kit (Qiagen) and 1 µg of total RNA was subjected to cDNA synthesis using the iScript cDNA synthesis kit (BioRad). Real time PCR was conducted using the Rotor Gene SYBR green PCR kit (Qiagen) with 25 ng of cDNA on a Rotor Gene Q instrument (Qiagen) and the following primers (Microsynth, Switzerland):

E7-fwd: CAGCTCAGAGGAGGAGGATG,	E7-rev: GCCCATTAACAGGTCTTCCA,
H2Db-fwd: AGTGGTGCTGCAGAGCATTACAA,	H2Db-rev: GGTGACTTCACCTTTAGATCTGGG,
B2M-fwd: TTCTGGTGCTTGTCTCACTGA,	B2M-rev: CAGTATGTTCGGCTTCCCATTC,
TAP1-fwd: GGACTTGCCTTGTTCGAGAG,	TAP1-rev: GCTGCCACATAACTGATAGCGA,
Psmb5-fwd: GAGCCGCGAATCGAAATGC,	Psmb5-rev: ATCCGCTGCAACAATGACTCC,

RPL13a-fwd: CTGTGAAGGCATCAACATTTCTG, RPL13a-rev: GACCACCATCCGCTTTTCTT.

The relative amount of cDNA was calculated with the $\Delta\Delta C_T$ method using *RPL13a* as the reference gene and the TC-1 tumor sample as calibrator.

DNA sequencing. cDNA from TC-1 tumors was amplified with the E7-specific primers ATGCATGGAGATACACCTAC and ATTATGGTTTCTGAGAACAGA by Platinum Taq polymerase (Invitrogen) and cloned into pSC-A employing the StrataClone PCR cloning kit (Agilent Technologies). The insert containing the HPV16 E7 gene sequence was evaluated by Sanger sequencing using the T3 primer: TTAACCCTCACTAAAGG (Microsynth, Switzerland).

Statistical analyses. Statistical analyses were performed in GraphPad Prism 7. Flow cytometry data and CD8 T cells quantification by histology on SC1 tumors were compared using t test. Survival curves were compared using Log-rank (Mantel-Cox) Test. Normalized growth curves of SC1 tumors were compared using 2-way anova.

Acknowledgements. We thank B. Torchia for technical support; Dr. R. Guet and the bioimaging and optics platform (BIOP) core facility at EPFL for developing image analyses tools; Professor T.C. Wu from Johns Hopkins University for providing TC-1 cells; and Professor Daniel E. Speiser and Professor Pedro Romero for comments.

2.5 Important notes

Data presented in chapter 2 are part of a manuscript entitled: “Nanoparticle conjugation of human papillomavirus 16 E7-long peptides enhances therapeutic vaccination efficacy against well-established solid tumors in mice” that is, at the moment of writing, under review for publication in Cancer Immunology Research.

Authors: Gabriele Galliverti, Mélanie Tichet, Sonia Domingos-Pereira, Sylvie Hauert, Denise Nardelli-Haeffliger, Melody Swartz, Douglas Hanahan and Stephan Wullschlegel.

Authors contribution: G.G., M.A.S, D.H. and S.W. designed research; G.G., M.T., S.D.P. and S.W. performed research; G.G. and S.H. produced the nanoparticles (NPs); G.G. analyzed data; D.N.H., M.A.S., D.H. and S.W. directed the project and G.G. and D.H. wrote the manuscript.

2.6 Supplementary information

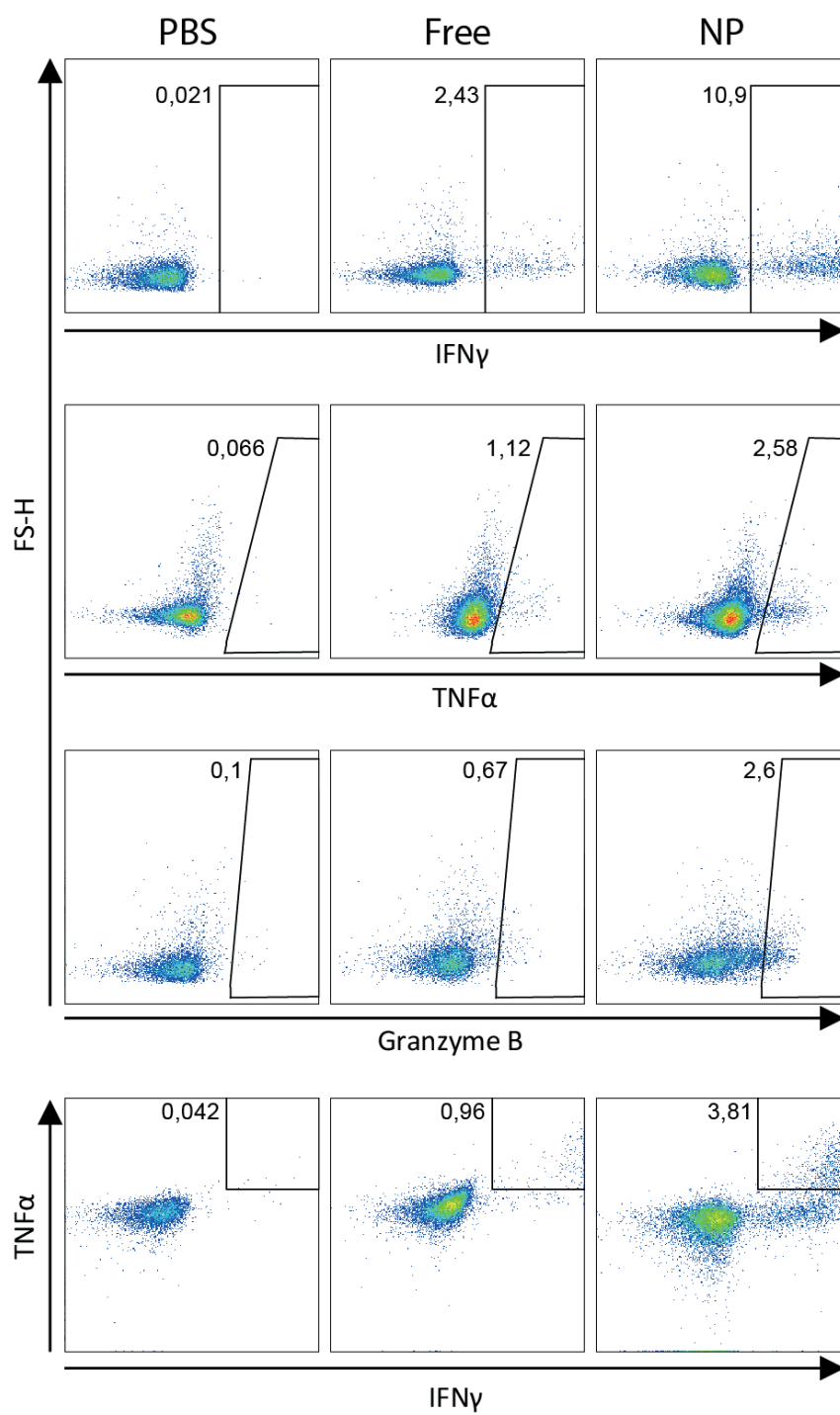


Figure S1. Representative flow cytometry plots of IFN γ +, TNF α +, GZB+ and double positive TNF α +IFN γ + CD8 T cells after in-vitro re-stimulation. Populations are gated on single cell live CD3+CD8+ lymphocytes. 0.5x10⁶ TC-1 cells were implanted into the flank of the mice at day 0. The vaccine and the control treatments were administered at day 12 when the mean tumor size was ~100 mm³. Mice received subcutaneous injections of PBS (n=8), or 15 μ g of E7LP either in a free form (free E7LP, n=8) or conjugated to NPs (NP-E7LP, n=8); both vaccinated groups also received 20 μ g of CpG as adjuvant. Mice were sacrificed 9 days after immunization and spleens were harvested for analyses. Whole splenocytes were re-stimulated in vitro with the HPV16 E7 CD8 peptide RAHYNIVTF and intracellular staining for IFN γ , TNF α and GZB was performed.

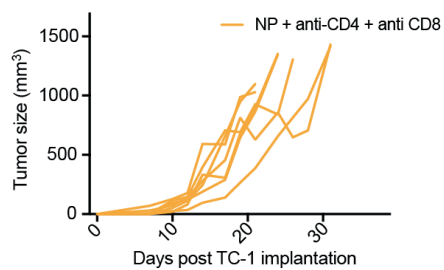
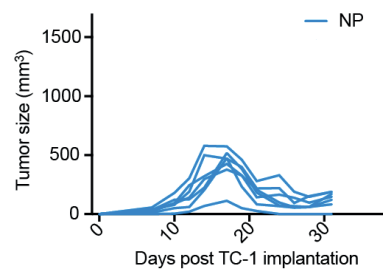
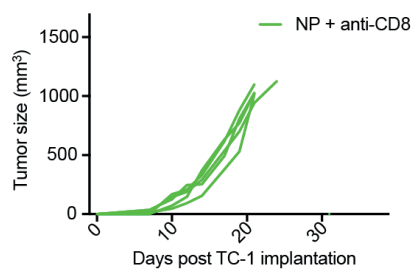
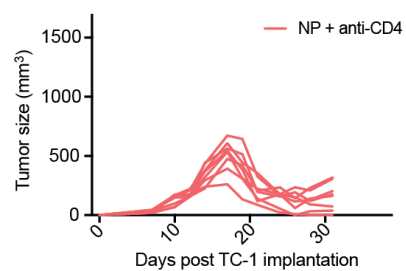
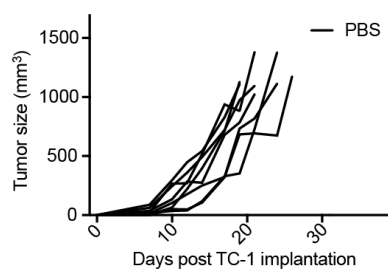
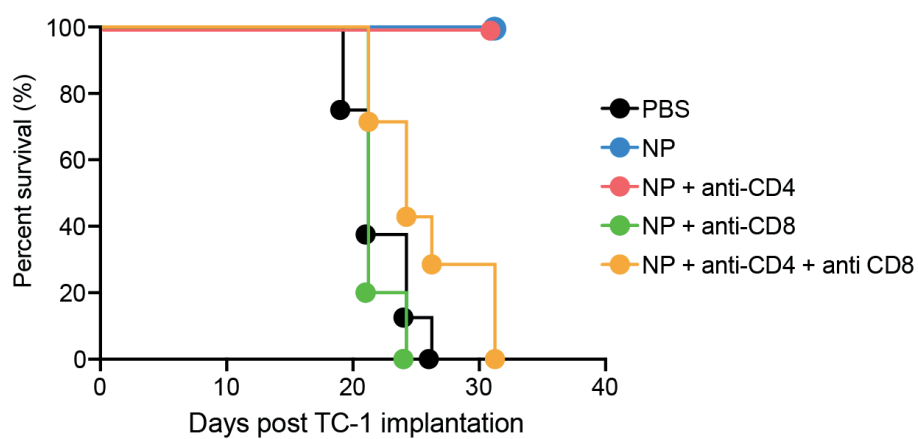


Figure S2. Survival of subcutaneous TC-1 tumor-bearing mice and TC-1 tumor growth curves of the different treatment groups. 0.5×10^6 TC-1 cells were implanted into the flank of the mice at day 0. The vaccine and the control treatments were administered when the mean tumor size was $\sim 100 \text{ mm}^3$. Mice received subcutaneous injections of PBS (n=8) or 15 μg of E7LP conjugated to NPs (NP-E7LP, n=28) combined with 20 μg of CpG as adjuvant. The NP-E7LP treated mice were then split into 4 different groups that remained untreated (n=7), received 10mg/kg of anti-CD8 depleting antibody (n=6) every 4 days, or 10 mg/kg of anti-CD4 depleting antibody (n=8) every 4 days, or both (n=7). Mice were monitored to follow tumor growth and survival. Mice that showed CD4 or CD8 T cell depletion less than 95% were excluded from the analyses.

Statistics: PBS vs NP $p=0.0001$, PBS vs NP+anti-CD4 $p<0.0001$, PBS vs NP+anti-CD8 $p=0.7944$, PBS vs NP+anti-CD4+anti-CD8 $p=0.0684$, NP vs NP+anti-CD4 $p=1$, NP vs NP+anti-CD8 $p=0.0004$, NP vs NP+anti-CD4+anti-CD8 $p=0.0002$, NP+anti-CD4 vs NP+anti-CD8 $p=0.0002$, NP+anti-CD8 vs NP+anti-CD4+anti-CD8 $p=0.0505$, NP+anti-CD4 vs NP+anti-CD4+anti-CD8 $p<0.0001$.

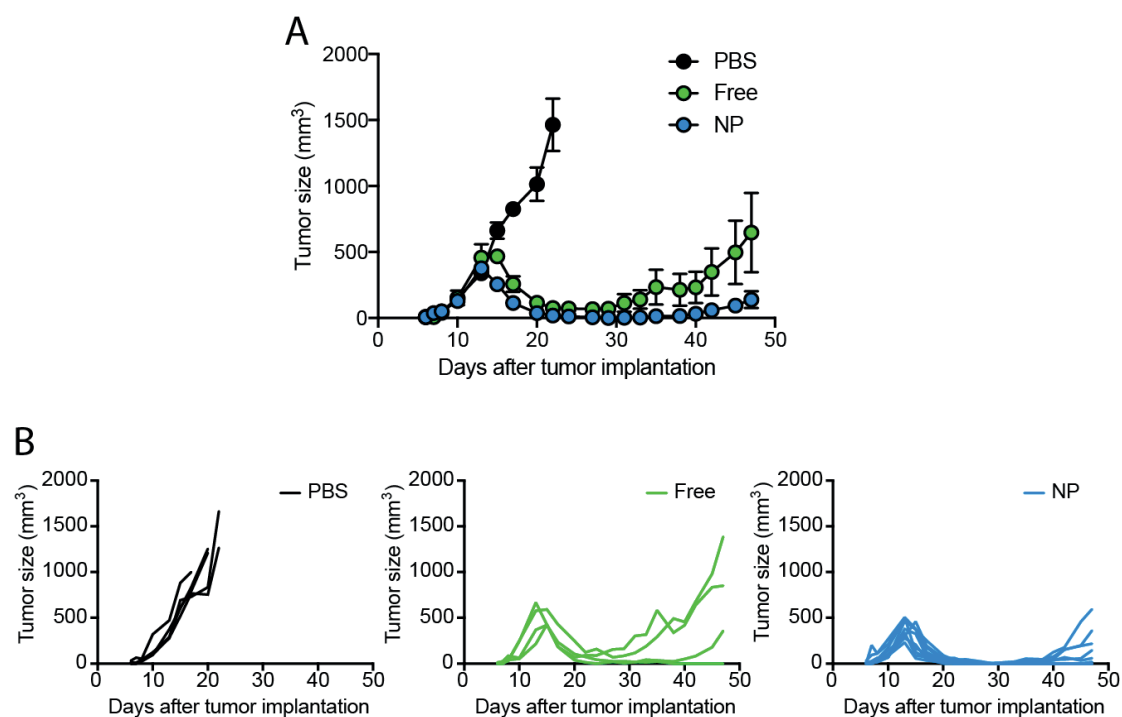


Figure S3. Tumor growth curves of early-immunized TC-1 tumor-bearing mice. 0.5×10^6 TC-1 cells were implanted into the flank of the mice at day 0. The vaccine and the control treatments were administered at day 7 when the mean detectable tumor volume was 22 mm³, and 32% of the mice lacked a palpable mass. Mice received subcutaneous injections of PBS ($n=5$) or 15 μ g of E7LP either in a free form (free E7LP, $n=4$) or conjugated to NPs (NP-E7LP, $n=10$); both vaccinated groups also received 20 μ g of CpG as adjuvant. (A) Mean tumor volume per group. (B) Individual tumor volumes.

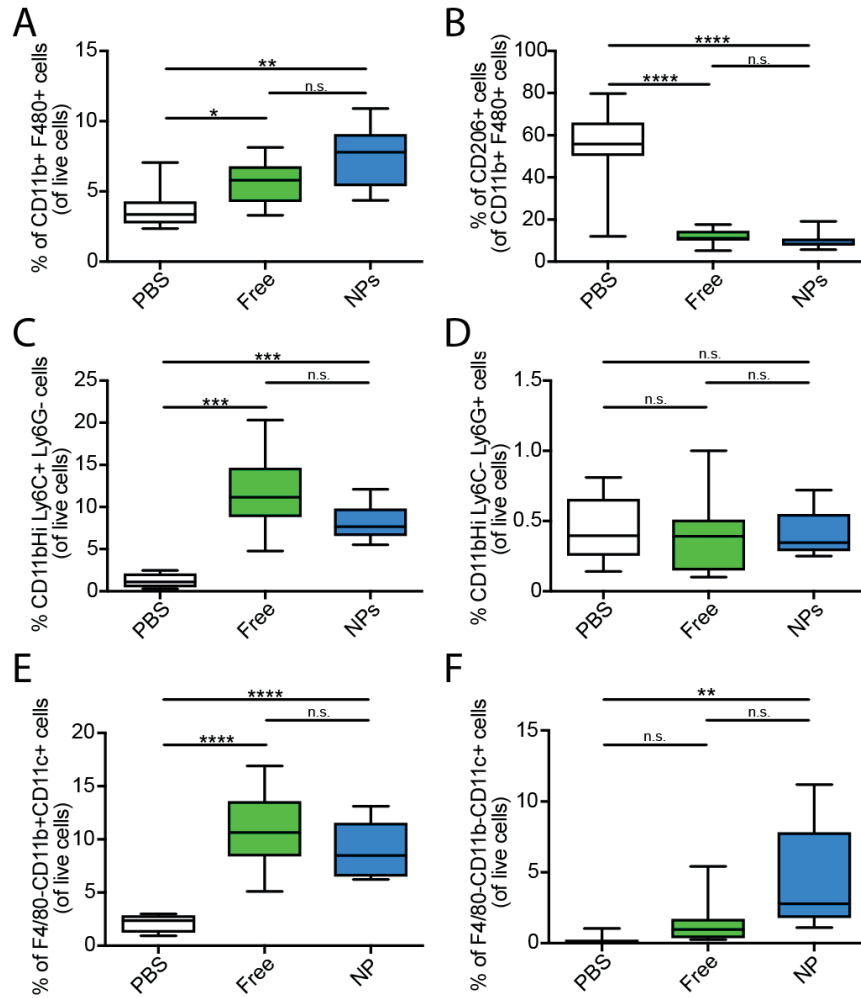


Figure S4. Intra-tumoral innate immune cells. Flow cytometry analyses of intra-tumoral (A) CD11b⁺F4/80⁺ macrophages, (B) CD206⁺CD11b⁺F4/80⁺ "M2 like" macrophages, (C) CD11b^{High}Ly6C⁺Ly6G⁻ monocytes, (D) CD11b^{High}Ly6C⁻Ly6G⁺ neutrophils, (E) F4/80⁻CD11b⁺CD11c⁺ DCs and (F) F4/80⁻CD11b⁻CD11c⁺ DCs. 0.5×10^6 TC-1 cells were implanted into a flank of each mouse at day 0. The vaccine and the control treatments were administered when the mean tumor size was $\sim 100 \text{ mm}^3$. Mice received subcutaneous injections of PBS (n=8) or 15 μg of E7LP either in a free form (free E7LP, n=8) or conjugated to NPs (NP-E7LP, n=8); both vaccinated groups also received 20 μg of CpG as adjuvant. Mice were sacrificed 9 days after immunization and tumors were harvested and processed for flow cytometry analyses. All the cells were gated on single, live cells. Gating strategy for these populations can be found in the Appendix Fig. 5.

Statistics: *p < 0.05; **p < 0.01; ***p < 0.001; ****p < 0.0001; n.s. = not significant.

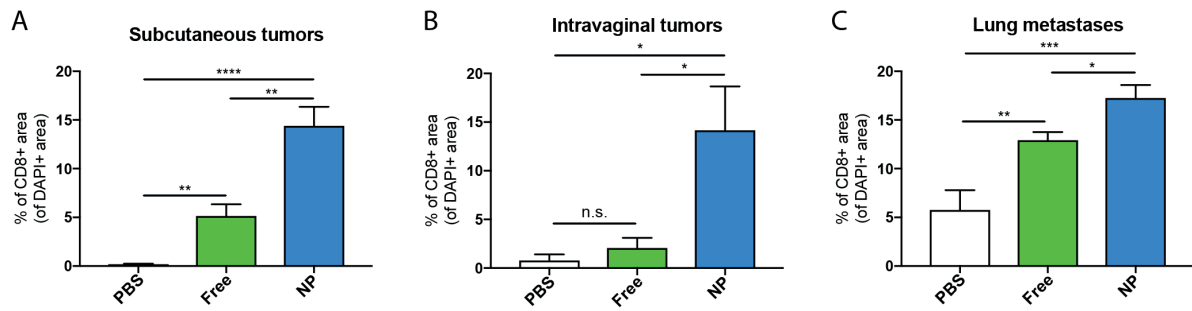


Figure S5. Quantification of intra-tumoral CD8 T cells performed on histological sections. The values are calculated as the percentage of the DAPI+ CD8 T cell nuclei area on the total DAPI+ area. Each mouse is represented by a data point obtained either by the mean calculated between every field or by quantification performed on the whole tissue section. (A) Subcutaneous TC-1 tumors. 4 samples per group were stained and 2 fields per samples were analyzed using Fiji. (B) 3 (PBS and NP) or 4 (Free) samples were stained and images of the whole tissue were acquired and analyzed using Fiji. (C) 4 (PBS) or 8 (Free and NP) samples were stained and images of the whole tissue were acquired. All the lung metastases identified on each sample were selected and analyzed using Fiji.

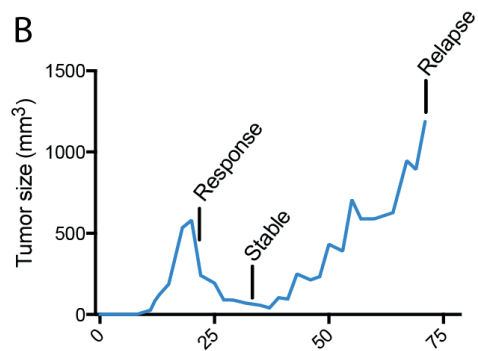
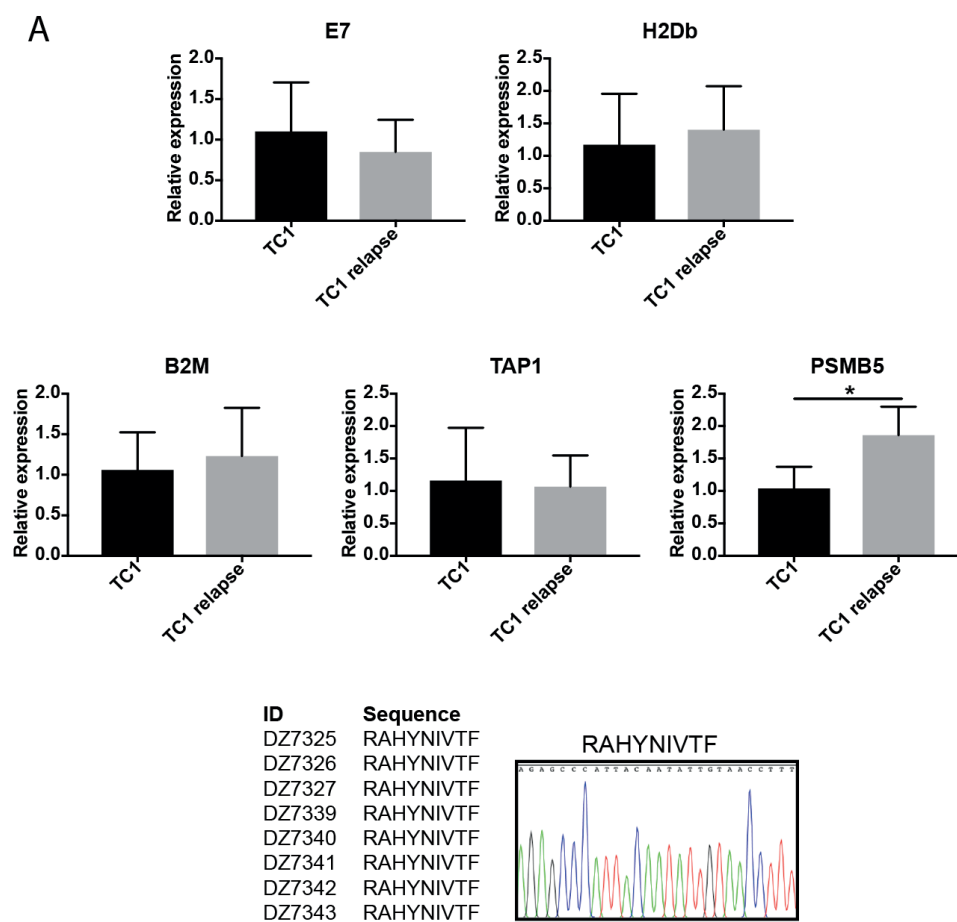


Figure S6. Antigen presentation machinery in TC1 tumors. (A) Gene expression and E7 sequence analysis comparing untreated TC-1 tumors with TC-1 tumors after relapsing from NP-E7LP treatment. E7, H2Db, B2M, TAP1 and PSMB5 gene expression of TC-1 (n=3) and TC-1 relapse (n=6) tumors were determined by real time PCR. The E7 sequence encoding for the MHC-I restricted CD8 peptide of 8 relapsing TC-1 tumors was sequenced by Sanger sequencing (5 clones per tumor). (B) Tumor growth curve of TC-1 tumor treated with E7LP vaccine, depicting response, stable disease and relapse phase.

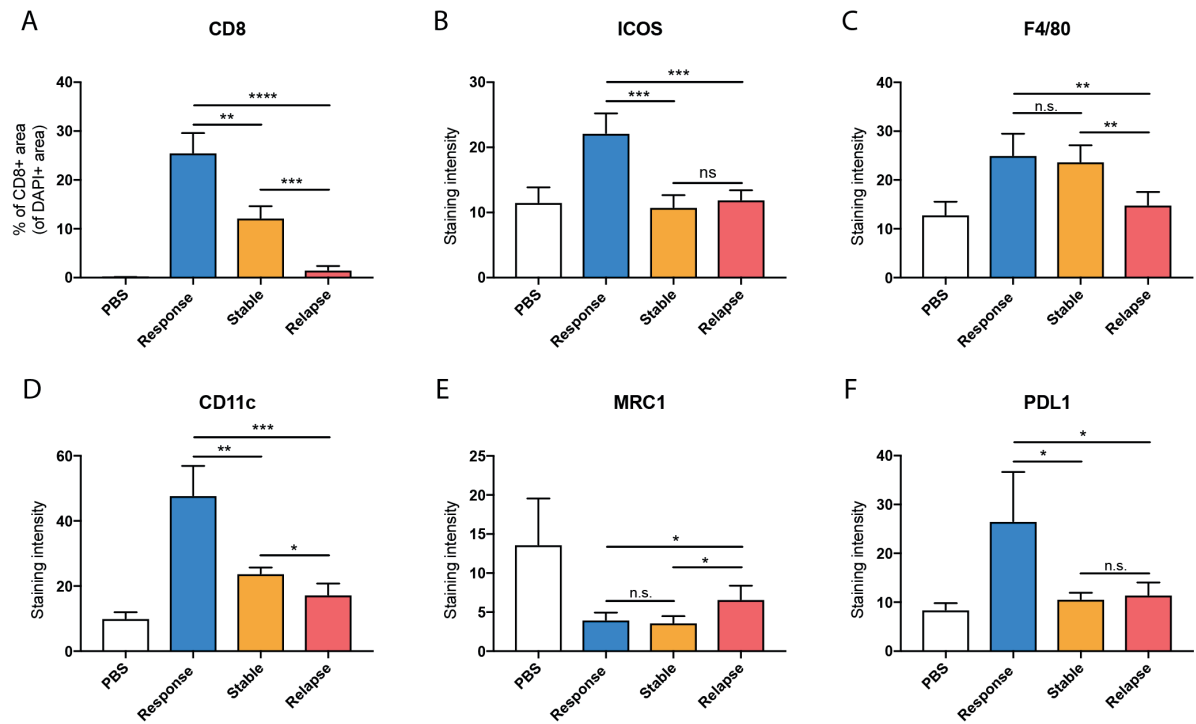


Figure S7. Quantification of immunological markers evaluated by immuno-histology on tumor tissue sections at different phases of therapeutic response. Treatment groups: PBS n=2; Response n=4; Stable n=4; Relapse n=4. As the tumor sections were very homogeneous in cell distribution and staining intensity in each separate treatment phase, three representative field per sample were imaged and subsequently analyzed using Fiji. Each mouse tumor is represented as a data point averaging the values calculated for each field for that tumor. The panels show A) mean CD8 T cells infiltrates per field, calculated as the percentage of the DAPI+/CD8+ area relative to the total DAPI+ nuclear area; and the mean staining intensity per field for: B) ICOS; C) F4/80; D) CD11c; E) MRC1; and F) PDL1. Statistics: * $p < 0.05$; ** $p < 0.01$; *** $p < 0.001$; **** $p < 0.0001$; n.s. = not significant. Additional statistics:

CD8: PBS vs Response $p=0.0011$, PBS vs Stable $p=0.0026$, PBS vs Relapse $p=0.0843$.

ICOS: PBS vs Response $p=0.0131$, PBS vs Stable $p=0.6762$, PBS vs Relapse $p=0.8011$.

F4/80: PBS vs Response $p=0.0265$, PBS vs Stable $p=0.0182$, PBS vs Relapse $p=0.4305$.

CD11c: PBS vs Response $p=0.0053$, PBS vs Stable $p=0.0012$, PBS vs Relapse $p=0.0596$.

MRC1: PBS vs Response $p=0.0222$, PBS vs Stable $p=0.0192$, PBS vs Relapse $p=0.0716$.

PDL1: PBS vs Response $p=0.0753$, PBS vs Stable $p=0.1279$, PBS vs Relapse $p=0.2043$.

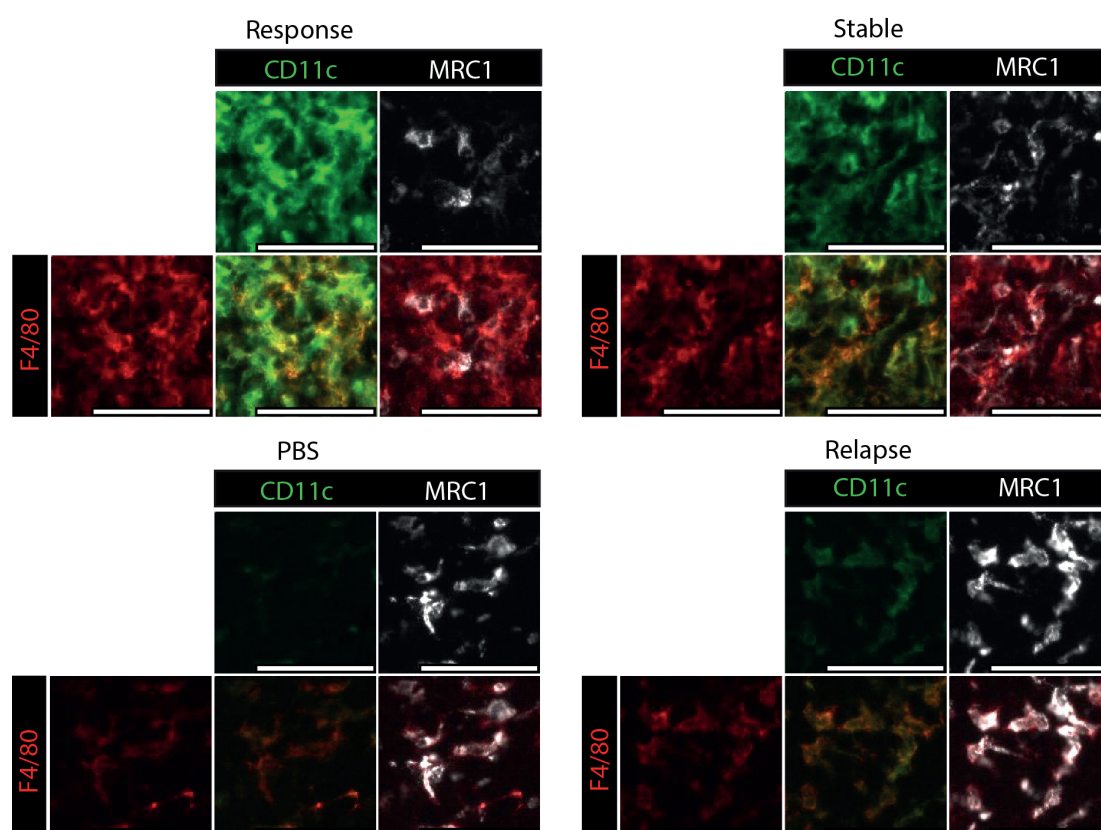


Figure S8. Magnified images of macrophages in the tumor microenvironment at different stages of disease progression. Images are derived from the fields shown In Fig. 6. Immuno-fluorescent staining for F4/80, CD11c and MRC1 is shown in 10µm sections derived from frozen OCT-embedded tumors that were collected at the indicated time-points as in Fig S6B. PBS treated tumors were collected at the endpoint. Scale bars are 50µm. Single channel images of F4/80, CD11c, MRC1 (top lane and bottom left) and overlays of F4/80+CD11c and F4/80+MRC1 (bottom center and bottom right) are shown.

Chapter 3

Immunosuppressive myeloid cells impair immunotherapy in a transgenic mouse model of HPV-related cancer

This chapter of the thesis will discuss how I took advantage of a transgenic mouse model of HPV+ cancers to identify a myeloid-cell dependent immunosuppressive mechanism that seems to play a key central role in blocking anti-tumor immunity and in masking the effects of combinatorial immunotherapies.

3.1 Introduction

The TC1 model used in the previous chapter is undoubtedly a useful tool to compare the efficacy of different vaccines formulations. However, apart from expressing E6 and E7 in tumor cells, it does not fully recapitulate all the features of the disease that are found in patients. The poor responses to therapeutic vaccination and immunotherapy observed against advanced cervical cancer (74, 166) suggest that in these patients the tumors might have developed mechanisms to suppress the anti-tumor immune response compared to the earlier stages of the disease. Several publications described that HPV-related cancer patients, mainly cervical cancers, have been found to have several alterations in the immune system that might account for the resistance of these type of cancers to immunotherapy-based approaches (73, 126, 155, 228). Interestingly, such alterations are not necessarily present only at the tumor site but they have also been found to be systemic and include: the generation of poorly active cytotoxic lymphocytes CTLs, the presence of immature and poorly functional dendritic cells, elevated counts of myeloid cells in the circulation, altered Th1 to Th2 balance in CD4 T cells, accumulation of Tregs in the TME and altered expression of TLRs on keratinocytes (126, 155, 228). Considering all these factors that might suppress the generation of antitumor immune responses even following therapeutic vaccination, and without forgetting all the other potential mechanisms possessed by the virus to avoid recognition by the immune system (32, 126), it is perhaps not surprising that therapeutic approaches based on vaccination or immunotherapy are ineffective in advanced cervical-cancer patients.

However, it is still not clear if and how these alterations are linked, what is their individual contribution to the suppression of anti-tumor responses, and if there are upstream mechanisms that are predominant in respect to the others, and therefore could represent a key therapeutic target.

To conduct research on these questions in a mouse model that would be more representative of the patients, I took advantage of the K14HPV16 H2b mouse model (182). These mice are derived from the “old” non-H2b K14HPV16 mouse (178, 179, 224). The non-H2b K14HPV16 mouse has an FVB background that is permissive for the development of SCC however, due to its MHC haplotype it does not allow the presentation of E7-derived peptides to CD8 T cells. To generate the “new” K14HPV16 H2b mouse capable of eliciting anti-E7 CD8 responses, the non-H2b K14HPV16 mice had to be backcrossed to C57BL/6 to obtain the H2b locus only. Thus allowing for the presentation of the HPV E7 protein-derived peptide to CD8 T cells while maintaining the FVB background. Additionally, this GEMM was chosen because the non-H2b K14HPV16 mouse was previously reported to mimic very closely both the stepwise development of cervical cancer (upon estradiol treatment) seen in patients, and the development squamous cell carcinomas of the skin (178, 179, 224). The new mouse would allow the study of anti-tumor CD8 responses while maintaining a relevant disease setting.

Additionally, given the widespread and constitutive expression of the HPV genes, this novel K14HPV16 H2b mode could mimic the long-term infected cancer patients and could potentially show some of the HPV-related alteration of the immune system and of the anti-tumor immune response. The results presented below show that therapeutic vaccination is ineffective as a single treatment and that these mice are also characterized by poor generation of CTLs, suppression of DCs activation, altered Tregs, and increased myeloid cells. Interestingly, all these features are seen at the systemic levels, thereby resembling the situation reported in patients and warranting for the relevance of these studies (126, 155, 228).

I identified the expansion of immunosuppressive myeloid cells as an upstream and seemingly predominant mechanism of suppression that is generally related to the presence of HPV gene expression. Interestingly, our results suggest that these cells can exert inhibition on both CD8 T cells and antigen presenting cells and moreover, that the immunosuppressive myeloid cells are

capable of completely masking the beneficial effects of combinatorial therapies with checkpoint blockade antibodies and other treatments.

Collectively, in this chapter, I have characterized the immune response to therapeutic vaccination and immunotherapeutic combinatorial approaches in HPV+ transgenic mice, and illustrated how a systemic increase in myeloid cells provide a robust mechanism of defense against such treatments by acting to suppress immunity even outside of the TME, in the peripheral lymphoid organs. As this mechanism seem to be acting upstream of all the other putative barriers, it could represent a very attractive target to unlock the potential of immunotherapy for the treatment of HPV+ cancers.

3.2 Results

3.2.1 Characterization of the MHC haplotype expression and changes in the tumor microenvironment in K14HPV16 H2b mice.

It is widely recognized that CD8 T cells play a major role in anti-tumor immune responses. In order to perform relevant therapeutic vaccination studies in the HPV+ GEMM, APCs need to be able to load E7-derived peptides on MHCI molecules.

I first began my study by checking that the “new” K14HPV16 H2b mice expressed the correct MHCI haplotype that allows for the loading and presentation of E7 peptides to CD8 T cells, namely the H2Db molecule. FACS analyses were performed on immune cells in the blood of BL6, FVB and K14HPV16 H2b mice. As expected the MHC haplotype of K14HPV16 H2b mice matched that of BL6, characterized by the presence of H2Db and H2Kb and by the absence of H2Kq, that was instead present in the FVB background (Fig. 1A).

I next assessed the changes in the immune cell population infiltrates in the tumor microenvironment of the cervix of the HPV transgenic K14HPV16 H2b (HPV+) mice comparing it to a normal cervix from non-HPV transgenic FVB H2b littermates (HPV-) mice. Services were harvested from 6 months old age-matched female mice. I found that the HPV+ mice had a general increase in total T cells, CD8 T cells, CD4 T cells and Tregs in the TME (Fig. 1B, C, D and E) that,

although appeared relatively scarce and scattered, suggest the presence of inflammation that is consistent with the presence of malignant cells. The number of macrophages appeared to be unchanged, suggesting that the cervix is already heavily infiltrated by these cells in normal conditions (Fig. 1F).

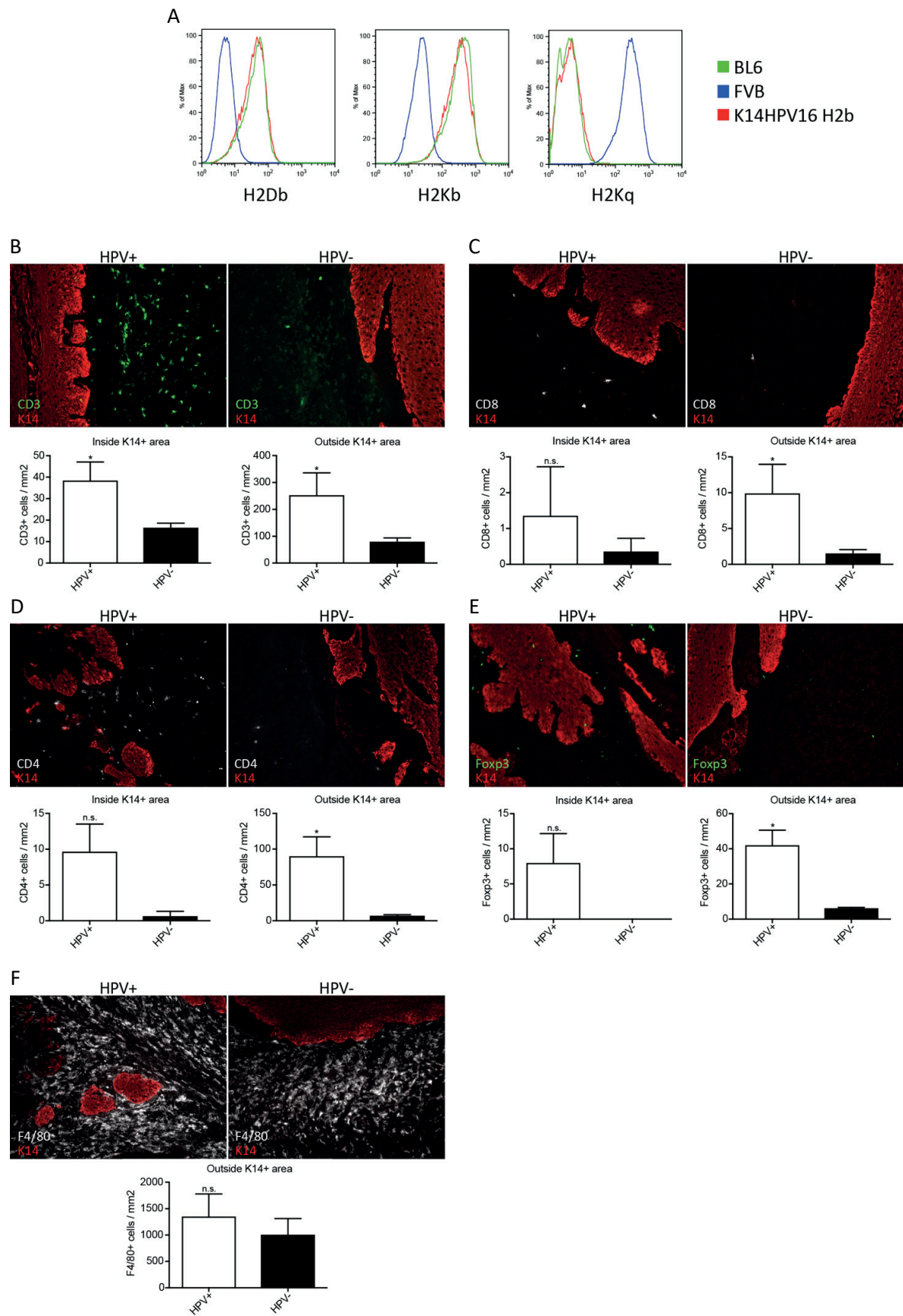


Figure 1. Characterization of MHCI expression on immune cells and of immune infiltrates in the cervical TME. (A) Flow cytometry analyses of MHCI expression performed on blood lymphocytes of mice of different strains. Representative graphs are shown. (B) Immuno-fluorescent staining for keratin 14 (red), CD3 or CD8 (green) and CD4 or F4/80 (white) on 10µm sections derived from frozen OCT-embedded cervixes of tumor-bearing HPV+ mice and the relative age-matched HPV-non-transgenic littermates and quantifications. Staining for keratin14 was performed to distinguish the tumor/epithelium from the surrounding tissue. Quantifications were performed using Fiji (ImageJ) and have been performed separately for cells inside the tumors in HPV+ mice or inside the normal epithelium in HPV- mice (Inside K14+ area) and in the surrounding stroma (Outside K14+ area). Quantification of F4/80+ macrophages is shown only outside the K14+ areas since there were no cells infiltrating the tumors/epithelium. Representative fields of the tissue are shown (n=4 per group). At least 3 fields per mouse were acquired. Values per mouse are the averaged measurement of the acquired fields. Statistics: * $p < 0.05$; ** $p < 0.01$; *** $p < 0.001$; **** $p < 0.0001$; n.s. = not significant.

3.2.2 NP-conjugation of E7 is required to elicit an immune response in K14HPV16 H2b (HPV+) mice upon vaccination.

The constitutive expression of E7, the same protein used in our therapeutic vaccination approach, by the HPV+ GEMM could lead to the generation of tolerance towards this antigen that, although it could represent a point of similarity with long-term HPV infected patients (126), might constitute an obstacle that prevents the generation of anti-E7 responses following therapeutic vaccination. To assess the ability of our vaccine at eliciting anti-E7 responses, similarly to what we did in the previous chapter, I compared the immune response by the two vaccine formulations, namely the NP-bound and free, using the full-length E7 protein as antigen.

5 months old HPV+ mice were immunized at day 0, boosted at day 14 and sacrificed at day 19 when I harvested the vaccination site-draining popliteal and brachial lymph nodes for analyses. Flow cytometry analyses of tetramer positive - E7-specific CD8 T cells revealed that only the NP formulation was capable of eliciting an immune response in the GEMM, with the free formulation showing only background staining from the tetramers that was similar to the one in the PBS or adjuvant only treated groups (Fig. 2A). Ex-vivo re-stimulation assay with the E7-derived CD8-restricted peptide of whole lymph-node cells confirmed the previous observation, showing that

only CD8 T cells from NP-immunized mice were producing IFN γ and TNF α upon re-encounter with their cognate antigen (Fig. 2B). The requirement of NP-conjugation for the generation of an anti-E7 response is in contrast with the results presented in the previous chapter, where the free formulation was already capable of generating antitumor responses, although to a limited degree compared to the NP vaccine. These results suggests that there could indeed be a certain degree of tolerance to E7 in the HPV+ mice. However, I show that the eventual partial tolerance can be overcome, at least to a certain extent, by using a potent NP-based vaccine that allows for the generation of an anti-E7 response.

To check that E7 specific cells generated in the HPV+ GEMM upon vaccination could still kill their target cells despite the apparent partial tolerance, and at the same time, assess for the presence of spontaneous responses in untreated mice, I performed in-vivo killing assay comparing NP-immunized with untreated HPV+ mice. 5 months old HPV+ mice received the NP vaccine and were boosted 14 days later. 19 days after the first shot of vaccine, HPV-non transgenic FVB H2b (HPV-) littermates-derived splenocytes were loaded with the E7-derived CD8-restricted peptide or with an OVA-derived CD8-restricted peptide as control, differentially labeled with high or low concentrations of CFSE respectively, mixed 1:1 and administered I.V. to both vaccinated and unvaccinated HPV+ mice. 6 hours after the transfer, splenocytes were harvested and analyzed for the presence of CFSE high and low cells. Flow cytometry analyses revealed that E7-peptide-loaded splenocytes were getting killed only in the immunized mice (Fig. 2C and D), showing that E7 specific CD8 T cells elicited upon vaccination possessed killing activity and confirming that untreated mice are unable to kill the E7-presenting splenocytes indicating the absence of spontaneous anti-E7 responses. These data show that, despite the potential presence of a partial tolerance to E7, the NP vaccine can elicit E7-specific CD8 T cells in HPV+ mice that possess killing activity. However, the absence of a comparison with non-transgenic HPV- mice prevents me from assessing if the killing activity of E7-specific CD8 T cells in HPV+ mice is normal or defective in comparison.

Additionally, I performed a comparison of different vaccine formulations in HPV+ mice. For all the formulations, 5 months old mice received 1 shots of vaccine and were boosted 14 days later. At day 19, vaccination site-draining lymph nodes were harvested and analyzed by flow cytometry,

observing that the dose of 40 μ g NP-E7protein and 40 μ g CPG (used in the previous experiments) was among the most effective ones and that the addition of MPLA, a TLR4 receptor agonist, to the vaccine was not significantly improving its effectiveness (Fig. 2E). Surprisingly, doubling the dose of antigen and adjuvant failed to produce an increase in the number of E7 specific CD8 T cells.

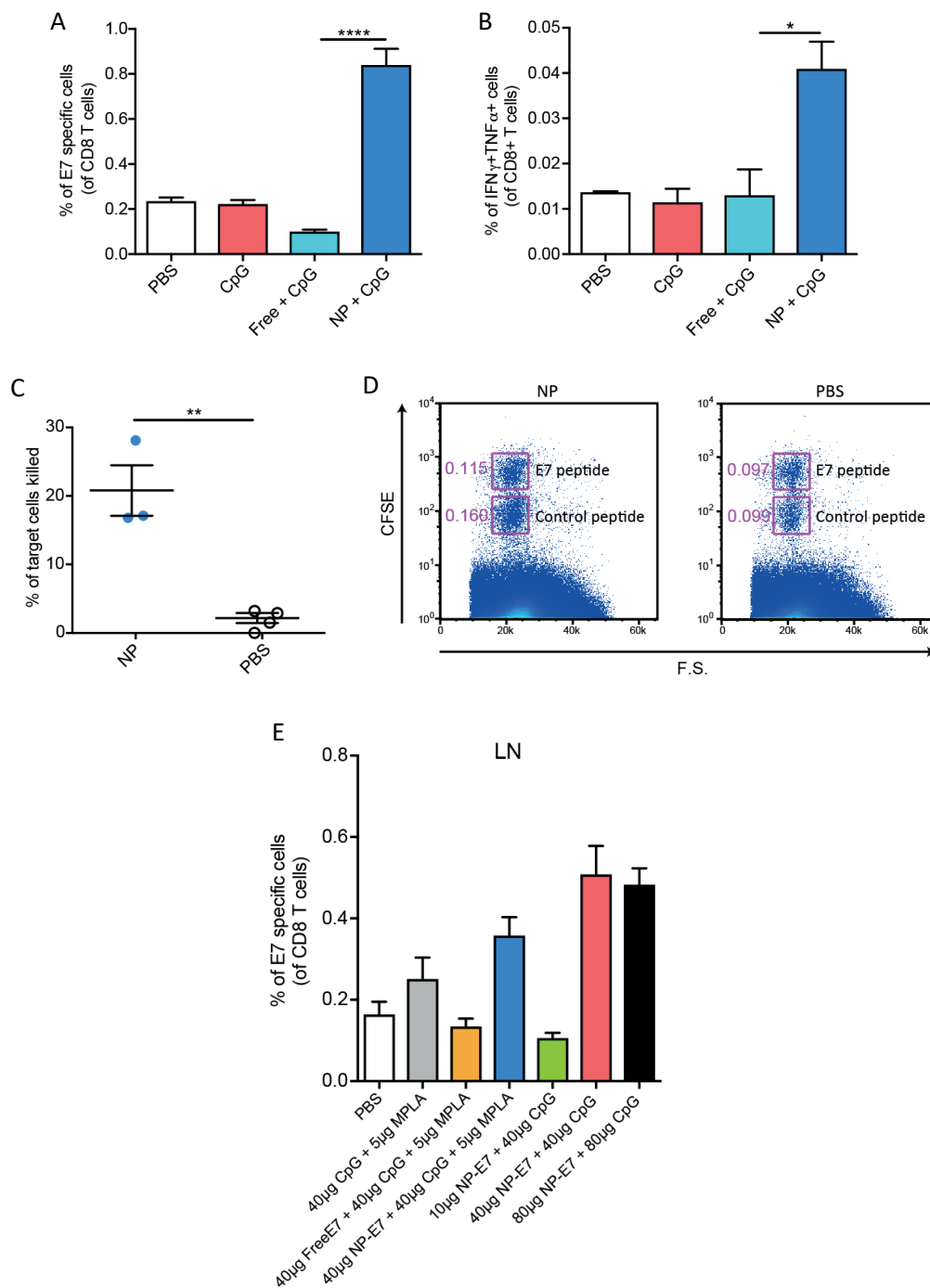


Figure 2. Comparison of different vaccine formulations and killing assay in K14HP16 H2b mice.

(A) Flow cytometry analyses of E7-specific CD8 T cells in the lymph nodes using tetramers recognizing the HPV16 E7 CD8 peptide RAHYNIVTF presented on H2Db. Groups: PBS n=6, CpG n=8, Free+CpG n=8, NP+CpG n=11. (B) Flow cytometry analyses of IFN γ and TNF α production by CD8 T cells after in-vitro re-stimulation with the HPV16 E7 CD8 peptide RAHYNIVTF. (C) Percentage of target E7 CD8 peptide RAHYNIVTF -loaded cells killed calculated from flow cytometry analyses by comparison with the control OVA CD8 peptide SIINFEKL -loaded cells. (D) Representative dot plot from flow cytometry analyses of mice used for the in-vivo killing assay. (E) Flow cytometry analyses of E7-specific CD8 T cells in the lymph nodes of mice treated with different vaccine formulations using tetramers recognizing the HPV16 E7 CD8 peptide RAHYNIVTF presented on H2Db (n=4 for all the groups, except n=8 for 40 μ g NP-E7 + 40 μ g CpG + 5 μ g MPLA). Statistics: *p < 0.05; **p < 0.01; ***p < 0.001; ****p < 0.0001; n.s. = not significant.

3.2.3 NP-vaccination caused only minor changes in CD8 T cell infiltrates in the tumor microenvironment that were not accompanied by a reduction in cervical tumor size.

Given the ability of the NP formulation at eliciting anti-E7 responses, I then analyzed changes in the TME. Mice were immunized at day 0 and boosted at day 14. To follow the changes in the TME associated with vaccination, the cervixes of NP immunized mice were collected at two different time-points, namely day 14 and day 24 after vaccination, and analyzed for the presence of CD8 T cells and E7 specific CD8 T cells. FACS analyses revealed that there were no changes in the total CD8 T cell presence that remained unchanged (Fig. 3A). E7 specific CD8 T cells were absent at day 14 and increased at day 24 post-immunization but remained relatively modest, around 3% of the total CD8 T cells (Fig. 3B).

I repeated a similar experiment and analyzed the TME by histology. This time, I compared mice that received the NP-E7protein vaccine and mice treated with adjuvants only or PBS harvesting the cervixes 24 days post immunization. Analyses of the cervical TME revealed that NP-vaccination was associated with a modest but not significant increase in CD8 T cells both inside the K14+ tumor foci and in the surrounding stroma (Fig. 3C). These changes were accompanied by a similar increase in Tregs that was observed only inside the K14+ areas (Fig. 3D). Overall, the CD8/Treg ratio was slightly improved, but the difference between the NP-vaccine and the adjuvant only

treated groups were not significant (Fig. 3E). Given the small changes in CD8 T cell infiltrates, I was not surprised by seeing that vaccination had no impact on the tumor size that was similar in all the three groups (Fig 3F). These data are in marked contrast to what we described in chapter 2 with TC-1 (and SC-1) tumors that were massively infiltrated with CD8 T cells upon vaccination with the NP formulation.

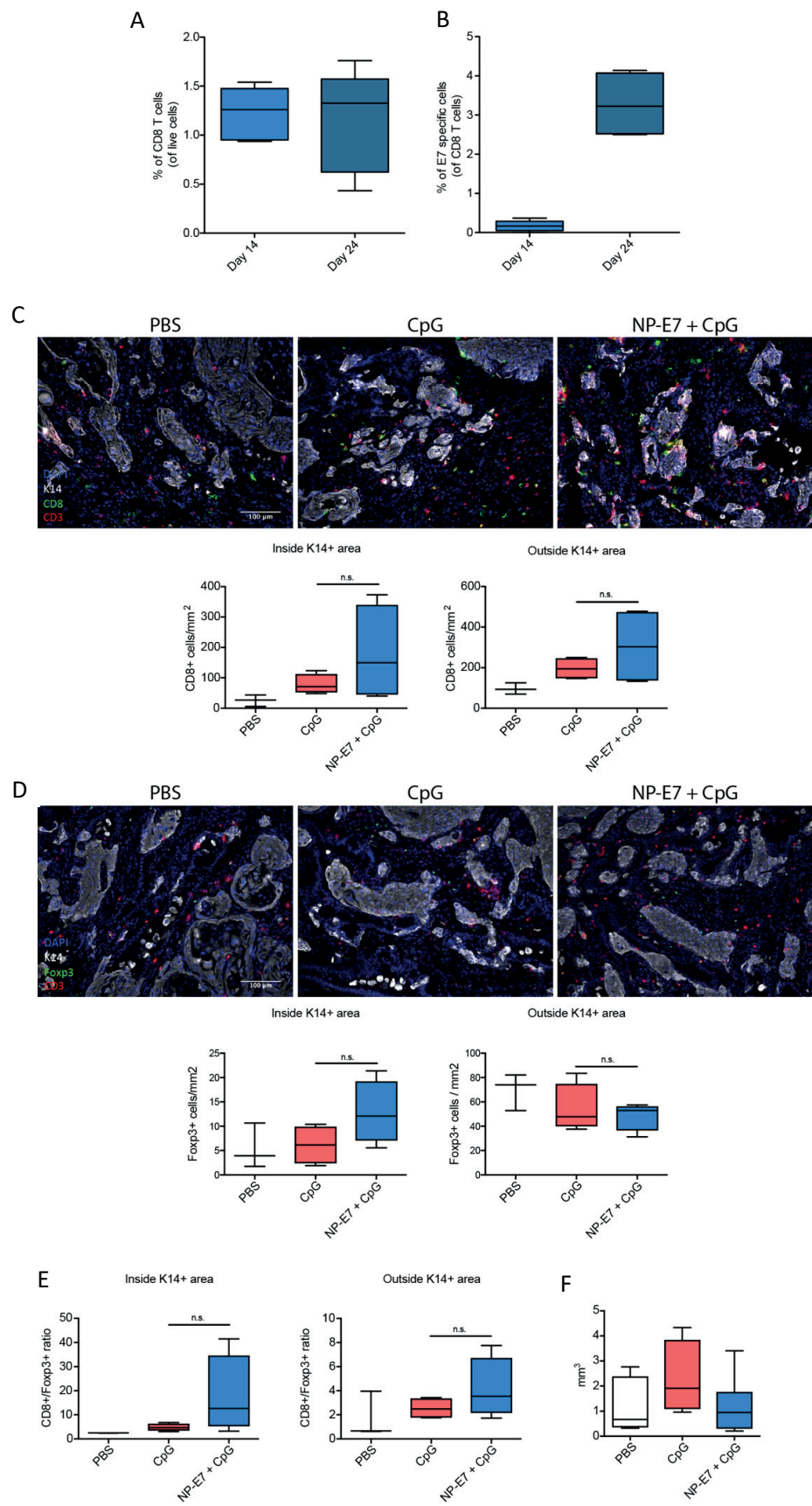


Figure 3. Vaccination-elicited changes at the tumor site and their impact on tumor burden. (A, B) Flow cytometry analyses of CD8 T cells in the cervix of HPV+ mice at different time-points following vaccination (n=4). B) Flow cytometry analyses of E7-specific CD8 T cells in the cervix of HPV+ mice using tetramers recognizing the HPV16 E7 CD8 peptide RAHYNIVTF presented on H2Db at different time-points after vaccination (n=4). (C, D) Immuno-fluorescent staining for keratin 14 (white), CD3 (red) and CD8 or Foxp3 (green) on 10 µm sections derived from frozen OCT-embedded cervixes and relative quantifications. Staining for keratin14 was performed to distinguish the tumor/epithelium from the surrounding tissue. Quantifications were performed using Fiji (ImageJ) and have been performed separately for cells inside the tumors in HPV+ mice or inside the normal epithelium in HPV- mice (Inside K14+ area) and in the surrounding stroma (Outside K14+ area). Representative fields of the tissue are shown. At least 3 fields per mouse were acquired. E) CD8/Treg cells ratio calculated on the tissue slides. Values per mouse are the averaged measurement of the acquired fields (F) Quantification of the cervical tumor size (n=4). Statistics: * $p < 0.05$; ** $p < 0.01$; *** $p < 0.001$; **** $p < 0.0001$; n.s. = not significant.

I reasoned that one possibility is that E7 specific CD8 T cells are migrating to the E7+ skin rather than specifically accumulating in the cervix of the HPV+ mice. I therefore performed histologic analyses of the skin from NP-E7protein immunized mice without seeing increased CD8 T cell infiltration, suggesting that E7-specific CD8 T cells are not preferentially migrating to this site (Fig 4).

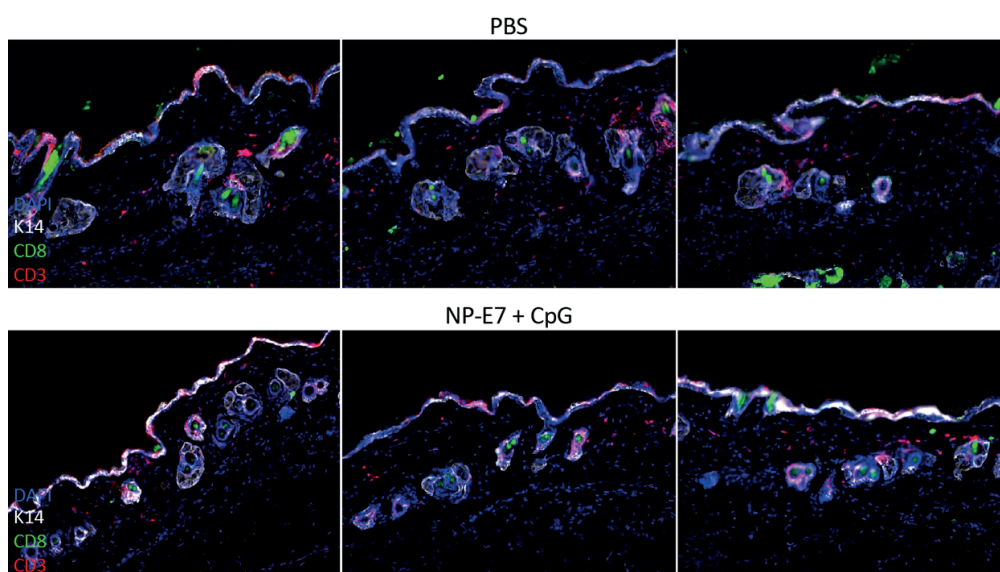


Figure 4. CD8 T cell infiltrates in the skin. Immuno-fluorescent staining for keratin 14 (white), CD3 (red) and CD8 (green) on 10 μ m sections derived from frozen OCT-embedded skin from HPV+ mice. Staining for keratin14 was performed to highlight the epithelium. Representative fields from individual mice are shown (n=3).

3.2.4 Assessing local barriers in the TME that might impair CD8 T cells infiltration and functions.

I reasoned that the negligible effect of therapeutic vaccination on the tumor and the associated TME, could be explained by the presence of local immunosuppressive barriers that are affecting the anti-tumor immune response by preventing infiltration or by suppressing their activity. Immunofluorescence analyses of the cervix harvested from 6 months old mice revealed expression of PDL1 and FasL on the K14+ cancer cells (Fig 5A and B) and a diffused infiltration of macrophages in the tumor-surrounding stroma that were expressing the M1 marker CD11c and/or the M2 marker CD206 (MRC1) in different combinations (Fig 5C). Moreover, cancer cells in the cervix stained positive for IDO and Arg1 (Fig 5D). These results show the presence of multiple barriers at the tumor site that could play a role in dampening antitumor immune responses. Particularly PDL1, IDO, Arg1 and the M2-like macrophages might be suppressing the CD8 T cells functions and/or accumulation at the tumor site, while the expression of FasL could lead to direct killing of activated effector CD8 T cells. Several of these factor have also been found to be present in patients (80, 117, 155, 228).

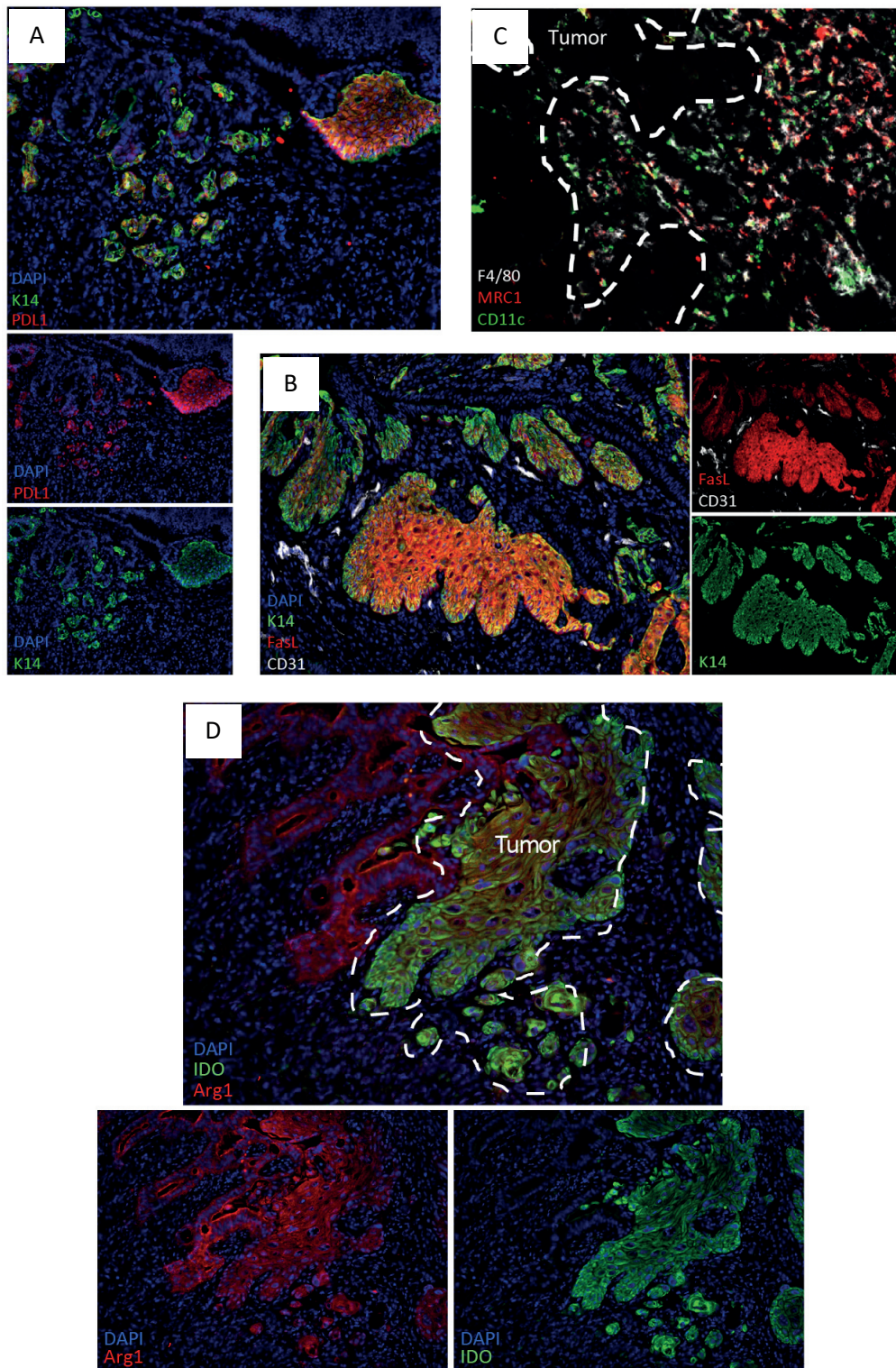


Figure 5. Potential immunosuppressive barriers in the TME. Immuno-fluorescent staining for (A) keratin 14 (green) and PDL1 (red), (B) F4/80 (white), MRC1/CD206 (red) and CD11c (green), (C)

keratin 14 (green), FasL (red) and CD31 (white) and (D) IDO (green) and Arg1 (red) on 10 μ m sections derived from frozen OCT-embedded cervixes from 6-months old HPV+ mice. Representative fields of the tissue are shown. At least 3 fields per mouse were imaged (n=4).

3.2.5 The E7-specific immune response is impaired in HPV+ mice.

We have previously shown in chapter 2 that HPV+ mice-derived SC-1 tumors respond to vaccination and get infiltrated by CD8 T cells despite having similar barriers compared to the spontaneous cervical tumors (unpublished data from our lab). I reasoned that this could either be because SC-1 tumors do not fully recapitulate the barriers seen in the spontaneous tumors of the HPV+ GEMM, or because the immune response following vaccination is stronger in HPV- mice, allowing the tumor-specific cells to overcome these barriers.

To compare the immune response in HPV+ and HPV- mice, I immunized age-matched 5 months old female mice with either 40 μ g NP-E7protein (Fig. 6A) or 15 μ g of NP-E7LP (Fig 6B) both combined with 40 μ g of CpG. These different doses were chosen so that the number of molecules containing the E7 CD8 epitope was the same between the two formulations. Additionally, 8-12 weeks old HPV+ and HPV- male mice were also immunized with the 15 μ g of NP-E7LP + CpG formulation (Fig 6C). All the mice were immunized once and then boosted 14 days later. The immune response was analyzed 19 days after the first show of vaccine in the vaccination site-draining lymph nodes. Flow cytometry analyses revealed that all the NP formulations performed similarly in mice with the same background irrespectively of the vaccine formulation or the sex, with HPV- mice always showing significantly higher responses than HPV+ mice.

These data indicate that the reduced response to therapeutic vaccination is characteristic of the HPV+ GEMM and is not related to the presence of cervical cancer. As all the HPV+ mice carry the transgene in the skin, it has to be expected that certain characteristics are shared between males and females and may not be related to cervical cancer but instead, to the widespread presence of the HPV16 genes or to the formation of skin lesions. As the results in males (Fig. 6C) and females (Fig. 6B) were virtually identical, only the data coming from female mice will be shown in the next part.

The lower numbers of E7 specific CD8 T cells detected in both spleen and lymph nodes suggest that there could be a defect in the generation of the immune response. Immunization in these mice is performed subcutaneously, making the vaccination-site draining lymph nodes, the location

where the anti-E7 response develops. Focusing on these lymph nodes, I checked the tetramers mean fluorescent intensity (Fig. 6D), as well as the effector/memory phenotype (Fig. 6E) of the E7 specific CD8 T cells. The lower tetramer MFI suggests a lower affinity for the cognate MHCI-peptide complex of the E7 specific CD8 in HPV+ mice, while the different phenotypic distribution seems to indicate a reduced generation of effector cells that would be consistent with an overall lower proliferation of the antigen-specific cells, ultimately leading to the previously observed lower frequencies. A reduced proliferation by CD8 T cells could also explain the lower affinity for the cognate peptide-MHC complexes indicated by the tetramer staining. Namely, a defective affinity maturation could ensue from reduced competition for the antigen, caused by the presence of a relatively lower number of competing cells.

I then tested cytokine production by E7-specific CD8 T cells by performing the re-stimulation assay on whole lymph node cells in the presence of increasing concentrations of the cognate peptide. While there was a trend showing a dose-dependent increase in IFN γ and TNF α positive cells in the HPV- mice, I measured minimal production of these cytokines in HPV+ mice, which did not increase regardless of the peptide concentration (Fig. 6F). I also assessed cytokine production from CD4 T cells by performing the re-stimulation assay with the full-length E7 protein. While I was able to clearly measure cytokine production from HPV- mice, the CD4 response was barely detectable in the HPV+ GEMM (Fig. 6G).

Collectively these data show that HPV+ mice have a defect in the generation of both anti-E7 CD8 and CD4 responses, that this defect is irrespective of the antigen form (full-length E7 or E7LP) and it's shared between male and female mice, suggesting that it is related to the presence of the HPV genes rather than to the presence of cervical cancer. The fact that relatively young male mice already show a reduction in the immune response, further strengthen the hypothesis that this phenotype is linked just to the presence of the HPV genes and the relative proteins.

Before continuing, it is important to point out that both the NP-E7 protein and the NP-E7LP formulations were used for the experiments presented in the following sections. This is because when I first started doing experiments in this mouse model, the E7 protein was used as antigen, and only later, I switched to the more clinically relevant E7LP. However, as it was shown in Figure 6, the two formulations were very similar, and up to date, I did not find any significant differences between the two, both in terms of systemic immune responses, local changes in the TME or

efficacy in combinatorial trials. Therefore, from here on, the anti E7 nanoparticle vaccine coupled with CpG will generally be regarded to as NP-VAX, to avoid generating unnecessary confusion with the two formulations.

Additionally, the fact that the lower responses to the vaccine were seen in both young males and old female mice suggested the existence of a similar mechanism that is active early on, thereby allowing me to use both for my experiments.

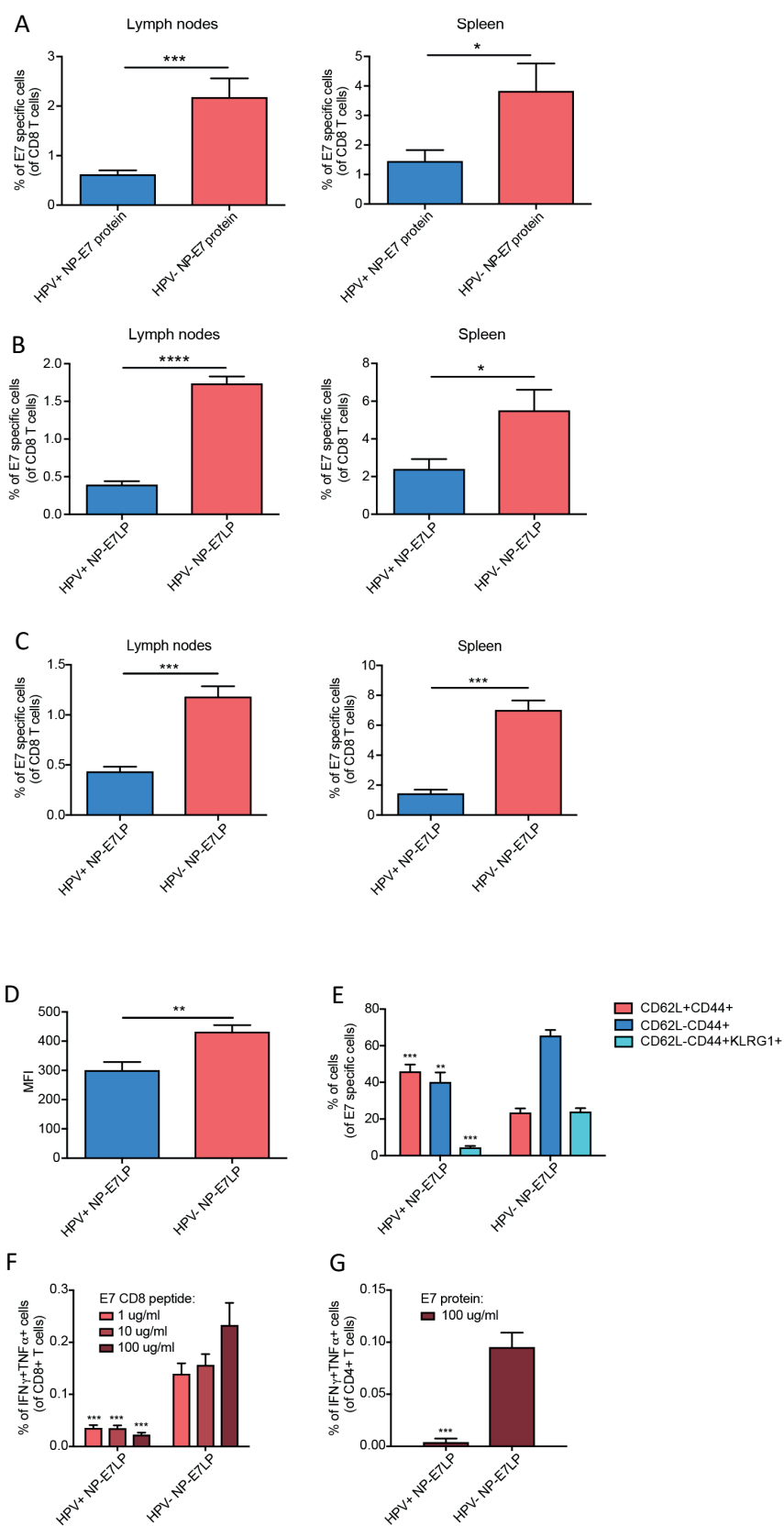


Figure 6. Comparison of the E7-specific immune response in lymph nodes and spleen of HPV+ and HPV- mice. Flow cytometry analyses were performed using tetramers recognizing the HPV16 E7 CD8 peptide RAHYNIVTF presented on H2Db. Analyses were performed on female mice treated with (A) nanoparticle-conjugated E7 full-length protein (n=4) or (C) nanoparticle-conjugated E7 long peptide (n=6), or on (B) male mice treated with nanoparticle-conjugated E7 long peptide (n=4). (D) Flow cytometry analyses of the mean fluorescence intensity of E7-specific tetramers on tetramer+ cells. (E) Flow cytometry analyses of the phenotype of E7-specific CD8 T cells. Cells are divided into CD62L+CD44+ Memory cells, CD62L-CD44+ Effector cells and CD62L-CD44+KLRG1+ Terminal effector cells. Gating strategy for these populations can be found in the Appendix Fig. 1. (F) Flow cytometry analyses of IFN γ and TNF α production by CD8 T cells after in-vitro re-stimulation with increasing concentrations of the HPV16 E7 CD8 peptide RAHYNIVTF. (G) Flow cytometry analyses of IFN γ and TNF α production by CD4 T cells after in-vitro re-stimulation with the full-length E7 protein. Gating strategy for this population can be found in the Appendix Fig. 4. (D, E, F, G) n=6. Statistics: * $p < 0.05$; ** $p < 0.01$; *** $p < 0.001$; **** $p < 0.0001$; n.s. = not significant.

3.2.6 Local barriers do not prevent tumor infiltration by CD8 T cells and shrinking of FVB H2b transplanted SC-1 tumors.

To compare how SC-1 tumor-bearing HPV+ and HPV- males would respond to therapeutic vaccination, me and my colleagues transplanted SC-1 cells into 8-12 weeks old HPV- and HPV+ male mice that were then immunized with a single shot of the NP-VAX or treated with PBS as control. Tetramer staining performed on the blood 9 days after vaccination revealed that spontaneous E7-specific responses were virtually absent in both untreated groups (Fig. 7). On the other hand, similarly to what was already described, administration of the vaccine led to the generation of E7 specific CD8 T cells in both HPV+ and HPV- mice that were, however, significantly more abundant in the non-HPV transgenic ones (HPV-) (Fig. 7).

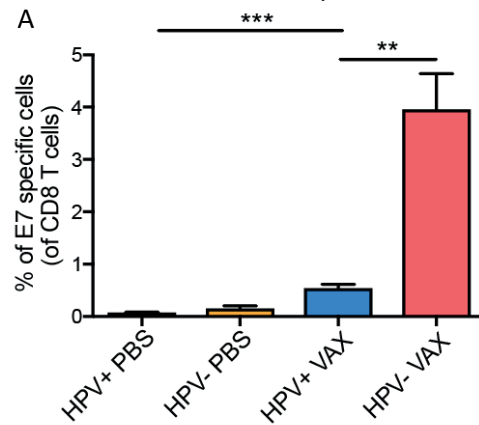


Figure 7. Flow cytometry analyses of E7-specific CD8 T cells in the lymph nodes of SC-1 tumor-bearing mice. Analyses were performed using tetramers recognizing the HPV16 E7 CD8 peptide RAHYNIVTF presented on H2Db (n=4). Statistics: * $p < 0.05$; ** $p < 0.01$; *** $p < 0.001$; **** $p < 0.0001$; n.s. = not significant.

3 weeks after immunization, mice were sacrificed and, when I looked at histological sections of whole SC-1 tumors, I found that HPV- PBS treated mice already had some degree of CD8 T cells infiltrates that further increased upon vaccination and that led to tumor shrinkage (as already reported in chapter 2). In neat contrast, SC-1 tumors transplanted in HPV+ mice showed no sign of CD8 T cell infiltrates that did not change upon vaccination (Fig 8A). No obvious changes in Treg infiltrates were detected in either of the groups seemingly ruling out Treg accumulation as a possible mechanism accounting for the differential infiltration in the TME by CD8 T cells (Fig. 8B). These results suggest that HPV+ mice have a defect in the generation of anti-E7 responses following vaccination compared to their HPV- counterparts and that the strength of the anti-E7 response could be a major factor influencing the outcome of therapeutic vaccination, as a robust response was able to overcome the local barriers in SC1 tumors.

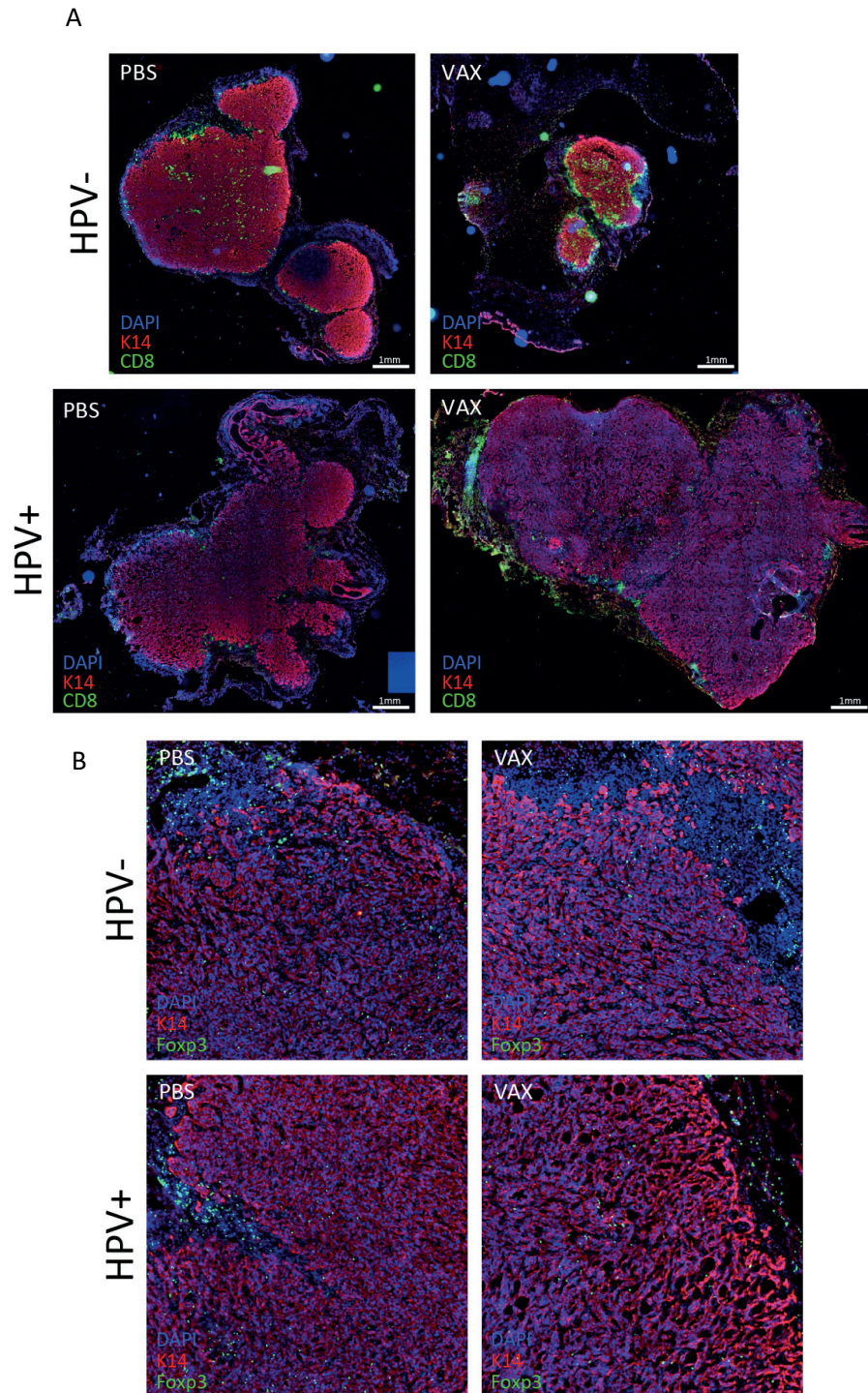


Figure 8. Immune infiltrates in subcutaneous SC-1 tumors. Immuno-fluorescent staining for keratin 14 (red) and (A) CD8 or (B) Foxp3 (green) on 10 μ m sections derived from frozen OCT-embedded SC1 tumors implanted in HPV+ or HPV- mice. Keratin 14 staining was used to visualize

SC1 cells. The whole tumor (n=4) was imaged. As Tregs were smaller than CD8 T cells, representative higher-magnification fields of the tissue extracted from whole tumor images are shown in (B).

3.2.7 HPV+ mice show impaired CD8 responses against OVA and LCMV-derived peptides.

As already mentioned, HPV+ mice constitutively express the HPV protein E7, possibly leading to the establishment of partial tolerance that could explain the low responsiveness to the therapeutic vaccine. To check if the defects in the immune response are a feature that is specific to E7, and therefore linked to tolerance, or if it is shared among other antigens, I immunized HPV+ and HPV- mice either with OVA or with an LCMV-derived CD8 short peptide using CpG as adjuvant. 8-12 weeks old HPV+ and HPV- mice were immunized once, and the immune response was analyzed 9 days later in the vaccination site-draining lymph nodes by flow cytometry and ex-vivo re-stimulation.

Similarly to what I saw with the NP-E7 vaccine, I observed significant defects in the immune response to OVA. Namely, OVA-specific CD8 T cells were reduced in HPV+ mice (Fig. 9A), and cytokine production was lower compared to the HPV- counterpart (Fig. 9B). As for the LCMV CD8 peptide, although I measured similar amounts of LCMV-specific CD8 T cells (Fig. 9C), cytokine production after re-stimulation was severely impaired and barely detectable in HPV+ mice (Fig. 9D).

Although for these antigens NP-conjugation was not required to elicit an immune response, I showed nonetheless that the overall immune responses were still impaired in HPV+ mice.

These results suggest that, although there might be a partial tolerance to E7 which can be broken by using an NP-based vaccine, HPV+ mice are characterized by a more profound state of immunosuppression that is affecting all immune responses to vaccination, regardless of the antigen used. I speculate that this mechanism could be responsible for the scarce impact of therapeutic vaccination in the HPV+ GEMM, and will likely need to be targeted to fully unleash the potential of immunotherapy in this model. Interestingly, these mechanisms seem to be already active at a systemic level, dampening the antitumor immune response even before it reaches the tumor site.

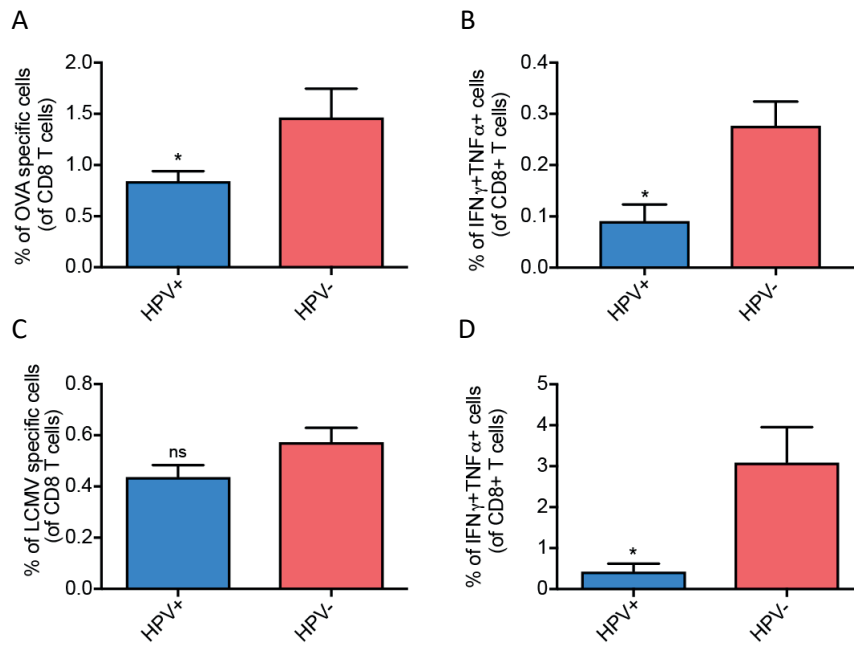


Figure 9. Flow cytometry analyses of the immune response against OVA and LCMV-derived peptides. (A) Flow cytometry analyses of OVA-specific CD8 T cells in the lymph nodes using tetramers recognizing the OVA CD8 peptide SIINFEKL and (B) Flow cytometry analyses of IFN γ and TNF α production by CD8 T cells after in-vitro re-stimulation with the OVA CD8 peptide SIINFEKL (n=5). (C) Flow cytometry analyses of LCMV-specific CD8 T cells in the lymph nodes using tetramers recognizing the LCMV CD8 peptide KAVYNFATC and (D) Flow cytometry analyses of IFN γ and TNF α production by CD8 T cells after in-vitro re-stimulation with the LCMV CD8 peptide KAVYNFATC (n=5). Gating strategy for these populations are similar for the one used for E7-specific CD8 T cells that can be found in the Appendix Fig. 1. Statistics: * $p < 0.05$; ** $p < 0.01$; *** $p < 0.001$; **** $p < 0.0001$; n.s. = not significant.

3.2.8 CD8 T cells activation and proliferation is not intrinsically defective in HPV+ mice.

Before proceeding further, I wanted to assess if the activation and the subsequent proliferation of CD8 T cells is intrinsically defective in HPV+ mice-derived CD8 T cells. To test for this, I isolated CD8 T cells from the spleen of HPV+ and HPV- mice, labeled them with CFSE and cultured them for 48h in the presence of anti-CD3 and anti-CD28. I then harvested the cells 48h later and quantified the amount of CFSElow cells by flow cytometry. The analyses showed that the cells proliferated similarly irrespective of their origin (Fig. 10), suggesting that the differences in

the percentage of vaccine-elicited E7-specific CD8 T cells between HPV+ and HPV- mice are not due to an intrinsic lower proliferative capacity of the T cells in the HPV+ GEMM.

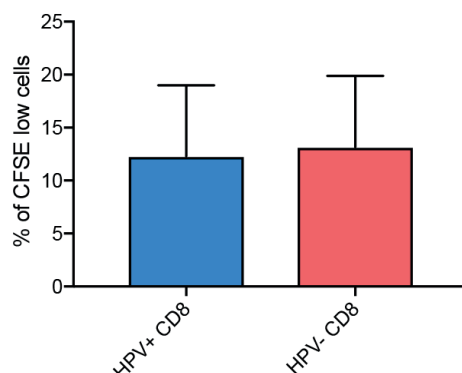


Figure 10. In-vitro HPV+ and HPV- -derived CD8 T cell proliferation. Flow cytometry analyses of CFSE low CD8 T cells after 48h culture in an anti-CD3 anti-CD28 coated plate (n=4). Gating strategy for this population can be found in the Appendix Fig. 7.

3.2.9 Lymphoid organs of HPV+ mice are characterized by the presence of phenotypically different regulatory T cells and show a general increase in all the major myeloid cell populations.

Since the systemic immunosuppression is not specific to E7, I then started to look for immune cell populations that could be responsible for generally suppressing responses to vaccination. Therefore, I focused my attention on regulatory T cells and myeloid cells, both of which have been widely studied as possible immunosuppressive populations in tumor-bearing mice and patients (111, 155, 158, 161, 163).

To characterize these cells at a systemic level, I looked at both spleen and lymph nodes and compared 6-months old HPV+ and HPV- female mice. I found similar percentages of total CD4+CD25+Foxp3+ T regulatory cells in the two strains (Fig. 11A) however, when I looked at the expression of the IL-7 receptor (CD127), I found a significant increase in the CD127+ Tregs in HPV+ mice (Fig. 11B). Tregs that express the IL-7 receptor have been shown to have a higher suppressive function when engaged with the receptor's ligand, leading to increased sequestration of IL-2 that ultimately suppresses T cell responses (229).

HPV+ mice also showed a general increase in all the major myeloid cells populations namely, total CD11b+ cells, CD11b+Ly6G+ neutrophils/G-MDSCs, CD11b+Ly6C+ monocytes/Mo-MDSCs and

CD11b+Ly6G-Ly6C-F4/80+ macrophages (Fig. 11C). The overall representation of each population in the mouse's spleen was virtually similar between HPV+ and HPV- mice (Fig. 11D) indicating that there was a similar increase in all these populations. On the other hand, neutrophils were constituting the majority of the CD11b+ myeloid cells in the lymph nodes suggesting that they could be playing a predominant role in this organ.

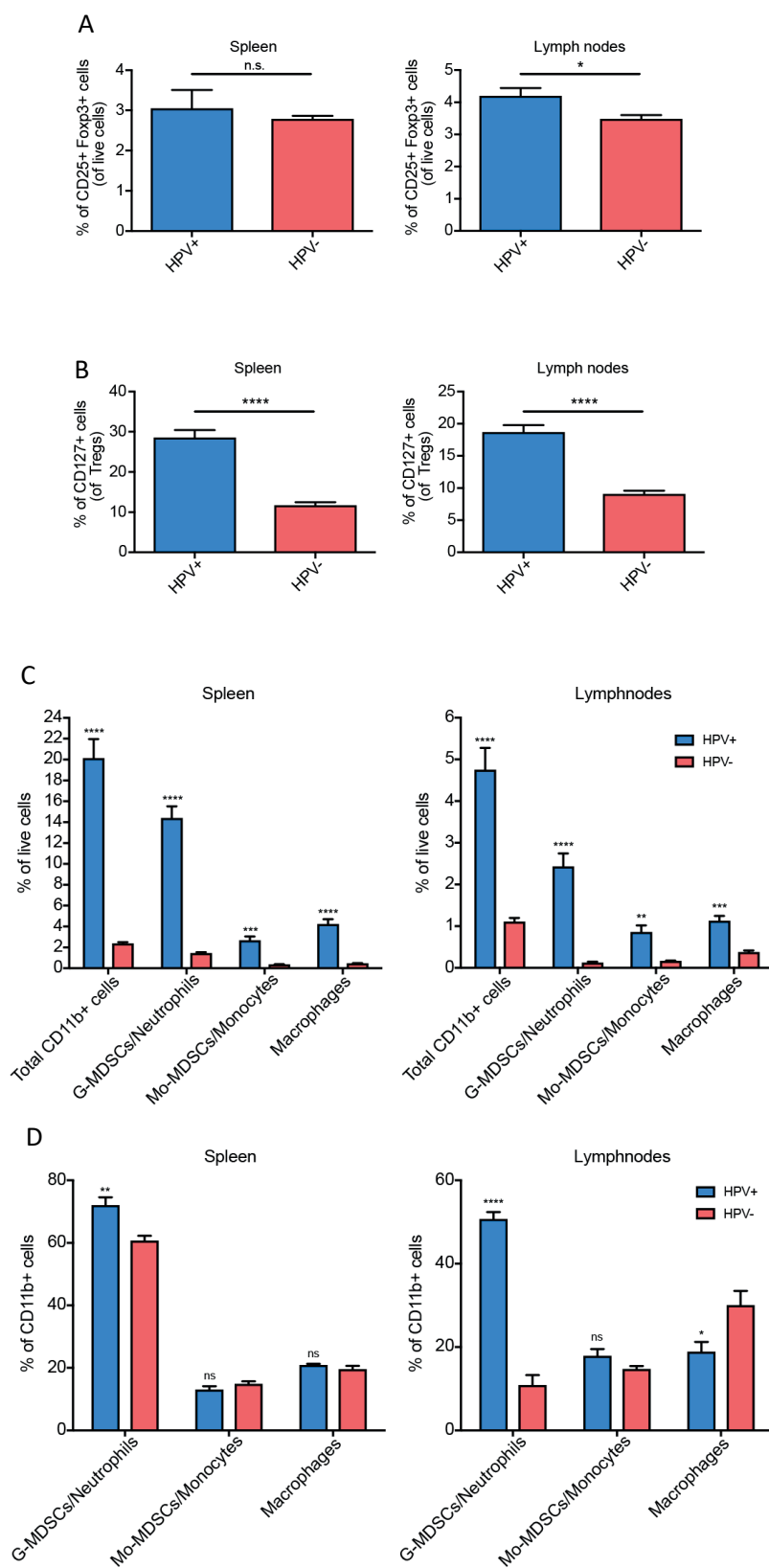


Figure 11. Analyses of Tregs and myeloid cells in lymph nodes and spleen of HPV+ and HPV- mice. (A) Flow cytometry analyses of CD25+Foxp3+ Tregs in the spleen and lymph nodes of HPV+ and HPV- mice. (B) Flow cytometry analyses of CD127+ Tregs in the spleen and lymph nodes of HPV+ and HPV- mice. Gating strategy for this population can be found in the Appendix Fig. 2. (C) Flow cytometry analyses of myeloid cells in the spleen and lymph nodes of HPV+ and HPV- mice indicated as percentage of live cells. (D) Flow cytometry analyses of myeloid cells in the spleen and lymph nodes of HPV+ and HPV- mice indicated as percentage of CD11b+ cells. Myeloid cells populations are defined as: CD11b+ Total CD11b+ cells, CD11b+Ly6G+Ly6C- G-MDSCs/Neutrophils, CD11b+Ly6G-Ly6C+ Mo-MDSCs/Monocytes, CD11b+Ly6G-Ly6C-F4/80+ macrophages. Gating strategy for these populations can be found in the Appendix Fig. 6. n=6. Statistics: * $p < 0.05$; ** $p < 0.01$; *** $p < 0.001$; **** $p < 0.0001$; n.s. = not significant.

Consistently with the massive increase in myeloid cells measured by flow cytometry, all HPV+ mice had a larger spleen and lymph nodes (Fig. 12).

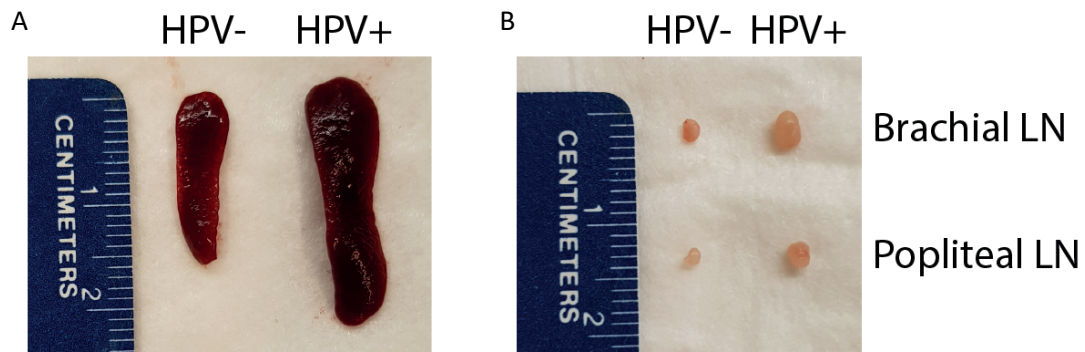


Figure 12. Comparison of spleen and lymph nodes of HPV+ and HPV- mice. Images of a representative (A) spleen and (B) lymph nodes (LN) harvested from 12 weeks old male mice. Brachial and Popliteal lymph nodes are also the vaccination-site draining lymph node analyzed in my experiments.

The presence in the HPV+ mice of phenotypically different Tregs, and a substantial increase in myeloid cells likely due to massive production of myeloid-derived suppressor cells (MDSCs), could represent two major immunosuppressive barriers that can potentially affect the response to

vaccination. Preliminary experiments conducted in 8-12 weeks old HPV+ and HPV- male mice revealed a similar situation (not shown), further adding to the hypothesis that these cells (one population or both) might be the ones playing a role in the systemic immunosuppression of HPV+ mice.

Interestingly, both Tregs accumulation, although only measured at the tumor site, and high numbers of myeloid cells in the circulation have been reported in cervical cancer patients (111, 126, 155, 228).

3.2.10 The lymph nodes of HPV+ mice are bathed in immunosuppressive factors.

Since the immune response to the subcutaneously-delivered NP-VAX is generated in the lymph nodes, to further characterize the situation in these lymphoid organs in HPV+ mice, I performed western blotting on whole lymph node protein extracts to look for factors that could impair immune responses. I found that several immunosuppressive molecules were significantly more abundant in HPV+ mice. In fact, I found increased levels of COX2, IL-10, IDO and Arg1 (Fig. 13A and B), all of which have well documented immunosuppressive functions that could directly affect both CD8 T cells and APCs. The presence of all these factors simultaneously, could also explain why I observed a generalized low immune-responsiveness in HPV+ mice.

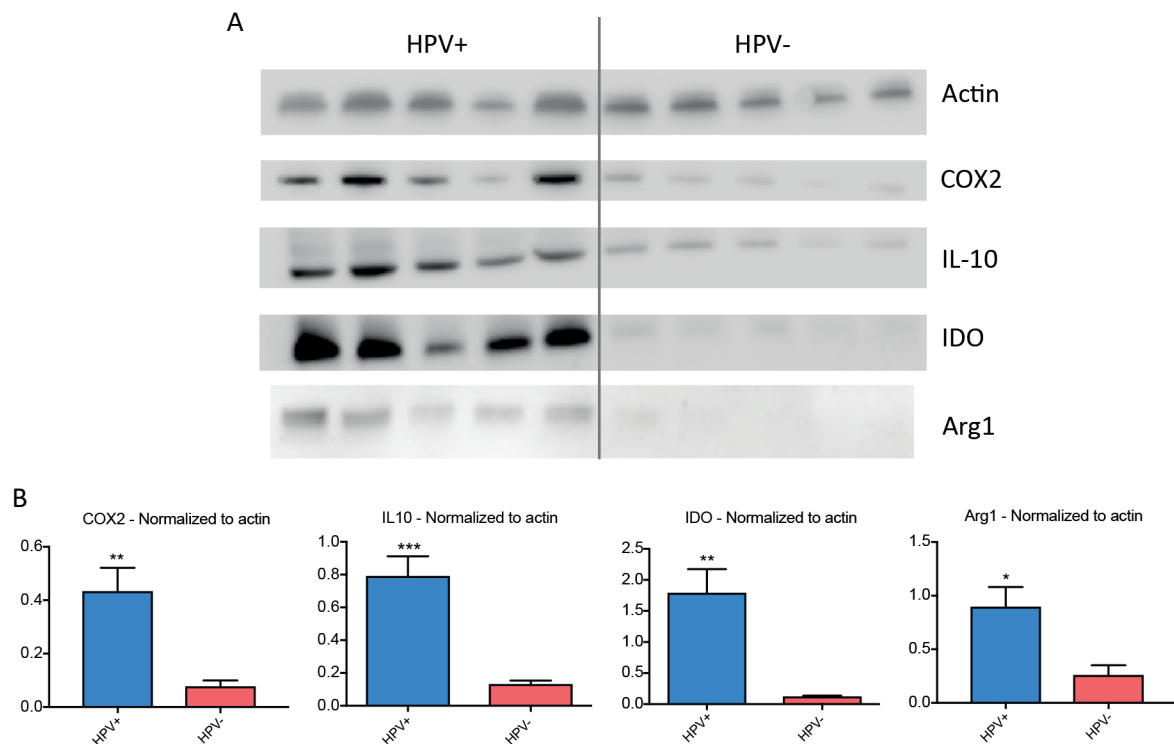


Figure 13. Immunosuppressive factors in the lymph nodes of HPV+ and HPV- mice. A) Western blot of whole lymph node protein extracts from HPV+ and HPV- mice -derived lymph nodes. 1 popliteal lymph node and 1 brachial lymph node per mouse were lysed together. B) Quantification of the western blot bands normalized to actin. Statistics: * $p < 0.05$; ** $p < 0.01$; *** $p < 0.001$; **** $p < 0.0001$; n.s. = not significant.

3.2.11 APC activity is suppressed in HPV+ mice.

The immunosuppressive factors and cells that I observed in the HPV+ mice could not only impact CD8 T cells directly, but also block the activation of APCs, leading to a defect in the first step of the generation of an immune response that would also explain the non-antigen specific nature of the observed defects.

To assess if this is the case, I administered the NP-VAX to HPV+ and HPV- mice or PBS as control and 24h later, I harvested the vaccination site-draining lymph nodes to measure DCs activation. I then analyzed by flow cytometry the expression of activation markers on the surface of CD11b-CD11c+ DCs. The percentage of CD80+ DCs was significantly increased in both HPV+ and HPV- mice upon vaccination, but its upregulation remained significantly lower in HPV+ mice (Fig. 14A).

Expression of all the other activation markers was significantly increased in the HPV- mice that received the vaccine compared to the PBS treated control group (Fig. 14A, B, C and D) however, I saw no changes in the percentages of CD86+ (Fig. 14B) and CD40+ (Fig. 14C) or in the mean fluorescence intensity of MHCII (Fig. 14D) on DCs in vaccinated HPV+ mice, that remained identical to the ones of the PBS treated mice. Similar results were obtained for CD11b+CD11c+ DCs (not shown). DCs activation at this early time-point should be entirely mediated by CpG, and it is therefore reasonable to exclude that it could be influenced by the presence of E7. These results show that DCs activation following vaccination is severely impaired in HPV+ mice. Poor DC activation is a feature that has also been observed in HPV-related cancer patients (126, 230), and could account for the low responses to the different vaccines described above.

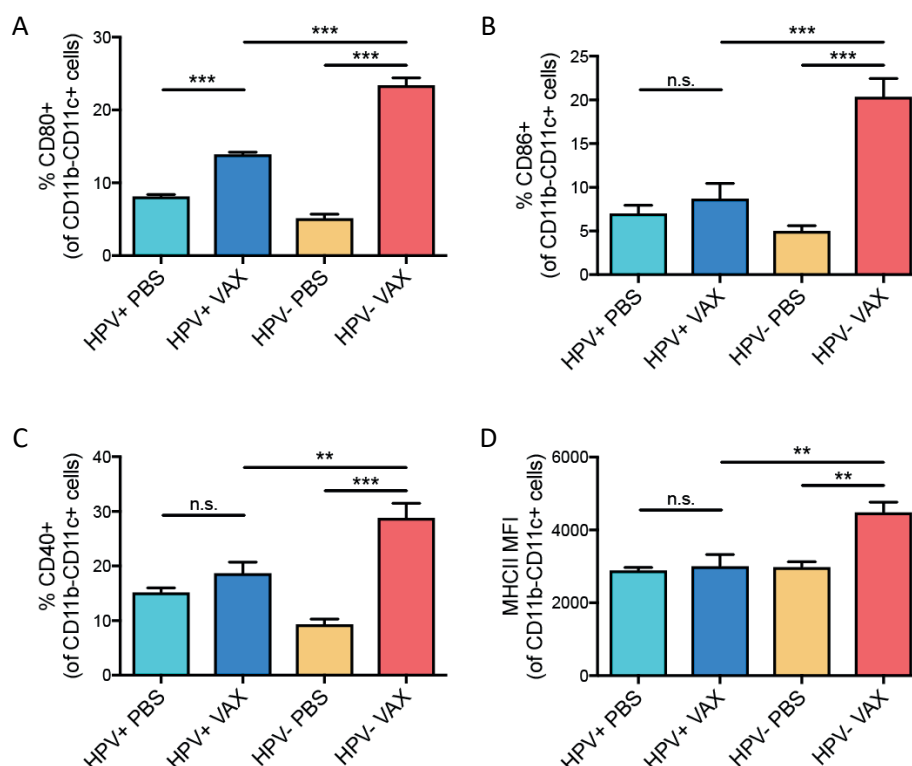


Figure 14. Analyses of APC activation in lymph nodes following immunization. (A, B, C) Flow cytometry analyses on lymph node -derived CD11b-CD11c+ dendritic cells activation markers indicated as percentage on the total CD11b-CD11c+ dendritic cells and (D) Mean fluorescence intensity of MHCII measured by flow cytometry analyses on lymph node -derived CD11b-CD11c+

(n=4). Gating strategy for this population can be found in the Appendix Fig. 8. Statistics: * $p < 0.05$; ** $p < 0.01$; *** $p < 0.001$; **** $p < 0.0001$; n.s. = not significant.

3.2.12 Activation of DCs derived from HPV+ mice is not intrinsically defective.

The HPV genes are present in the genome of HPV+ mice, and one possibility is that they are directly having an impact on DCs maturation and activation. In fact, it has been shown that HPVs can downregulate TLR9 (136) and since our vaccine uses CpG (a TLR9 agonist) as adjuvant, I wanted to exclude the possibility that the poor activation of HPV+ DCs is an intrinsic characteristic of HPV+ GEMM-derived cells.

To test for this, I generated bone marrow-derived dendritic cells from both HPV+ and HPV- mice bone marrow and I treated them in-vitro with LPS (that should activate them regardless of the TLR9 status) or CpG overnight to assess their activation in the absence of other factors. Expression of CD80, CD86, CD40, and MHCII were similarly upregulated in both HPV+ and HPV- -derived BMDCs and were similar between LPS and CpG treated groups (Fig. 15). These results indicate that HPV+ mice-derived BMDCs can fully activate in the presence of CpG and that their activation is similar to HPV- derived BMDCs, suggesting that other factors that are present in the HPV+ mice might be affecting their maturation or might be responsible for their poor in-vivo activation in the LNs upon immunization.

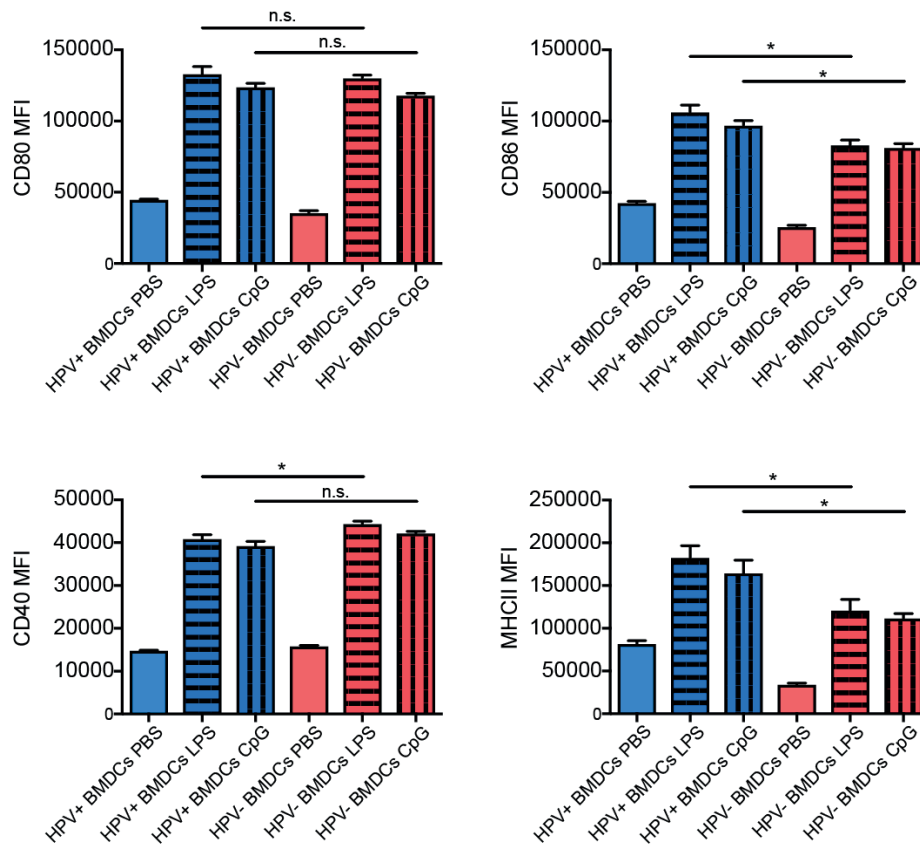


Figure 15. In-vitro activation of BMDCs. Mean fluorescence intensity of MHCII measured by flow cytometry analyses on HPV+ and HPV- bone marrow dendritic cells (BMDCs) activation markers following in-vitro overnight activation (n=3). Statistics: * $p < 0.05$; ** $p < 0.01$; *** $p < 0.001$; **** $p < 0.0001$; n.s. = not significant.

3.2.13 E7LP-loaded DC-vaccines are also poorly effective in HPV+ mice, and activation of adoptively-transferred DCs is suppressed in the lymph nodes and spleen of HPV+ mice.

I then wondered if it could be possible to overcome the poor activation/maturation of endogenous DCs in HPV+ mice, by administering a DC vaccine (DC-VAX). To completely avoid any potential interferences of the HPV proteins, I generated BMDCs from the bone marrow of HPV- mice, loaded them with the E7-LP, activated them overnight with LPS and then administered them subcutaneously to HPV+ and HPV- mice with the addition of CpG. Mice received one shot of the DC-VAX and were sacrificed 9 days later to assess the immune response. When I looked at the

anti-E7 CD8 response in the vaccination site-draining lymph nodes by flow cytometry, I observed a situation that was identical to the one measured after vaccination with the NP formulation. Namely, DC vaccine-treated HPV+ mice were still showing fewer E7 specific CD8 T cells (Fig. 16A), a different phenotype distribution (Fig. 16B) and a lower cytokine production (Fig. 16C) compared to the HPV- mice.

To monitor the activation of the exogenous DCs upon administration, I repeated the experiment and labeled the BMDCs contained in the DC-VAX with CFSE prior to injection. 24h later I collected the vaccination-site draining lymph nodes, and I analyzed the expression of activation markers on the CFSE+ exogenous BMDCs. I found that their expression was lower in the cells that were administered to HPV+ mice (Fig. 16D), suggesting that their activation was suppressed upon administration in the GEMM.

To test if this was an effect of the subcutaneous administration, potentially linked to the fact that the cells were injected closely to the HPV+ skin, I repeated the same set of experiments but this time I injected the vaccine intravenously and monitored the immune response and CFSE+ DCs activation in the spleen. Flow cytometry analyses revealed in the HPV+ mice a situation similar to what I observed in the lymph nodes, with fewer E7-specific CD8 T cells (Fig. 16E) and a different phenotype distribution (Fig. 16F) measured 9 days after vaccination and decreased expression of activation markers (Fig. 16G) measured 24h after cell transfer, suggesting that both lymph nodes and spleen present a similar immunosuppressive environment that is capable of impairing DCs activation and possibly suppressing other immune cells.

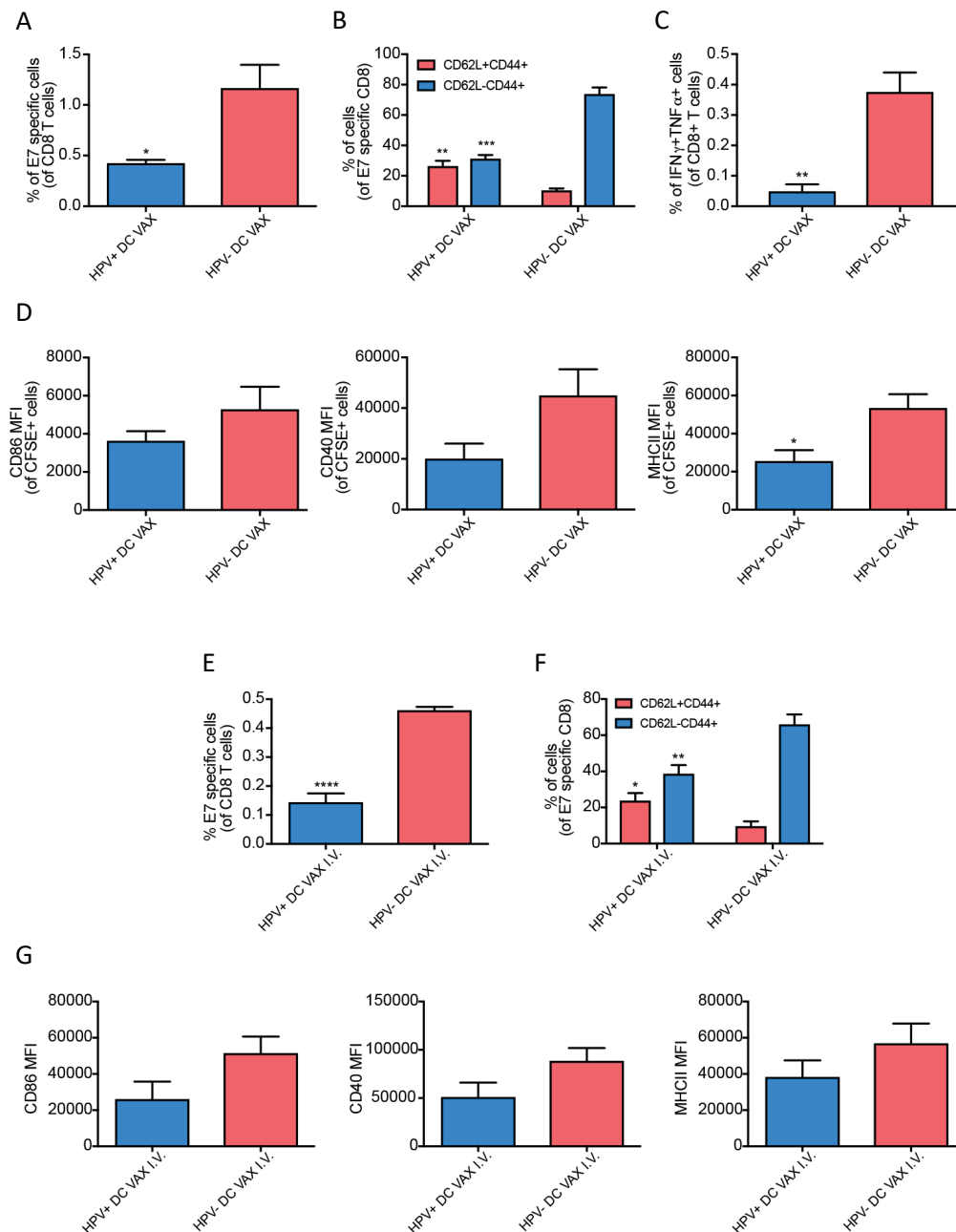


Figure 16. Flow cytometry analyses of E7-specific CD8 T cells and BMDCs activation following administration of a DC vaccine. Flow cytometry analyses in the lymph nodes and spleen using tetramers recognizing the HPV16 E7 CD8 peptide RAHYNIVTF presented on H2Db on (A) subcutaneously or (E) intravenously -delivered dendritic cells vaccine (DC VAX) treated mice. Flow cytometry analyses of the phenotype of lymph node -derived E7-specific CD8 T cells on (B)

subcutaneously or (F) intravenously -delivered dendritic cells vaccine (DC VAX) treated mice. Cells are divided into CD62L+CD44+ Memory cells, CD62L-CD44+ Effector cells and CD62L-CD44+KLRG1+ Terminal effector cells. (C) Flow cytometry analyses of IFN γ and TNF α production by lymph node - derived CD8 T cells after in-vitro re-stimulation with the HPV16 E7 CD8 peptide RAHYNIVTF. Flow cytometry analyses of CFSE+ DCs activation markers on (D) subcutaneously or (G) intravenously - delivered dendritic cells vaccine (DC VAX) treated mice. Gating strategy for this population can be found in the Appendix Fig. 9. (A, B, C) n=5, (D) n=3, (E, F) n=4, (G) n=3. Statistics: *p < 0.05; **p < 0.01; ***p < 0.001; ****p<0.0001; n.s. = not significant.

3.2.14 Testing combinatorial strategies aimed to directly boost the immune response and increase tumor infiltration

The results presented above show that the immune response generated by therapeutic vaccination alone is not sufficient to have an impact at the tumor site. The efficacy of the vaccine seem to be impaired by a poor activation of APCs and possibly by the presence of Tregs and MDSCs. Therefore, I reasoned that the anti-E7 immune response needs to be improved in order to achieve effective anti-tumor immunity.

The first approach I decided to take in order to improve the anti-tumor immune response in HPV+ mice, was to combine our nanoparticle-based vaccine with different checkpoint inhibitors or agonistic antibodies and/or with other treatments aimed at blocking potentially harmful ligands for the T cells found at the tumor site (PDL1, FasL) or at increasing their intra-tumoral infiltration in the cervix. Some of these experiments will be discussed in detail, while other additional preliminary experiments are summarized in Table 1.

The goal of these approaches was to try enhancing the generation of anti-E7 CD8 T cells aiming at obtaining a strong enough immune response capable of overcoming the immunosuppressive barriers. At the same time, I layered treatments to enhance the recruitment of the E7 specific effector cells to the tumor, hoping to generate a feedback loop that would ultimately enhance the antitumor response.

Treatment	Goal
NP-VAX + anti-GITR + anti-CTLA4	Test the effect of agonistic anti-GITR
NP-VAX + Intravaginal CpG and PolyI:C (tested successfully in a preliminary experiment on BL6 mice)	Increase CD8 T cells infiltration at the tumor site by local delivery of pro-inflammatory adjuvants
NP-VAX + anti-PD1 + anti-CTLA4 + Intravaginal CpG and PolyI:C	Increase CD8 T cells infiltration at the tumor site by local delivery of pro-inflammatory adjuvants
NP-VAX + anti-PD1 + anti-CTLA4 + Intravaginal imiquimod cream	Increase CD8 T cells infiltration at the tumor site by local delivery of pro-inflammatory adjuvants clinically used to treat pre-malignant lesions and warts
NP-VAX + anti-PD1 + anti-CTLA4 + Intravaginal CXCL9/10	Increase effector CD8 T cells infiltration at the tumor site by local delivery of chemokines
NP-VAX + anti-PD1 + anti-CTLA4 + anti-FasL + Intravaginal CXCL9/10	Increase CD8 T cells infiltration at the tumor site by local delivery of chemokines and by block CD8 T cells killing by tumor cells with anti-FasL
NP-VAX + all-trans retinoic acid	Use ATRA to increase the generation of CD8 T cells capable of migrating to mucosal sites

Table 1. Summary of the additional immunotherapy treatments that were performed in HPV+ mice. Unfortunately, none of these treatments showed improvement in the immune response to the vaccine nor elicited significant changes at the tumor site.

3.2.15 Combination of vaccination with anti-PD1 and anti-CTLA4 does not boost the generation of E7-specific CD8 T cells and does not elicit changes in the TME

I started by combining therapeutic vaccination against E7 using our NP-VAX with anti-PD1 (aPD1) treatment in HPV+ mice.

HPV+ females were immunized with the NP-VAX when they were 5 months old (day 0) and received a second shot at day 14. aPD1 treatment was administered 2 times per week starting at day 0 and continued throughout the experiment. Mice were sacrificed at day 24.

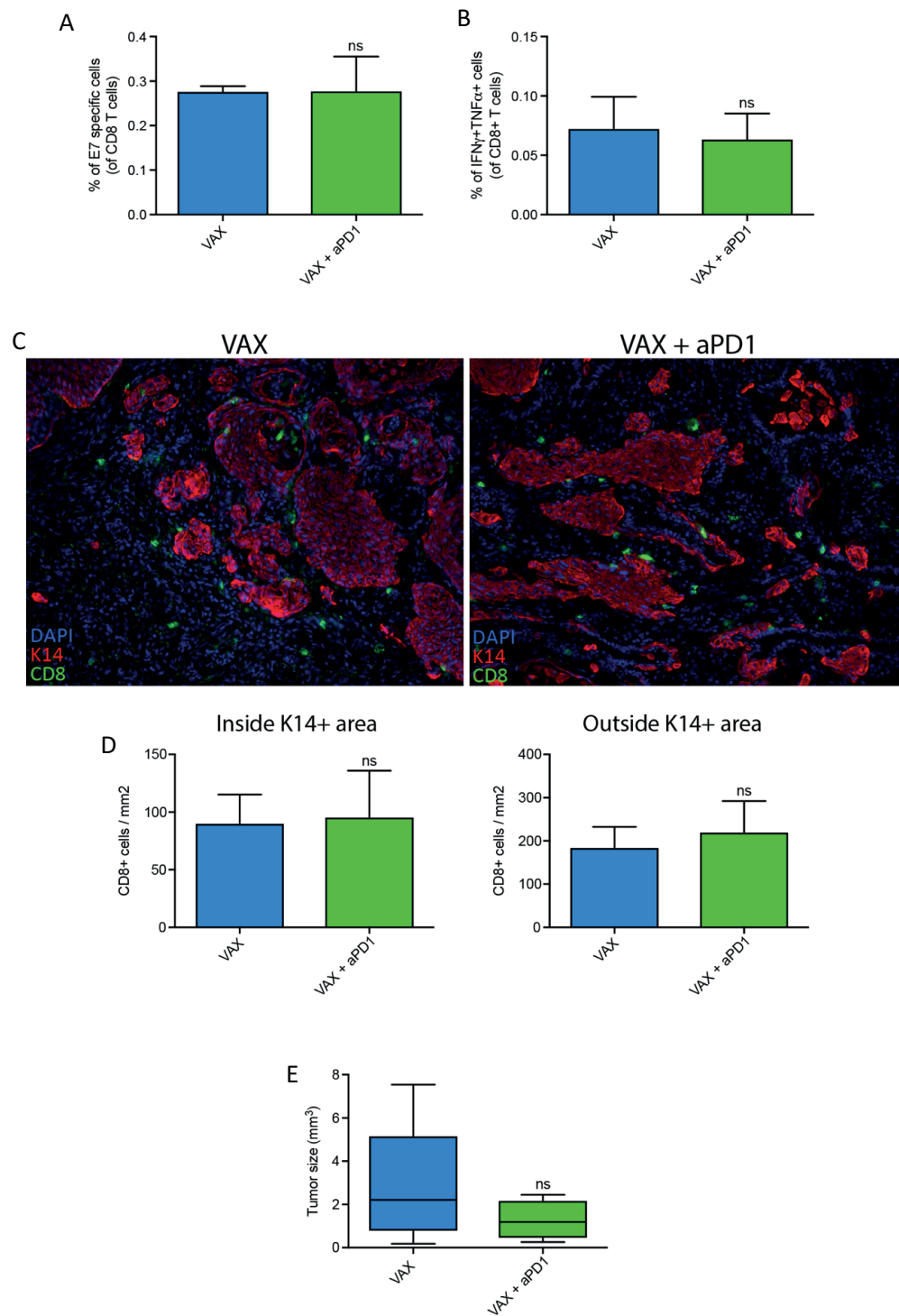
Flow cytometry analyses of the lymph nodes of mice treated with VAX+aPD1 failed to detect an increase in either the percentage of E7-specific CD8 T cells (Fig. 17A) or in the cytokine production after re-stimulation of whole lymph node cells (Fig. 17B) indicating that the combinatorial treatment provided no benefit in the generation of the anti-E7 response. I then moved my attention to the tumor site in the cervix. Both groups showed similar degree of CD8 T cell infiltrates in both the K14+ tumor foci and in the surrounding stroma (Fig. 17C and D). Reflecting the absence of an increase in the immune cells infiltrating the TME, tumor burden was similar in both groups (Fig. 17E).

In light of these results, I decided to add anti-CTLA4 (aCTLA4) to the combination. Mice received the same treatment as the previous experiment with the addition of the aCTLA4 treatment that was carried out together with aPD1, 2 times per week. Once again, I did not observed any significant increase in either the percentage of E7 specific CD8 T cells in the mouse lymph nodes (Fig. 17F) nor in cytokine production after re-stimulation of whole lymph nodes cells (Fig. 17G), although it's worth noting that for the latter I did measure a trend toward a slight increase in the VAX+aPD1+aCTLA4 treated mice. The addition of aCTLA4 to the treatment was not sufficient to prompt any obvious change in CD8 T cell infiltrates in the cervix (Fig. 17H), and it resulted in similar tumor burdens in all the groups (Fig. 17I).

These results, along with the ones obtained in preliminary experiments listed in Table 1, suggest that the combination of therapeutic vaccination with aPD1 and aCTLA4 (and others) checkpoint inhibitors and agonistic antibodies is not sufficient to provide a significant boost to the anti-E7 immune response. This result could be explained either by a model-dependent feature by which the tested antibodies are not beneficial (similarly to what has been observed in TC-1 tumor-bearing mice, that seem to be responsive only to combinations involving anti-41BB (204)) or, more in accordance with my previously discussed data, by an overwhelming presence of systemic immunosuppressive barriers that might mask or completely cancel the benefit of these combinatorial approaches.

Additionally, my preliminary experiments (Table 1) indicate that intravaginal delivery of adjuvants (CpG+PolyI:C), of effector CD8 T cells-attracting chemokines (CXCL9, CXCL10) or of an imiquimod-containing cream, do not lead to an increased recruitment of CD8 T cells in the TME and do not

cause any significant change at the tumor site. The ineffectiveness of the intravaginal delivery approaches could again be due to the overwhelming presence of immunosuppressive cells that fail to get activated and promote CD8 T cells recruitment upon treatment or in some cases, by the poor responsiveness of the HPV+ keratinocytes to pro-inflammatory stimuli.



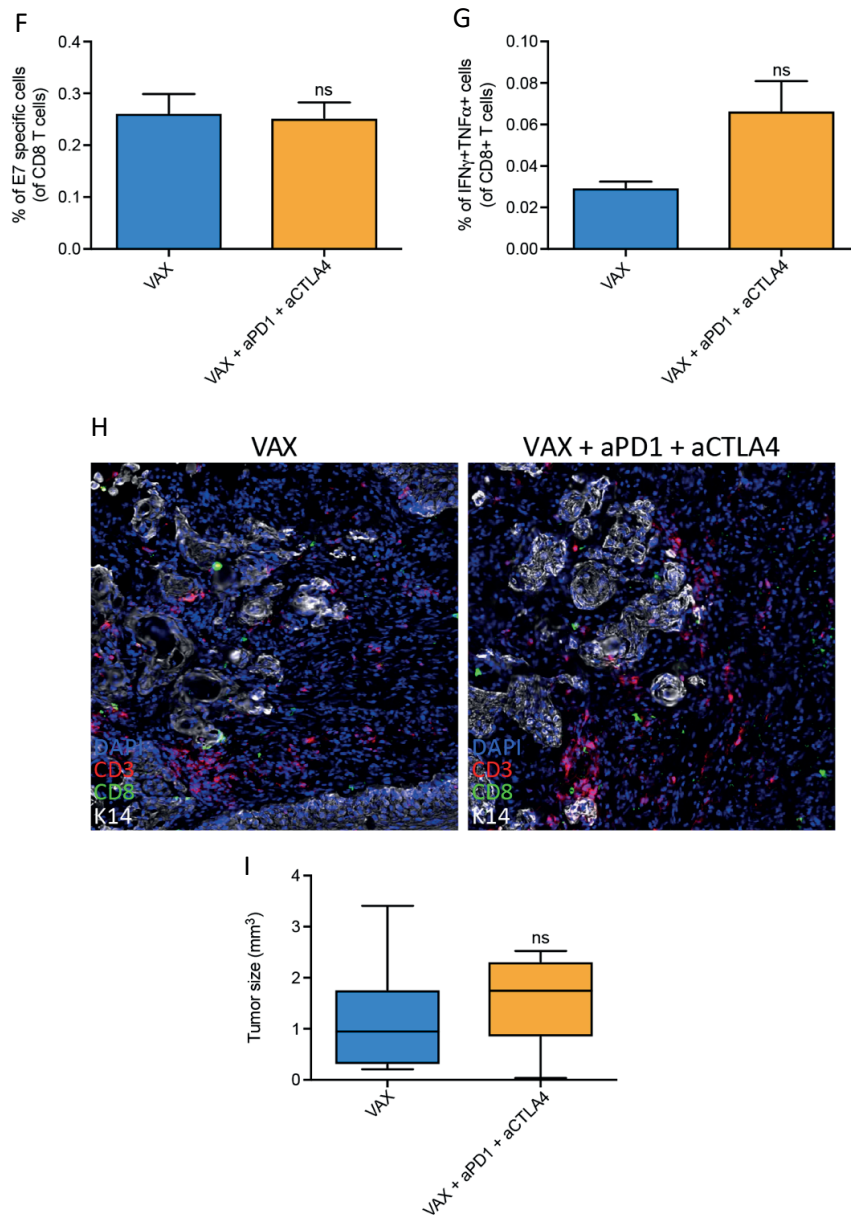


Figure 17. Analyses of the anti-E7 immune response, the TME and the tumor burden following combinatorial immunotherapy in HPV+ mice. (A, F) Flow cytometry analyses of E7-specific CD8 T cells in the lymph nodes using tetramers recognizing the HPV16 E7 CD8 peptide RAHYNIVTF presented on H2Db. (B, G) Flow cytometry analyses of IFN γ and TNF α production by lymph node - derived CD8 T cells after in-vitro re-stimulation with the HPV16 E7 CD8 peptide RAHYNIVTF. (C) Immuno-fluorescent staining for keratin 14 (red) and CD8 (green) on 10 μ m sections derived from frozen OCT-embedded cervixes. Representative fields of the tissue is shown. (D) Quantification of CD8 T cell infiltrates. Staining for keratin14 was performed to distinguish the tumor/epithelium

from the surrounding tissue. Quantifications were performed using Fiji (ImageJ) and have been performed separately for cells inside the tumors (Inside K14+ area) and in the surrounding stroma (Outside K14+ area). D) CD8/Treg cells ratio calculated on the tissue slides. (E, I) Quantification of the cervical tumor size. (H) Immuno-fluorescent staining for keratin 14 (white), CD3 (red) and CD8 (green) on 10µm sections derived from frozen OCT-embedded cervixes. Representative fields of the tissue are shown. At least 3 fields per mouse were imaged. Values per mouse are the averaged measurement of the acquired fields. All the groups are n=4. Statistics: * $p < 0.05$; ** $p < 0.01$; *** $p < 0.001$; **** $p < 0.0001$; n.s. = not significant.

3.2.16 Targeting APCs with anti-CD40 agonistic antibody does not boost the anti-E7 immune response following vaccination.

I previously determined that APCs functions are impaired in HPV+ mice, and therefore, I reasoned that boosting their activation might improve the anti-E7 immune response elicited by the NP vaccine. To test for this, I delivered the anti-E7 NP vaccine with an anti-CD40 (aCD40) agonistic antibody, administered at the same time as the vaccine.

Female HPV+ mice received a first shot of the combined treatment at 5 months of age (day 0) and a second one 14 days later. Mice were sacrificed at day 24. The immune response in the vaccination site-draining lymph nodes of the mice was analyzed by flow cytometry and by re-stimulation of whole lymph nodes cells. My analyses showed that the combinatorial treatment failed to significantly improve the anti-E7 CD8 T cell response (Fig. 18A and B) and consequently, there was no reduction in the cervical tumor burden (Fig. 18C).

These results indicate that therapeutic engagement of the CD40 ligand is not sufficient to improve the immune response to the vaccine in HPV+ mice. Similarly to combinations with the antibodies mentioned above and in table 1, these results could be explained by a model-dependent non-responsiveness to certain antibodies or by the presence of potentially overwhelming immunosuppressive mechanisms.

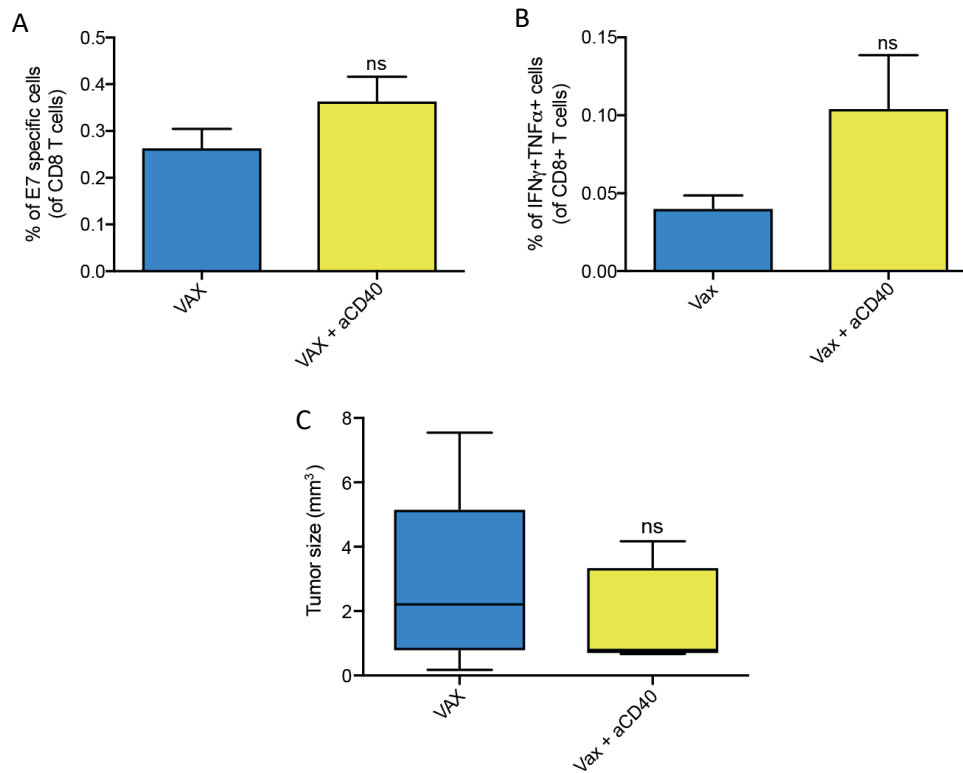


Figure 18. Analyses of the anti-E7 immune response and of the tumor burden following combinatorial immunotherapy with therapeutic vaccination and anti-CD40 in HPV+ mice. (A) Flow cytometry analyses of E7-specific CD8 T cells in the lymph nodes using tetramers recognizing the HPV16 E7 CD8 peptide RAHYNIVTF presented on H2Db. (B) Flow cytometry analyses of IFN γ and TNF α production by lymph node -derived CD8 T cells after in-vitro re-stimulation with the HPV16 E7 CD8 peptide RAHYNIVTF. (C) Quantification of the cervical tumor size. $n=4$. Statistics: * $p < 0.05$; ** $p < 0.01$; *** $p < 0.001$; **** $p < 0.0001$; n.s. = not significant.

3.2.17 Investigating the role of Tregs as potential immunosuppressive cells in HPV+ mice

The previous paragraphs illustrated how approaches based on the combination of therapeutic antibodies and the NP vaccine were not successful at boosting the anti-E7 response. I reasoned that the next step was to try disabling the immunosuppressive barriers present at the systemic level in the HPV+ mice starting from T regulatory cells, which have also been previously implicated in the general immunosuppression in a similar mouse model (182).

Although the percentage of Tregs is similar in the lymph nodes and spleen of HPV+ and HPV- mice, the higher expression of the IL-7 receptor (CD127) measured in HPV+ suggests that these cells

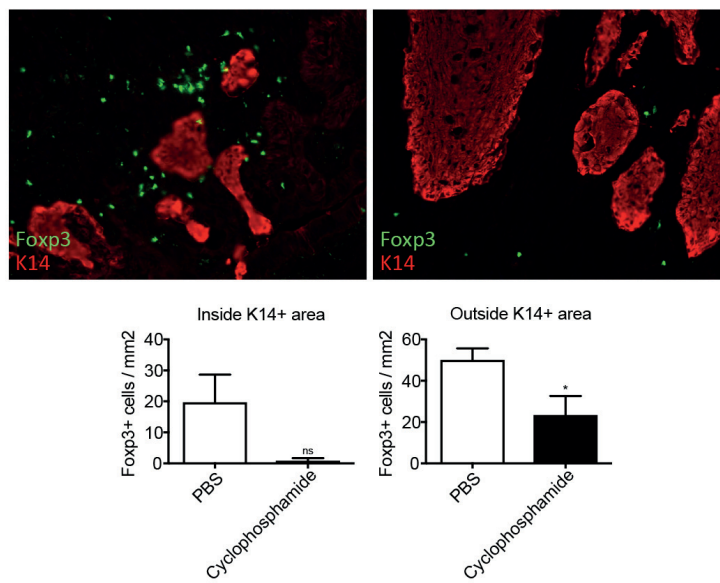
might be playing a role in suppressing immune responses in the HPV+ GEMM. In fact, CD127+ Tregs have been reported to be more suppressive than the CD127- counterpart (229).

3.2.18 Metronomic cyclophosphamide treatment depletes Tregs at the tumor site but kills the vaccine-elicited E7 specific CD8 T cells.

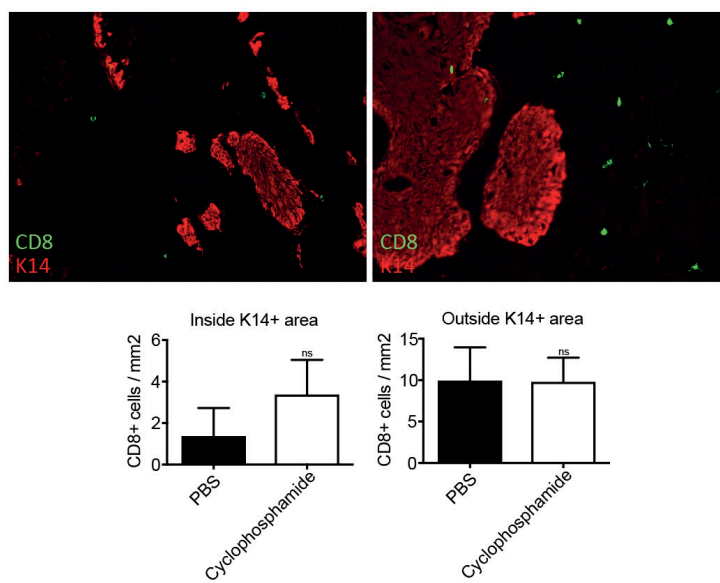
Treatment of 5 months old female HPV+ mice with continuous low dose cyclophosphamide for 4 weeks showed that this regimen can deplete Tregs in the TME (Fig. 19A) without affecting CD8 T cells infiltrates (Fig. 19B). Therefore, I decided to combine this treatment with our therapeutic NP-VAX against E7. Cyclophosphamide treatment was administered in the drinking water starting 5 days before vaccination and suspended for 2 days prior and after each vaccine shot. Mice were immunized twice at 5 months of age (day 0), boosted at day 14, and were sacrificed 5 days after the second shot at day 19. Flow cytometry analyses of the LNs showed that the cyclophosphamide treatment completely abrogated the generation of the E7-specific CD8 T cell response (Fig. 19C), suggesting that metronomic chemotherapy can kill the vaccine-specific CD8 T cells that are proliferating following immunization, at least with this regimen.

These results suggest that, although continuous low dose cyclophosphamide can deplete Tregs in the TME and possibly improve the CD8/Treg ratio, a potential successful combination with therapeutic vaccination, if feasible, might require a careful timing in order to avoid killing the immune cells generated following immunization.

A



B



C

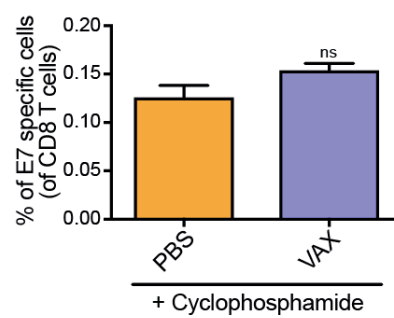


Figure 19. Analyses of the effects of metronomic cyclophosphamide on the TME and the anti-E7 response in HPV+ mice. (A, B) Immuno-fluorescent staining for keratin 14 (red) and Foxp3+ or CD8 (green) on 10 μ m sections derived from frozen OCT-embedded cervixes and relative quantifications. Representative fields of the tissue are shown. Staining for keratin14 was performed to distinguish the tumor/epithelium from the surrounding tissue. Quantifications were performed using Fiji (ImageJ) and have been performed separately for cells inside the tumors (Inside K14+ area) and in the surrounding stroma (Outside K14+ area). Groups: PBS n=4, Cyclophosphamide n=3. At least 5 fields per mouse were imaged. Values per mouse are the averaged measurement of the acquired fields. (C) Flow cytometry analyses of E7-specific CD8 T cells in the lymph nodes using tetramers recognizing the HPV16 E7 CD8 peptide RAHYNIVTF presented on H2Db. Groups: Cyclophosphamide n=5, Cyclophosphamide + VAX n=6. Statistics: * $p < 0.05$; ** $p < 0.01$; *** $p < 0.001$; **** $p < 0.0001$; n.s. = not significant.

3.2.19 Combinatorial strategies to target Tregs employing anti-CD25, anti-CD4 and anti-CTLA4 show poor depleting activity and fail to significantly boost immune responses.

Given the results with chemotherapy, I next resorted to the use of depleting antibodies to eliminate the T regulatory cells in HPV+ mice.

I first used an anti-CD25 (aCD25) depleting antibody that has been widely used to preferentially target Tregs in virtue of their high expression of CD25. As CD25 is also expressed on activated CD8 T cells so, to avoid depleting the newly generated E7 specific CD8 T cells following vaccination, I pre-treated HPV+ mice for 3 days before administering the NP-VAX against E7. Mice received 2 shots of the NP-VAX at day 0 and day 14 and were sacrificed at day 19. Unfortunately, flow cytometry analyses on the blood performed 6 days after immunization revealed that Foxp3+CD4+ Tregs were not depleted by the antibody treatment. Interestingly, there was a shift in the CD25 staining (performed using the same antibody clone) of the CD4+Foxp3+ population (Fig. 20A) that suggest that, although the depleting antibody was still present and bound to the Tregs, the cells were not getting eliminated. As expected given the results of the depletion, when I looked at the vaccination-site draining lymph nodes at day 19, there was no reduction of Tregs (Fig. 20B) nor in the CD127+ Tregs (Fig. 20C) and the immune response to the vaccine was unchanged (Fig. 20D).

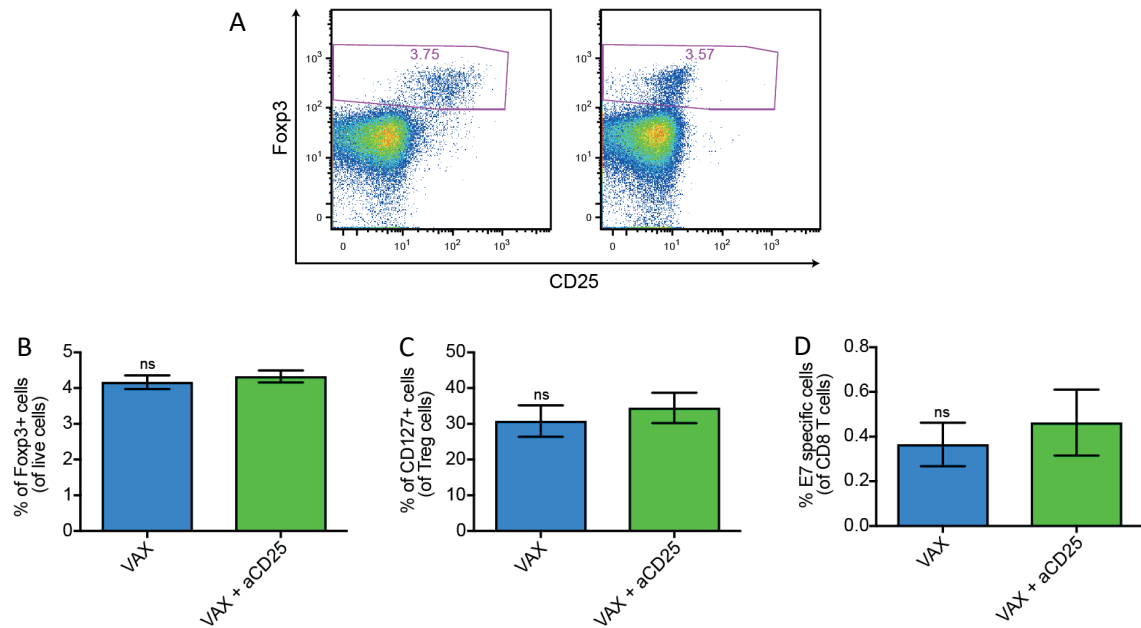


Figure 20. Analyses of Treg depletion with anti-CD25 and its effect on the anti-E7 response in HPV+ mice. (A) Representative dot plot from flow cytometry analyses of HPV+ mice lymph nodes. Cells were gated on live CD3+CD4+ cells. (B) Flow cytometry analyses of Foxp3+ Tregs in the lymph nodes of HPV+ mice. (C) Flow cytometry analyses of CD127+ Tregs in the lymph nodes of HPV+ mice. (D) Flow cytometry analyses of E7-specific CD8 T cells in the lymph nodes using tetramers recognizing the HPV16 E7 CD8 peptide RAHYNIVTF presented on H2Db. n=4. Statistics: *p < 0.05; **p < 0.01; ***p < 0.001; ****p < 0.0001; n.s. = not significant.

I then decided to try a different approach and use an anti-CD4 (aCD4) depleting antibody to eliminate the whole CD4+ population that includes the Tregs. I reasoned that depletion of the CD4 T cells should not negatively impact the response to the NP-VAX against E7 since we previously reported in the TC1 model how the CD8 response is independent from CD4 T cells. In addition, I showed that the CD4 response is anyway severely defective in HPV+ mice, as previously demonstrated by the almost undetectable cytokine production by these cells in vaccinated mice. I used the same schedule as the previous experiment but, contrarily to what I did with aCD25, the aCD4 antibody was administered 3 times per week throughout the experiment. Since depletion of CD4 T cells could lead to an improvement of the immune response (231), as a control, both HPV+ and HPV- mice were used in this experiment comparing vaccine alone or vaccine combined with

aCD4. When I sacrificed the mice, I measured by flow cytometry a significant CD4 depletion in the lymph nodes (Fig. 21A) that was also accompanied by a similar reduction in the Tregs (Fig. 21B). Importantly, reduction of the CD4⁺ T cells was not simply due to a shift in the population caused by the presence of the depleting antibody indicating that CD4 T cells were actually getting eliminated. As previously reported, both the percentage of E7-specific CD8 T cells (Fig. 21C) and the cytokine production after re-stimulation (Fig. 21D) were higher in HPV⁻ mice. Although CD4 T cells depletion did not cause any significant changes in HPV⁻ mice, CD4 T cells-depleted HPV⁺ mice showed a significant increase in the percentage of E7-specific CD8 T cells and a small increase in cytokine production from re-stimulated whole lymph node cells. However, the change in IFN γ and TNF α production was not significant, and it remained substantially lower than what was measured in HPV⁻ mice. These results show that there might be a beneficial effect coming from CD4 depletion, although I cannot determine if the benefit is due to the elimination of Tregs. However as already mentioned, a similar effect has already been reported following CD4 depletion (231), implicating that the small improvement seen in HPV⁺ mice might not be happening as a consequence of a reduced immunosuppressive population specific to these mice.

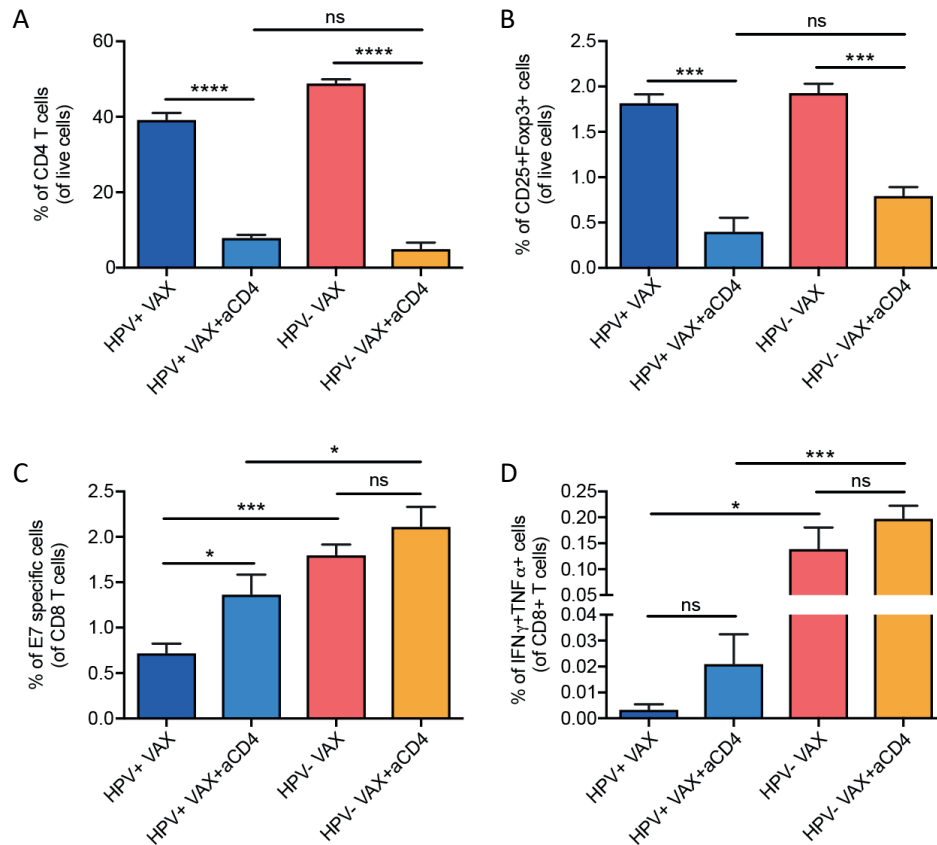


Figure 21. Analyses of the effects of CD4 T cell depletion on the anti-E7 immune response. (A) Flow cytometry analyses of CD4⁺ T cells in the lymph nodes of HPV⁺ mice. (B) Flow cytometry analyses of CD25⁺Foxp3⁺ Tregs in the lymph nodes of HPV⁺ mice. (C) Flow cytometry analyses of E7-specific CD8 T cells in the lymph nodes using tetramers recognizing the HPV16 E7 CD8 peptide RAHYNIVTF presented on H2Db. (D) Flow cytometry analyses of IFN γ and TNF α production by lymph node -derived CD8 T cells after in-vitro re-stimulation with the HPV16 E7 CD8 peptide RAHYNIVTF. $n=4$. Statistics: * $p < 0.05$; ** $p < 0.01$; *** $p < 0.001$; **** $p < 0.0001$; n.s. = not significant.

I next tried to perform a preliminary experiment combining aCD25 and aCD4 treatment. Although the aCD25 showed poor depletion capabilities as a single treatment, I reasoned that layering these 2 antibodies might help further reducing the Treg numbers compared to aCD4 alone.

HPV⁺ mice were treated as previously shown, aCD25 was given as a pre-treatment while aCD4 was administered throughout the experiment and mice received 2 shots of the NP-VAX either alone or

in combination with both depleting antibodies. When mice were sacrificed at day 19, I performed flow cytometry analyses on the lymph nodes where, although I measured a significant decrease in total CD4⁺ cells (Fig. 22A), the reduction in the Treg numbers was limited and not significant (Fig. 22B) almost as if aCD25 interfered with the depletion of Tregs. Similarly to the previously shown combination of VAX+aCD4, I measured a significant increase in the percentage of E7-specific CD8 T cells (Fig. 22C) while cytokine production was not improved (Fig. 22D). These results show that combining aCD4 and aCD25 does not lead to a better Treg depletion but, surprisingly, it seems to make the Treg depletion less effective. The less effective Treg depletion observed in this experiment suggests that the benefits elicited by aCD4 treatment in terms of percentage of E7 specific CD8 T cells, might not be related to a reduction in Tregs.

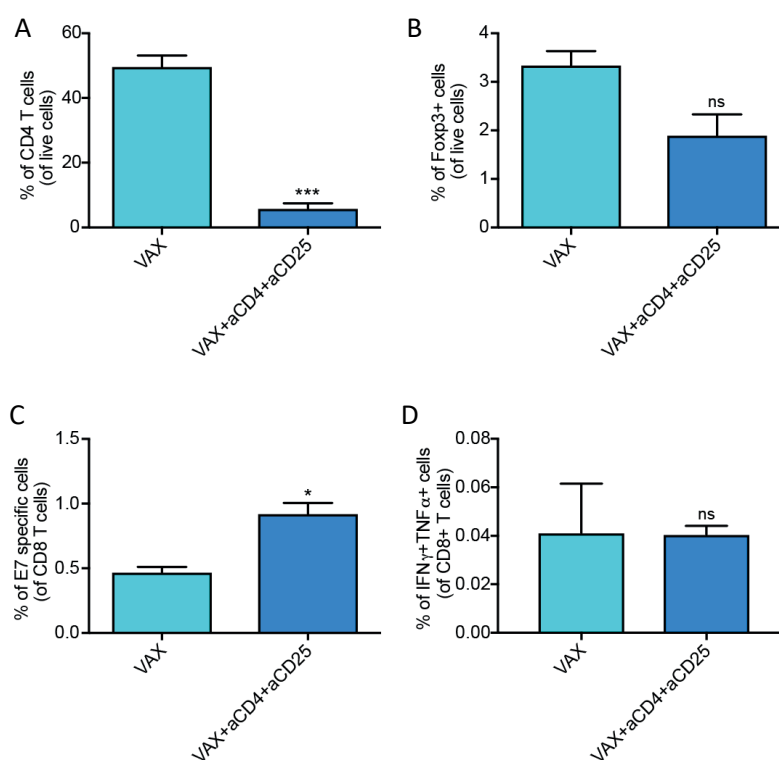


Figure 22. Analyses of the effects of combined anti-CD4 and anti-CD25 treatment on the anti-E7 immune response. (A) Flow cytometry analyses of CD4⁺ T cells in the lymph nodes of HPV⁺ mice. (B) Flow cytometry analyses of Foxp3⁺ Tregs in the lymph nodes of HPV⁺ mice. (C) Flow cytometry analyses of E7-specific CD8 T cells in the lymph nodes using tetramers recognizing the HPV16 E7 CD8 peptide RAHYNIVTF presented on H2Db. (D) Flow cytometry analyses of IFN γ and TNF α

*production by lymph node -derived CD8 T cells after in-vitro re-stimulation with the HPV16 E7 CD8 peptide RAHYNIVTF. Groups: VAX n=2, VAX + aCD4 + aCD25 n=3. Statistics: * $p < 0.05$; ** $p < 0.01$; *** $p < 0.001$; **** $p < 0.0001$; n.s. = not significant.*

Finally, in a last attempt at specifically target Tregs, I combined the aCD25 antibody with a non-commercially available anti-CTLA4 (aCTLA4) antibody (kindly provided by BMS) that has been observed to be capable of targeting and depleting Tregs (232).

HPV+ mice were immunized with the NP-VAX against E7 either alone or in combination with aCD25 pre-treatment with or without the addition of aCTLA4 that started 1 day before vaccination and was administered throughout the experiment 2 times per week. As in the previous experiments, mice received 2 shots of vaccine 14 days apart and were sacrificed 19 days after the first shot. Upon sacrifice, I analyzed the vaccination site-draining lymph nodes of the mice by flow cytometry. The analyses showed that CD4 T cells were not affected by the treatment (Fig. 23A) while Tregs were only slightly lower in the group that received aCD25 (Fig. 23B) confirming the poor depleting activity by this antibody observed in our model. Treatment with aCD25+aCTLA4, on the other hand, did not show Treg depletion (Fig. 23B). Consistent with the poor depletion and with the previously reported combinatorial trials involving aCTLA4, I did not measure any significant improvement in the anti-E7 immune response either as percentage of E7-specific CD8 T cells (Fig. 23C) or as cytokine production by these cells after re-stimulation (Fig. 23D).

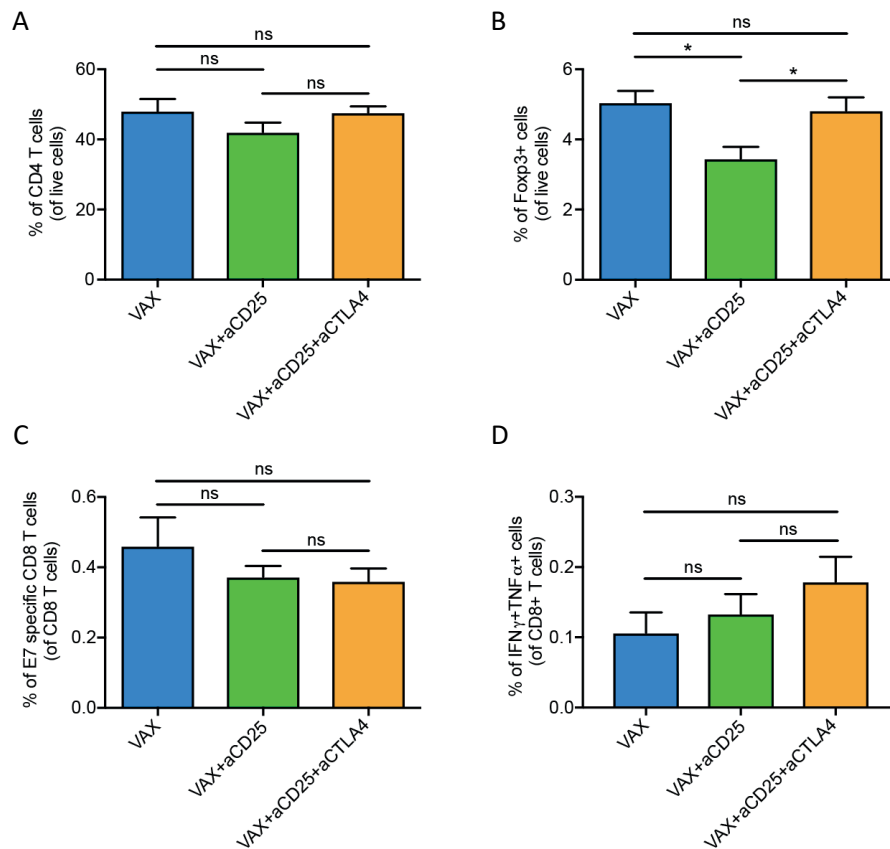


Figure 23. Analyses of the effects of combined anti-CD4 and anti-CTLA4 treatment on the anti-E7 immune response. (A) Flow cytometry analyses of CD4⁺ T cells in the lymph nodes of HPV⁺ mice. (B) Flow cytometry analyses of Foxp3⁺ Tregs in the lymph nodes of HPV⁺ mice. (C) Flow cytometry analyses of E7-specific CD8 T cells in the lymph nodes using tetramers recognizing the HPV16 E7 CD8 peptide RAHYNIVTF presented on H2Db. (D) Flow cytometry analyses of IFN γ and TNF α production by lymph node -derived CD8 T cells after in-vitro re-stimulation with the HPV16 E7 CD8 peptide RAHYNIVTF. $n=4$. Statistics: * $p < 0.05$; ** $p < 0.01$; *** $p < 0.001$; **** $p < 0.0001$; n.s. = not significant.

For this last experiment, I decided to also look at the cytokine production after re-stimulation of whole splenocytes, measuring a situation virtually identical to the one in the lymph nodes (Fig. 24A). However, I decided to specifically isolate the CD8 T cells from the splenocytes mix by magnetic bead-mediated negative selection, and perform my re-stimulation assay with CD8 T cells

only. Surprisingly, I measured a significant increase in cytokine production in both groups that was rather small in the VAX+aCD25 group but was 2-fold in the VAX+aCD25+aCTLA combination (Fig. 24B).

Since these differences were not shown when the re-stimulation was performed on the whole splenocytes, these results suggest that these combinatorial treatments were actually able to generate higher numbers of E7-specific CD8 T cells capable of cytokine production, but that these beneficial effects were masked in the splenocytes mix, possibly by the presence of a suppressive cell population.

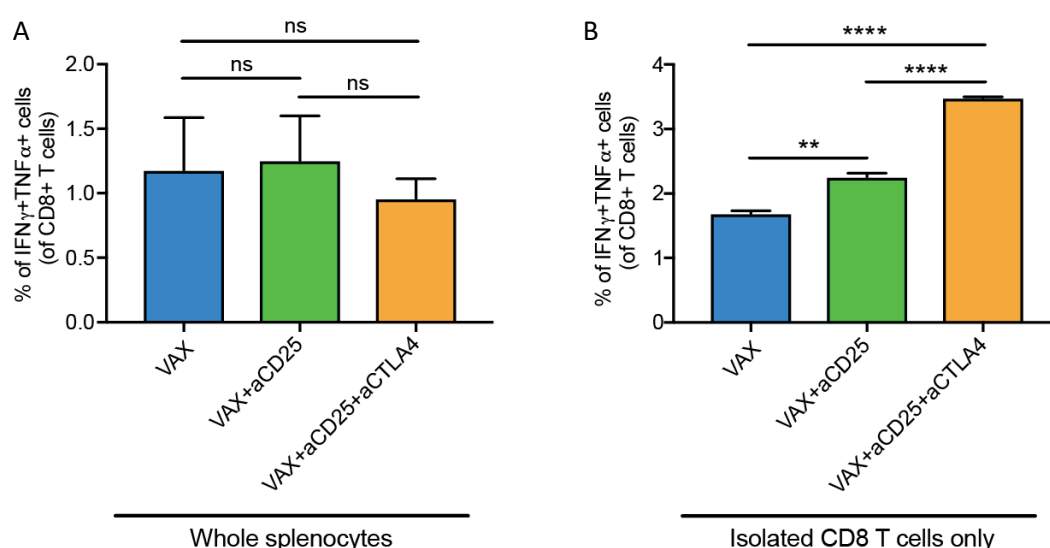


Figure 24. Ex-vivo re-stimulation assay on whole splenocytes and isolated CD8 T cells. Flow cytometry analyses of IFN γ and TNF α production from CD8 T cells after in-vitro re-stimulation with the HPV16 E7 CD8 peptide RAHYNIVTF ($n=4$). A) Whole splenocytes or B) isolated CD8 T cells only were used for the assay. Statistics: * $p < 0.05$; ** $p < 0.01$; *** $p < 0.001$; **** $p < 0.0001$; n.s. = not significant.

In conclusion, the Treg depletion experiments in HPV+ mice presented above, illustrate a situation where specifically eliminating Tregs is unfeasible, at least with the approaches that I tried, making it impossible to clearly determine if they are playing a part in the systemic immunosuppression in

HPV+ mice. However, the results from the last ex-vivo re-stimulation experiment presented, suggests that there is indeed a suppressive population in the splenocytes mix, whose activity is maintained in vitro.

3.2.20 In-vitro co-culture of Tregs with CD8 T cells and DCs does not increase in the suppressive activity of HPV+ mice-derived Tregs over the HPV- counterparts.

To further look into the role of Tregs, I set up a series of in-vitro co-culture assays to compare the suppressive activity of HPV+ and HPV- -derived Tregs on CD8 T cells proliferation, on E7-specific CD8 T cells cytokine production, and on BMDCs activation. The aim of this series of experiment was to check if Tregs isolated from HPV+ mice had a superior immunosuppressive activity compared to Tregs from HPV- mice that could explain the reduced responses to the NP-VAX seen in the GEMM.

To assess the effects of Tregs on CD8 T cells proliferation, I isolated CD4+CD25+ Tregs-enriched cells from both HPV+ (HPV+ Tregs) and HPV- (HPV- Tregs) mice and CD8 T cells from HPV- mice using magnetic beads. CD8 T cells were labeled with CFSE to follow their proliferation, they were mixed with the CD4+CD25+ Treg-enriched population in a 1:10 CD8:Treg ratio and cultured in an anti-CD3 anti-CD28 coated plate. As control, I co-cultured the CFSE-labeled CD8 with the CD4+CD25- Treg-depleted cell population (HPV+CD4 and HPV-CD4) that I recovered from the magnetic separation. After 48h in culture, the cells were recovered, and CFSE+ CD8 T cells proliferation was measured by flow cytometry by gating on the CFSElow cells. Although the Tregs-enriched cells suppressed the CD8 T cells proliferation compared to the control condition with the Treg-depleted CD4 T cells, there was no difference between cells derived from HPV+ and HPV- mice (Fig. 25A).

I then performed a similar assay, but this time CD8 T cells were isolated from an HPV- mouse that has been previously immunized with the NP-VAX against E7. CD8 T cells were mixed with either the Treg-enriched population or with the Treg-depleted CD4 population in a 1:10 ratio and I performed a re-stimulation assay. Cytokine production was lower when CD8 T cells were co-cultured with the Tregs-enriched population compared to the Tregs-depleted CD4 control

condition, however, consistently to what I observed for the CD8 T cells proliferation, there was no difference in suppressive activity between cells derived from HPV+ or HPV- mice (Fig.25B).

Finally, to assess if the suppressive activity of Tregs was affecting APCs I generated BMDCs from an HPV- mouse bone marrow and, after overnight activation with CpG, BMDCs were co-cultured in the same conditions used for the previous assays, namely in the presence of the Tregs-enriched population or with the Tregs-depleted CD4 cells in a 1:10 ratio. After 24h of co-culture, the cells were harvested and analyzed by flow cytometry. MFI analyses on CD11b-CD11c+ DCs revealed that, although Tregs were also suppressing BMDCs activation, there was once again no difference in the suppressive ability of HPV+ or HPV- derived cells (Fig. 25C).

These in-vitro results show that, despite the difference in phenotype evidenced by an increased expression of the IL-7 receptor expression (CD127) by Tregs from HPV+ mice, there seems to be no difference in the suppressive capability of these cells compared to Tregs isolated from HPV- mice. Although it is possible that the in-vitro results might not reflect the in-vivo activity of these cells (that could have lost CD127 expression in the co-culture), it seems nonetheless reasonable to assume that Tregs are not a key immunosuppressive barriers in HPV+ mice and therefore, do not represent an attractive population to target in order to relieve the systemic immunosuppression.

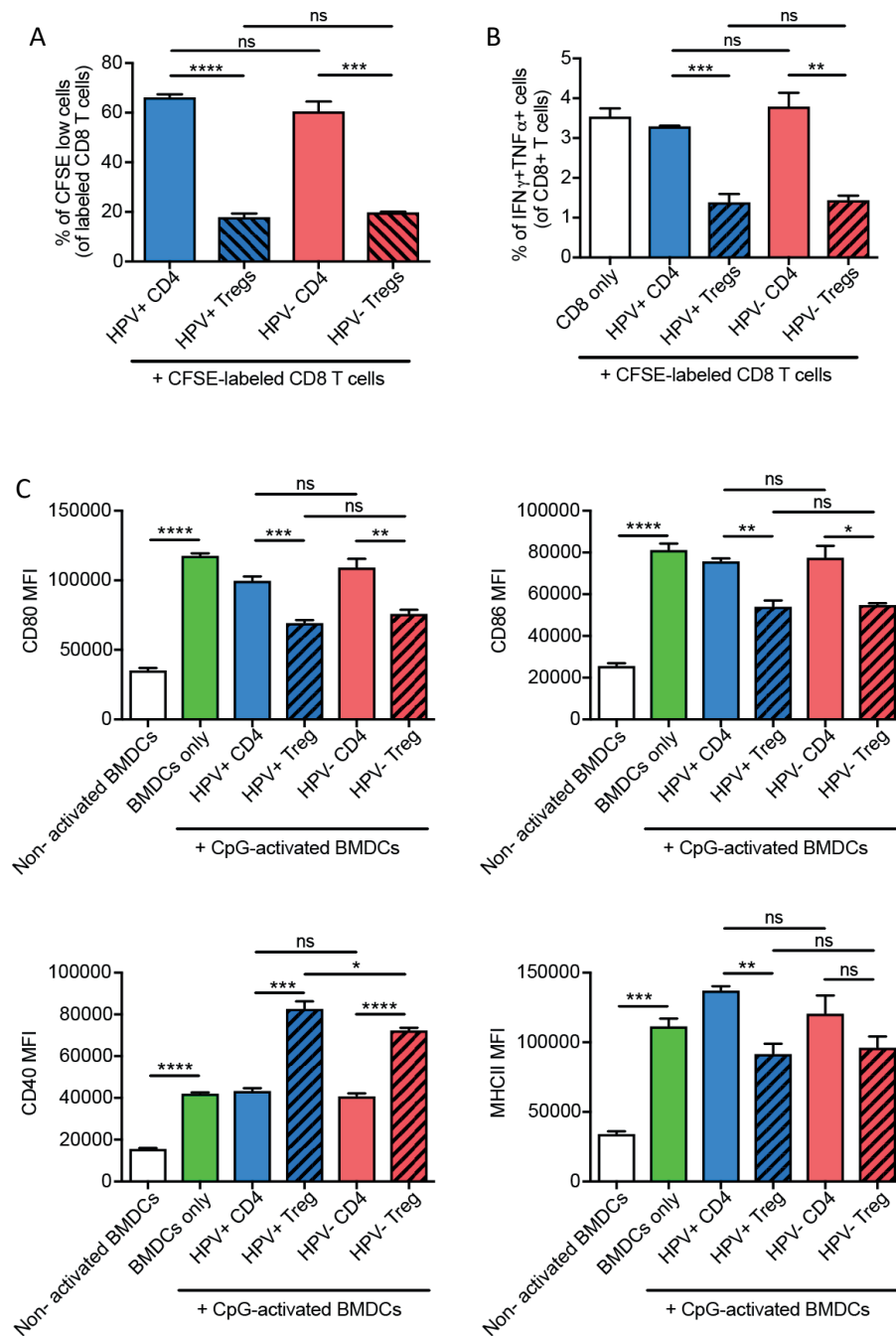


Figure 25. In-vitro co-cultures of CD8 T cells or BMDCs with HPV+ or HPV- mice -derived Tregs. (A) Flow cytometry analyses of CFSE low CD8 T cells after 48h co-culture in the presence of HPV+ or HPV- spleen-derived CD4+CD25+ Tregs-enriched cells in an anti-CD3 anti-CD28 coated plate (n=3). (B) Flow cytometry analyses of IFN γ and TNF α production from CD8 T cells after in-vitro re-

*stimulation with the HPV16 E7 CD8 peptide RAHYNIVTF in the presence of HPV+ or HPV- spleen-derived CD4+CD25+ Tregs-enriched cells (n=3). (C) Mean fluorescence intensity measured by flow cytometry analyses on HPV+ and HPV- CD11b-CD11c+ cells activation markers after overnight activation of BMDCs with CpG followed by 24h co-culture in the presence of HPV+ or HPV- spleen-derived CD4+CD25+ Tregs-enriched cells (n=3). Gating strategy for this population can be found in the Appendix Fig. 10. Statistics: * $p < 0.05$; ** $p < 0.01$; *** $p < 0.001$; **** $p < 0.0001$; n.s. = not significant.*

3.2.21 Myeloid cells from HPV+ mice suppress CD8 T cells proliferation and cytokine production and impair DCs activation.

I next focused my attention on the myeloid cells. I reasoned that given the substantial increase that I measured in HPV+ mice, these cells could be immature cells playing a major role in suppressing the immune response, the so-called myeloid-derived suppressor cells (MDSCs). Importantly, a recent update on a previous report by Sjoerd van der Burg at the ESMO conference (Geneva, 2017) suggested that these cells might be playing a predominant suppressive role towards vaccine-elicited anti-tumor immune responses in patients with cervical cancer (111). According to the literature on the field, in order to be able to classify myeloid cells as MDSCs, they need to be capable of suppressing CD8 T cells proliferation and cytokine production (233). Therefore, I conducted ex-vivo assays to assess their suppressive functions.

To test the effects of myeloid cells on CD8 T cells proliferation, I performed an in-vitro co-culture experiment with isolated CD11b+ cells and CFSE-labeled CD8 T cells isolated from a naïve HPV- mouse. The assay was performed in an anti-CD3 and anti-CD28 –coated plate to trigger CD8 T cell proliferation. Similarly to what I saw for cytokine production, CD8 T cells proliferation was significantly impaired in the presence of HPV+ mice -derived myeloid cells as indicated by the lower amount of CFSElow cells recovered from the co-culture (Fig. 26A).

I then isolated CD11b+ cells from HPV+ and HPV- as well as CD8 T cells from an immunized HPV- mouse using magnetic separation. An in-vitro re-stimulation assay using the E7-derived CD8 peptide was performed by mixing CD8 T cells and myeloid cells at a 1:10 ratio, after which I assessed IFN γ and TNF α production from CD8 T cells by flow cytometry. A significantly lower

percentage of IFN γ and TNF α double positive cells was measured when the CD8 T cells were in the presence of HPV+ mice -derived myeloid cells (Fig. 26B).

Additionally, a preliminary experiment conducted using a trans-well to separate the myeloid cells (in the upper part) from CFSE-labeled CD8 T cells (on the bottom, also coated with anti-CD3 antiCD28), suggests that the suppressive activity of the former could be mediated by a soluble factor (Fig. 26C).

Since APCs activation is also impaired in HPV+ mice, I then set out to test if myeloid cells isolated from HPV+ mice could also suppress DCs activation. To test for this, I generated BMDCs from the bone marrow of HPV- mice and activated them overnight with LPS or with PBS as negative control for activation. The following day, CD11b+ cells isolated from either HPV+ or HPV- mice were added to the BMDCs and were co-cultured for 24h in a 1:10 BMDCs to CD11b+ cells ratio. Prior to mixing the cells, BMDCs were labeled with CFSE in order to distinguish them from other DCs that might have been included in the isolated CD11b+ cell mix. Flow cytometry analyses of CFSE+ BMDCs revealed that upregulation of the activation markers CD40, CD86 and MHCII were lower when the cells were co-cultured with HPV+ derived myeloid cells compared to the HPV- -derived ones (Fig. 26D). Interestingly, the expression of these markers in the co-culture with HPV+ myeloid cells was similar to the condition with BMDCs alone. This result suggests that at least in-vitro, rather than performing a direct inhibition of the APCs activation, the myeloid cells in HPV+ mice could be lacking the ability to promote the complete activation of the BMDCs that is instead seen in the presence of HPV- derived myeloid cells.

Collectively, these data show that CD11b+ myeloid cells (now also definable as bonafide MDSCs) isolated from HPV+ mice can impair both CD8 T cells responses and APCs activation in-vitro, establishing them as a potential major barrier to immunotherapy that could be acting systemically to impair immune responses and suppress tumor-specific CD8 T cells even before they reach the tumor site. As previously mentioned, high levels of myeloid cells have been reported in the circulation of HPV-related cancer patients (111, 126, 155, 158). These observations potentially make the study of immunosuppression by MDSCs in the K14HPV16 H2b (HPV+) mouse model of great interest and relevance for the treatment of cervical and other HPV-related forms of cancer.

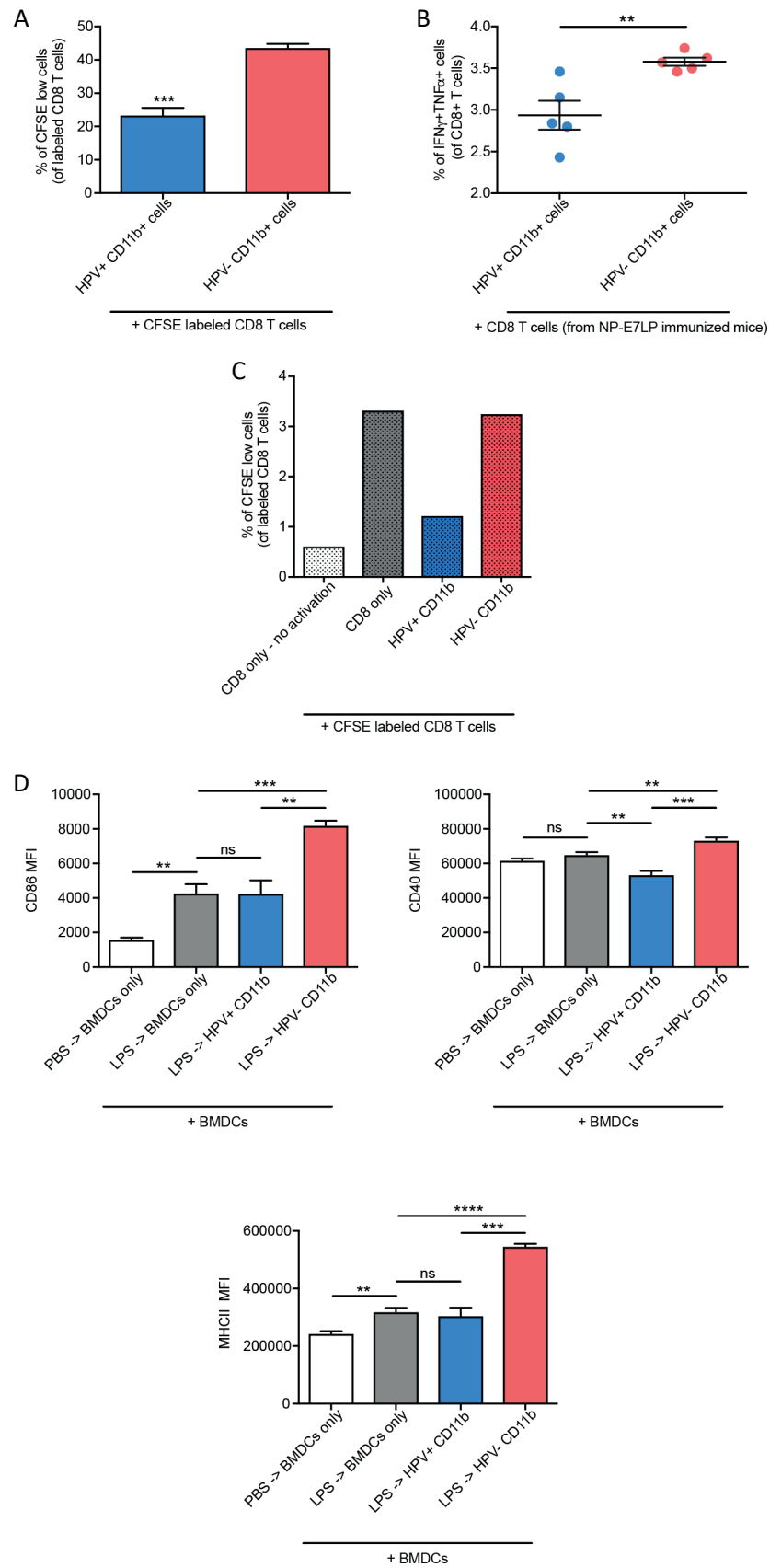


Figure 26. In-vitro co-culture of CD8 T cells and BMDCs with HPV+ or HPV- mice –derived CD11b+ myeloid cells. (A) Flow cytometry analyses of CFSE low CD8 T cells after 48h co-culture in the presence of HPV+ or HPV- spleen-derived CD11b+ cells in an anti-CD3 anti-CD28 coated plate (n=4). (B) Flow cytometry analyses of IFN γ and TNF α production from CD8 T cells after in-vitro re-stimulation with the HPV16 E7 CD8 peptide RAHYNIVTF in the presence of HPV+ or HPV- spleen-derived CD11b+ cells (n=5). (C) Flow cytometry analyses of CFSE low CD8 T cells after 48h co-culture in a trans-well in the presence of HPV+ or HPV- spleen-derived CD11b+ cells in an anti-CD3 anti-CD28 coated plate (n=1). CD8 T cells were plated on the bottom while CD11b+ cells were plated inside a trans-well. (D) Flow cytometry analyses HPV+ and HPV- CD11b-CD11c+ cells activation markers after overnight activation of BMDCs with CpG and 24h co-culture in the presence of HPV+ or HPV- spleen-derived CD11b+ cells (n=4). Statistics: * $p < 0.05$; ** $p < 0.01$; *** $p < 0.001$; **** $p < 0.0001$; n.s. = not significant.

3.2.22 Myeloid cells in HPV+ mice are a source of immunosuppressive factors and produce increased reactive oxygen species.

Since I measured increased immunosuppressive factors in the LNs of HPV+ mice, I then wanted to test if myeloid cells could constitute a source for them. I isolated CD11b+ cells from the spleen of HPV+ and HPV- mice and used as control the myeloid cells -depleted splenocytes that were recovered after isolation. I then performed protein extraction followed by western blotting. The same amount of protein was loaded into each well, therefore, it is important to keep in mind that HPV+ mice have a higher number of myeloid cells compared to HPV- mice and that these results might not account for this difference in numbers.

My results showed that IL-10 and IDO were significantly more abundant in the CD11b+ cells isolated from HPV+ mice compared to the HPV- -derived myeloid cells and to both the splenocytes preparations (Fig. 27A and B). COX-2 was instead increased in the myeloid cells -depleted splenocytes compared to the isolated CD11b+ cells (Fig. 27A and B) suggesting that its main source could be a non-myeloid population. Arginase 1 (Arg1) was instead upregulated in the HPV- myeloid cells by 3-fold (Fig. 27C and D). The increase Arg1 presence detected in the HPV+ mice lymph nodes could come from the tumor cells directly, or it could still be coming from the myeloid

cells, in fact, although they seem to be expressing it at lower levels, their higher numbers might compensate for this difference.

Additionally, to assess the capacity of myeloid cells to produce immunosuppressive reactive oxygen species (ROS) (234), I stained HPV+ and HPV- mice -derived myeloid cells with the ROS reactive dye DCFDA. Positive controls for ROS production were performed by treating the cells with PMA. This assay revealed that HPV+ mice- derived CD11b+ cells are capable of producing higher levels of ROS (Fig. 27E).

These results show that HPV+ mice-derived CD11b+ myeloid cells are a major source of at least some the immunosuppressive factors that are present in the LNs and that they can produce higher quantities of ROS compared to the HPV- -derived counterparts. These and the previously shown in-vitro data collectively suggest that myeloid cells might be playing a major role in suppressing immune responses in the HPV+ GEMM.

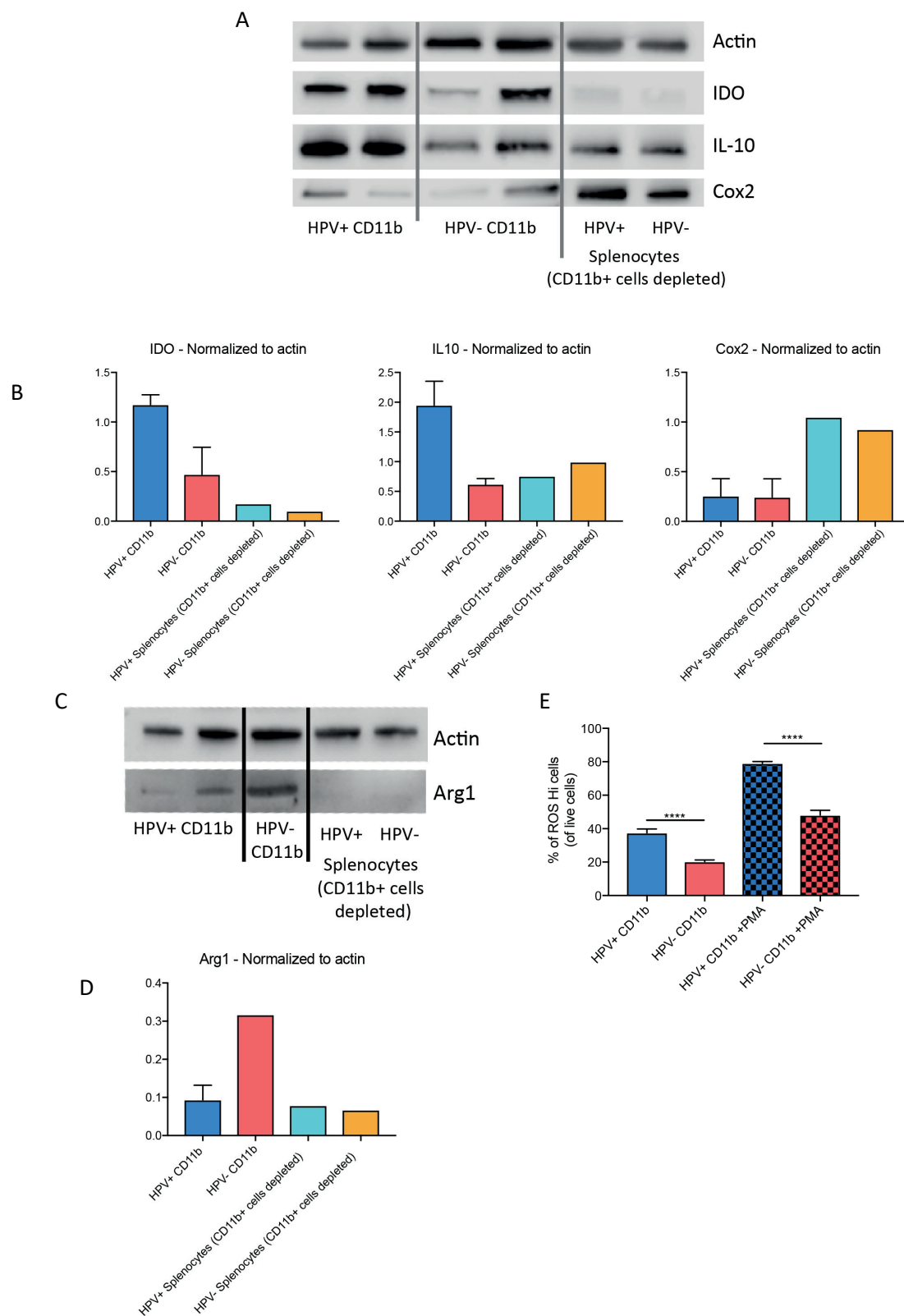


Figure 27. Production of immunosuppressive factors by myeloid cells. (A, C) Western blot of protein extracts from HPV+ and HPV- mice spleen -derived CD11b+ cells or from the respective CD11b+ cells-depleted whole splenocytes. (B, D) Quantification of the western blot bands normalized to actin. (E) Flow cytometry analyses of HPV+ and HPV- spleen -derived CD11b+ cells stained with DCFDA (n=5, PMA treated groups n=4). Statistics: * $p < 0.05$; ** $p < 0.01$; *** $p < 0.001$; **** $p < 0.0001$; n.s. = not significant.

3.2.23 In-vitro blocking of IL-10 does not rescue the immunosuppression by MDSCs.

After discovering that MDSCs are a major source of immunosuppressive factors in the LNs of HPV+ mice, I set out to block these factors in my in-vitro assays to assess their role in the immunosuppression.

I first focused my attention on IL-10 as it can be specifically blocked with neutralizing antibodies. After confirming that HPV+ -derived MDSCs were releasing higher levels of IL-10 in the supernatant when kept in culture (Fig. 28A and B), I performed the CD8 proliferation and BMDCs activation assays as previously described, with and without the addition of an anti-IL-10 antibody in the culture media. Unfortunately, blocking IL-10 did not show any benefit in both CD8 proliferation (Fig. 28C) of BMDCs activation (Fig. 28D), suggesting that IL-10, at least in-vitro, might not be exerting a predominant role in suppressing immune responses or alternatively, that other redundant mechanisms are compensating or are enough to maintain a similar level of suppression even in the absence of IL-10.

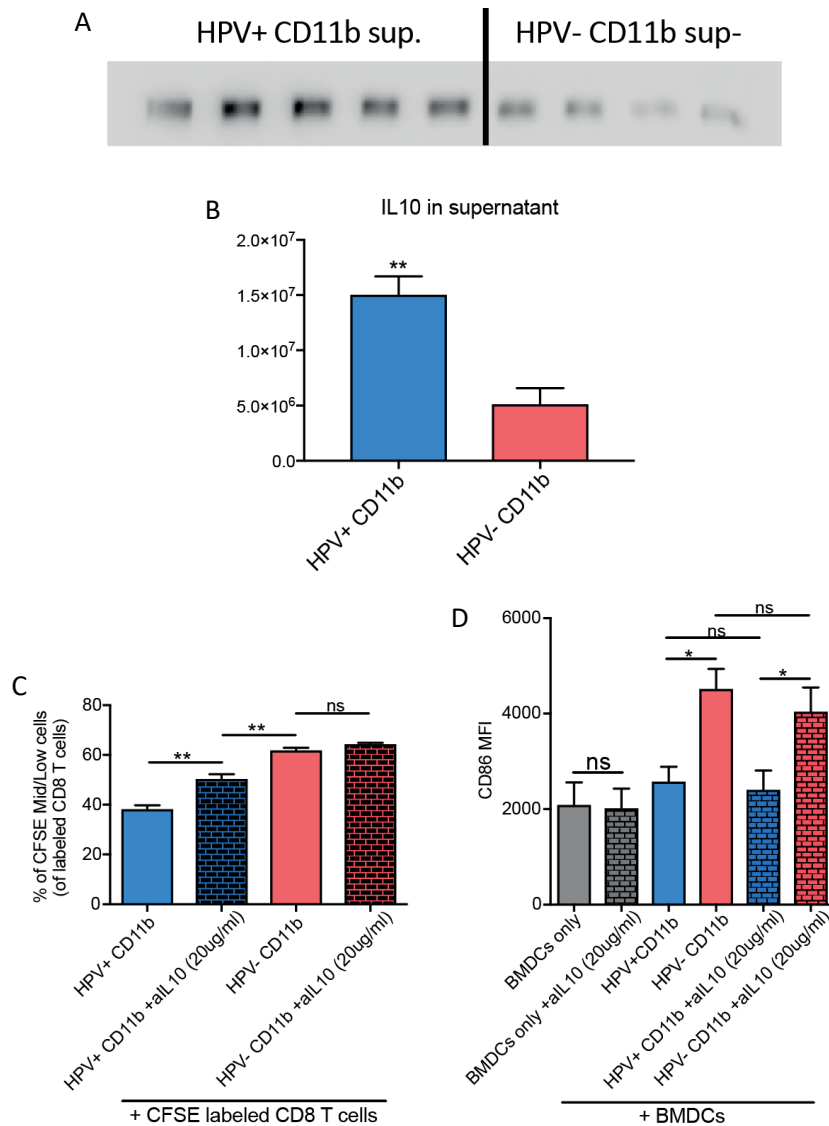


Figure 28. In-vitro analyses of the role of IL-10 in myeloid cell-mediated suppression. (A) Western blot for IL-10 of supernatant derived from 48h culture of HPV+ and HPV- spleen-derived CD11b+ cells. The same volume of supernatant was loaded into each well. (B) Quantification of the western blot bands. (C) Flow cytometry analyses of CFSE Mid/Low CD8 T cells after 48h co-culture in the presence of HPV+ or HPV- spleen-derived CD11b+ cells in an anti-CD3 anti-CD28 coated plate and in the presence of an anti-IL10 neutralizing antibody (n=4). (D) Flow cytometry analyses of IFN γ and TNF α production from CD8 T cells after in-vitro re-stimulation with the HPV16 E7 CD8 peptide

*RAHYNIVTF in the presence of HPV+ or HPV- spleen-derived CD11b+ cells and of an anti-IL10 neutralizing antibody (n=4). Statistics: * $p < 0.05$; ** $p < 0.01$; *** $p < 0.001$; **** $p < 0.0001$; n.s. = not significant.*

3.2.24 In-vitro treatment with IDO inhibitors do not rescue CD8 T cell proliferation but causes a generalized improvement in BMDC activation.

I then decided to block IDO, another immunosuppressive enzyme that I found to be present in the LNs of HPV+ mice and was produced by myeloid cells. Similarly to what I did for testing the blockade of IL-10, I set up in vitro assays to test for CD8 T cells proliferation with different conditions with and without a small molecule IDO inhibitor (IDOinhib) at two different concentrations and with the competitive IDO inhibitor 1-methyltryptophan (1MT). Unfortunately, the small molecule inhibitor killed all the CD8 T cells at both concentrations, making it impossible to be tested in-vitro, while the 1-MT did not affect the CD8 T cell proliferation, that remained low when the cells were co-cultured with HPV+ mice –derived CD11b+ MDSCs (Fig. 29A). On the other hand, when the small molecule inhibitor was tested in the co-culture experiment with BMDCs, it was able to increase the cells activation in both the condition with HPV+ and HPV- -derived CD11b+ cells (Fig. 29B).

My results have shown that blocking IDO with 1-MT was not successful in restoring the proliferation of CD8 T cells hinting that, similarly to IL-10, it is either not a major player in the immunosuppression of CD8 T cells or its blockade alone is not sufficient to restore the proliferation of those T cells. However, the fact that the small molecule inhibitor was capable of ameliorating BMDCs activation in all the conditions (with both HPV+ and HPV- mice derived myeloid cells), suggests that IDO could play a physiological role in controlling DCs activation. It could be speculated, given the higher levels of IDO measured in the HPV+ mice's lymph nodes, that this immunosuppressive enzyme could have a more profound impact and restrain the activation of the APCs in the HPV+ GEMM.

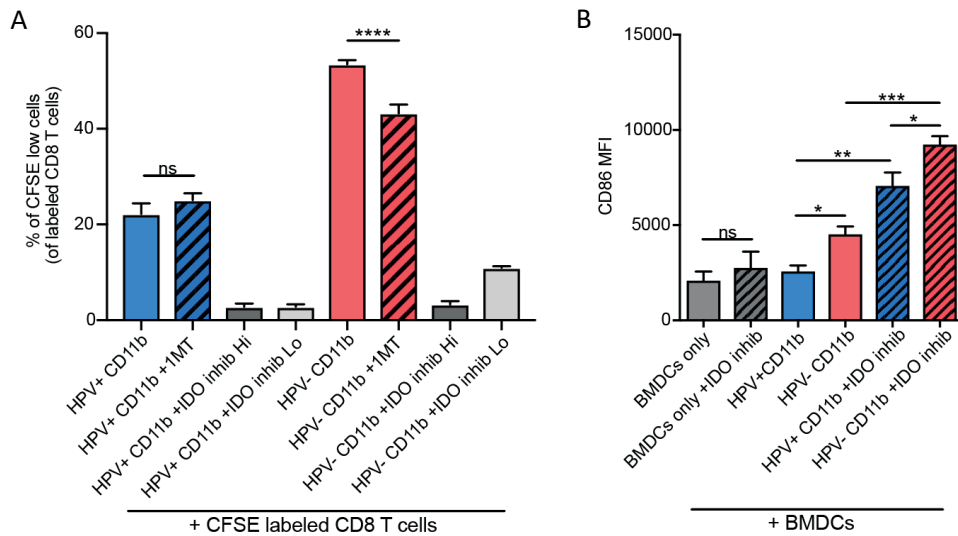


Figure 29. In-vitro analyses of the role of IDO in myeloid cell-mediated suppression. (A) Flow cytometry analyses of CFSE Mid/Low CD8 T cells after 48h co-culture in the presence of HPV+ or HPV- spleen-derived CD11b+ cells in an anti-CD3 anti-CD28 coated plate and in the presence of different concentrations of a small molecule IDO inhibitor or of 1 methyltryptophan 1MT (n=4). (B) Flow cytometry analyses of BMDs cultured in the presence of HPV+ or HPV- spleen-derived CD11b+ cells and of different concentrations of a small molecule IDO inhibitor (n=4). Statistics: * $p < 0.05$; ** $p < 0.01$; *** $p < 0.001$; **** $p < 0.0001$; n.s. = not significant.

3.2.25 Inhibition of Arg1, iNOS or reactive oxygen species does not rescue CD8 T cells proliferation in vitro.

I then conducted a preliminary experiment to assess the effects of ROS and other potentially immunosuppressive factors, namely Arg1 and iNOS, that have been reported to be employed by MDSCs for suppressing immune responses (235).

I took advantage of the in-vitro CD8 T cell proliferation assay in the presence of HPV+ and HPV- derived CD11b+ cells and added to the culture media N-Acetyl-L-Cysteine (NAC) to block the activity of ROS, N^G-Monomethyl-L-arginine (NG) to block Arg1 and Nw-Hydroxy-nor-L-arginine (NW) to block iNOS.

My results showed that none of these treatments managed to completely restore CD8 T cells proliferation (Fig. 30) indicating that these factors might not be involved in the immunosuppression or that, similarly to IL-10 and IDO, blocking them singularly, is not sufficient. Additional experiments will be required to obtain more definitive data on the role of all these factors.

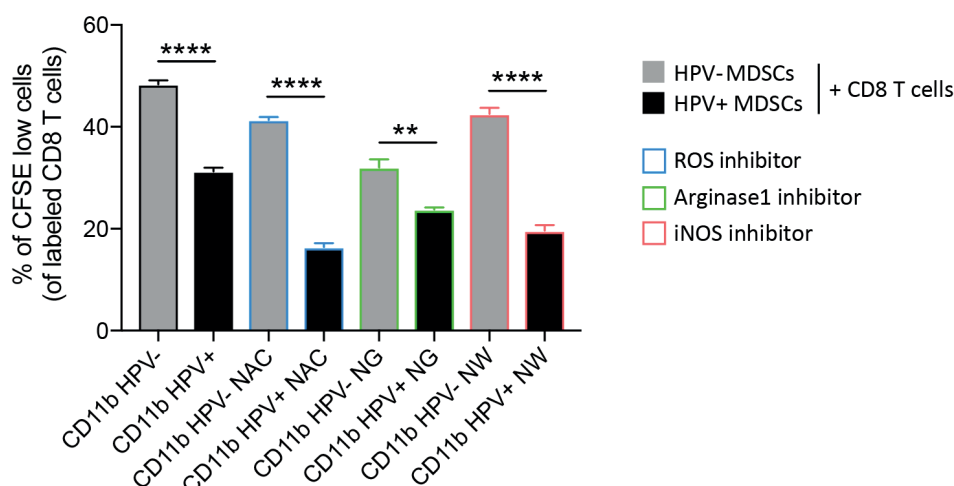


Figure 30. Co-culture assay of CD8 T cells and HPV+ mice -derived myeloid cells in the presence of different inhibitors. Flow cytometry analyses of CFSE low CD8 T cells after 48h co-culture in the presence of HPV+ or HPV- spleen-derived CD11b+ cells in an anti-CD3 anti-CD28 coated plate and in the presence of different small molecule inhibitors of ROS (NAC), Arginase 1 (NG) or iNOS (NW) respectively (n=4). Statistics: * $p < 0.05$; ** $p < 0.01$; *** $p < 0.001$; **** $p < 0.0001$; n.s. = not significant.

3.2.26 HPV+ mouse derived neutrophils show distinctive gene expression profiles

I next shifted my attention to the different myeloid cell population contained in the CD11b+ cells pool trying to characterize them separately. I first focused on neutrophils, as they have already been suspected to be implicated in immunomodulation in patients bearing cervical cancer (158, 163) and because they are the most abundant myeloid population in the HPV+ mice. I began by isolating neutrophils from the spleen of HPV+ and HPV- mice using FACS and, together with my colleagues, performed RNAseq on the isolated CD11b+Ly6G+Ly6C- population.

Neutrophils from HPV+ mice clustered separately from HPV- neutrophils (Fig. 31), indicating that they could be in fact, phenotypically different. Interestingly, 2 separate analyses revealed upregulation of the IL6-JAK-Stat3 pathway in neutrophils from HPV+ mice (Table 2 and Fig. 32) that could represent a potential target to interfere with the functions of these cells.

Following our RNAseq analyses, to assess if neutrophils have suppressive activity on CD8 T cells, I performed the previously-described in-vitro CD8 T cell proliferation assay by co-culturing CD8 T cells with HPV+ or HPV- -derived magnetically isolated neutrophils plated at a 1:10 ratio in an anti-CD3 anti-CD28 coated plate. Unfortunately, neutrophils did not remain alive for the duration of the assay and were mostly dead after 48h (not shown), and I did not measure suppression of the CD8 T cell proliferation (Fig. 33). From this experiment, it was not possible to determine if these cells possess immunosuppressive functions. A shorter assay, like the re-stimulation assay, might be better suited for this assessment as the neutrophils will be required for a much shorter amount of time (6h vs 48h).

Collectively, the RNAseq results revealed that the neutrophils in the HPV+ mice are substantially different from the ones found in non-transgenic HPV- mice, suggesting that they might still be a potential target that needs to be eliminated to disable the systemic immunosuppression in the HPV+ GEMM, although it was not possible to directly assess their suppressive activity with the performed assay.

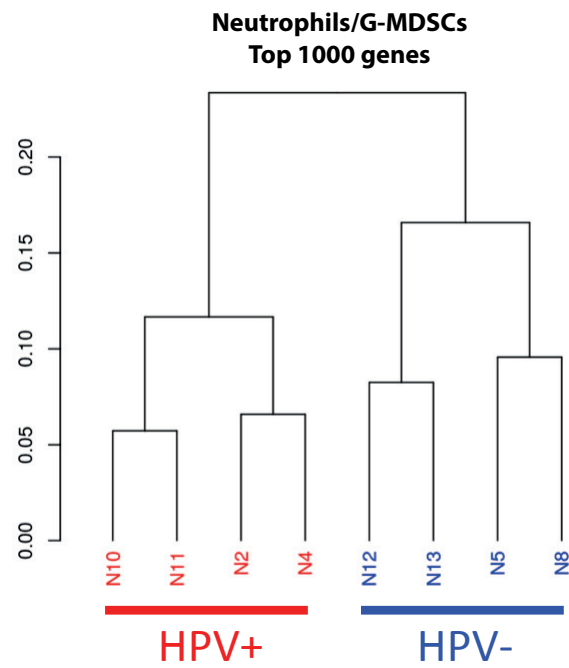


Figure 31. Clustering of CD11b+Ly6G+Ly6C- neutrophils sorted from HPV+ and HPV- mice.

KEGG genesets

Enrichment in up-regulated genes

Significant genesets in POSvsNEG up-regulated genes

Geneset	Score	NES	P	FDR	LeadingEdge
KEGG_CYTOKINE_CYTOKINE_RECEPTOR_INTERACTION	0.61	1.6	1e-03	6.2e-02	IL13RA1, CSF2RB, CCR1, IL4R, TNFRSF13B, IL1R2, ACVRL1, CSF3R, IL10RA, CXCR2, RELT, IL6R, TNFRSF18, TNFRSF1A, IL17RA, IFNGR1, LTBR, PRL, IL- 10RB, IFNAR2, TNFSF14, TNFRSF10B, IFNGR2, IL1RAP, CXCR5, CRLF2, TN- FRSF1B, FAS
KEGG_JAK_STAT_SIGNALING_PATHWAY	0.57	1.5	1e-03	6.2e-02	IL13RA1, CSF2RB, IL4R, CISH, IRF9, SOCS3, JAK3, CCND3, CSF3R, IL10RA, STAT2, STAT3, PIK3CD, BCL2L1, IL6R, PIK3R5, IFNGR1, PRL, IL10RB, IFNAR2, SOCS1, IFNGR2, CRLF2
KEGG_AMINO_SUGAR_AND_NUCLEOTIDE_SUGAR_METABOLISM	0.69	1.7	1e-03	6.2e-02	NPL, GALE, PGM2, GMDS, GPI, CMAS, HK3
KEGG_NEUROACTIVE_LIGAND_RECEPTOR_INTERACTION	0.64	1.5	2e-03	9.3e-02	ADORA3, TSPO, P2RY1, F2RL2, P2RX4, C5AR1, P2RY2, P2RY13, KISS1R, PTAFR, FPR1, PRL

Hallmark genesets

Enrichment in up-regulated genes

Significant genesets in POSvsNEG up-regulated genes

Geneset	Score	NES	P	FDR	LeadingEdge
HALLMARK_INTERFERON_ALPHA_RESPONSE	0.66	1.7	1e-03	1.7e-02	TRIM5, IFITM2, RTP4, IL4R, OAS1, IRF7, IRF9, GBP2, MOV10, ISG15, TRIM25, PARP9, ADAR, TRAFD1, EIF2AK2, RSAD2, PSME2, ISG20, STAT2, TRIM21, IFI27, OGFR, CD47, IRF1, CNP, LY6E, DHX58, UBE2L6, CMPK2, PARP14, IFI35, HERC6, PSME1, CASP1, DDX60
HALLMARK_INTERFERON_GAMMA_RESPONSE	0.61	1.7	1e-03	1.7e-02	IFITM2, OAS2, RTP4, MVP, CSF2RB, IL4R, XAF1, OAS3, IRF7, IRF9, MYD88, UPP1, GCH1, ZBP1, ISG15, SELP, SOCS3, HIF1A, TRIM25, ST8SIA4, ADAR, TRAFD1, EIF2AK2, RSAD2, PTPN1, IL10RA, PSME2, ISG20, STAT2, TRIM21, DDX58, SAMHD1, STAT3, RIPK1, IFI27, OGFR, SPPL2A, IRF1, LY6E, TNFAIP2, DHX58, FPR1, IFNAR2, UBE2L6, CMPK2, PARP14, IFI35, SOCS1, HERC6, PSME1, CASP1, MARCH1, DDX60, FAS, SRI, NAMPT, TXNIP, NCOA3, NFKB1, RIPK2, EIF4E3
HALLMARK_INFLAMMATORY_RESPONSE	0.56	1.5	1e-03	1.7e-02	RTP4, SLC31A1, IL4R, PROK2, IRF7, MXD1, GCH1, SLC28A2, TLR2, P2RX4, HIF1A, KCNJ2, EIF2AK2, CSF3R, IL10RA, C5AR1, P2RY2, SGMS2, TLR1, AQP9, LYN, PIK3R5, IRF1, PTAFR, KIF1B, LY6E, RHOG, FPR1
HALLMARK_IL6_JAK_STAT3_SIGNALING	0.60	1.6	2e-03	2.5e-02	IL13RA1, CSF2RB, CCR1, IL4R, IRF9, MYD88, TLR2, IL1R2, SOCS3, ACVRL1, PTPN1, CSF3R, STAT2, STAT3, HMOX1, PIK3R5, TNFRSF1A, IRF1, IL17RA, IFNGR1, LTBR, IL10RB, SOCS1, CD44, IFNGR2, CRLF2, TNFRSF1B, FAS
HALLMARK_ALLOGRAFT_REJECTION	0.49	1.3	8e-03	8.0e-02	CCR1, IL4R, TLR6, IRF7, GBP2, TLR2, BCL3, HIF1A, ST8SIA4, RPS9, CCND3, SPI1, GCNT1, TLR1, FGR, LYN, MMP9, CD47, BCL10, CFP, IFNGR1, SRGN, IT- GB2, SIT1, DEGS1, NME1, IFNAR2, SOCS1, IFNGR2, PTPRC, FAS, NCF4, RIPK2, RPL3L, AKT1, TAPBP
HALLMARK_KRAS_SIGNALING_DN	0.66	1.6	1e-02	8.5e-02	TGM1, LFNG, RSAD2, ASB7, SGK1, MTHFR, PROP1, MFSD6, MEFV

Table 2. Pathway analyses in neutrophils from HPV+ vs HPV- mice.



Figure 32. Heat-map of the IL6-JAK-STAT3 pathway in CD11b+Ly6G+Ly6C- neutrophils. Neutrophils were sorted from HPV+ (dark grey) or HPV- (light grey) mice.

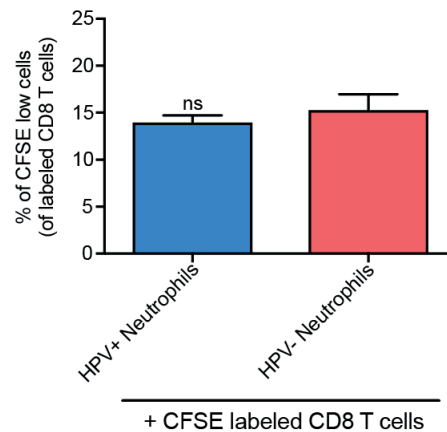


Figure 33. In-vitro co-culture of CD8 T cells and HPV+ or HPV- mice -derived neutrophils. A) Flow cytometry analyses of CFSE low CD8 T cells after 48h co-culture in the presence of HPV+ or HPV- spleen-derived neutrophils cells in an anti-CD3 anti-CD28 coated plate (n=4). Statistics: * $p < 0.05$; ** $p < 0.01$; *** $p < 0.001$; **** $p < 0.0001$; n.s. = not significant.

3.2.27 Monocytes/macrophages suppress CD8 T cells proliferation in-vitro

In light of the in vitro-results obtained with neutrophils, I performed a similar co-culture experiment where I mixed CFSE-labeled CD8 T cells with monocytes/macrophages isolated by magnetic separation from HPV+ and HPV- mice. The monocyte/macrophages mix constituted the majority of the isolated cells (see materials and methods), that were comprised of roughly equal numbers of Ly6C+ F4/80- cells and Ly6C-F4/80+ cells. CD8 T cells were mixed as previously in a 1:10 ratio with the macrophages/monocytes mix. Contrarily to the experiment with neutrophils, the majority of the cells remained alive for the duration of the experiment. Analyses of CFSE low CD8 T cells after 48h of co-culture revealed that monocytes/macrophages isolated from HPV+ mice had a significant suppressive activity on CD8 T cells proliferation (Fig. 34). Further experiments will be required to characterize monocytes and macrophages separately and to assess their suppressive activity on cytokine production and APCs activation.

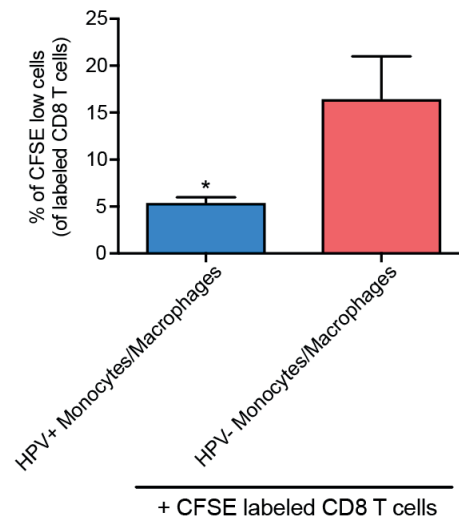


Figure 34. In-vitro co-culture of CD8 T cells and HPV+ or HPV- mice –derived Monocytes/Macrophages. Flow cytometry analyses of CFSE low CD8 T cells after 48h co-culture in the presence of HPV+ or HPV- spleen-derived monocytes/macrophages cells in an anti-CD3 anti-CD28 coated plate. Groups: HPV+ Monocytes/Macrophages n=6, HPV- Monocytes/Macrophages n=5. Statistics: * $p < 0.05$; ** $p < 0.01$; *** $p < 0.001$; **** $p < 0.0001$; n.s. = not significant.

3.2.28 Testing alternative approaches for targeting myeloid cells

Previous results established myeloid cells as a suppressive cell population in the HPV+ mice. Given their significant systemic expansion measured in the lymphoid organs of HPV+ mice and the previous reports about their expansion and potential involvement in suppressing immune responses in patients (111, 155, 158, 161, 163), I sought out to test approaches to target them, aiming at relieving the systemic immunosuppression in the HPV+ GEMM and boost the antitumor immune response generated upon vaccination with the NP-VAX.

As it seems that all the major CD11b+ cell populations might be playing a role in impairing systemic immune responses, although it was not possible to assess the suppressive activity of neutrophils directly, I took approaches both widely aimed at all the myeloid cells or at their suppressive functions and also at specific populations.

3.2.29 Antibiotic treatment does not affect myeloid cells nor ameliorate the response to the vaccine

HPV+ mice develop spontaneous skin lesions often causing the mice to scratch and wound their skin. I reasoned that this could potentially lead to bacterial infiltration past the skin barrier that might be a cause of inflammation and be at least partially responsible for the increase in myeloid cells. To exclude that bacterial infections might be linked to the systemic increase in CD11b+ cells and/or to the systemic immunosuppression, I pre-treated mice with a mix of antibiotics for 1 week before proceeding with vaccination. The antibiotics treatment continued throughout the experiment and mice were sacrificed 9 days after receiving the NP-VAX. Antibiotics treatments did not improve the immune response to vaccination (Fig. 35A and B), and it did not cause changes in the myeloid cells (Fig. 35C, D, E, and F). Although it could be that the antibiotics of choice, or the regimen used, was not capable of eradicating the bacteria, this result suggest that the skin phenotype might not be linked to bacterial infections or at least, that there is no link between potential bacterial infiltration past the skin barrier and the increase in myeloid cells or the systemic immunosuppression.

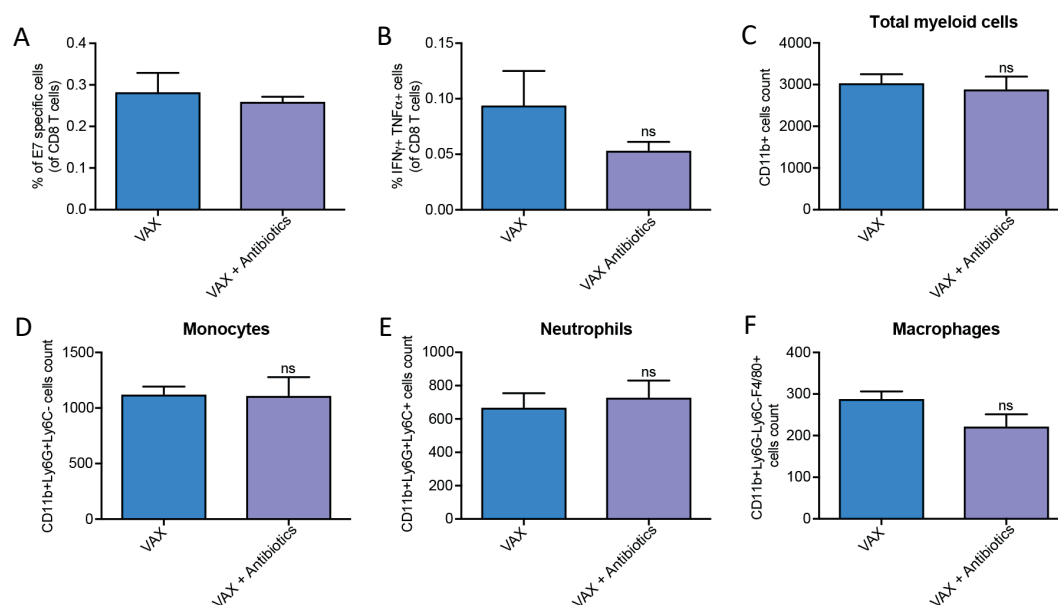


Figure 35. Flow cytometry analyses of the effects of antibiotic treatment on the anti-E7 response and on myeloid cells. (A) Flow cytometry analyses of E7-specific CD8 T cells in the lymph nodes using tetramers recognizing the HPV16 E7 CD8 peptide RAHYNIVTF presented on H2Db. (B) Flow

cytometry analyses of IFN γ and TNF α production by lymph node -derived CD8 T cells after in-vitro re-stimulation with the HPV16 E7 CD8 peptide RAHYNIVTF. Flow cytometry analyses of (C) CD11b+ total myeloid cells cells, (D) CD11b+Ly6G+Ly6C- neutrophils, (E) CD11b+Ly6G-Ly6C+ monocytes and (F) CD11b+Ly6G-Ly6C-F4/80+ macrophages in the lymph nodes of HPV+ mice. Groups: VAX n=4, VAX + antibiotics n=5. Statistics: * $p < 0.05$; ** $p < 0.01$; *** $p < 0.001$; **** $p < 0.0001$; n.s. = not significant.

3.2.30 Targeting myeloid cells with depleting antibodies is poorly effective in HPV+ mice

My first attempt at directly targeting myeloid cells took advantage of depleting antibodies against Ly6G, Ly6C, and CD11b.

In light of my results and the previous observations by others, I started with anti-Ly6G (aLy6G) treatment to eliminate neutrophils in HPV+ mice. Antibody treatments started 1 day before vaccination and mice received 2 shots of vaccine at day 0 and day 14. aLy6G was administered for the duration of the experiment 3 times per week. Myeloid cells depletion in the blood was monitored at day 7 and day 14. Mice were sacrificed at day 19 and flow cytometry analyses on vaccination site draining lymph node were performed. At day 0 the total amount of CD11b+ cells was not significantly lower (Fig. 36A) but the aLy6G antibody was bound to all the neutrophils as suggested by the absence of Ly6G staining (Fig. 36B). The concomitant increase in monocytes (Fig. 36C) or macrophages (measured, but not significant) (Fig. 36D) does not seem enough to compensate for the potential depletion of neutrophils on the total CD11b+ cells shown by Ly6G staining. Therefore I concluded that, although the depleting antibody was bound to the target cells, for unknown reasons this population was only partially depleted by the treatment. At day 7, in the blood I measured a slight increase in total CD11b+ cells (Fig. 36E) accompanied by a decrease in the antibody binding to neutrophils, as suggested by the appearance of Ly6G staining (Fig. 36F), and an increase in monocytes (Fig. 36G) and macrophages (Fig. 36H). Analyses of the lymph nodes at day 19 revealed similar numbers of myeloid cells (Fig. 36I) between the two groups and an increase in neutrophils (Fig. 36L), possibly due to a rebound of these cells caused by an initial partial depletion by aLy6G, that was however no longer associated with increased monocytes (Fig. 36M) and macrophages (Fig. 36N). Following these results, not surprisingly, I did not measure an increase in the numbers of E7-specific CD8 T cells (Fig. 36O) or on cytokine production after re-stimulation (Fig. 36P).

To assess if the apparently limited neutrophils depletion was due to an intrinsic poor efficacy of the antibody or if it was dependent on the GEMM, I repeated the same experiment in HPV- mice. Contrarily to what I observed at day 0 in HPV+ mice, anti-Ly6G treatment caused a substantial decrease in the total amount of CD11b+ (Fig. 37A) cells accompanied by loss of Ly6G staining (Fig. 37B) and no concomitant increase in monocytes (Fig. 37C) or macrophages (Fig. 37D) indicating that the treatment was indeed depleting neutrophils and compensatory mechanism did not intervene yet.

At day 7, albeit to a lesser extent, neutrophil depletion seemed to be still working quite well as indicated by the loss in CD11b+ (Fig. 37E) cells and in the complete absence of Ly6G staining (Fig. 37F) with no concomitant increase in the other populations (Fig. 37G and H). At day 19 however, the HPV- mice lymph nodes showed no significant changes in the myeloid cells population (Fig. 37I) as well as what appears to be a sign of a loss of binding of the α Ly6G depleting antibody as suggested by the appearance of Ly6G+ cells at the FACS (Fig. 37L). Monocytes (Fig. 37M) and macrophages (Fig. 37N) were similar between the groups. As expected from the non-HPV transgenic mice, neutrophils depletion did not cause changes to the immune response against E7 (Fig. 37O and P), likely because these cells are not suppressive to begin with.

These results show that a significant neutrophils depletion can be easily achieved in HPV- mice for up to 2 weeks while in the HPV+ counterparts, it is not detectable as early as 7 days after the beginning of the treatment. Moreover, in HPV+ mice neutrophils targeting was accompanied by an increase in monocytes and macrophages that could compensate for the already limited neutrophils depletion. Overall, with the regimen I used, it was not possible to deplete neutrophils in HPV+ mice and the disappointing results compared to the HPV- mice suggests that it might be hard to achieve a significant depletion of these cells (and possibly others) in the GEMM.

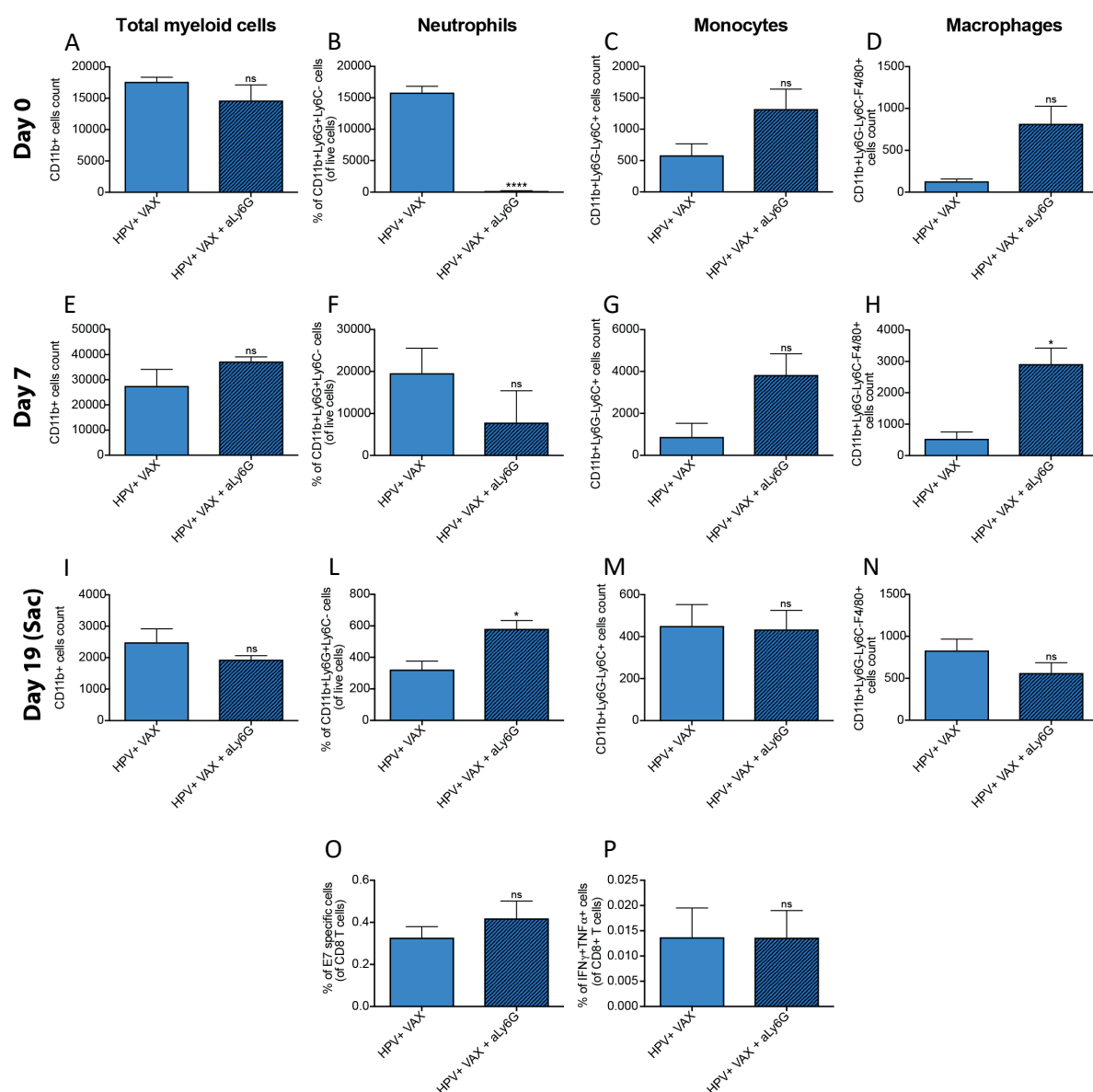


Figure 36. Flow cytometry analyses of myeloid cells and of the anti-E7 response following anti-Ly6G treatment. Flow cytometry analyses at different time-points of (A, E, I) CD11b+ total myeloid cells, (B, F, L) CD11b+Ly6G+Ly6C- neutrophils, (C, G, M) CD11b+Ly6G-Ly6C+ monocytes and (D, H, N) CD11b+Ly6G-Ly6C-F4/80+ macrophages in the blood (day 0 and day 7) or in the lymph nodes (day 19) of HPV+ mice. (O) Flow cytometry analyses of E7-specific CD8 T cells in the lymph nodes using tetramers recognizing the HPV16 E7 CD8 peptide RAHYNIVTF presented on H2Db. (P) Flow cytometry analyses of IFN γ and TNF α production by lymph node -derived CD8 T cells after in-vitro re-stimulation with the HPV16 E7 CD8 peptide RAHYNIVTF. $n=4$. Statistics: * $p < 0.05$; ** $p < 0.01$; *** $p < 0.001$; **** $p < 0.0001$; n.s. = not significant.

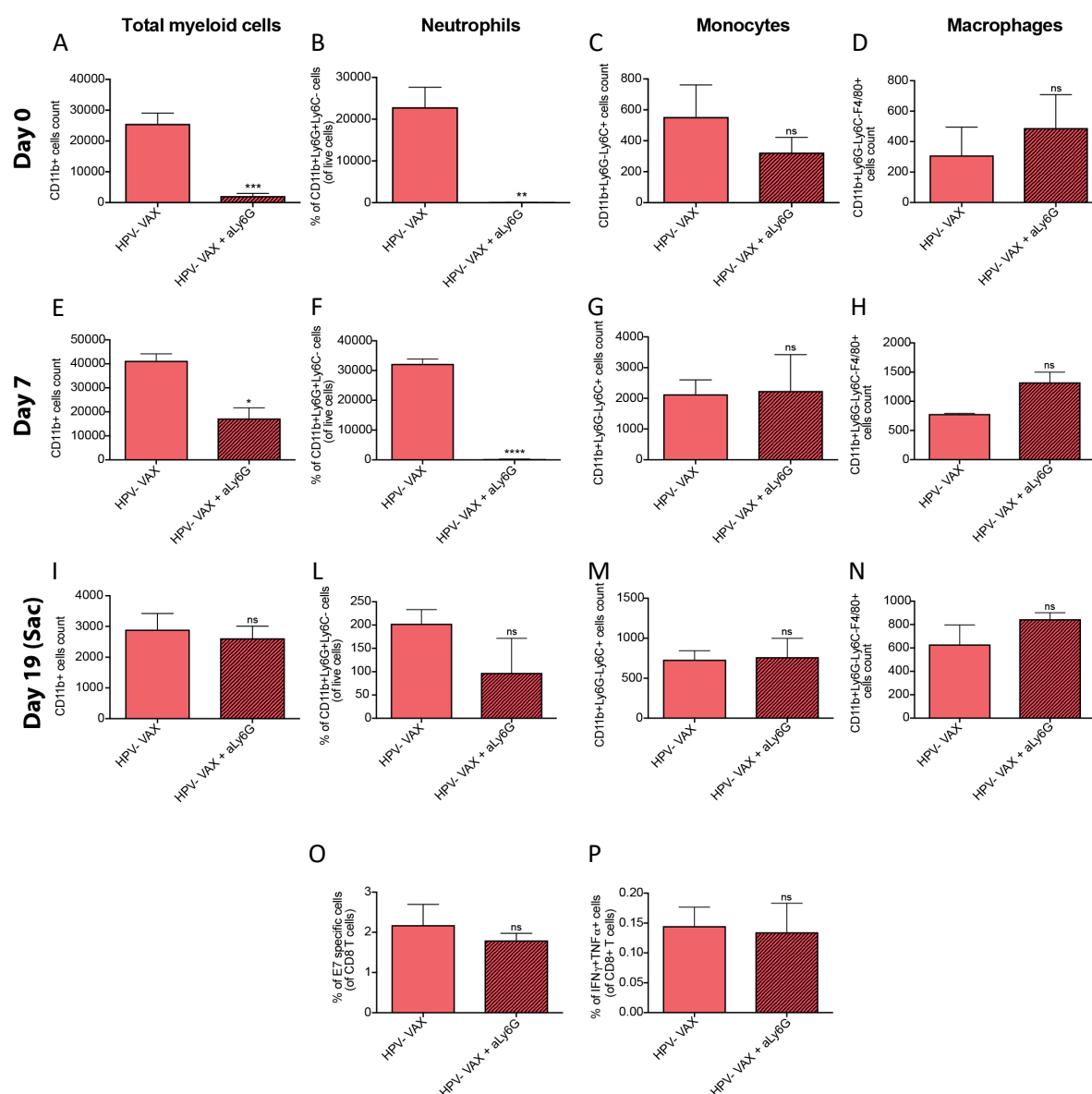


Figure 37. Flow cytometry analyses of myeloid cells and of the anti-E7 response following anti-Ly6G treatment. Flow cytometry analyses at different time-points of (A, E, I) CD11b+ total myeloid cells, (B, F, L) CD11b+Ly6G+Ly6C- neutrophils, (C, G, M) CD11b+Ly6G-Ly6C+ monocytes and (D, H, N) CD11b+Ly6G-Ly6C-F4/80+ macrophages in the blood (day 0 and day 7) or in the lymph nodes (day 19) of HPV- mice. (O) Flow cytometry analyses of E7-specific CD8 T cells in the lymph nodes using tetramers recognizing the HPV16 E7 CD8 peptide RAHYNIVTF presented on H2Db. (P) Flow cytometry analyses of IFN γ and TNF α production by lymph node -derived CD8 T cells after in-vitro re-stimulation with the HPV16 E7 CD8 peptide RAHYNIVTF. $n=4$. Statistics: * $p < 0.05$; ** $p < 0.01$; *** $p < 0.001$; **** $p < 0.0001$; n.s. = not significant.

I next aimed at depleting monocytes using anti-Ly6C (aLy6C). Given the quick repopulation of the myeloid compartment observed in the previous experiment, I also decided to shorten the duration of the treatment. HPV+ mice were pre-treated for 7 days with aLy6C and then immunized once at day 0 with the NP-VAX, the depleting antibody treatment was given 3 times per week throughout the experiment. Similarly to what I did before, depletion in the blood was assessed at day 0 and at day 7, but this time I sacrificed the mice at day 9 post-immunization and performed flow cytometry analyses on the vaccination site draining lymph nodes. Analyses of myeloid cells in the blood revealed a general depletion of all the observed populations at day 0 (Fig. 38A, B, C, and D) and the loss of Ly6C staining (Fig. 38C) showed that the depleting antibody was at least bound to its target cells. Interestingly I detected an unexpected depletion of neutrophils (Fig. 38B) that suggested that these cells express low levels of Ly6C. At day 7 in the blood and at day 10, when mice were sacrificed, the depletion of myeloid cells was lost (Fig. 38E-N) while the Ly6C staining suggested that the depleting antibody was still bound to monocytes (Fig. 38C and M). Unfortunately, this treatment did not produce any benefit to the immune response to the vaccine as both the percentage of E7-specific CD8 T cells (Fig. 38O) and cytokine production from E7-specific CD8 T cells (Fig. 38P) was not improved, with the latter that was instead lower compared to the vaccine only treated group. Given the degree of depletion in the blood, and the lower number of monocytes relatively to the neutrophils it was not possible to assess if there was indeed a depletion of the former, however, this result suggests that similarly to aLy6G, aLy6C is also a not viable strategy to treat immunosuppression in HPV+ mice. The reasons behind this result could again be attributable to a poor and short-term antibody-mediated cell depletion in the GEMM. Although I did not test the anti-Ly6C antibody in HPV- mice, judging from previous results, it could be speculated that the monocyte depletion would have been more successful in the non-transgenic mice setting.

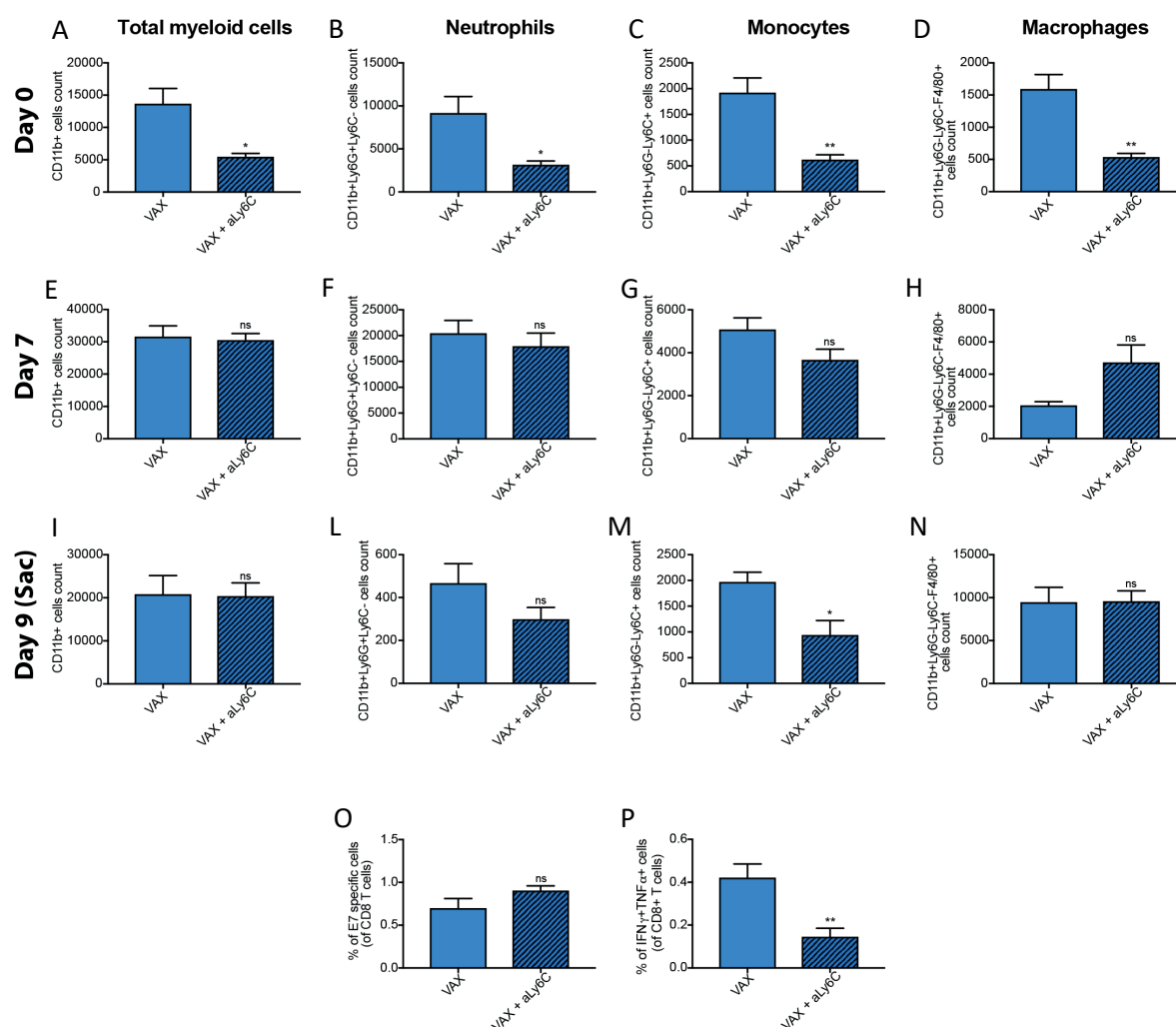


Figure 38. Flow cytometry analyses of myeloid cells and of the anti-E7 response following anti-Ly6C treatment. Flow cytometry analyses at different time-points of (A, E, I) CD11b+ total myeloid cells, (B, F, L) CD11b+Ly6G+Ly6C- neutrophils, (C, G, M) CD11b+Ly6G-Ly6C+ monocytes and D, H, N) CD11b+Ly6G-Ly6C-F4/80+ macrophages in the blood (day 0 and day 7) or in the lymph nodes (day 9) of HPV+ mice. (O) Flow cytometry analyses of E7-specific CD8 T cells in the lymph nodes using tetramers recognizing the HPV16 E7 CD8 peptide RAHYNIVTF presented on H2Db. (P) Flow cytometry analyses of IFN γ and TNF α production by lymph node-derived CD8 T cells after in-vitro re-stimulation with the HPV16 E7 CD8 peptide RAHYNIVTF. $n=4$. Statistics: * $p < 0.05$; ** $p < 0.01$; *** $p < 0.001$; **** $p < 0.0001$; n.s. = not significant.

Despite the unsuccessful approaches tried so far, I then decided to use an anti-CD11b (aCD11b) depleting antibody to test if targeting the whole population of myeloid cells could lead to better results. For this experiment, I employed the same schedule used for aLy6C, namely mice were pre-treated for 7 days, vaccinated with the NP-VAX and bled at day 0, bled at day 7 and sacrificed at day 9 when flow cytometry analyses of the vaccination site draining lymph node were performed. Binding of the depleting antibody was characterized by a shift in the CD11b staining that resulted in the loss of CD11b^{High} cells. This result showed that, although there was a complete disappearance of CD11b^{High} cells at day 0 in the blood (Fig. 39A), I observed a progressive re-gain of the CD11b staining (Fig. 39E and I), indicating that less antibody was binding to the target cells, perhaps as a consequence of the development of neutralizing antibodies, that culminated in the return of normal levels of CD11b^{High} cells by day 9 in the lymph nodes (Fig. 39I). However, generally lower, although not always statistically significant, numbers of neutrophils, monocytes, and macrophages were detected at day 0 (Fig. 39B, C, and D) and day 7 (Fig. 39F, G and H) in the blood, suggesting at least that a partial depletion was happening. However, by day 9, this trend was lost (Fig. 39L, M, and N) along with the loss of aCD11b depleting antibody binding (Fig. 39I). Expectedly, the very limited differences observed in myeloid cells in the blood did not lead to an improvement of the anti-E7 response to the NP-VAX in the lymph nodes (Fig. 39O and P) casting reasonable doubts on the feasibility of this approach to eliminate myeloid cells.

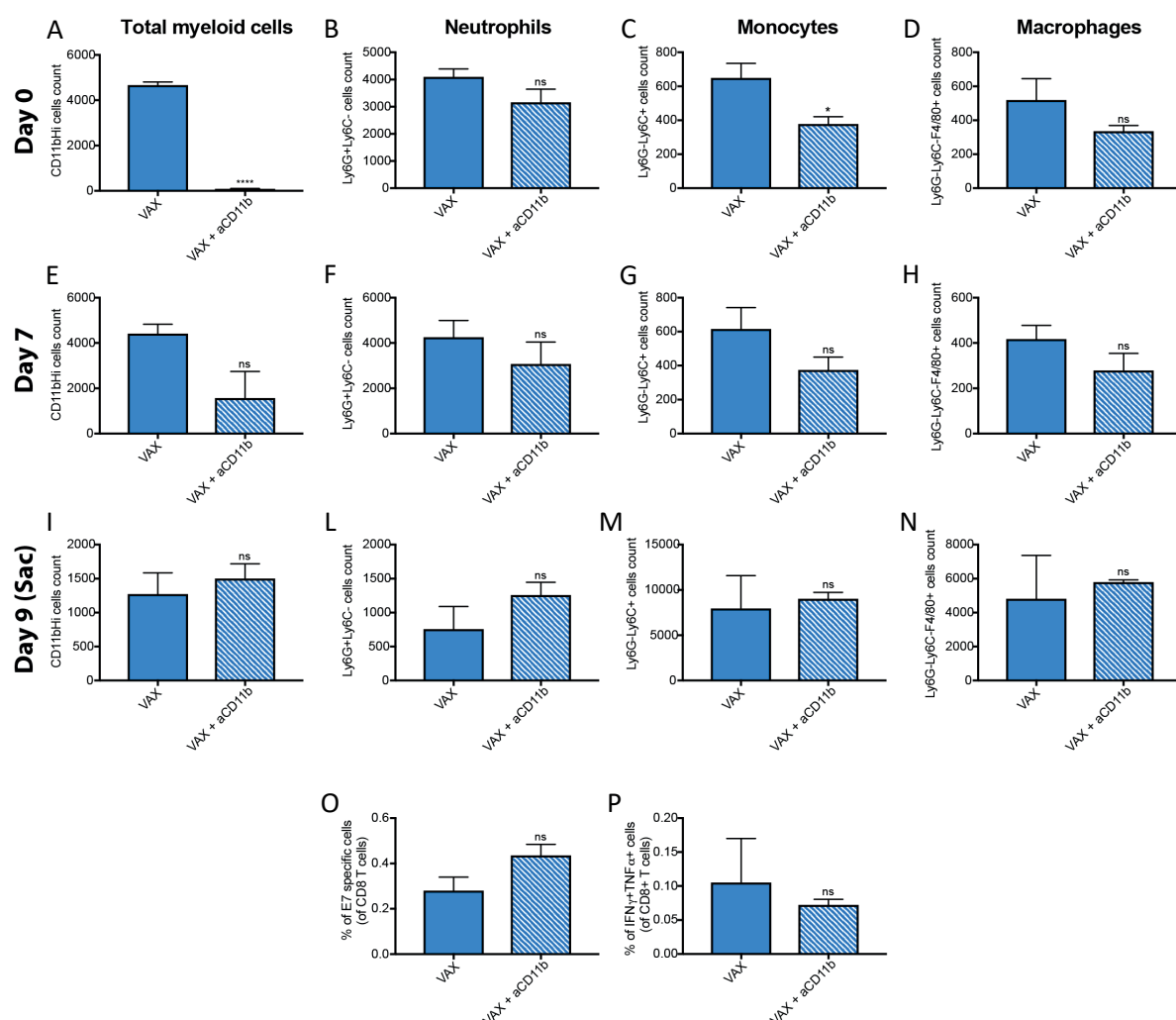


Figure 39. Flow cytometry analyses of myeloid cells and of the anti-E7 response following anti-CD11b treatment. Flow cytometry analyses at different time-points of (A, E, I) CD11bHi myeloid cells, (B, F, L) Ly6G+Ly6C- neutrophils, (C, G, M) Ly6G-Ly6C+ monocytes and (D, H, N) Ly6G-Ly6C-F4/80+ macrophages in the blood (day 0 and day 7) or in the lymph nodes (day 9) of HPV+ mice. (O) Flow cytometry analyses of E7-specific CD8 T cells in the lymph nodes using tetramers recognizing the HPV16 E7 CD8 peptide RAHYNIVTF presented on H2Db. (P) Flow cytometry analyses of IFN γ and TNF α production by lymph node -derived CD8 T cells after in-vitro re-stimulation with the HPV16 E7 CD8 peptide RAHYNIVTF. Groups: VAX n=3, VAX + α CD11b n=4. Statistics: * $p < 0.05$; ** $p < 0.01$; *** $p < 0.001$; **** $p < 0.0001$; n.s. = not significant.

Collectively, these results suggest that depleting myeloid cells in the HPV+ mice using conventional depleting antibodies appears to be a difficult and unfeasible strategy. These approaches might be hindered by either or a combination of: the large amount of antibodies required to eliminate the unusually high numbers of myeloid cells, by the fast neutralization of the depleting antibodies, or by the presence of potent mechanisms that allows for a rapid re-expansion of the depleted cells and/or for the concomitant compensatory expansion of the other populations. Mechanisms that might be even boosted by the presence of the HPV genes. Additionally, the poor efficacy of these depleting strategies could be due to a defect in macrophages, that have been reported to be required for cell depletion following aLy6G treatment (236), or in other cells and factors required for the efficacy of depleting antibodies, like the complement system or natural killer cells. The presence of these defects is supported by the fact that, although the depleting antibodies are bound to their targets, the cells are not getting eliminated.

3.2.31 Strategies targeting monocytes/macrophages are also poorly effective in HPV+ mice

My in-vitro results showed that monocytes/macrophages had a direct suppressive activity on CD8 T cells proliferation. Additionally, monocytic-MDSCs, which are phenotypically indistinguishable from monocytes by flow cytometry, are usually more suppressive on a per-cell basis than the granulocytic counterpart. Thus making the monocyte/macrophages good candidates to be targeted. Specifically, I employed 3 different treatments that I combined with our NP-VAX namely IPI549, clodronate liposomes (CLDlip) and antiCSF1R (aCSF1R).

IPI549 is a PI3K-gamma inhibitor that has been previously shown to be able to target macrophages and lead to an improvement in anti-tumor immunity by inhibiting immunosuppression (237). Treatment with IPI549 was initiated 1 day before vaccination with the NP-VAX and given daily until the end of the experiment. Mice received only 1 shot of the NP-VAX at day 0 and were sacrificed at day 9. Unfortunately, flow cytometry analyses on the vaccination site draining lymph nodes revealed that the treatment impaired the generation of E7 specific CD8 T cells as indicated by their significantly lower numbers compared to the vaccine only group (Fig. 40A). Additionally, cytokine production was also lower, although the difference was not significant (Fig. 40B). These results show that the combination of IPI549 with therapeutic vaccination in this model might not be feasible or it will require a different schedule of treatment.

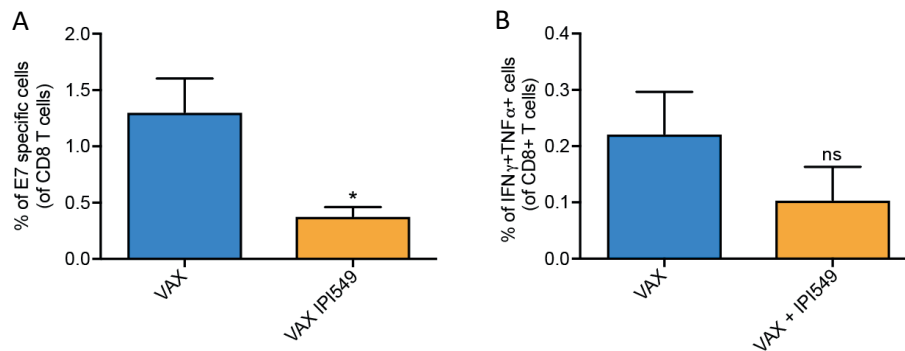


Figure 40. Flow cytometry analyses of the anti-E7 response following IPI549 treatment. (A) Flow cytometry analyses of E7-specific CD8 T cells in the lymph nodes using tetramers recognizing the HPV16 E7 CD8 peptide RAHYNIVTF presented on H2Db and (B) Flow cytometry analyses of IFN γ and TNF α production by lymph node -derived CD8 T cells after in-vitro re-stimulation with the HPV16 E7 CD8 peptide RAHYNIVTF (n=3). Statistics: * $p < 0.05$; ** $p < 0.01$; *** $p < 0.001$; **** $p < 0.0001$; n.s. = not significant.

I next combined the NP-VAX with CLDlip that are established as a macrophages-depleting compound. I pre-treated HPV+ mice with CLDlip administered 3 times per week starting 7 days before vaccination, and I continued the treatment throughout the experiment. Mice received the NP-VAX at day 0 and were sacrificed at day 9 when I performed flow cytometry analyses on the vaccination site draining lymph nodes that revealed no improvement in the immune response against E7 (Fig. 41A and B). The results obtained showed no depletion of macrophages (Fig. 41C) nor of monocytes (Fig. 41D) that were instead increased upon CLDlip treatment. Interestingly, unpublished data from our lab showed that a similarly-scheduled CLDlip treatment was consistently depleting macrophages in the spleen and lymph nodes but not in the tumors from BRAF-melanoma transgenic mice, and that the reason for the lack of intra-tumoral depletion was attributable to the lack of phagocytic activity by the immunosuppressive TAMs. In light of these results, it is tempting to speculate that macrophages in peripheral lymphoid organs of the HPV+ mice already have an altered phenotype similar to what is usually seen in TAMs, and that it could be associated with a defective in phagocytosis. Defects in macrophages functions could, as already mentioned, account for the poor depleting activity of the aLy6G treatment (and possibly of aLy6C, aCD11b and a portion of the Treg-depleting treatments mentioned earlier).

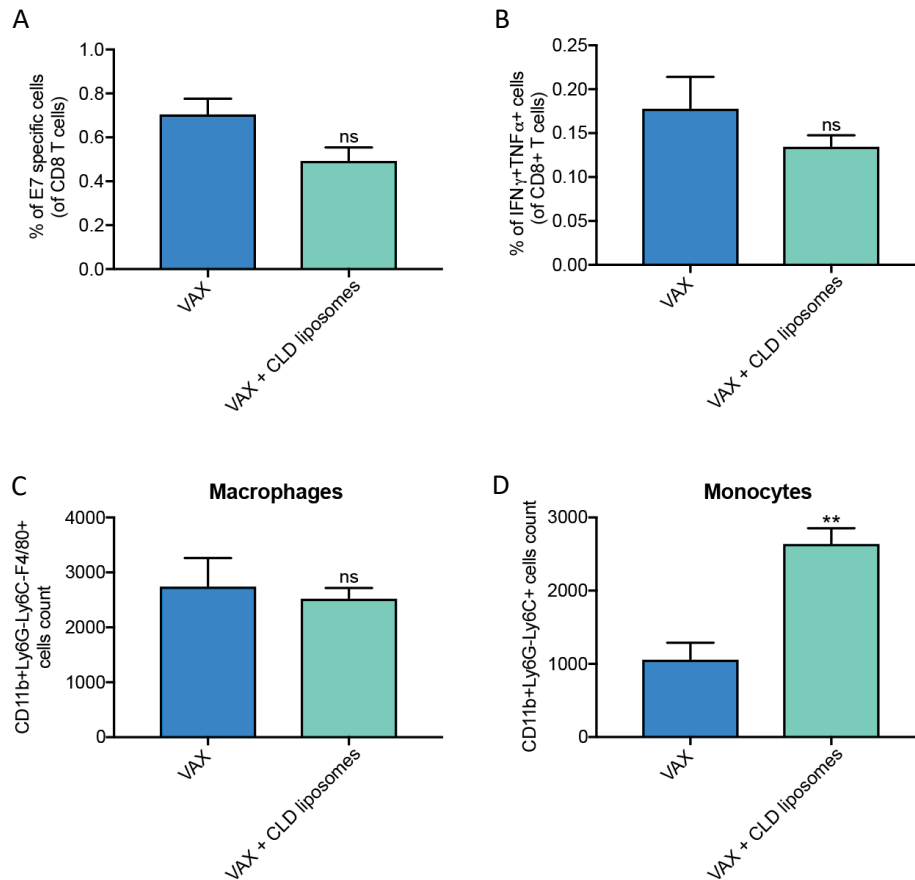


Figure 41. Flow cytometry analyses of the effect of CLD liposomes on the anti-E7 immune response and on macrophages and monocytes. (A) Flow cytometry analyses of E7-specific CD8 T cells in the lymph nodes using tetramers recognizing the HPV16 E7 CD8 peptide RAHYNIVTF presented on H2Db. (B) Flow cytometry analyses of IFN γ and TNF α production by lymph node - derived CD8 T cells after in-vitro re-stimulation with the HPV16 E7 CD8 peptide RAHYNIVTF. Flow cytometry analyses of (C) CD11b+Ly6G-Ly6C-F4/80+ macrophages and (D) CD11b+Ly6G-Ly6C+ monocytes in the lymph nodes of HPV+ mice. Groups: VAX n=6, VAX + CLD liposomes n=4. Statistics: * $p < 0.05$; ** $p < 0.01$; *** $p < 0.001$; **** $p < 0.0001$; n.s. = not significant.

As a last attempt to specifically eliminate monocytes/macrophages I resorted to the use of aCSF1R, whose activity was proven to be sufficient for eliminating TAMs in TC-1 tumor-bearing mice (unpublished data from the lab). Treatment with aCSF1R was administered 3 times per week starting 7 days before immunization and was continued for the duration of the experiment. Mice

received the NP-VAX at day 0 and were sacrificed at day 9 when flow cytometry analyses on the vaccination site draining lymph nodes were performed. Differences in myeloid cells were not significant (Fig. 42A, B, C, and D) but I measured a trend showing a slight reduction in monocytes (Fig. 42C) and macrophages (Fig. 42D). However, possibly due to the extremely limited changes in these cells, the immune response to the vaccine was identical in the two groups (Fig. 42E and F). These results show that strategies involving aCSF1R are also not significantly affecting the macrophages in lymphoid organs of HPV+ mice nor are they improving the anti-E7 immune response.

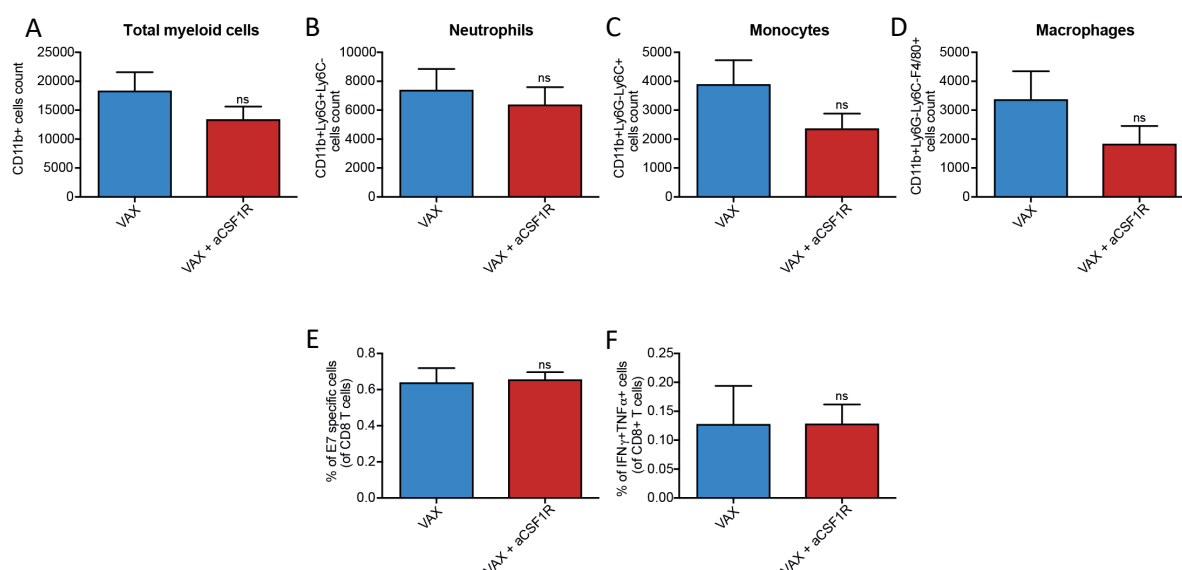


Figure 42. Flow cytometry analyses of the effects of anti-CSF1R on myeloid cells and on the anti-E7 response. Flow cytometry analyses of (A) CD11b+ total myeloid cells, (B) CD11b+Ly6G+Ly6C- neutrophils, (C) CD11b+Ly6G-Ly6C+ monocytes and (D) CD11b+Ly6G-Ly6C-F4/80+ macrophages in the lymph nodes of HPV+ mice. (E) Flow cytometry analyses of E7-specific CD8 T cells in the lymph nodes using tetramers recognizing the HPV16 E7 CD8 peptide RAHYNIVTF presented on H2Db. (F) Flow cytometry analyses of IFN γ and TNF α production by lymph node-derived CD8 T cells after in-vitro re-stimulation with the HPV16 E7 CD8 peptide RAHYNIVTF. Groups: VAX n=4, VAX + aCSF1R n=7. Statistics: * $p < 0.05$; ** $p < 0.01$; *** $p < 0.001$; **** $p < 0.0001$; n.s. = not significant.

Collectively, these data show that the treatments I tried were not sufficient to ameliorate the immune response to the NP-VAX due to their detrimental effects on E7-specific CD8 T cells

(IPI549) or due to their limited ability to deplete monocytes/macrophages. Importantly, however, the data collected with the CLDlip treatments helped shedding some light on the poor efficacy of the previously illustrated depletion experiments, indicating that such strategies might have a reduced efficacy in this model.

3.2.32 Chemotherapy aimed to eliminate myeloid cells are only transiently effective

Chemotherapy is the next class of myeloid cells-depleting treatments that I tested in HPV+ mice. Namely, I choose 5-fluorouracil (5FU) and gemcitabine for their reported ability of depleting MDSCs (109, 110) and carboplatin (carboplatin + paclitaxel), that is the standard of care for cervical cancer patients and it has been shown to be able to reduce the numbers of myeloid cells in TC1 tumor-bearing mice and in patients (111).

HPV+ mice were treated once with either 5FU or gemcitabine 3 days prior to vaccination. Mice were then vaccinated at day 0 with the NP-VAX and sacrificed at day 9 when flow cytometry analyses on the vaccination site draining lymph nodes were performed. Myeloid cells depletion was measured in the blood 5 days after the chemo treatment (2 days after vaccination) (Fig. 43A, B, C and D) and the results revealed that mice treated with 5FU had a significant decrease in monocytes (Fig. 43C) and lower, although not significantly, numbers of macrophages (Fig. 43D) while gemcitabine treatment did not cause a reduction in myeloid cells (Fig. 43A, B, C and D) but was rather associated with a small but significant increase in neutrophils (Fig. 43B). Analyses on the lymph nodes at day 9 after immunization showed similar numbers of all the myeloid populations in mice that received gemcitabine while I detected a trend showing an increase in total CD11b+ cells, neutrophils and monocytes in mice that were treated with 5FU (Fig. 43E, F, G, and H). These changes are perhaps reflecting the activation of compensatory mechanisms following the 5FU-dependant decrease measured in the blood at the earlier time-point that led to a subsequent expansion of several myeloid populations. CD8 T cells at the time of sac were not significantly altered by the chemotherapy combination (Fig. 43I). The percentage of E7-specific CD8 T cells and cytokine production after re-stimulation were similar between the groups (Fig. 43L and M).

These results show that, although 5FU was capable of decreasing the numbers of some myeloid cells populations, this depletion was not sufficient, either because not enough cells were

eliminated, because neutrophils were spared, or because was not lasting long enough to be translated into a detectable improvement in the response to the vaccine.

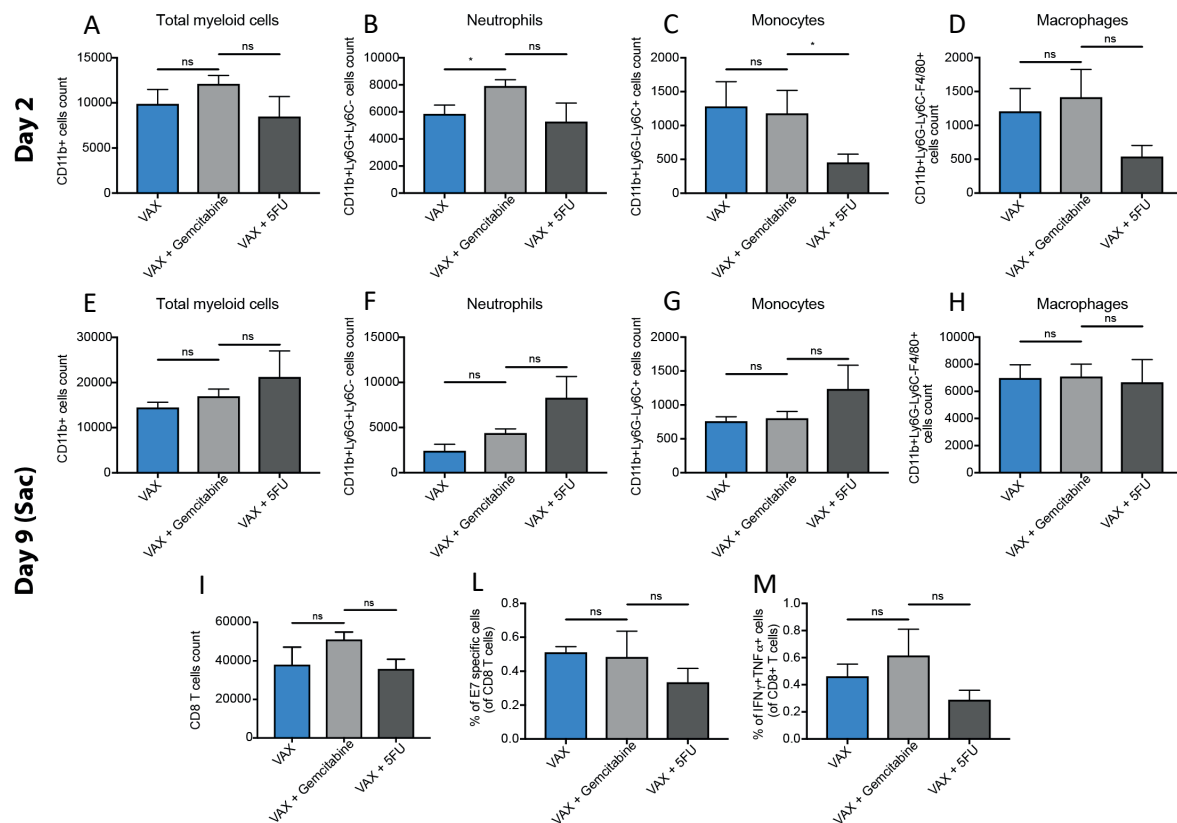


Figure 43. Flow cytometry analyses of the effects of chemotherapy with gemcitabine and 5FU on myeloid cells and on the anti-E7 response. Flow cytometry analyses at different time-points of (A, E) CD11b+ total myeloid cells, (B, F) CD11b+Ly6G+Ly6C- neutrophils, (C, G) CD11b+Ly6G-Ly6C+ monocytes and (D, H) CD11b+Ly6G-Ly6C-F4/80+ macrophages in the blood (day 2) or in the lymph nodes (day 9) of HPV+ mice. (I) Flow cytometry analyses of CD8 T cells in the lymph nodes. (L) Flow cytometry analyses of E7-specific CD8 T cells in the lymph nodes using tetramers recognizing the HPV16 E7 CD8 peptide RAHYNIVTF presented on H2Db. (M) Flow cytometry analyses of IFN γ and TNF α production by lymph node -derived CD8 T cells after in-vitro re-stimulation with the HPV16 E7 CD8 peptide RAHYNIVTF. Groups: VAX n=4, VAX + gemcitabine n=4, VAX + 5FU n=5. Statistics: * $p < 0.05$; ** $p < 0.01$; *** $p < 0.001$; **** $p < 0.0001$; n.s. = not significant.

Combinatorial treatment of an E7 containing vaccine with carbotaxol has previously been reported to be feasible in both TC1 tumor-bearing mice and in patients with pre-cancerous HPV+ lesions (111). Therefore, I used the same regimen utilized by others. Namely HPV+ mice received a first round of chemotherapy (day -14) followed by a second one 7 days later (day -7). For this experiment, I decided to use a DC vaccine instead of the nanoparticle formulation that I usually employ. The reason behind this choice, was to eliminate any possible interference that could be due to the killing of DCs and other APCs by the chemo treatment. The DC vaccine was prepared as illustrated in previous experiments. 7 days after the second chemo treatment, mice received the DC VAX (day 0). Myeloid cells depletion in the blood was checked 5 days after the second dose of chemo (day -2), and mice were sacrificed at day 9 after immunization when flow cytometry analyses on the vaccination site draining lymph nodes were performed. Analyses on the blood at the early time point (day -2) showed a decrease in the total CD11b+ cells (Fig. 44A) that was caused by diminished neutrophils (Fig. 44B) and macrophages (Fig. 44D) but not monocytes (Fig. 44C) while CD8 T cells remained untouched by the chemo treatment (Fig. 44E). When I looked at the lymph nodes at day 9 the depletion was gone and all the populations were back to similar levels to the group that did not receive carbotaxol (Fig. 44A, B, C, and D), indicating that, although capable of depleting myeloid cells, the effect of chemotherapy in HPV+ mice was lost by the end of the experiment. As I expected from these results and from the return of myeloid cells to normal levels, there were no changes in total CD8 T cells (Fig. 44E), in the percentage of E7-specific CD8 (Fig. 44F) or in their ability at producing cytokines (Fig. 44G) in mice that received the combination of NP-VAX and carbotaxol.

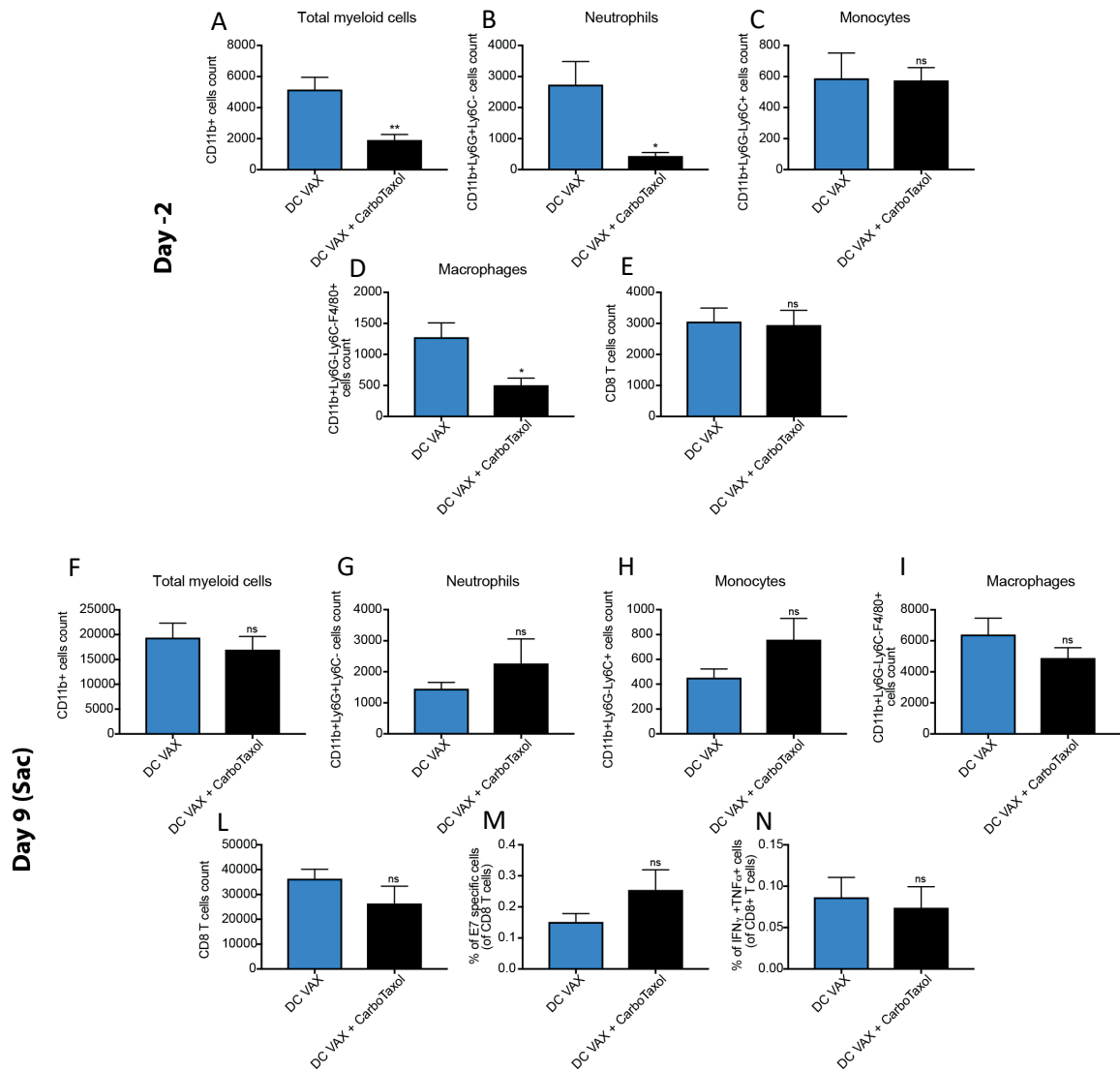


Figure 44. Flow cytometry analyses of the effects of chemotherapy with carbottaxol on myeloid cells and on the anti-E7 response. Flow cytometry analyses at different time-points of (A, F) CD11b+ total myeloid cells, (B, G) CD11b+Ly6G+Ly6C- neutrophils, (C, H) CD11b+Ly6G-Ly6C+ monocytes, (D, I) CD11b+Ly6G-Ly6C-F4/80+ macrophages and (E, L) CD8 T cells in the blood (day -2) or in the lymph nodes (day 9) of HPV+ mice. (M) Flow cytometry analyses of E7-specific CD8 T cells in the lymph nodes using tetramers recognizing the HPV16 E7 CD8 peptide RAHYNIVTF presented on H2Db. (N) Flow cytometry analyses of IFN γ and TNF α production by lymph node - derived CD8 T cells after in-vitro re-stimulation with the HPV16 E7 CD8 peptide RAHYNIVTF. $n=4$. Statistics: * $p < 0.05$; ** $p < 0.01$; *** $p < 0.001$; **** $p < 0.0001$; n.s. = not significant.

Collectively, these data show that chemotherapy can be used to trigger a substantial depletion in the myeloid cells compartment, but its effect remains time-limited and additionally, not all the cell populations are equally affected by the treatments. I anticipate that alternative schedules and/or combinations will have to be considered in order to extend the window of myeloid cells depletion before improvements in the response to the vaccine can be achieved. However, it is important to keep in mind that a careful timing of these treatments will likely be absolutely required to avoid killing the effector cells generated upon vaccination.

3.2.33 Blocking IL-10 or IDO does not relieve the systemic immunosuppression

In light of the poor efficacy of depleting strategies, I set out to block the immunosuppressive factors produced by myeloid cells directly. Previous results showed that two of the most prominently expressed ones that I previously found in the LNs of HPV+ mice, IDO and IL-10, seems to be produced by myeloid cells. In vitro results suggested that blocking IDO was improving on the activation of DCs while blocking IL-10 failed to show improvements in either CD8 T cells proliferation or on DCs activation. However, IL-10 might still be acting indirectly on CD8 T cells in-vivo. Therefore, I decided to block these factors either alone or in combination.

Treatment with the small molecule IDO inhibitor started 7 days before vaccination and was administered daily while the anti-IL10 antibody was administered 3 times per week starting at the time of vaccination. Mice were sacrificed 9 days after immunization with the NP-VAX and flow cytometry analyses on the vaccination-site draining lymph nodes were performed. Unfortunately, blocking these factors in HPV+ mice did not increase the numbers of E7-specific CD8 T cells or the cytokine production upon vaccination either when administered as single treatments (Fig. 45A and B) or in combination (Fig. 45C and D). These results suggest that either the pharmacological inhibition was not strong enough to completely cancel the activity of IDO and/or IL10, or that these factors are not playing a major role in the immunosuppression and are possibly secondary, or even that their blockade is simply compensated by other mechanisms.

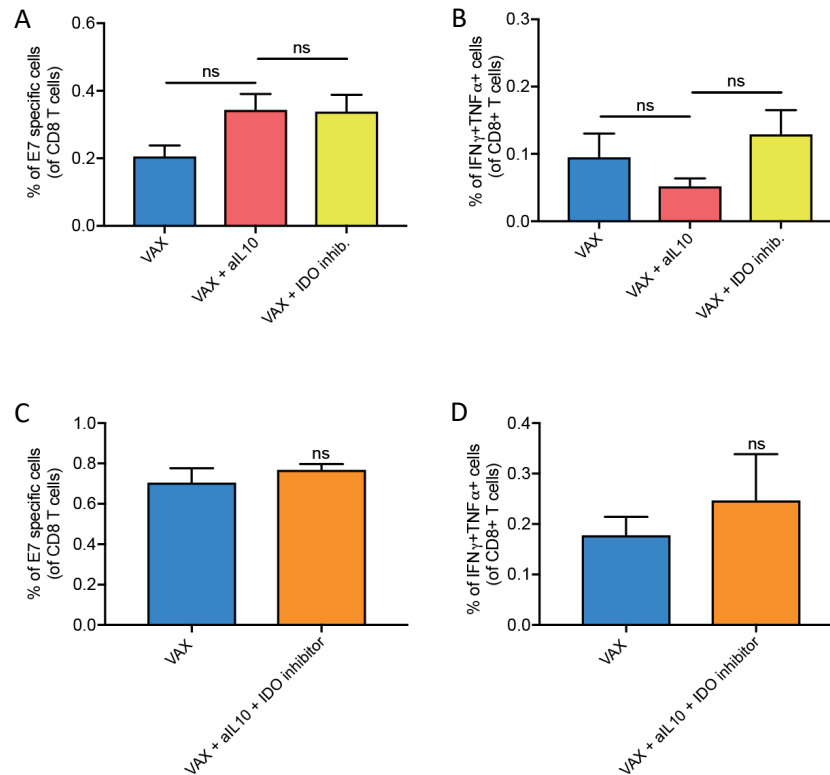


Figure 45. Flow cytometry analyses of the anti-E7 immune response following blockade of IDO and/or IL-10. (A, C) Flow cytometry analyses of E7-specific CD8 T cells in the lymph nodes of HPV+ mice using tetramers recognizing the HPV16 E7 CD8 peptide RAHYNIVTF presented on H2Db. (B, D) Flow cytometry analyses of IFNγ and TNFα production by HPV+ mice lymph node -derived CD8 T cells after in-vitro re-stimulation with the HPV16 E7 CD8 peptide RAHYNIVTF. Groups: (A, B) VAX n=3, VAX + aIL10 n=4, VAX + IDO inhibitor n=5; (C, D) VAX n= 6, VAX + aIL10 + IDO inhibitor n=4. Statistics: * $p < 0.05$; ** $p < 0.01$; *** $p < 0.001$; **** $p < 0.0001$; n.s. = not significant.

3.2.34 Sildenafil does not abrogate the suppressive activity of myeloid cells

It has been reported that treatment with sildenafil, a phosphodiesterase-5 (PDE5) inhibitor, was able to reduce the suppressive functions of myeloid cells by downregulating Arg-1 and NOS-2 in a setting similar to the one of HPV+ mice and lead to improved anti-tumor responses (238). Following the previously published dosage, sildenafil treatment started 7 days before immunization and was given daily to HPV+ mice. Mice received a single dose of NP-VAX and, when sacrificed 9 days later, flow cytometry analyses on the vaccination-site draining lymph nodes were performed. My results showed that sildenafil treatment did not improve the immune response to

the vaccine in HPV+ mice (Fig.46 A and B). Failure of this treatment suggests that PDE5 inhibitors alone cannot block the systemic immunosuppression possibly because this enzyme is not playing a role in the setting of HPV+ mice or because of the presence of multiple-redundant immunosuppressive mechanisms.

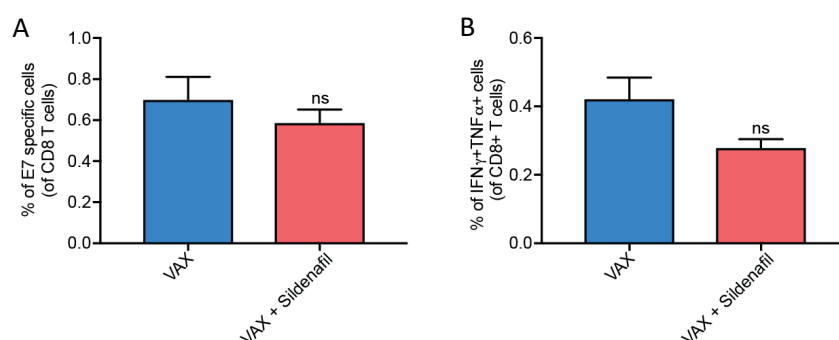


Figure 46. Flow cytometry analyses of the effect of sildenafil on the anti-E7 immune response.

(A) Flow cytometry analyses of E7-specific CD8 T cells in the lymph nodes of HPV+ mice using tetramers recognizing the HPV16 E7 CD8 peptide RAHYNIVTF presented on H2Db and (B) Flow cytometry analyses of IFN γ and TNF α production by HPV+ mice lymph node-derived CD8 T cells after in-vitro re-stimulation with the HPV16 E7 CD8 peptide RAHYNIVTF (n=4). Statistics: * $p < 0.05$; ** $p < 0.01$; *** $p < 0.001$; **** $p < 0.0001$; n.s. = not significant.

3.2.35 Increased levels of G-CSF and GM-CSF in HPV+ mice could explain the increase in myeloid cells.

Direct targeting of the myeloid cells, either with depleting antibodies or by trying to block their suppressive function, proved to be hard to achieve and/or ineffective in HPV+ mice. Therefore, I decided to investigate which factors, that could be responsible for driving the myeloid cell expansion, are increased in HPV+ mice compared to the non-transgenic HPV- littermates. Since HPV+ mice have a systemic increase in myeloid cells, I reasoned that the increase in these factors should also be measurable at a systemic level in the periphery. Therefore, I performed additional western blots analyses on LNs from HPV+ and HPV- mice. Interestingly, I found upregulation of G-CSF and GM-CSF but not M-CSF, indicating that there is indeed a systemic increase in these growth factors (Fig. 47A and B). The higher levels of G-CSF and GM-CSF could

easily be responsible for the increased systemic accumulation of myeloid cells seen both in spleen and lymph nodes of the HPV+ GEMM.

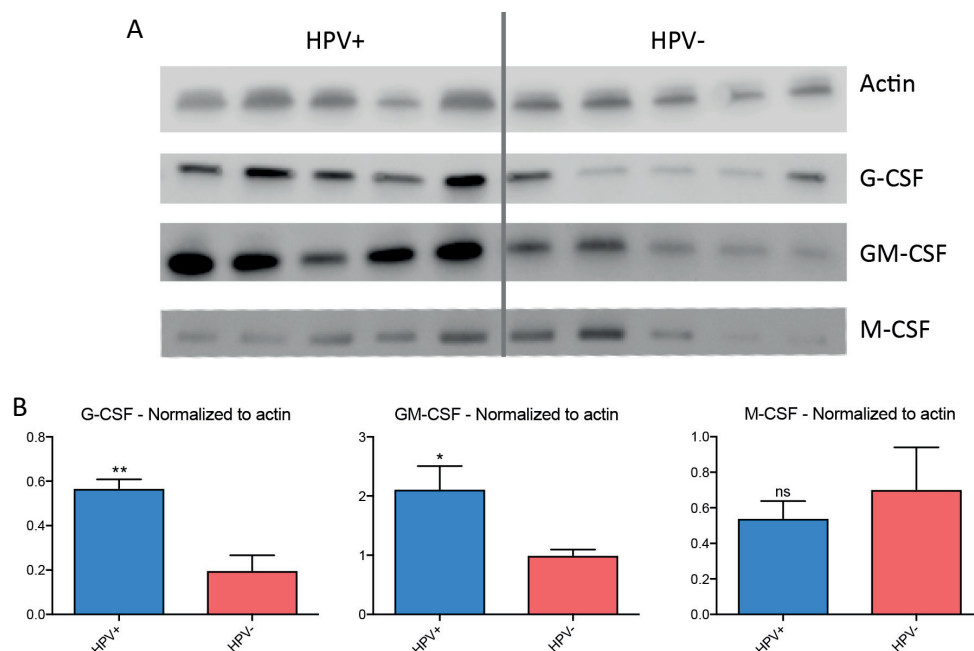


Figure 47. Expression of growth factors driving myeloid cell expansion in the lymph nodes of HPV+ and HPV- mice. A) Western blot of whole lymph node protein extracts from HPV+ and HPV- mice -derived lymph nodes. 1 popliteal lymph node and 1 brachial lymph node per mouse were lysed together. B) Quantification of the western blot bands normalized to actin. Statistics: *p < 0.05; **p < 0.01; ***p < 0.001; ****p < 0.0001; n.s. = not significant.

3.2.36 Blocking growth factors to reduce myeloid cells number seems feasible but requires additional testing

The most abundant CD11b+ population in HPV+ mice are neutrophils. Therefore, I decided to start with a short preliminary experiment where I blocked G-CSF, a factor mainly involved in promoting granulocytes proliferation. Anti-G-CSF (aG-CSF) treatment started 1 day before vaccination and mice were sacrificed 7 days after administration of the NP-VAX. Analyses on the vaccination site draining lymph nodes showed a reduction in the total numbers of CD11b+ (Fig. 48A) cells along with a significant reduction in neutrophils (Fig. 48B) (that went down 10-fold) and in monocytes (Fig. 48C) but not in macrophages (Fig. 48D). Unfortunately, the immune response

against E7 was not improved (Fig. 48 F and G) possibly either because depletion did not start early enough to rescue the phenotype of the dendritic cell, that were likely still suppressed at the time of vaccination, or because the remaining macrophages and monocytes could still exert their suppressive functions.

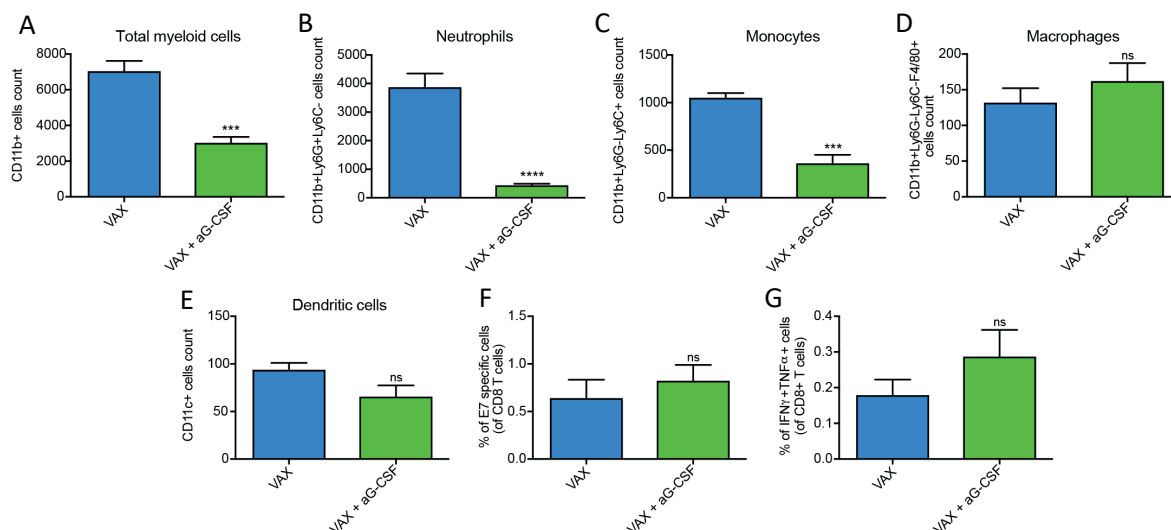


Figure 48. Flow cytometry analyses of the effects of G-CSF blockade on myeloid cells and on the anti-E7 response. Flow cytometry analyses of (A) CD11b+ total myeloid cells, (B) CD11b+Ly6G+Ly6C- neutrophils, (C) CD11b+Ly6G+Ly6C+ monocytes, (D) CD11b+Ly6G+Ly6C+F4/80+ macrophages and (E) CD11c+ dendritic cells in the lymph nodes of HPV+ mice. Gating strategy for this population can be found in the Appendix Fig. 6. (F) Flow cytometry analyses of E7-specific CD8 T cells in the lymph nodes of HPV+ mice using tetramers recognizing the HPV16 E7 CD8 peptide RAHYNIVTF presented on H2Db. (G) Flow cytometry analyses of IFN γ and TNF α production by HPV+ mice lymph node -derived CD8 T cells after in-vitro re-stimulation with the HPV16 E7 CD8 peptide RAHYNIVTF. Groups: VAX n=4, VAX + aG-CSF n=5. Statistics: * $p < 0.05$; ** $p < 0.01$; *** $p < 0.001$; **** $p < 0.0001$; n.s. = not significant.

As a last attempt at depleting myeloid cells, I decided to combine multiple treatments hoping to achieve a substantial reduction in all the populations. Namely, I combined aG-CSF treatment with anti-GM-CSF (aGM-CSF) and anti-Gr1 (aGr1). The rationale behind this treatment was to block both growth factors and at the same time, use aGr1 to deplete any remaining Ly6G+ neutrophils

and Ly6C⁺ monocytes. Blocking of GM-CSF might potentially have an impact on macrophage too, collectively reducing all the major myeloid cells population.

As blocking these factors might have a detrimental impact on DCs, I decided to use a DC vaccine similarly to what I did with the combination with carbotaxol. Treatment of HPV⁺ mice with aG-CSF and aGM-CSF was initiated 7 days before vaccination, while treatment with aGr1, that is known to quickly lose its efficacy after beginning the treatment, was given starting 1 day before vaccination. At day 0, all the mice received the DC VAX and were then sacrificed 9 days later when flow cytometry analyses on the vaccination-site draining lymph nodes were performed. Surprisingly, I did not measure a reduction in myeloid cells in the LNs of the mice treated with the triple combo of antibodies (Fig. 49A, B, C, and D). Consequently, there was no improvement of the immune response to the vaccine (Fig. 49 E and F). Seeing that aG-CSF alone worked nicely at depleting neutrophils and monocytes I was expecting to see a similar situation, if not better in this experiment. Perhaps the treatment against G-CSF and GM-CSF also have a short window of efficacy and, once it's passed, myeloid cells quickly re-expand and return to normal levels masking the benefit of the combination similarly to what I observed previously. Alternatively, these treatments might somehow interfere with each other and cancel themselves out, although it seems an unlikely situation, at least for this specific treatments combination.

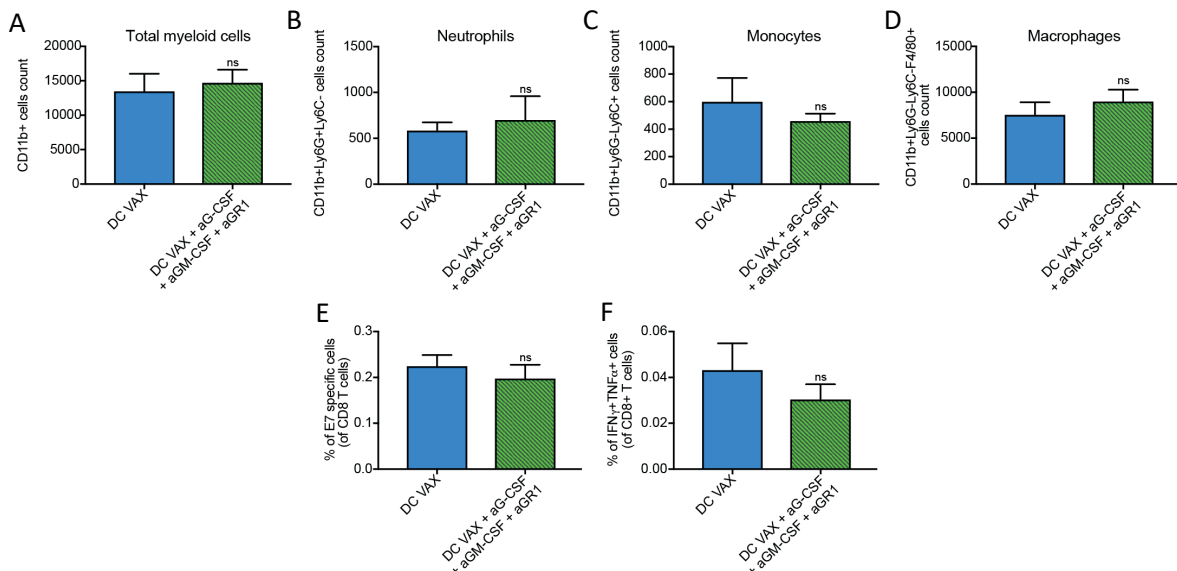


Figure 49. Flow cytometry analyses of the effects of a combinatorial treatment with anti-G-CSF, anti-GM-CSF and anti-GR1 on myeloid cells and on the anti-E7 response. Flow cytometry analyses

of (A) CD11b⁺ total myeloid cells, (B) CD11b⁺Ly6G⁺Ly6C⁻ neutrophils, (C) CD11b⁺Ly6G⁻Ly6C⁺ monocytes and (D) CD11b⁺Ly6G⁻Ly6C⁻F4/80⁺ macrophages in the lymph nodes of HPV⁺ mice. (F) Flow cytometry analyses of E7-specific CD8 T cells in the lymph nodes of HPV⁺ mice using tetramers recognizing the HPV16 E7 CD8 peptide RAHYNIVTF presented on H2Db. (G) Flow cytometry analyses of IFN γ and TNF α production by HPV⁺ mice lymph node -derived CD8 T cells after in-vitro re-stimulation with the HPV16 E7 CD8 peptide RAHYNIVTF. Groups: DC VAX n=4, DC VAX 1 aG-CSF + aGM-CSF + aGR1 n=5. Statistics: * $p < 0.05$; ** $p < 0.01$; *** $p < 0.001$; **** $p < 0.0001$; n.s. = not significant.

However, to assess if the combination was indeed able to generate better CD8 T cells but its effect got masked by the return of the myeloid cells, I isolated whole splenocytes from the mice used in the previous experiment and performed re-stimulation assay with the E7-CD8 peptide. Additionally, I magnetically isolated CD8 T cells from the splenocytes and performed the same assay with just CD8 T cells present in culture.

Interestingly, there was no difference in cytokine production from CD8 T cells in the splenocytes mix and isolated CD8 T cells from mice that received DC VAX alone, indicating that their functions were already defective and removal of the immunosuppressive populations contained in the spleen did not ameliorate their functionality. On the other hand, isolated CD8 T cells from mice treated with the combination of aG-CSF, aGM-CSF and aGR1 showed a more than 3-fold increase in cytokine production compared to the CD8 T cells in the whole splenocytes mix (Fig. 50). This result suggests that the combinatorial treatment was capable of inducing the generation of more potent CD8 T cells, possibly due to a transient depletion of myeloid cells at the time of vaccination, but their superior cytokine production capacity was masked in the presence of the immunosuppressive cells contained in the splenocyte mix.

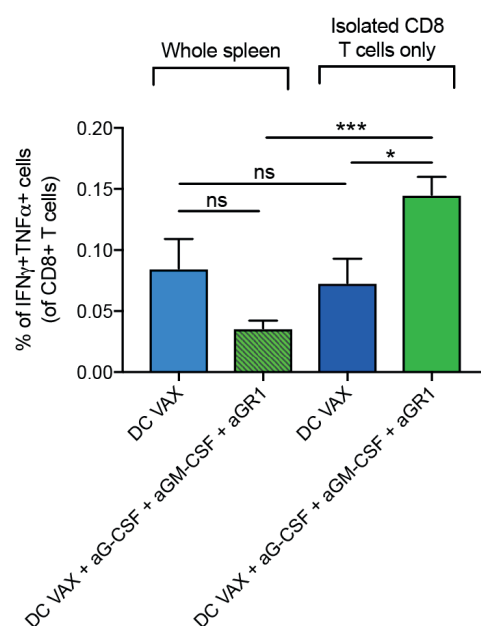


Figure 50. Ex-vivo re-stimulation of whole splenocytes and isolated CD8 T cells from mice that received anti-G-CSF, anti-GM-CSF and anti-GR1. Flow cytometry analyses performed of IFN γ and TNF α production from CD8 T cells after in-vitro re-stimulation with the HPV16 E7 CD8 peptide RAHYNIVTF of whole splenocytes or of isolated CD8 T cells (n=4). Statistics: *p < 0.05; **p < 0.01; ***p < 0.001; ****p < 0.0001; n.s. = not significant.

Collectively these data strengthen the fact that depleting myeloid cells in HPV+ mice might be hard to achieve, and will likely require completely different approaches or a carefully thought combination of the ones illustrated above. Also, it is clear that the beneficial effects of possibly many of the treatments that I tried, including immunotherapy with agonistic and checkpoint blockade antibodies, might have been masked by the presence of immunosuppressive myeloid cells in the analyzed lymphoid organs.

3.2.37 Investigating mechanisms behind expansion of the myeloid cell compartment and the production of G-CSF and GM-CSF

The attempt at eliminating the immunosuppressive myeloid cells proved to be unsuccessful so far. Therefore, I decided to start investigating the mechanism behind their expansion. This

information might shed some light on this phenomenon that is also seen in patients, and possibly help identify additional strategies for targeting these cells or their functions.

3.2.38 HPV+ mice have systemic inflammation as indicated by an increase in several factors related to inflammatory conditions

It has been previously reported, both in patients and in the old K14HPV16 non-H2b mouse model, that squamous cell carcinoma (SCC) of the skin is associated with local tumor-promoting chronic inflammation (239). I reasoned that local inflammation in large regions of the skin, like it could be for HPV+ mice, or at the tumor site (in both mice and patients) might lead to the release of inflammatory mediators and other factors that could trigger systemic effects, like the increase in myeloid cells. In fact, myeloid cells expansion is known to happen under inflammatory conditions (240, 241). Additionally, the presence of systemic chronic inflammation might also have a negative impact on immune responses (242, 243).

To test for this hypothesis, I first performed western blot analyses on the lymph nodes of HPV+ and HPV- mice looking for factors that are usually upregulated under inflammatory conditions. Interestingly, I observed that IL-1beta, HSP90, IL-23, and CRP were all upregulated in HPV+ mice suggesting that there is a chronic inflammatory state in these lymphoid organs and possibly systemically (Fig. 51A and B). Interestingly, IL-23 is a potent inducer of IL-17 (WB analyses for this cytokine gave unclear results), a cytokine involved in other inflammatory conditions of the skin like psoriasis.

These results suggest the presence of a chronic inflammatory state in HPV+ mice that could explain the increase in G-CSF and GM-CSF. It could be speculated that the induction of immunosuppressive myeloid cells might be a response of the organism that is trying to stop the excess of inflammation.

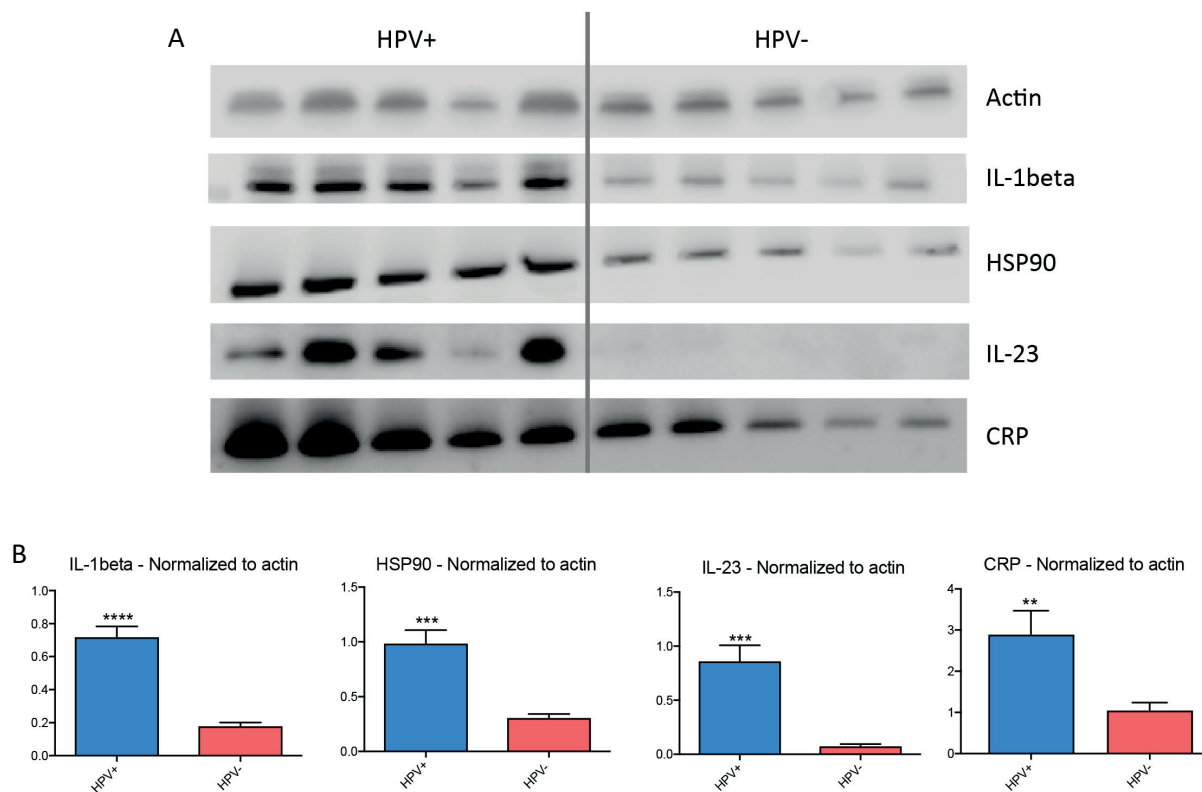


Figure 51. Expression of pro-inflammatory and inflammation-related factors in the lymph nodes of HPV+ and HPV- mice. (A) Western blot of whole lymph node protein extracts from HPV+ and HPV- mice -derived lymph nodes. 1 popliteal lymph node and 1 brachial lymph node per mouse were lysed together. (B) Quantification of the western blot bands normalized to actin. Statistics: * $p < 0.05$; ** $p < 0.01$; *** $p < 0.001$; **** $p < 0.0001$; n.s. = not significant.

3.2.39 GM-CSF is produced locally in the skin

I then started looking for the source of G-CSF and GM-CSF. I first decided to look at the skin surfaces of HPV+ mice as these factors might be produced locally. I collected whole ears, the back skin and the tail epidermis from HPV+ and HPV- mice and performed western blot on the protein extracts. I found a substantial upregulation of GM-CSF (Fig. 52A and C) but not G-CSF (Fig. 52A and B) in all the samples derived from HPV+ mice suggesting that, at least for GM-CSF, the production might be mainly happening locally in the skin. However, the site of G-CSF production remained elusive. Interestingly, the ear seemed to be containing the highest levels of GM-CSF, perhaps due to the severe phenotype observed in this organ (Fig. 53).

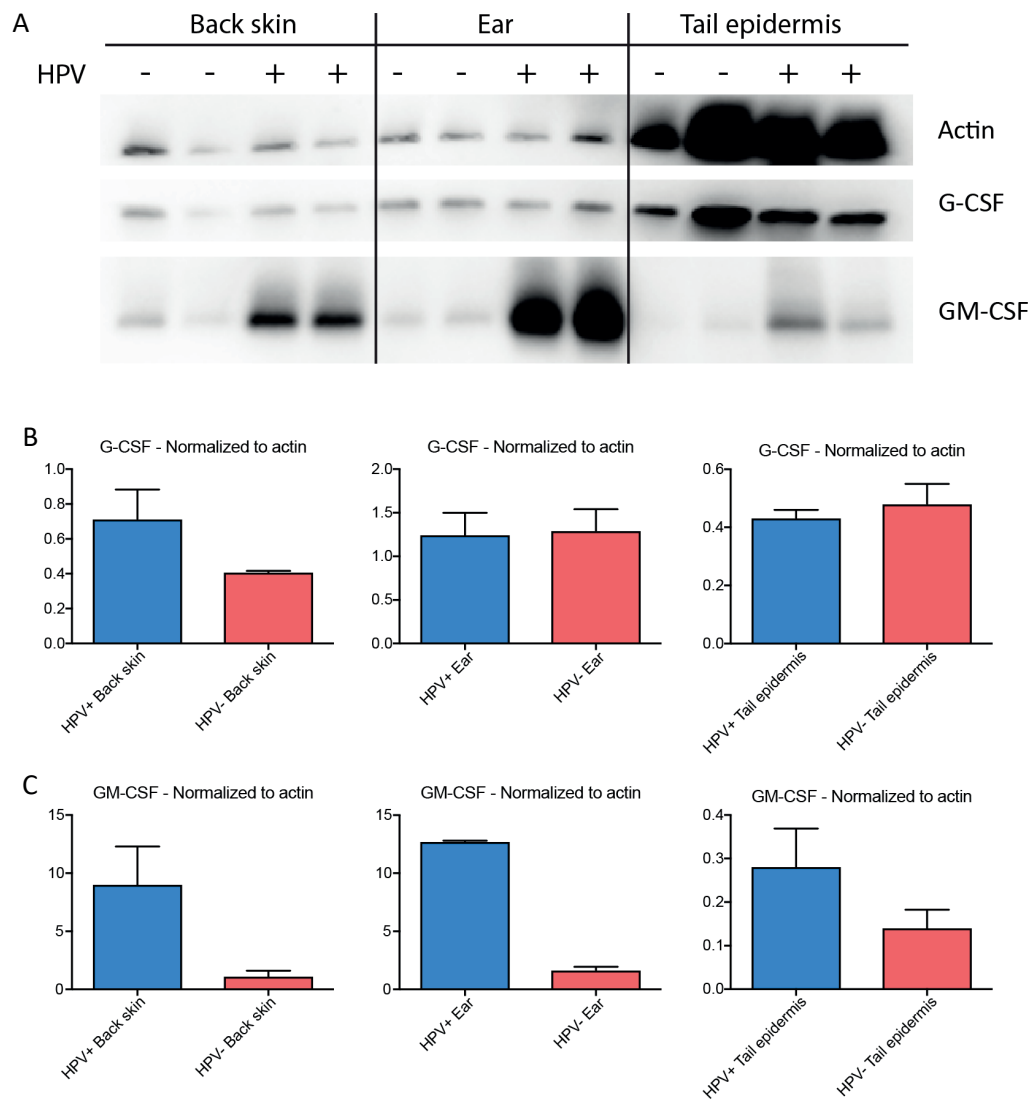


Figure 52. Analyses of GM-CSF and G-CSF production at various skin surfaces. (A) Western blot of protein extracts from ear, back skin or tail epidermis from HPV+ and HPV- mice. (B,C) quantification of the western blot bands normalized to actin. Statistics: * $p < 0.05$; ** $p < 0.01$; *** $p < 0.001$; **** $p < 0.0001$; n.s. = not significant.

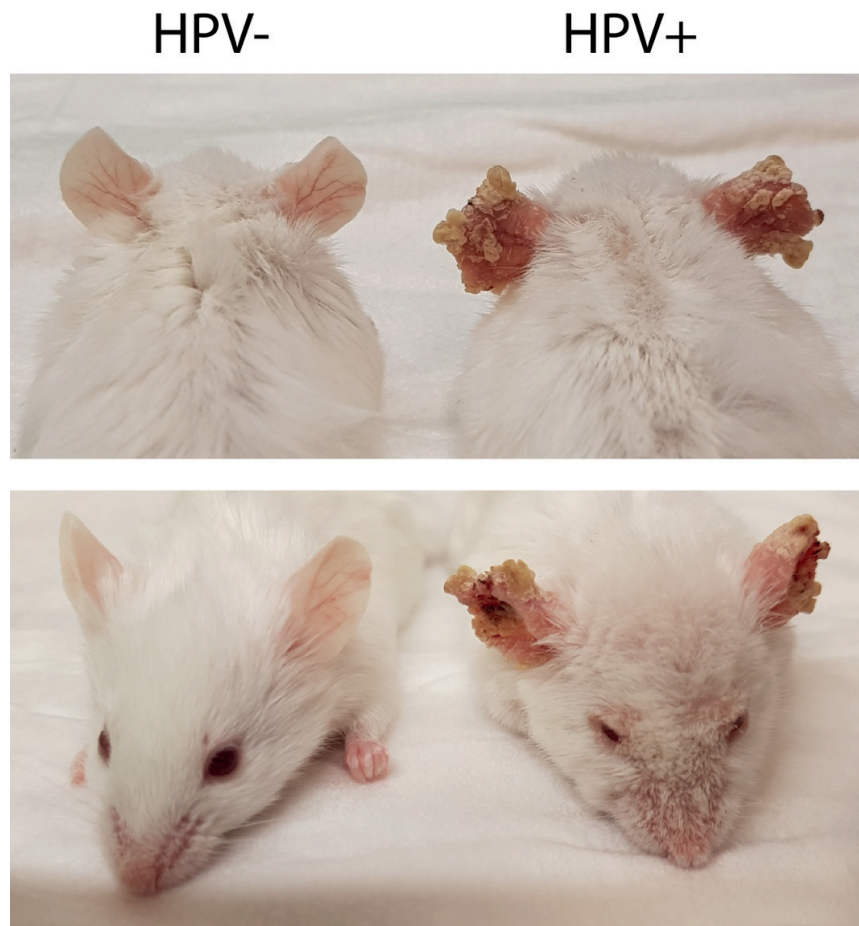


Figure 53. Comparison of the ear phenotype in HPV- and HPV+ mice. Images of representative HPV- (left) and HPV+ (right) 12 weeks old mice. Keratinocytic masses can be seen on the ears of HPV+ mice. Statistics: * $p < 0.05$; ** $p < 0.01$; *** $p < 0.001$; **** $p < 0.0001$; n.s. = not significant.

Preliminary flow cytometry analyses of the ear, back skin or tail skin of HPV+ and HPV- mice was also performed to quantify the presence of immune cells, keratinocytes, and fibroblasts.

The results revealed that in both ears and skin all these populations were increased in HPV+ mice (Fig. 54 A-F), while in the tail they remained similar between both strains (Fig. 54G, H and I). The increase in immune cells (Fig. 54A and D) suggests that there is an important inflammatory cells component associated with the skin. These results also show the expansion in keratinocytes that should be expected from the HPV expression in these cells. Additionally, the increase in fibroblasts (Fig. 54 C and F) could represent an expansion in CAFs, a cell type that has already been reported to play a role in tumor growth in the K14HPV16 non-H2b mouse model (244).

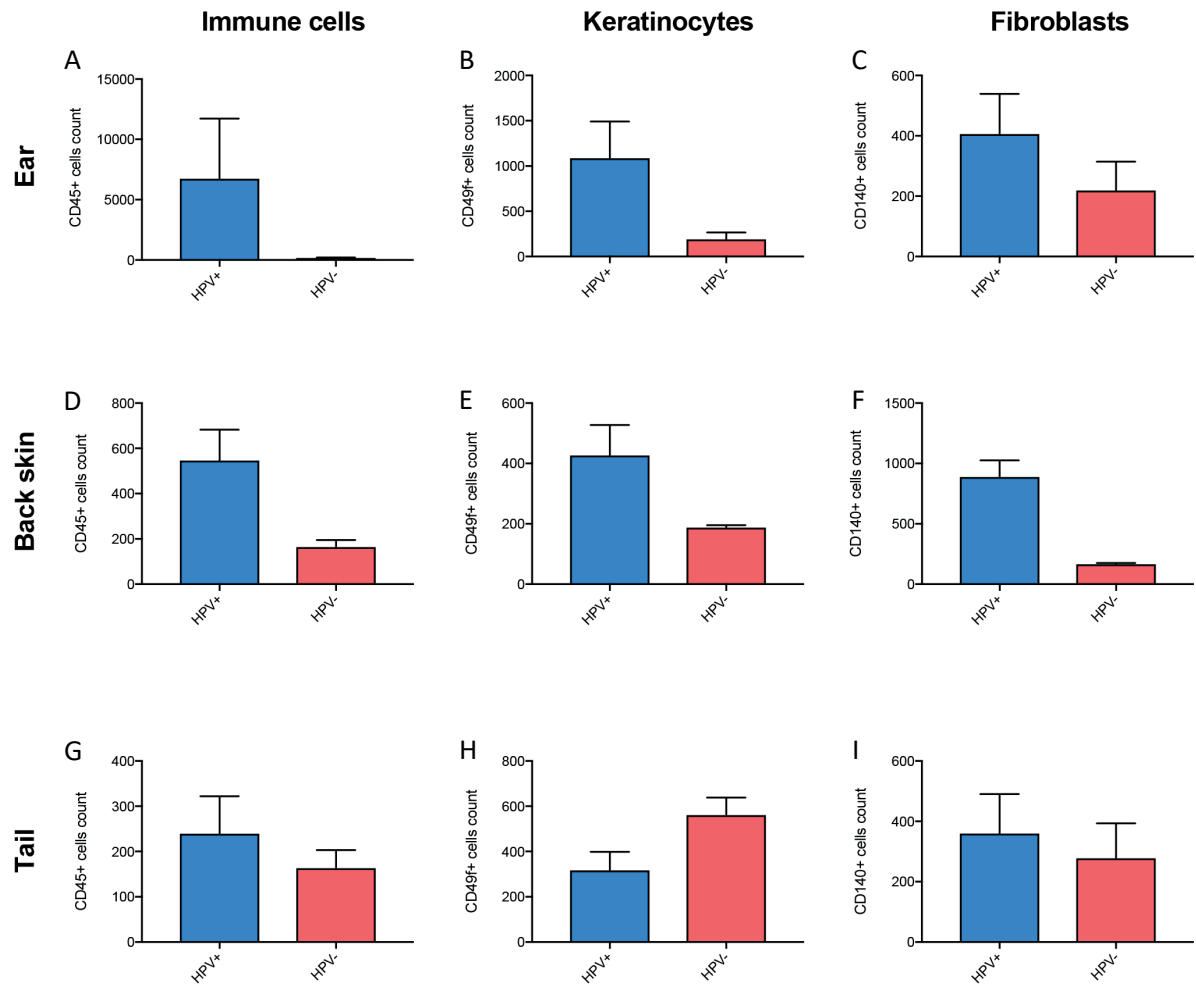


Figure 54. Flow cytometry analyses of different cell populations at various skin surfaces. Flow cytometry analyses performed on different skin surfaces for (A, D, G) CD45+ immune cells, (B, E, H) CD49f+CD140- keratinocytes and (C, F, I) CD49f-CD140+ fibroblasts. $n=2$. Statistics: * $p < 0.05$; ** $p < 0.01$; *** $p < 0.001$; **** $p < 0.0001$; n.s. = not significant.

Collectively, these results show that production of GM-CSF happens at the skin surfaces, possibly as a consequence of local inflammation. However, as all the analyzed populations were similarly increased in the HPV+ mice, it is currently unclear which one could represent the main source of this factor and further analyses on the specific populations will be required.

3.2.40 B lymphocyte depletion causes a reduction in the number of circulating macrophages but does not alter the local immune infiltrates in the ear skin.

In K14HPV16 non-H2b mice, the local inflammatory reaction was found to be linked to B cells, and it has been shown that IgG deposition at the site of skin SCCs was altering the phenotype of macrophages that could be rescued upon B cell depletion (164, 239). I reasoned that B cell depletion with a similar anti-CD20 (aCD20) antibody might alleviate local and systemic inflammation, potentially leading to a reduction in the production of inflammatory mediators and factors responsible for expanding the immunosuppressive myeloid cells.

To test this hypothesis, HPV+ mice were pre-treated with aCD20 once per week for 5 weeks. The long treatment was chosen to leave enough time to reach substantial cell depletion, and to allow for the antibodies to be cleared from the skin. B cell depletion in the blood remained stable for the duration of the treatment with these cells almost completely disappearing from the circulation (Fig. 55A). After 5 weeks of aCD20 treatment, mice were immunized with the NP-VAX and sacrificed 9 days later. Treatment with aCD20 continued until the end of the experiment. Flow cytometry analyses of the vaccination site draining lymph nodes showed that B cell depletion was also effective at this site (Fig. 55B). When I looked at myeloid cells, however, I found no significant reduction in total CD11b+ cells (Fig. 55C), neutrophils (Fig. 55D) and monocytes (Fig. 55E). Consistent with the previously published link between B cells and macrophages, I found that latter were significantly lower in the lymph nodes (Fig. 55F). To exclude interferences with antigen presentation, I checked dendritic cells and found that were not changed by this treatment (Fig. 55G). When I looked at the immune response against E7 elicited by vaccination, however, I found no significant improvement in mice that received aCD20 treatment (Fig. 55H and I).

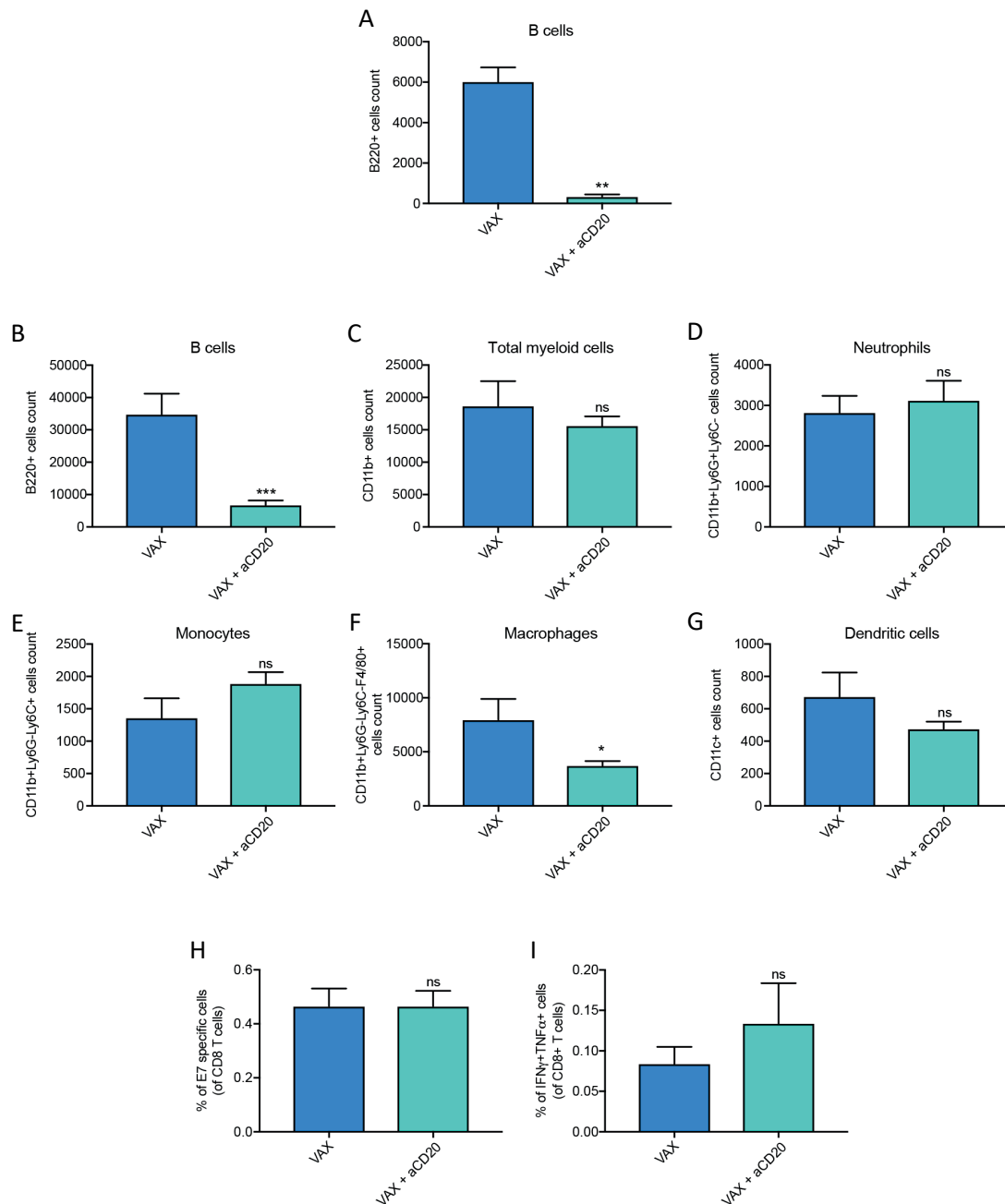


Figure 55. Flow cytometry analyses of the effects of B lymphocyte depletion on various immune population and on the anti-E7 response. (A) Flow cytometry analyses of B220+ B cells in the blood of HPV+ mice 4 weeks after the start of aCD20 treatment. Gating strategy for this population can be found in the Appendix Fig. 11. Flow cytometry analyses of (B) B220+ B cells, (C) CD11b+ total myeloid cells, (D) CD11b+Ly6G+Ly6C- neutrophils, (E) CD11b+Ly6G-Ly6C+ monocytes, (F) CD11b+Ly6G-Ly6C-F4/80+ macrophages and (G) CD11c+ dendritic cells in the lymph nodes of HPV+

*mice. (H) Flow cytometry analyses of E7-specific CD8 T cells in the lymph nodes of HPV+ mice using tetramers recognizing the HPV16 E7 CD8 peptide RAHYNIVTF presented on H2Db. (I) Flow cytometry analyses of IFN γ and TNF α production by HPV+ mice lymph node -derived CD8 T cells after in-vitro re-stimulation with the HPV16 E7 CD8 peptide RAHYNIVTF. Groups: VAX n=4, VAX + aCD20 n=6. Statistics: * $p < 0.05$; ** $p < 0.01$; *** $p < 0.001$; **** $p < 0.0001$; n.s. = not significant.*

A previous publication in the old K14HPV16 non-H2b mouse model reported a local effect of the aCD20 treatment on macrophages and T cell infiltrates, therefore, I performed immunofluorescence staining on the mouse ears. Preliminary results showed no obvious change in CD8 T cells (Fig. 56A) or macrophages (Fig. 56B) infiltrates were observed, although the F4/80 staining appeared to be slightly dimmer upon aCD20 treatment. I also checked local neutrophils that were also not changed by the treatment (Fig. 56B).

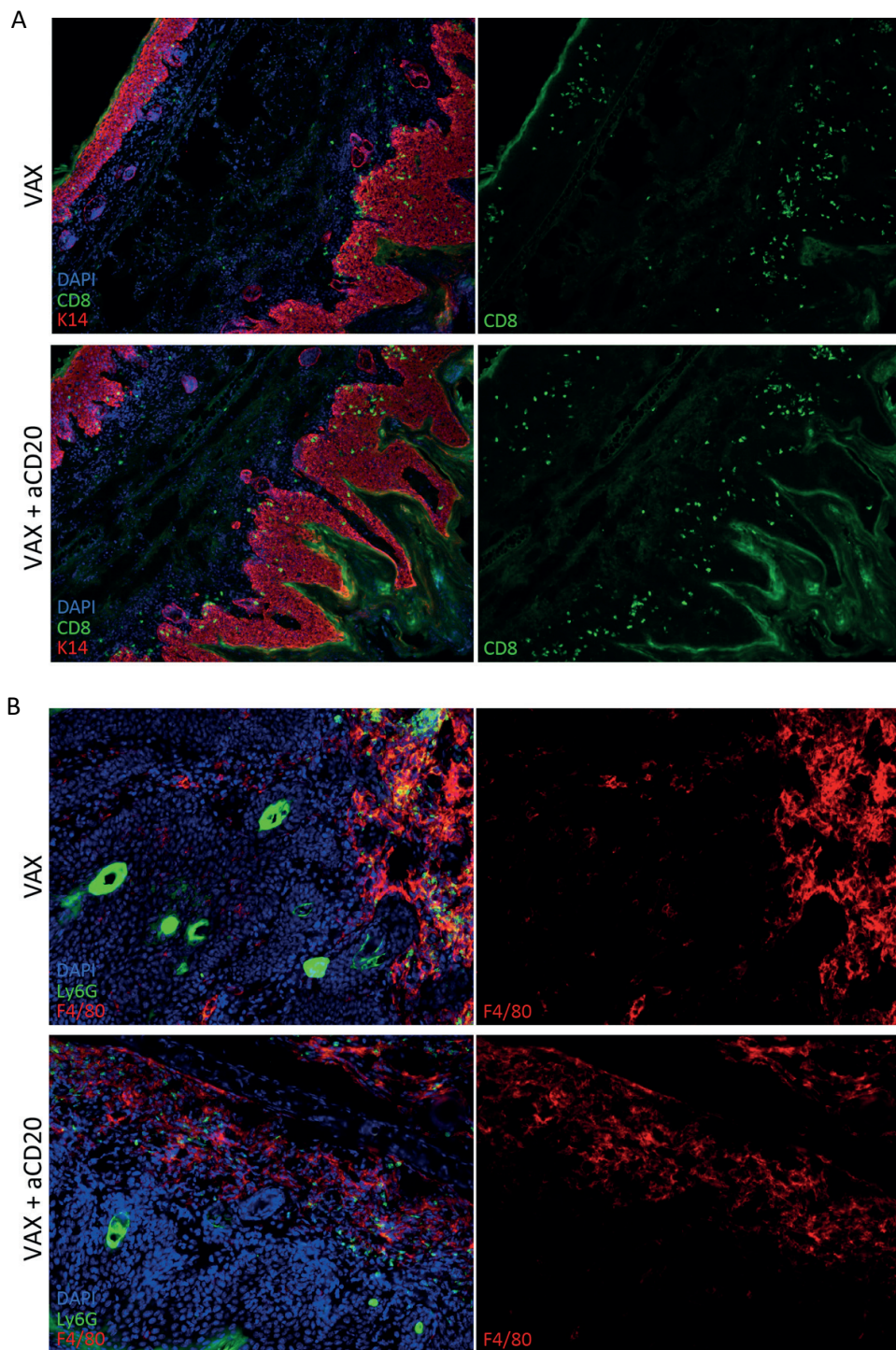


Figure 56. Immune infiltrates in the ear. Immuno-fluorescent staining for (A) keratin 14 (red) and CD8 (green) or (B) F4/80 (red) and Ly6G (green) on 10 μ m sections derived from frozen OCT-embedded ears from HPV+ mice. Staining for keratin14 was performed to distinguish the

tumor/epithelium from the surrounding tissue. Groups: VAX n=4, VAX + aCD20 n=6. At least 4 fields were imaged per mouse. Representative fields of the tissue are shown.

These results suggest that aCD20 treatment can elicit a systemic reduction in macrophages that is however not sufficient to cause major changes at the site of skin lesions in the ear or in the immune response to the vaccine. Further analyses on macrophages phenotype, both locally and systemically, and on the local production of GM-CSF in the ears will be required to better characterize the effects of aCD20 and to evaluate if it could represent a valid treatment that requires consideration as an addition to a potential combinatorial regimen aimed at relieving immunosuppression.

3.2.41 Aspirin treatment further suppress the anti-E7 immune response

I have previously detected increased levels of COX2 in the HPV+ mice lymph nodes, and further analyses suggested this enzyme is mainly expressed by non-myeloid cells. COX2 activity has been correlated with immunosuppression and increased activity of suppressive myeloid cells in tumor models (245, 246) and its blockade, by widely available drugs such as aspirin, has anti-inflammatory effects (247). Therefore, I set out to treat HPV+ mice with aspirin hoping to relieve the chronic inflammatory state as well as the immunosuppressive activity by myeloid cells.

Aspirin treatment was carried out in the drinking water starting 7 days prior to vaccination and was terminated at the end of the experiment. Mice were vaccinated with the NP-VAX at day 0 and sacrificed 9 days later when I performed flow cytometry analyses of the vaccination site draining lymph nodes. Myeloid cells status was also measured in the blood at day 2 after immunization. Surprisingly, when I looked at the blood, I found a slight trend that, although not significant, suggested an increase of several myeloid cells populations including total CD11b+ cells (Fig. 57A), neutrophils (Fig. 57B), and macrophages (Fig. 57D) while monocytes (Fig. 57C) and DCs (Fig. 57E) remained similar. Later, when I sacrificed the mice, I observed that this trend disappeared (Fig. 57F-L). However, the percentage of E7-specific CD8 T cells (Fig. 57M) and cytokine production from E7-specific CD8 T cells (Fig. 57N) were both significantly lower in the HPV+ mice lymph nodes. These results could be explained by the transitory increase in myeloid cells resulting that

was perhaps detrimental for the antigen presenting cells or because of an important role of COX2 in the generation of the immune response to the vaccine that was lacking as a consequence of the inhibition of the enzyme.

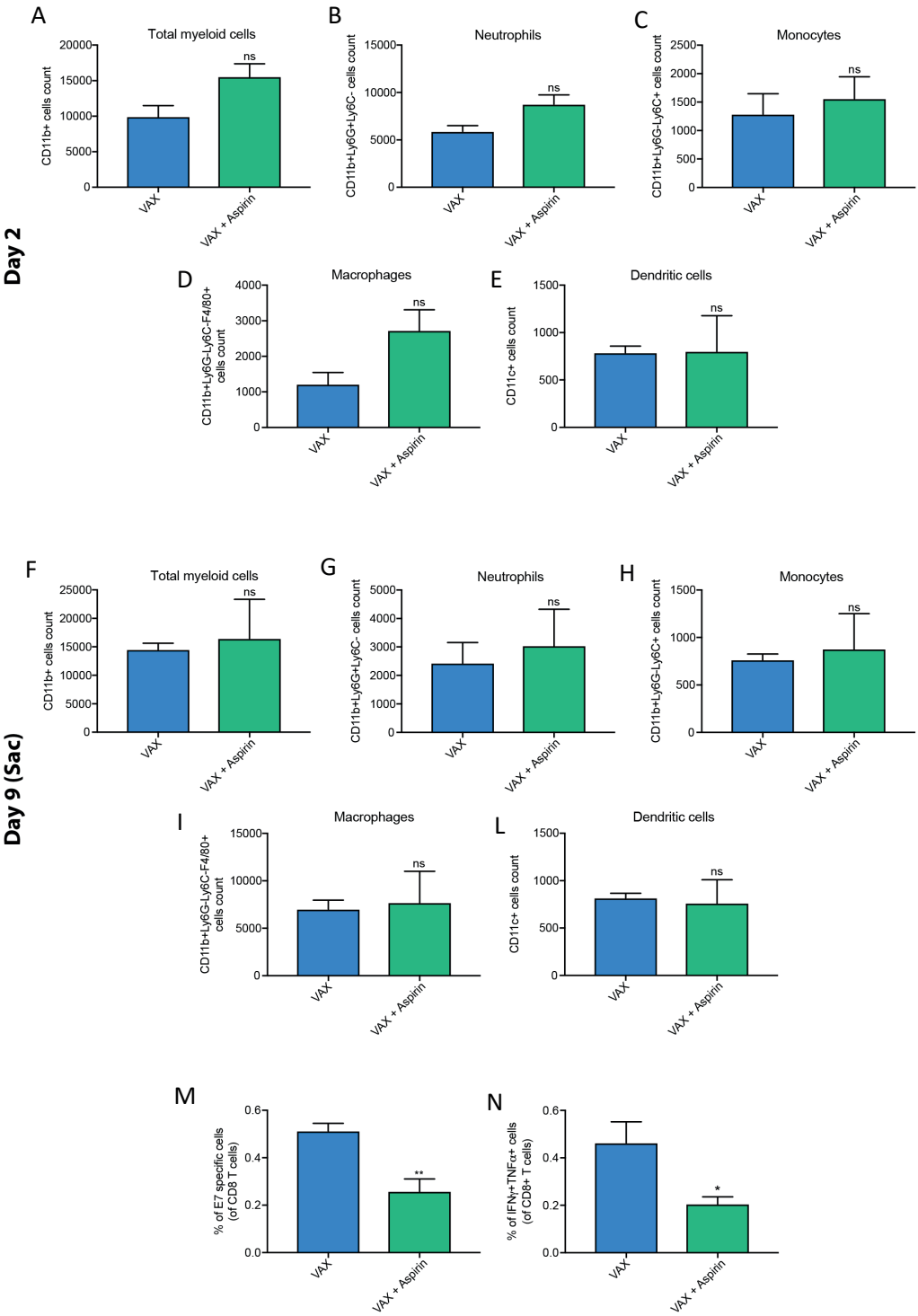


Figure 57. Flow cytometry analyses of the effects of aspirin on several immune populations and on the anti-E7 response. Flow cytometry analyses at different time-points of (A, F) CD11b⁺ total myeloid cells, (B, G) CD11b⁺Ly6G⁺Ly6C⁻ neutrophils, (C, H) CD11b⁺Ly6G⁺Ly6C⁺ monocytes, (D, I) CD11b⁺Ly6G⁺Ly6C⁻F4/80⁺ macrophages and (E, L) CD11c⁺ dendritic cells in the blood (day 2) or in the lymph nodes (day 9) of HPV⁺ mice. (M) Flow cytometry analyses of E7-specific CD8 T cells in the lymph nodes of HPV⁺ mice using tetramers recognizing the HPV16 E7 CD8 peptide RAHYNIVTF presented on H2Db. (N) Flow cytometry analyses of IFN γ and TNF α production by HPV⁺ mice lymph node -derived CD8 T cells after in-vitro re-stimulation with the HPV16 E7 CD8 peptide RAHYNIVTF. n=4. Statistics: * $p < 0.05$; ** $p < 0.01$; *** $p < 0.001$; **** $p < 0.0001$; n.s. = not significant.

3.2.42 Prednisolone treatment shuts down the immune system of HPV⁺ mice and could represent an attractive future component of combinatorial regimens

Given the results obtained with aspirin, I decided to try a more potent approach. Prednisolone is a very strong anti-inflammatory drug that is used to treat several inflammatory conditions (248). Since this drug is capable of basically shutting down multiple arms of the immune system, I thought to use it in our HPV⁺ mice in an attempt to reduce the local inflammation in the skin and consequently relieve the systemic inflammatory state. The goal of this experiment was also to monitor the levels of myeloid cells and determine if the anti-inflammatory effects of prednisolone could bring to a reduction in these cells as a consequence of the lower general inflammation.

The first experiment I performed involved treatment of HPV⁺ mice with 350 μ g of prednisolone per day in the drinking water. The treatment started 2 weeks before vaccination and was terminated at the end of the experiment. Mice immunized at day 0 with the NP-VAX and sacrificed 9 days later when flow cytometry analyses were performed on the vaccination site draining lymph nodes.

As expected, prednisolone treatment caused a general reduction in all the analyzed immune cells populations namely in total CD11b⁺ cells (Fig. 58A), neutrophils (Fig. 58B), monocytes (Fig. 58C), macrophages (Fig. 58D) (although not significant), DCs (Fig. 58E), CD4 T cells (Fig. 58F), Tregs (Fig. 58G) and CD8 T cells (Fig. 58H). When I analyzed the percentage of E7-specific CD8 T cells and their cytokine production I did not measure a significant difference between the groups but (Fig.

58I and M), due to the general reduction in CD8 T cells, their absolute numbers were lower in mice that received prednisolone (Fig. 58L and N).

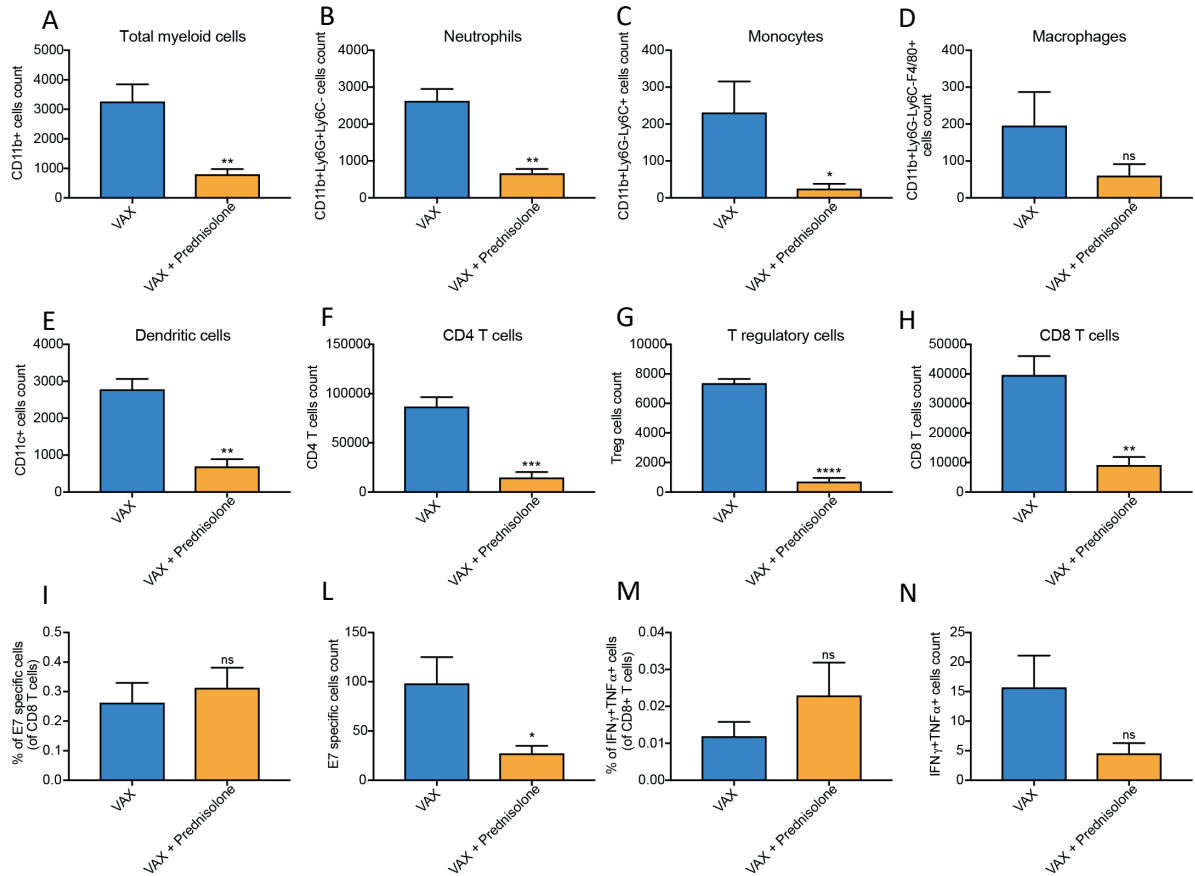


Figure 58. Flow cytometry analyses of the effects of prednisolone on several immune populations and on the anti-E7 response. Flow cytometry analyses at different time-points of (A) CD11b+ total myeloid cells, (B) CD11b+Ly6G+Ly6C- neutrophils, (C) CD11b+Ly6G-Ly6C+ monocytes, (D) CD11b+Ly6G-Ly6C-F4/80+ macrophages, (E) CD11c+ dendritic cells, (F) CD4+ T cells, (G) CD4+CD25+Foxp3+ Tregs and (H) CD8 T cells in the lymph nodes (day 9) of HPV+ mice. (I, L) Flow cytometry analyses of E7-specific CD8 T cells in the lymph nodes of HPV+ mice using tetramers recognizing the HPV16 E7 CD8 peptide RAHYNIVTF presented on H2Db. (M, N) Flow cytometry analyses of IFN γ and TNF α production by HPV+ mice lymph node -derived CD8 T cells after in-vitro re-stimulation with the HPV16 E7 CD8 peptide RAHYNIVTF. Groups: VAX n=4, VAX + prednisolone n=5. Statistics: * $p < 0.05$; ** $p < 0.01$; *** $p < 0.001$; **** $p < 0.0001$; n.s. = not significant.

This experiment was carried out in female HPV+ mice, and therefore, I decided to analyze the changes at the tumor site caused by the prednisolone treatment. CD8 T cells completely disappeared from the tissue (Fig. 59A) along with Ly6G+ neutrophils (Fig. 59B), and additionally, I saw a slight reduction in macrophages (Fig. 59B).

These results suggest that prednisolone can potentially be used to shut down the immune system and that this could potentially help reversing the inflammatory state of the mouse by lowering immune cell infiltrates in the skin, as the effects there should mimic what happened at the tumor site.

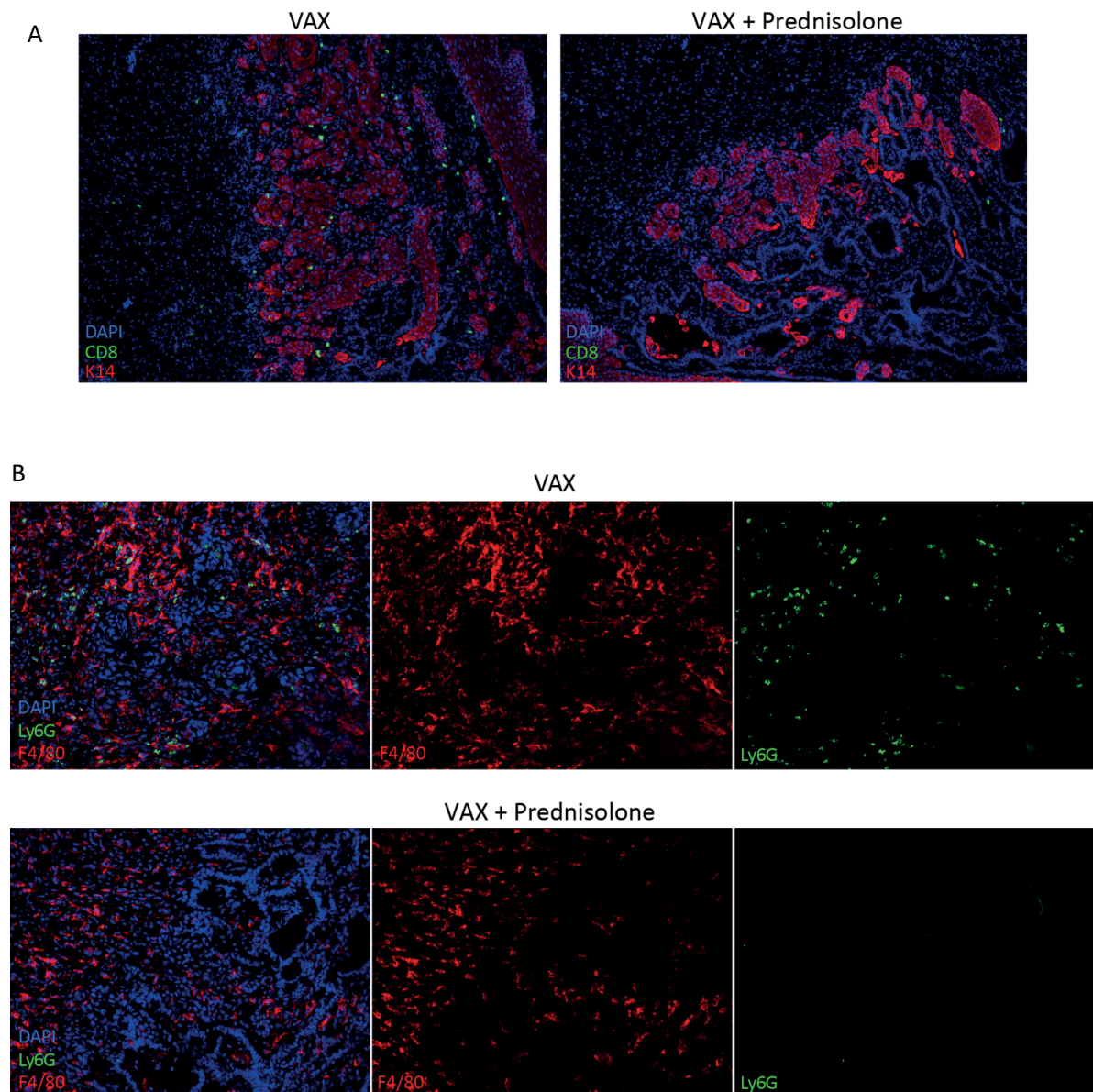


Figure 59. Immune infiltrates in the cervical TME. Immuno-fluorescent staining for (A) keratin 14 (red) and CD8 (green) or (B) F4/80 (red) and Ly6G (green) on 10 μ m sections derived from frozen OCT-embedded ears from HPV+ mice. Staining for keratin14 was performed to distinguish the tumor/epithelium from the surrounding tissue. Groups: VAX n=4, VAX + prednisolone n=5. At least 3 fields were imaged per mouse. Representative fields of the tissue are shown.

In the second experiment that I performed using prednisolone, I decided to compare different treatment doses and schedules as illustrated in Fig. 60. All the treatments were carried out in the drinking water. For all the three doses of prednisolone, the treatment was stopped 1 day before vaccination while only for the lowest dose I had a group of mice where it was continued until the end of the experiment. Mice were immunized at day 0 with the NP-VAX and sacrificed 9 days later when I performed flow cytometry analyses on the vaccination site draining lymph nodes. When I sacrificed the mice, I measured no significant changes in total CD11b+ cells (Fig. 61A), monocytes (Fig. 61C), macrophages (Fig. 61D), DCs (Fig. 61E) or CD8 T cells (Fig. 61F). However, neutrophils were significantly increased in the groups that received the high and middle dose of prednisolone and were clearly increased, although it was not significant, in the group that received the low dose that was interrupted before vaccination (Fig. 61B). Interestingly, neutrophils were significantly lower in the group that received the low dose of prednisolone throughout the entire experiment (Fig. 61B).

The immune response to the vaccine was not significantly different between the groups (Fig. 61G, H, I and L) with the only exception of a lower percentage of E7 specific CD8 T cells in the group treated with the middle dose (Fig. 61G).

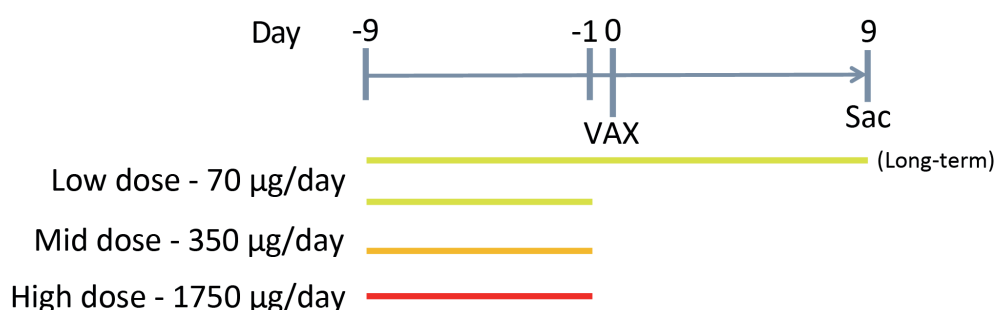


Figure 60. Schematic of the experimental design.

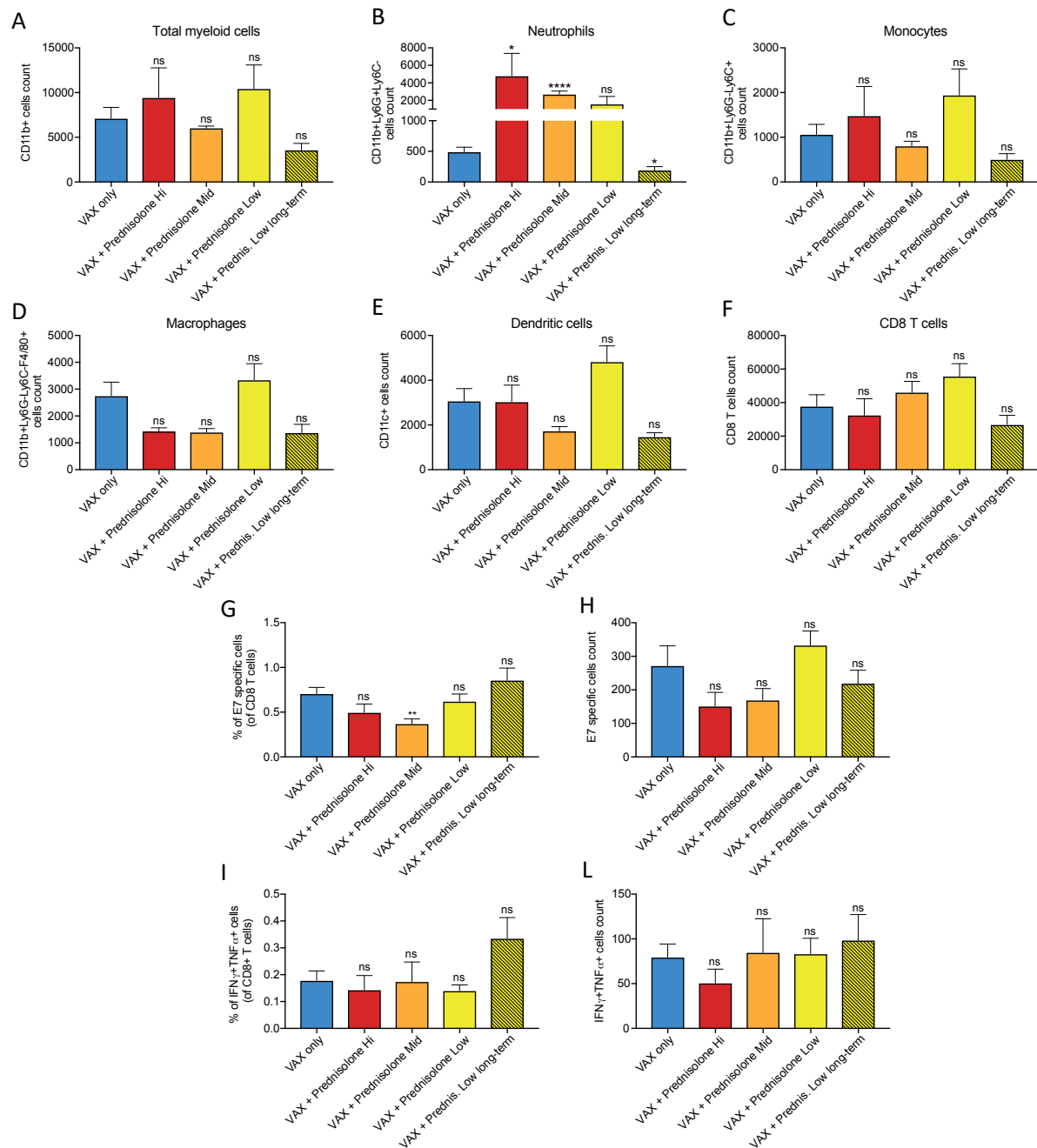


Figure 61. Flow cytometry analyses of the effects of prednisolone on several immune populations and on the anti-E7 response. Flow cytometry analyses of (A) CD11b⁺ total myeloid cells, (B) CD11b+Ly6G+Ly6C⁻ neutrophils, (C) CD11b+Ly6G-Ly6C⁺ monocytes, (D) CD11b+Ly6G-Ly6C-F4/80⁺ macrophages, (E) CD11c⁺ dendritic cells and (F) CD8 T cells in the lymph nodes of HPV⁺ mice. (G, H) Flow cytometry analyses of E7-specific CD8 T cells in the lymph nodes of HPV⁺ mice using tetramers recognizing the HPV16 E7 CD8 peptide RAHYNIVTF presented on H2Db. (I, L)

*Flow cytometry analyses of IFN γ and TNF α production by HPV+ mice lymph node -derived CD8 T cells after in-vitro re-stimulation with the HPV16 E7 CD8 peptide RAHYNIVTF. Groups: n=3 except for VAX n=6 and VAX + Prednisolone Hi n=3. Statistics: * $p < 0.05$; ** $p < 0.01$; *** $p < 0.001$; **** $p < 0.0001$; n.s. = not significant.*

These results suggest that interrupting the prednisolone treatment 1 day before vaccination is enough, in most of the cases, to restore the normal response to the vaccine and that a continuous treatment with a low dose has no significant impact on it. Additionally, it appears that the immunosuppressive and anti-inflammatory effects of prednisolone cause a rebound of neutrophils once the treatment is lifted, perhaps as a result of compensatory mechanisms that come in play when neutrophils numbers went down or as a result of suddenly being re-exposed to an inflammation-prone environment. Interestingly, the continuous low dose administration of prednisolone was associated with a reduction in neutrophils that was still measurable at the end of the experiment.

Collectively this data establish prednisolone as a potent anti-inflammatory drug that is effective also in HPV+ mice. Although I did not manage to boost the response to the NP-VAX, this treatment could potentially be used as a baseline to reset the immune system and alleviate the chronic inflammatory state of the mice both at the systemic level but also locally in the skin and at the tumor site. Careful and rational evaluation of the dosage and timing of the drugs will be required to achieve the optimal results. It seems reasonable to assume that the best strategy would be to pre-treat the mice with a medium dose and then sequentially switch to the lower one, before administering the vaccine.

Given the complexity of the mouse model, additional treatments will likely have to be layered on top of prednisolone to further reduce the numbers of immunosuppressive myeloid cells and reduce the systemic immunosuppression that is characteristic of HPV+ mice.

3.3 Discussion

In this chapter 3 of the thesis, I illustrated the results obtained in an HPV16 transgenic mouse model that spontaneously develops skin lesions and cervical cancer (when implanted with estradiol). Collectively, my data show that this mouse model presents, together with the stepwise development of cervical cancer previously characterized, many characteristics that have been implicated in patients to participate in the establishment of tolerance and unresponsiveness by the immune system against the tumor. Namely, tumor-specific cytotoxic CD8 T lymphocytes are generated in low numbers and have impaired functions, dendritic cells are poorly functional and there is a systemic increase in myeloid cells that have suppressive functions (MDSCs).

Patients diagnosed with cervical cancer have usually been infected for more than a decade by HPV (13) which, during this time, has “worked” towards the establishment of a certain degree of tolerance towards its antigens (126), perhaps partially explaining the low responsiveness of some cancer patients to therapeutic vaccination against the viral antigens (166). Our mouse model, although it cannot recapitulate the early steps of the viral life cycle, constitutively express the HPV proteins, thereby mimicking the later stage of chronic infection when the viral DNA is usually integrated into the host genome. My data support the hypothesis that this feature allows for the generation of a partial tolerance to the E7 protein, adding another extremely important element of similarity between these mice and the patients (126). Supporting this claim, the free formulation of our therapeutic vaccine cannot elicit anti-E7 CD8 T cells suggesting indeed the presence of tolerance towards this antigen. This tolerance however, seems to be only partial, and it can be broken by using a stronger NP-based formulation. The NP vaccine prompts the generation of an anti-E7 response that retains cytokine production and killing capabilities, further strengthening the fact that the use of nanoparticle-based formulations could represent a critical improvement in therapeutic vaccination strategies for HPV-related cancer patients.

Perhaps the most relevant feature I observed, is that this mouse model is characterized by the presence of profound systemic immunosuppression that impairs immune responses not only against the constitutively expressed HPV protein E7, but also against completely foreign antigens namely ovalbumin (OVA) and LCMV-derived short peptides. The mechanism responsible for the

impairment of the immune response targets CD8 T cells directly, and additionally, I demonstrated that it also involves the active suppression of dendritic cells. DCs cannot fully activate in HPV+ mice, even when they are exogenously delivered as part of a DC-based vaccine. Importantly, this aspect of the impaired APCs activation represents another point of similarity between patients and HPV+ mice (126).

Interestingly, this systemically suppressed phenotype is seen both in 5-6 month old cervical cancer-bearing female mice but also in relatively young, 8-12 week old males. This observation implies that this feature is likely to be a result of the expression of the HPV16 genes, present in the mouse genome, by keratinocytes. Although it is still unclear whether this is a direct effect dictated by altered keratinocytes or if this is part of a larger and more intricate pathway involving multiple cell types that are present at the skin surfaces, I have identified myeloid cells as the potential responsible for suppressing immune responses.

The expansion of these cells, which are found in much higher numbers in the HPV+ mice compared to their non-transgenic littermates, is likely to be driven by an increased production of G-CSF and GM-CSF which, at least for the latter, happens locally in the skin, perhaps as a consequence of the presence of a local inflammatory milieu. Moreover, these myeloid cells seem to be responsible for the increase of some of the suppressive factors that I measured in the mouse's lymph nodes (IL-10 and IDO), while others might be coming from the keratinocytes themselves (Arg-1). Thanks to in-vitro co-culture experiments I determined that myeloid cells isolated from HPV+ transgenic mice can indeed suppress both CD8 T cells and APCs. The large numbers of immunosuppressive myeloid cells found in both spleen and lymph nodes, and their ability to block different cell types that are critical for the generation of a strong systemic antitumor response, provides an explanation to the poor efficacy of immunotherapy strategies in this mouse model. Importantly, similar features have been reported for myeloid cells isolated from patients with HPV-related cancers (111, 126, 158), thus making these findings relevant and providing clues as to why immunotherapy has been ineffective so far in these individuals, and potentially, in patients with other types of cancer associated with increased MDSCs (249, 250).

Unfortunately, after testing several strategies to alleviate the systemic immunosuppression, it became apparent that the use of "classical" approaches, mostly based on depleting antibodies or chemotherapy, but also involving the direct targeting of some of the putative immunosuppressive

factors, would not suffice in this model. Although the increase in myeloid cells has also been reported for cervical cancer patients (111, 126, 158), it could be that their expansion is exacerbated in our HPV-transgenic mice by the fact that the entire skin, the largest organ of the body, expresses the viral genes. I reasoned that this could render the mechanisms driving the proliferation of this immunosuppressive cell population particularly strong and very hard to counteract.

Moreover, the poor efficacy of therapeutic approaches based on depleting antibodies in the HPV+ mice could be linked to defects in cell populations that are normally involved in the depleting activity of some these agents. In fact, for anti-Ly6G mediated depletion, the activity of macrophages plays a key role (236). In our mice, however, the poor efficacy of clodronate-liposomes at depleting macrophages suggest that they have a reduced phagocytic activity, hinting that they might be less prone to phagocytize, and consequently eliminate, the depleting antibody-coated cells. This defect in macrophages, and possibly other mechanisms, will need to be kept into consideration for the development of therapeutic strategies aimed at blocking the immunosuppressive cells. On the other hand, chemotherapy seems to be capable of depleting myeloid cells, a result that has provided promising preliminary results in patients treated with carbotaxol (111). However, In the GEMM its effects were too short-lived, not lasting long enough to appreciate an improvement in the antitumor response, further strengthening the notion that the mechanisms keeping the levels of myeloid cells high might be quite strong in these mice.

Another important observation that can be drawn from ex-vivo re-stimulation experiments is that at least some of the treatments I tried seemed to be capable of generating higher numbers of cytokine-producing E7 specific CD8 T cells. However, the beneficial effects of such treatments were simply masked if the CD8 T cells used in the assay were in the presence of the suppressive cells contained in the splenocytes mix, and were only evident when CD8 T cells were re-stimulated alone. Having partially excluded Tregs as a putative immunosuppressive population, my data indicate that myeloid cells could be the sole responsible for this effect.

These results suggest that combinatorial immunotherapy-based strategies that seemed to be poorly or completely ineffective in-vivo, have the potential of showing positive results, but only once the suppressive activity of myeloid cells is blocked. As the presence of suppressive myeloid cells is a common feature observed not only in cervical cancer patients (111, 126, 158), but also in

patients with other types of cancer (249, 250), my results argue that the study of therapies aimed at eliminating, re-programing or blocking these suppressive cells, should be a priority and could potentially lead to the success of immunotherapeutic strategies in currently non-responding patients.

I also started investigating the mechanisms behind the increase in myeloid cells and in the growth factors that are likely driving them. Interestingly, I measured a general systemic inflammatory state in the lymph nodes of the transgenic mice. Although at first glance, such a situation might seem to be in contrast with the general suppression of immune responses, the two could actually be tightly linked. In fact, it is known that chronic inflammatory conditions, similar to the one that has been previously characterized in the skin of K14HPV16 non-H2b mice and that has been found to be associated with squamous cell carcinomas in patients (164, 239), can cause an expansion of the myeloid compartment (240, 241). The ensuing increase in these cells proliferation can lead to the release of immature cells from the bone marrow that have a suppressive phenotype (MDSCs) (233, 240, 251). The increase in suppressive myeloid cells could be a feedback response generated with the goal of stopping the inflammatory state but ultimately, in the case of our mice and possibly in SCC patients, only leading to a general suppression of immune responses without really impacting chronic inflammation. Moreover, it has been recognized that under prolonged exposure to pro-inflammatory environments, the activity of dendritic cells becomes compromised (252), adding further elements to explain the poor responses obtained upon vaccination. Attempts at reducing the inflammatory state using prednisolone demonstrated that the drug can shut down the whole immune system and lower the numbers of all the major cell populations, but further testing will be required to find the optimal dose to consistently and continuously keep the inflammation low while at the same time allow for the generation of immune responses upon therapeutic vaccination.

To summarize, I believe that the local production of GM-CSF in the skin of the mice, together with the increase in G-CSF, collectively cause an expansion of suppressive myeloid cells that accumulate in the spleen and lymph nodes of the mice. Once there, together with other suppressive factors like IDO, IL10, and Arginase1, they act to suppress both dendritic cell activation and CD8 T cell proliferation and cytokine production (Fig. 62). Interestingly, this mechanism seems to be acting

upstream of the other potential immunosuppressive barriers that I described, including those localized in the tumor microenvironment, thereby blocking the anti-tumor immune response systemically before tumor-specific CD8 T cells can even reach the TME.

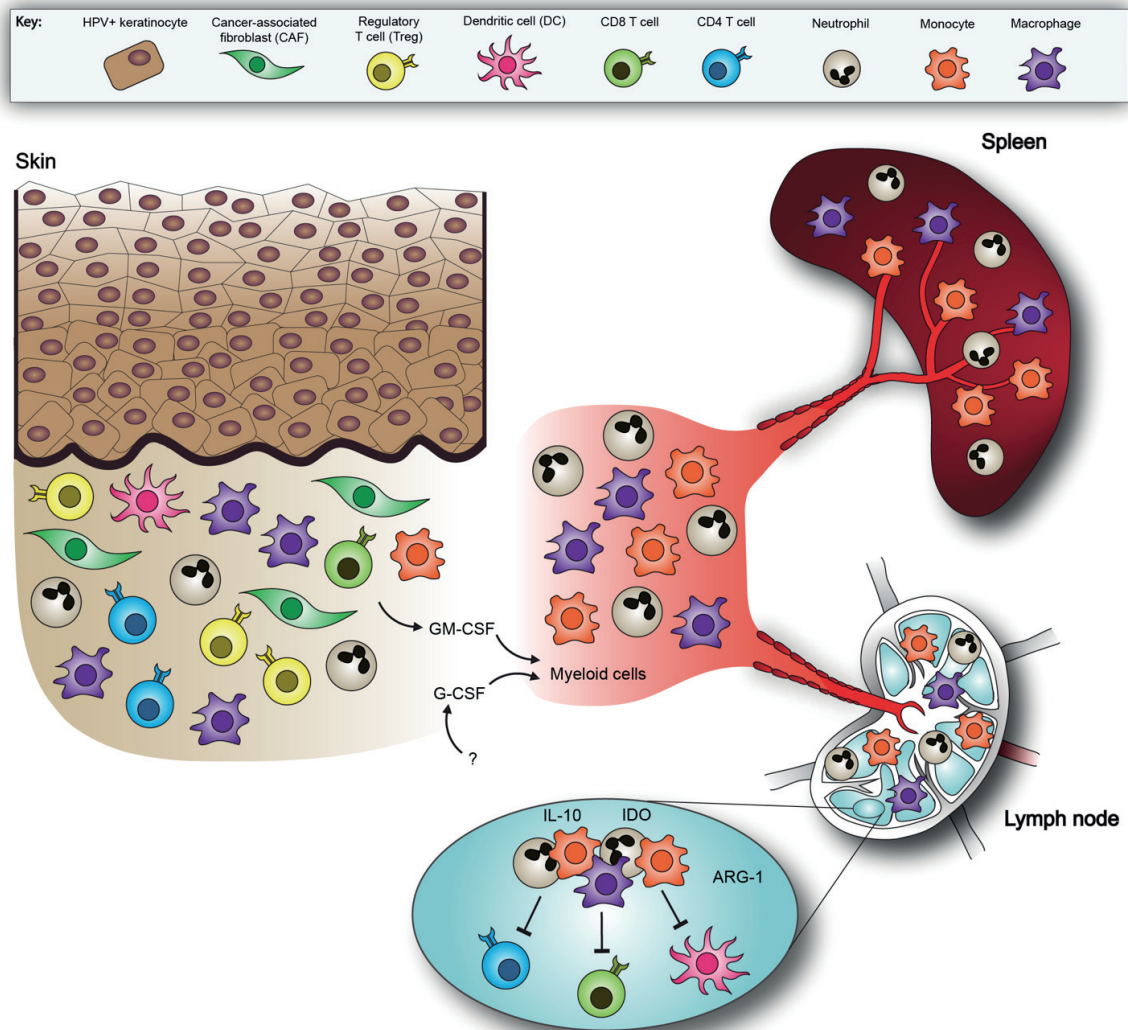


Figure 62. Schematic representation of the immunosuppressive mechanism observed in HPV+ mice. GM-CSF (produced locally in the skin) together with G-CSF promote the expansion of immunosuppressive myeloid cells that accumulate in the spleen and lymph nodes. Once there, myeloid cells likely act in concert with other immunosuppressive factors like IL-10, IDO and ARG-1

to suppress proliferation and function of CD8 T cells, CD4 T cells and antigen presenting cells (like DCs), collectively impairing the generation of the anti-tumor immune response.

In conclusion, although the HPV+ mouse might represent a model in which to analyze and characterize the suppressive mechanisms in detail, due to its severe phenotype, targeting the systemic immunosuppression might require complex combinatorial approaches or the development of novel more effective strategies.

However, accounting for all these observations, this mouse model clearly shares many useful similarities with patients, making the findings presented in this chapter of great potential relevance for humans. I believe that further studies and thorough characterization of these mechanisms of immunosuppression will help developing new strategies to improve the success of therapeutic approaches for HPV-related cancer patients. I anticipate that these results will also be helpful for patients with other types of cancer such as breast cancer (253), but also many others (254), that share a similar systemic alteration in the numbers and/or phenotype of myeloid cells.

3.4 Materials and methods

Mice, Tumor Cells, and Antibody Treatments. For all experiments, K14HPV16/H2b mice (HPV+) or their FVB/n/H2b (HPV-) littermates were used. The K14HPV16/H2b line was generated by crossing K14HPV16/FVB/n (H2q) mice (179, 180, 224) with C57BL/6 (H2b) mice to introduce the H2b locus. F1 mice were backcrossed for 11 generations to FVB/n, selecting for the H2b locus in every generation. This genetic configuration allows K14HPV16/H2b mice to present E7-derived peptides on MHC I molecules while maintaining the FVB/n background that is permissive for squamous carcinogenesis. All the mice were bred in-house and kept under pathogen-free conditions at the animal facility of Ecole Polytechnique Fédérale de Lausanne. Females were subcutaneously implanted with estrogen-releasing pellets at age 1, 3, and 5 months. 5 months old females or 8-12 weeks old males were used for the experiments. All experiments were performed in accordance with Swiss law and with the approval of the Cantonal Veterinary Office of Canton de Vaud, Switzerland.

SC1 cells were generated from a squamous cell carcinoma of the skin of a K14HPV16/H2b mouse. SC1 cells were cultured in DMEM medium (Gibco), 10% FBS (Gibco), P/S (100Units/ml penicillin, 100 µg/ml streptomycin; Gibco), and 1'000'000 SC1 cells resuspended in 100 µl HBBS/Matrigel (1:1 solution) were implanted s.c. on the flank of K14HPV16/H2B or FVB/n/H2b mice.

Antibodies and other treatment were administered with the scheduled indicated in the text. Doses and frequency of treatment are summarized in table 3.

Treatment	Dosage	Frequency	Source
anti-PD1	200 µg/mouse	2x week	Bioxcell
anti-CTLA4	200 µg/mouse	2x week	Bioxcell
anti-CD40	200 µg/mouse	2x week	Bioxcell
Cyclophosphamide	10 mg/kg per day	daily in drinking water	Sigma
anti-CD25	200 µg/mouse	3 consecutive days	Bioxcell
anti-CD4	200 µg/mouse	2x week	Bioxcell
Antibiotics (Vancomycin)	500 mg/L	daily in drinking water	TEVA
Antibiotics (Neomycin)	1 g/L	daily in drinking water	Fisher Scientific
Antibiotics (Imipenem/Cilastatin)	500 mg/L	daily in drinking water	Actavis
anti-Ly6G	400 µg/mouse	3x week	Bioxcell
anti-Ly6C	400 µg/mouse	3x week	Bioxcell
anti-CD11b	400 µg/mouse	3x week	Bioxcell
IPI549	15 mg/kg	daily	MedChem Express
Clodronate liposomes	200 µl	3x week	Liposoma
anti-CSF1R	10 mg/kg	2x week	Roche
Gemcitabine	120 mg/kg	1 shot	Sigma
5-fluorouracil	50 mg/kg	1 shot	Sigma
Carboplatin	40 mg/kg	1x week for 2 weeks	BMS
Paclitaxel	20 mg/kg	2x week for 2 weeks	Labatec
anti-IL10	200 µg/mouse	3x week	Bioxcell
IDO inhibitor	100 mg/kg	daily	BMS
Sildenafil	200 µg/mouse	daily	Sigma
anti-G-CSF	100 µg/mouse	3x week	R&D
anti-GM-CSF	100 µg/mouse	3x week	Bioxcell
anti-Gr1	200 µg/mouse	3x week	Bioxcell
anti-CD20	10 mg/kg	1x week	Roche
Aspirin	600 µg/ml	daily in drinking water	Sigma
Prednisolone	different doses (see text)	daily in drinking water	Sigma

Table 3. Summary of treatments and relative dosage. Cyclophosphamide was administered in drinking water containing 5% sugar; the 3 antibiotics were all administered together; IDO inhibitor was administered in 55% PEG-400, 20% TPGS, 20% Propylene glycol, 5% EtOH; the other treatments were administered in PBS or saline.

Immunization. Mice were immunized as stated in the text with a total amount of 40 µg of E7 protein (full length) or with 15 µg of E7LP either unconjugated (“free”) or in the NP-bound form, and 40µg of CpG was used as adjuvant unless it was stated otherwise. These doses were chosen in order to deliver the same number of molecules bearing the E7 CD8-specific antigenic peptide RAHYNIVTF. The NP formulations were prepared as indicated below. For the unconjugated formulation, the E7 protein or E7LP were first dissolved in DMSO and then diluted in PBS prior to immunization. The DC-vaccine was prepared as described below. Non-immunized mice were treated with PBS. All the mice from one experiment were immunized together on the same day except for the vaccine doses comparison experiment in Fig. 2 where data were pooled from different experiments. Mice received either 1 or 2 shots of vaccine as indicated in the text. Subcutaneous (s.c.) immunizations of mice were performed in the four limbs using the Hock method. Intravenous (I.V.) immunizations were performed in the tail vein.

Nanoparticle (NP) synthesis and Conjugation. NPs were synthesized, functionalized and characterized as previously described. For antigen conjugation, the HPV16 E7 long peptide or the HPV16 E7 protein was dissolved in DMSO and incubated for 12h in endotoxin-free water in the presence of NPs and guanidine hydrochloride (AppliChem) at room temperature. NP-E7LP or NP-E7protein were purified by size-exclusion chromatography using CL-6B matrix (Sigma-Aldrich), eluted and stored in PBS at room temperature. The size of NP before and after conjugation was determined by dynamic light scattering and remained around 30 nm. E7LP or E7protein loading on the nanoparticles was measured by BCA assay (Thermo Fisher Scientific). NPs alone have been shown to have no adjuvant activity.

Bone marrow dendritic cells (BMDCs) preparation. Femurs and tibiae of 4-6 weeks old mice were collected and cleaned. The bone marrow was extracted by flushing with a syringe, filtered and

plated in RPMI, 10% FBS, 1% PSA and 50 μ M B-mercaptoethanol in the presence of 20 ng/ml GM-CSF. New media was added at day 3, and half of it was replaced at day 6 (the cells contained in the replaced media were recovered and put back in culture). At day 8 the BMDCs in suspension were collected and used for the different assays.

DC vaccine (DC-VAX) preparation. BMDCs were collected at day 8 of culture as previously illustrated. Cells were incubated with the E7LP for 3h at 37°C for antigen loading. E7LP-loaded BMDCs were activated with 20 ng/ml LPS overnight for 12h. After the activation, the cells were extensively washed to remove the excess of LPS, harvested, and mixed with CpG. For certain experiments, when stated in the text, BMDCs were labeled with CFSE prior to mixing with CpG. Each mouse received a total of 2 million BMDCs and 40 μ g of CpG either s.c. or I.V. as indicated.

Co-culture experiments with BMDCs. BMDCs were collected at day 8 of culture as previously illustrated. Cells were activated overnight for 12h with either LPS (20 ng/ml) or CpG (0,1 μ M) as indicated in the text. After the activation, the cells were extensively washed to remove the excess of LPS and CpG and plated together with Tregs enriched cells or CD11b+ cells isolated from HPV+ and HPV- mice. The ratio of the co-culture was 1 BMDC to 10 Tregs/CD11b+ cells. Where stated, IDO inhibitor (BMS) was added at a final concentration of 10 μ M and anti-IL10 antibody was added at a final concentration of 20 μ g/ml. BMDCs were labeled with CFSE prior to mixing with CD11b+ cells. 24h later, cells were harvested and processed for flow cytometry analyses.

Reagents. CpG-B 1826 oligonucleotide (5'-TCCATGAGCTTCCTGACGTT-3' as phosphorothioated DNA bases) was purchased from Microsynth and used as adjuvant in various vaccine formulations or to activate BMDCs. HPV16 E7 long peptide (aa 43-77, purity>90%) was purchased from Think Peptides and the Protein and Peptide Chemistry Facility, UNIL and used for NP conjugation, immunization and re-stimulation of CD4 T cells. The E7 protein was purchased from the Protein and Peptide Chemistry Facility, UNIL and used for NP conjugation and immunization. The HPV16 E7 CD8 peptide RAHYNIVTF was purchased from Think Peptides and used for re-stimulation. OVA used for immunization and the OVA CD8 peptide SIINFEKL used for re-stimulation were provided by Prof. Melody Swartz and Jeffrey Hubbell labs. The LCMV CD8 peptide KAVYNFATC used for both

immunization and re-stimulation was purchased from the University of Lausanne (UNIL). Ultrapure LPS, used for BMDCs activation was purchased by Microsynth. MPLA, used as adjuvant where indicated in the text, was purchased from Microsynth.

Co-culture experiments with CD8 T cells. CD8 T cells were isolated from naïve mice or from mice that were previously immunized against E7 as stated in the text. CD8 T cells isolation was performed on the spleen using the Easysep Mouse CD8⁺ T cell Isolation Kit (Stemcell Technologies) for magnetic isolation according to the manufacturer's instructions. CD8 T cells purity was above 90% in all the experiments.

For proliferation assays, CD8 T cells were labeled with CFSE and added to a plate that has previously been coated overnight with 2 µg/ml anti-CD3 anti-CD28 in PBS. CD8 T cells were harvested 48h later, stained with a live-dead dye and analyzed by flow cytometry to assess their proliferation.

For re-stimulation experiments, isolated CD8 T cells were added to a plate, and the assay was performed as previously illustrated. When indicated, CD8 T cells were co-cultured with other cell types in a 1 CD8 to 10 other cells ratio. Where stated, 1-Methyltryptophan (1MT, Sigma) was added at a final concentration of 50 µM, IDO inhibitor (BMS) was added at a final concentration of 2 or 10 µM, anti-IL10 antibody (BioXcell) was added at a final concentration of 20 µg/ml, Arginase 1 inhibitor N^G-Monomethyl-L-arginine (NG) was added at a final concentration of 1 mM, iNOS inhibitor Nω-Hydroxy-nor-L-arginine (NW) was added at a final concentration of 50 µM and ROS inhibitor N-Acetyl-L-Cysteine (NAC) was added at a final concentration of 1 mM.

Cell isolations for co-culture experiments. Cell isolations were performed on the spleen. The CD4⁺ CD25⁺ Tregs enriched cells were isolated using a double step magnetic isolation CD4⁺CD25⁺ Regulatory T Cell Isolation Kit (Miltenyi). Cells purity was around 70% in all the experiments. CD11b⁺ cells were isolated using the magnetic isolation positive selection Easysep Mouse CD11b positive selection kit II (Stemcell Technologies). Collectively, monocytes, neutrophils, macrophages and DCs accounted for more than 80% of the isolated cells. Neutrophils were isolated using the magnetic isolation negative selection Easysep Mouse Neutrophil Enrichment Kit (Stemcell Technologies). Cells purity was higher than 80%. Monocytes/macrophages were isolated using the

magnetic isolation negative selection Easysep Mouse Monocyte Isolation Kit (Stemcell Technologies). Cells purity was higher than 80%. Ly6C-F4/80+ macrophages and Ly6C+F4/80-monocytes were equally represented in the isolated population. All the procedures were carried out according to the manufacturer's instructions

Killing assay. Whole splenocytes were harvested from HPV- mice, split into 2 and differentially labeled with High or Low CFSE concentrations. The High CFSE labeled splenocytes were loaded with the E7 CD8 peptide RAHYNIVTF while the Low CFSE labeled splenocytes were loaded with the control OVA CD8 peptide SIINFEKL. Both cells were then mixed 1:1 and a total of 2 million cells were injected I.V. in the tail vein of each mouse. 6h after the cell transfer, spleens were harvested and processed for flow cytometry analyses.

Skin, ear and tail preparation for flow cytometry. Hair were removed when necessary. The organs were incubated for 30 min at 37°C in RPMI 5%FBS with collagenase A and DNase I. The organs were then minced with a scalpel and disrupted through a 40 µm filter.

Cell preparation for flow cytometry and antigen-specific in-vitro re-stimulation. Blood was harvested from the tail vein while spleens and lymph nodes were harvested and gently disrupted through a 40-µm filter (Fisher Scientific). On blood and spleen samples, red blood cells were lysed using ACK lysis buffer, and cells were filtered again through a 40-µm filter before use. Cervices were harvested and minced using a scalpel and digested for 45min using collagenase A (0.33U/ml, Roche), dispase (0.85U/ml, Roche), DNaseI (144U/ml, Roche) in RPMI medium with intermittent shaking at 37°C. For CD8 T cell antigen-specific re-stimulation, cell suspensions from either spleen or lymph nodes were cultured at 37°C for 6h in a 96 well plate in the presence of 1µg/ml of the HPV16 CD8 peptide RAHYNIVTF or the OVA CD8 peptide SIINFEKL or the LCMV CD8 peptide KAVYNFATC. After the first 3h of culture, brefeldin A (Sigma-Aldrich) was added to a final concentration of 5 µg/ml. For CD4 T cells, antigen-specific re-stimulation cell suspensions from either lymph nodes were cultured at 37°C for a total of 15h in a 96 well plate in the presence of

100 µg/ml of the E7LP. After the first 3h of culture, brefeldin A (Sigma-Aldrich) was added to a final concentration of 1 µg/ml.

When indicated, CD8 T cell antigen-specific re-stimulation was performed on magnetically isolated CD8 T cells (performed as previously described).

All the cells were cultured in IMDM medium (Gibco) supplemented with 10% FBS (Gibco) and 1x penicillin/streptomycin (100Units/ml penicillin, 100 µg/ml streptomycin; Gibco).

Measurements of cervical tumors size. Serial 10 µm sections of the OCT-embedded cervixes were taken and stained with H&E. An image of the whole tissue was taken every 100 µm. Tumor area on each of the imaged sections was quantified manually. Tumor volume (V) was calculated using the following formula $V = 2/3 \times A \times Z$, where A is the maximal tumor area measured on a section and Z is the depth of tumor determined by the number of sections containing tumors as previously described.

Protein extractions and western blot. Popliteal and brachial lymph nodes as well as whole ears, back skin and tail skin were harvested from 12 weeks old naïve untreated mice. Mice had been previously shaved before collecting the skin from the back. The tail skin was left overnight at 4° in a solution containing 4 mg/ml dispase in KC growth medium (Gibco) to allow for the separation of dermis and epidermis. The next day the epidermis was peeled off and used for protein extraction. All the organs were snap frozen upon collection except for the tail where only the epidermis was snap frozen after isolation. The organs were put in RIPA buffer and mechanically lysed. Following mechanical disruption, the obtained lysate solutions were left on ice for 2h. CD11b⁺ cells were isolated from the spleen as previously described and the CD11b⁺ cells depleted splenocytes were also recovered from the kit. Cells were re-suspended in RIPA buffer and left on ice for 2h. After on-ice incubation, samples were centrifuged at high speed, and the protein-containing supernatant was collected and used for western blot. Protein concentration was determined by Bradford assay (BioRad) according to the manufacturer's instructions and 10-20 µg of total protein we used for the western blots. The same amount of total protein was loaded in each well. The following antibodies were used: Beta-actin (Cell Signaling), G-CSF (clone EPR3203(N)(B), Abcam), GM-CSF (clone MP122E9, R&D), M-CSF (Abcam), IL10 (clone JES052A5, R&D), IDO (clone mIDO-48, Biolegend), Arginase1 (Santa Cruz), IL1beta (Abcam), HSP90 (clone F-8, Santa Cruz), IL-23 (Abcam),

COX2 (Abcam) and C-reactive protein (CRP, R&D). Western blot bands were quantified using Fiji (ImageJ) and normalized for actin.

ROS production assay. CD11b⁺ cells were isolated as previously described and cultured in a 96 wells plate for 1h at 37°C in complete RPMI. Media was then removed, and the ROS-reactive dye 2',7'-Dichlorofluorescein diacetate (DCFDA, Sigma) was added at a final concentration of 10 µg/ml in PBS, and the cells were left for 30 min at 37°C. PMA at a final concentration of 1 µg/ml was used as positive control for ROS production. At the end of the experiment, cells were harvested, stained with a live/dead dye and analyzed by flow cytometry.

RNAseq on neutrophils. Live CD11b⁺Ly6G⁺Ly6C⁻ neutrophils were FACS sorted, and total RNA was isolated with the miRNeasy micro kit (Qiagen). The quality and quantity of the RNA was determined by a Fragment Analyzer (Advanced Analytical). The RQN for the RNA ranged from 9.6 to 10. 4 ng of total RNA was amplified using the SMATer reagents (Clontech). RNA-seq was performed on an Illumina HiSeq equipment at the CIG, University of Lausanne. Data analyses were performed by Dr. Nadine Zangger (SIB, University of Lausanne)

Flow cytometry. For surface staining and blocking, cells were incubated for 15min on ice with the antibodies diluted in PBS 2% FBS. Before tetramer and antibody staining, all cell suspensions from tumor or spleen were blocked with anti CD16/32 (BioLegend). Cells were then labeled with fixable live/dead cell viability reagent (Invitrogen) diluted in PBS for 15 min on ice. Staining with a tetramer recognizing HPV16 E7 peptide 49-57 presented by H2Db (University of Lausanne, UNIL) was performed before antibody staining for 30min at room temperature. Tetramer staining for OVA-specific and LCMV-specific CD8 T cells was performed similarly using tetramers recognizing the SIINFEKL (Proimmune) and KAVYNFATC (University of Lausanne, UNIL) peptide-MHC complexes. If no intracellular staining was performed after surface staining, cells were fixed with 2% PFA in PBS for 15min on ice. For intracellular staining, cells were permeabilized and fixed with the Foxp3/Transcription Factor Staining Buffer Set Kit (eBioscience) following the manufacturer instructions and then incubated overnight with the antibodies diluted in 1x Permeabilization buffer provided with the aforementioned kit. After staining, cells were washed and re-suspended

in PBS 2% FBS for analyses. Samples were acquired on a Cyan, or Gallios analyzer (Beckman Coulter) and data were analyzed using FlowJo software (Tree Star Inc.). Antibodies used for flow cytometry: CD3 (clone 145-2C11, ThermoFisher), CD4 (clone RM4-5, BioLegend), CD8a (clone 5H10, ThermoFisher), B220 (clone RA3-6B2, ThermoFisher), IFN γ (clone XMG1.2, BioLegend), TNF α (clone MP6-XT22, ThermoFisher), Foxp3 (clone FJK-16s, ThermoFisher), CD25 (clone PC61.5, ThermoFisher), CD45 (30-F11, ThermoFisher), CD11b (clone M1/70, ThermoFisher), CD11c (clone N418, BioLegend), Ly6G (clone 1A8, BioLegend), Ly6C (clone HK1.4, ThermoFisher), CD206 (clone C068C2, BioLegend), MHCII (clone M5/114.15.2, BioLegend), CD49f (GoH3, BioLegend), CD140a (APA5, ThermoFisher).

Immunofluorescence staining. SC1 tumors, cervixes, ears, and skin were harvested, embedded in OCT (Sakura) and fresh frozen on dry ice. 10 μ m thick sections were cut from OCT-embedded samples using a cryostat and collected on Superfrost Plus glass slides (Thermo Scientific). Tissue sections and OCT embedded samples were stored at -80°C. For immunofluorescence staining, sections were fixed in ice-cold methanol (Fisher Scientific) for 10min before proceeding. Slides were washed with PBS to remove the remaining OCT and then blocked for 45min at room temperature with PBS + 5% BSA + 2.5% FBS and then stained with primary antibodies diluted in PBS + 1% BSA overnight at 4° in a humidified chamber. On the following day, slides were washed with PBS and stained with secondary antibodies diluted in PBS + 1% BSA for 1h at room temperature. Before mounting, slides were washed again in PBS and then covered with mounting media (Dako) containing DAPI (Roche, 5 μ g/ml). Coverslips (Menzel Glaser) were applied to the slides and sealed using nail polish. Images were acquired using a Leica DM5500B and processed using Fiji (ImageJ). Antibodies used for immunofluorescence staining: CD8 (clone 53-6.7, eBioscience), keratin 14 (clone poly19053, BioLegend), F4/80-PE (clone BM8, eBioscience), CD11c-FITC (clone N418, BioLegend), MRC1-Alexa fluor 647 (clone C068C2, BioLegend), PD-L1-PE (MIH5, eBioscience), FasL (clone MFL3, BioLegend), IDO (clone mIDO-48, BioLegend), Arginase1 (Santa Cruz), Ly6G (clone 1A8, BioLegend), CD31 (clone MEC 13.3, BioLegend).

Statistical analyses. Statistical analyses were performed in GraphPad Prism 7. Flow cytometry data and cells quantification by histology on SC1 tumors were compared using t-test. Western blot results were compared using t-test.

3.5 Acknowledgments

I thank Dr. S. Wullschleger and Dr. M. Tichet for their help and for the always invaluable discussions; B. Torchia, M. Wen-Peng and M.A. Gaveta for technical support; Dr. R. Guet and the bioimaging and optics platform (BIOP) core facility at EPFL for developing image analyses tools; Dr. C. Cianciaruso for figure 62.

3.6 Specific contribution to experiments

I designed and performed most of the experiments, especially those concerning the characterization and treatment of the immunosuppressed phenotype of K14HPV16 mice, analyzed and interpreted the data, monitored and treated mice.

S. Wullschleger and M. Tichet provided scientific input and discussion.

S. Wullschleger managed the mouse colonies and extracted RNA from neutrophils.

S. Wullschleger and B. Torchia took care of the mice breeding and monitoring, treated mice, implanted subcutaneous SC1 tumors and helped me preparing mouse-derived samples for analyses.

M. Wen-Peng and M.A. Gaveta monitored the mice, treated mice and helped me preparing mouse-derived samples for analyses.

M. Tichet participated in the harvesting and analyses of the different skin surfaces (ear, back skin and tail epidermis) and helped me preparing mouse-derived samples for analyses.

RNAseq on neutrophils was performed at the UNIL GTF CIG facility and N. Zangger analyzed the data.

Chapter 4

Concluding remarks

4.1 Summary and general discussion

Immunotherapy of HPV-related cancers and pre-cancerous lesions currently revolve around the use of therapeutic vaccines since it is possible to target the viral proteins that, in this case, are also de-facto tumor-associated antigens. However, a recognized limitation of therapeutic vaccination is that it is only partially effective in patients with pre-malignant lesions and almost completely ineffective in those patients with more advanced cancer (74, 166). Moreover, a recent report (ESMO Geneva 2017) argues that combinations involving immunotherapy are generally poorly effective in patients with cervical cancer. The resistance of HPV+ cancers to the attack of the immune system is certainly linked to the profound manipulation of the immune response orchestrated by the virus in order to escape from its elimination (32, 126) and, unfortunately for the patients, HPV+ malignant lesions might have additional resistance mechanisms (126, 155, 228), making it very difficult to direct immunity against these tumors.

As illustrated in the introduction, HPVs and HPV-related cancers have several ways to manipulate the immune response but, up to date, it is still unclear which ones are the most important for tumor resistance against the immune-mediated attack. The goal of this thesis was, by taking advantage of different mouse models, to find strategies aimed at improving the success of therapeutic vaccination and, more generally, immunotherapy-based approaches against cancers driven by HPVs, and to identify mechanisms that could explain the poor responsiveness to immunotherapy of this cancer type, and that could therefore represent key therapeutic targets.

In chapter 2, I showed how it is possible to improve on the efficacy of therapeutic vaccination strategies based on the E7-derived synthetic long peptides, which are currently being evaluated in clinical trials (74, 75, 166, 186). Namely, I illustrated how the use of a potent vaccine formulation, based on the conjugation of the aforementioned E7-derived long peptides to 30 nm in diameter nanoparticles (NPs), could greatly improve both the systemic and the local anti-tumor immune response in mice bearing transplanted TC1 and SC1 (HPV+ GEMM-derived) tumors, leading to

superior tumor rejection. Survival of mice bearing TC1 tumors at different anatomical locations was significantly improved thanks to the use of the NP formulation, with a substantial percentage of mice achieving complete responses that were not seen in mice treated with the classical unconjugated vaccine. My results illustrate the capabilities of this NP-based platform, and potentially of other similar ones, at enhancing the efficacy of therapeutic vaccination. The advantages derived from the use of these novel formulations could help to generate stronger and broader immune responses even in those patients that poorly respond to immunization with classical formulations. Moreover, I showed that the NP vaccine, although already effective by itself in the TC1 model, can also be combined with therapeutic agonistic antibodies against-41BB, suggesting that these novel formulations could easily be coupled with other treatments to further boost their performances. It is also important to note that any thiol-bearing molecule can be easily coupled with our nanoparticles following a simple mixing step, making them a versatile platform that could potentially be used against a broad range of tumor-associated antigens-derived peptides.

In this part of the thesis, I also illustrated how NP-treated TC1 tumor-bearing mice potentially represent an attractive model in which to study changes occurring in the TME that leads to the stabilization of the disease and later, to the eventual relapse of the tumor. Although I have not yet uncovered the specific mechanism underlining these modifications I provided evidence that it is related to a loss of CD8 T cell activity. At the same time, I excluded some of the most common causes of immunosuppression and escape, like loss of antigen presentation, mutation of the antigenic peptide, M2-like TAMs, and PDL1 expression. Preliminary experiments that I recently conducted suggest that E7-specific CD8 T cells in the circulation of mice bearing stable tumors can still kill de-novo implanted TC1 cells. Moreover, a second shot of the vaccine performed while the tumor is in the stable phase, leads to an increase in the systemic anti-tumor CD8 T cell response but fails to have an impact on the tumor. Collectively, these data suggest that the events leading to the loss of tumor killing are happening locally in the TME, possibly due to mutations in the remaining TC1 cells that acquired the ability to suppress the CTLs response or perhaps because of changes in certain immune populations. These mechanisms could provide important insights into how to increase the efficacy of immunotherapies, either by prolonging the response phase and completely eliminate the tumor, by re-activating the immune response during a stable disease

phase to push towards complete eradication or alternatively, by prolonging the stabilization of the tumor size.

Although TC1-tumor-bearing mice are widely used and represent a valid model to compare different therapeutic vaccine formulations, they do not recapitulate all the features observed in patients with advanced forms of HPV-related cancers (126, 155, 228), who do not respond well to therapeutic vaccination alone. Consequently, despite the positive results of our vaccination approach, I suspect that as a single therapy, this strategy will still not be effective in patients with advanced disease because of the presence of several additional immunosuppressive barriers. Instead, I think that this could serve as a baseline treatment upon which to build combinatorial approaches.

Precisely to conduct studies in a more relevant setting, in chapter 3, I focused my attention on a transgenic mouse model of HPV+ cancers. The K14HPV16 mouse model, already reported to mimic the same stepwise development of cervical cancer seen in patients (178, 224), was previously modified to express the MHC molecule (H2b) capable of presenting an HPV E7-derived epitope to CD8 T cells (182). This allowed the study of E7-directed immunotherapeutic approaches in the new K14HPV16 H2b (HPV+) mouse model. My data have shown that these mice possess several characteristics that are commonly found in cervical cancer patients and that are likely playing a major role in these individuals at dampening the efficacy of different anti-cancer therapies including immunotherapy.

First of all, I showed how the use of a potent NP-based formulation is required in order to elicit an immune response in seemingly partially tolerant HPV+ mice, strengthening the need for using improved therapeutic vaccine formulations and providing additional data on the effectiveness of NP-based vaccines.

Next, my data suggest that an increase in a suppressive myeloid cells population could be the main mechanism responsible for both suppressing the anti-tumor immune response generated upon vaccination, and for rendering immunotherapy combinations ineffective. Interestingly, while the majority of the research done in this field focuses the attention on the tumor microenvironment (251, 255, 256), the seemingly entire myeloid cell-dependent immunosuppressive mechanism that I observed is already active at the systemic level in the lymphoid organs. There, this mechanism

impairs the generation of the immune response by blocking both the first step of antigen presentation by APCs, and the subsequent CD8 T cell proliferation and cytokine production. I have also shown that this mechanism appears to be capable of masking the combinatorial effects of other immunotherapies, implying that such combinations could be effective upon the elimination of the immunosuppressive cells. The implication of these observations could be of extreme importance, not only for cervical cancer and HPV-related cancer patients, but also for a wide variety of other cancer types. In fact, in contrast to most of the reports in the literature on suppressive myeloid cells that show how they can locally suppress anti-tumor immunity in the TME (161, 251), my data suggest that it might be necessary to take a more global look at the MDSCs, by taking into consideration their systemic accumulation and the effects of these cells on the systemic immune response. Their activity might, in fact, be blocking the generation of full-blown anti-tumor response even before the effector cytotoxic lymphocytes reach the tumor site. Such a potential bottleneck, present upstream in the cancer-immunity cycle (216) (Fig. 1), poses an important limitation to all immunotherapy approaches both in humans and in mice, and could explain, at least to a certain extent, why immunotherapies are still ineffective in a substantial percentage of patients. These patients might be characterized by an unusually high number of myeloid cells in the circulation that, as I have shown, could completely erase the beneficial effect of the therapies, misleading the clinician into thinking that the treatment is not working at all while in fact, a therapeutic effect might be masked by these suppressive cell populations.

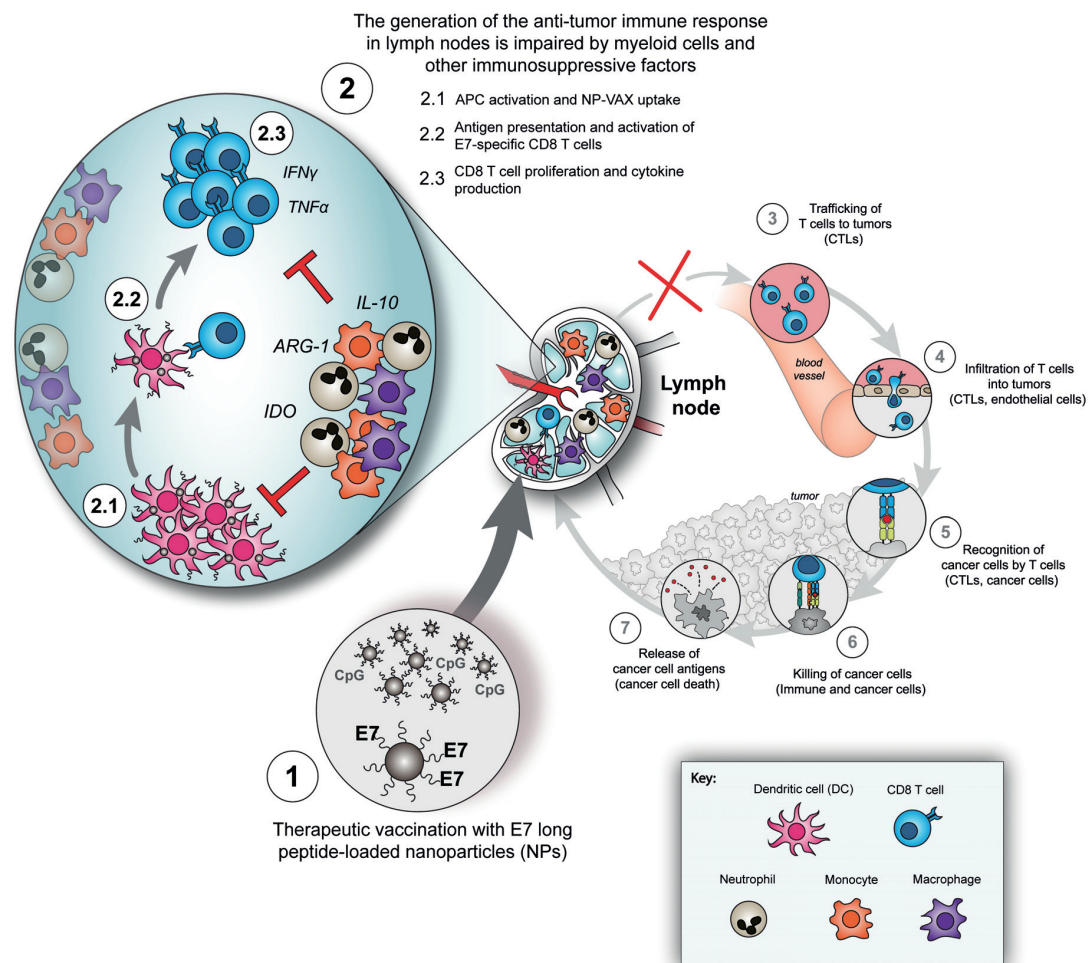


Figure 1. The cancer-immunity cycle in HPV+ mice and HPV-related cancer patients. Image was adapted from (216). The generation of immunity to cancer is a cyclic process that can be self-propagating, leading to an accumulation of immune-stimulatory factors that in principle should amplify and broaden T cell responses. This cycle can be divided into seven major steps, starting with the delivery of a therapeutic vaccine and ending with the killing of cancer cells. Each step is described above, with the primary cell types involved and the anatomic location of the activity listed. The data presented in this thesis show how the use of a nanoparticle-based vaccine loaded with HPV E7-derived long peptides can greatly boost the anti-tumor immune response (1). However, the generation of such response in the lymph node is inhibited by the presence of immunosuppressive myeloid cells and other suppressive factors (2). Namely, antigen presenting cells (APC) activation (2.1), CD8 T cell proliferation (2.3) and cytokine production by effector

antigen-specific CD8 T cells (2.3) are all impaired. These results in the generation of a defective and weak anti-tumor immunity that cannot lead to the next steps (3-7), thereby putting a premature halt to the cancer-immunity cycle. The addition of checkpoint blockade or agonistic antibodies to the therapeutic vaccination approach is also unable to improve step 2, as their beneficial effect is masked by myeloid cells.

Unfortunately, specific and clinically feasible treatments aimed at myeloid cells are still lacking, although certain chemotherapeutic agents have shown the ability to decrease the numbers of these cells. Carbotaxol in particular, has been used in a few patients in combination with an anti-E7 therapeutic vaccine, where it has shown promising results at depleting myeloid cells and improving the immune response following vaccination (111). Given this observation, it is important to comment on the fact that I was unable to replicate these results in the K14HPV16 mice by using this same treatment. As I discussed in the final part of the previous chapter, I believe that our GEMM is characterized by a huge expansion of myeloid cells that is possibly caused by the widespread presence of HPV protein expression in the epidermis at large. Because of this, it is likely that the expansion of CD11b+ cells, although very similar to the human condition, reaches an extent that might be exacerbated, representing an extreme case perhaps characteristic only of the most severe patients conditions, and hence possibly explaining the difference in results.

Targeting of these myeloid cells might be a key requirement to unleash the full potential of immunotherapy in HPV-related cancer patients, although depleting strategies that are commonly utilized in mice are generally poorly effective and are much less applicable to humans. Also, complete depletion of myeloid cells is undesirable in patients, mainly because these cells are of paramount importance in the host defense from pathogens, so much that a substantial decrease in their numbers can expose the patients to potentially life-threatening infections, thereby putting their lives at serious risk (257). Additionally, as I have seen in mice, probably because of the importance of these cells, the mechanisms that are in place to maintain a certain level of myeloid cells are very strong, and depletion can be achieved in the animals only for a limited time. Rather than trying to deplete them, I believe that strategies aimed at normalizing myeloid cells numbers, and at the same time re-program or re-activate them, will be the most successful ones. However, the research on targeting myeloid cells or their suppressive activity is still lagging behind, and I

believe that substantial improvements will need to be made before it will be consistently achievable.

This thesis presents new observations pertinent for strategies and future directions seeking to effectively improve therapeutic vaccination and immunotherapy approaches for HPV-related cancers.

I have shown that the use of a solid-phase vaccination platform represents a substantial improvement over a classical liquid-form vaccine. The use of an NP-based vaccine was not only capable of enhancing the anti-tumor immune response in mice bearing TC-1 tumors but was absolutely required in order to elicit an immune response in genetically engineered mice expressing the HPV16 oncogenes. My results suggest that the use of this or other conceptually similar formulations that have also shown promising results in tumor-bearing mice (196, 217–219), could be applied toward establishing an efficacious immunotherapeutic strategy for HPV-related cancer patients. The results obtained in the HPV16 GEMM suggests that the use of such vaccines have potential to elicit CD8-mediated immune responses even in situations where partial tolerance to the antigen exists and/or in the presence of potent immunosuppressive mechanisms, a result that I could not achieve with the classical unconjugated formulation. Therefore, solid phase vaccines could constitute a robust baseline treatment for cancer patients, with efficacy further enhanced in combinations with approaches aimed at relieving potential immunosuppressive mechanisms or, alternatively, stimulating responses with therapeutic agonistic antibodies (as we have shown with anti-CD137/4-1BB). Interestingly, therapeutic vaccination with unconjugated SLPs has shown remarkable results in combination with photodynamic therapy (258), and we anticipate that the use of a NP-based formulation would lead to further improvement in the anti-tumor responses involving this combinatorial treatment. Collectively these results establish NP-based, and solid-phase vaccines in general as a promising and versatile tool to enhance anti-tumor immune responses against HPV-related cancers. Moreover, this approach could also be employed against other types of cancers upon the identification of appropriate TAAs.

In this thesis I also propose that a key mechanism of immune-escape used by HPV-related cancers takes advantage of myeloid cells to suppress the early steps in the generation of systemic anti-

tumor immune responses. The data presented in Chapter 3 implicate MDSCs in orchestrating an overwhelming systemic immunosuppression that prevents the generation of fully functional anti-tumor CD8 T cell responses and completely masks the effects of combinatorial therapies involving checkpoint blockade antibodies. Such a condition could greatly diminish or even completely abolish the effectiveness of most of the immunotherapy-based approaches currently utilized in patients against a wide variety of cancers, much as it evidently does in the HPV16 GEMM. Importantly, given that an increase in MDSCs has been reported for multiple types of cancers, this myeloid-cell -dependent systemic suppression might be a common trait too often overlooked, as the attention is generally focused only on the TME. My data highlight the need for monitoring the systemic myeloid cell status in patients undergoing immunotherapy and could help in selecting the most appropriate treatment or, in some patients, provide a potential explanation as to why the treatment failed. I believe that it is very likely that this immunosuppressive mechanism will have to be mandatorily targeted in order for immunotherapy to show efficacy against tumors in patients with increased systemic accumulation of myeloid cells.

Collectively, this thesis illustrates promising approaches with potential to improve immunotherapies against HPV-related cancers. I believe that the use of a potent NP-based therapeutic vaccine, combined with blockade of the immunosuppressive myeloid cells, will lead to the generation of strong and fully functional anti-tumor CD8 T cells capable of infiltrating the tumor and eliminating malignant cells. However, I cannot exclude that local barriers in the TME will also have a negative impact on the anti-tumor immune response and therefore, additional combinations (e.g. with checkpoint blockade antibodies) might also be required to achieve substantial anti-tumor activity.

Finally, I believe that these data will help guide future research aiming to finally unlock the potential of therapeutic vaccination and immunotherapy against HPV-driven, and other human cancers.

4.2 Future directions

Although our nanoparticle platform showed promising data in mouse models, many other similar solid-phase vaccines are currently being developed and tested. A necessary future step would have to be a side by side comparison of the available formulations, in order to determine which one is the most promising for a potential translation to patients.

Our vaccination experiment on TC1 tumor-bearing mice also showed that it could be used as a tool to model a 3-phase anti-tumor response, consisting in initial shrinking, stable disease and relapse phase that could mimic the adaptive resistance mechanisms also seen in patients. Continuing this line of research could shed light on the mechanisms that are responsible for the loss of anti-tumor activity by the CTLs, on how the balance between tumor-specific immunity and tumor growth are maintained during the stable phase, on how this balance is eventually tilted towards tumor-growth causing the relapse, and hopefully, on how to manipulate these events to favor complete tumor eradication, to prolong the stable phase or to prevent relapse. To ensure that these results would be relevant to patients it will also be necessary to compare and contrast our data with observations made in humans. Analyzing patient-derived data on the systemic anti-tumor immune response and on tumor biopsies taken at different stages of the disease will be of high importance.

Regarding the data I obtained in the HPV+ transgenic mouse model on the predominant suppressive role of myeloid cells, this aspect seems to be relevant for the human disease too. Our mice give us the unique advantage of allowing the study and characterization of the pathways leading to the expansion of myeloid cells, and also the mechanisms used by these cells to restrain immune responses in great details. More specifically, future research on this HPV+ GEMM will be focused on fully characterizing the events and players leading to G-CSF and GM-CSF production, and on identifying other potential factors involved in the regulation of myeloid cells expansion and functions, in addition to the identification of the cells producing these factors. Moreover, as these mechanisms are linked to the presence of HPV proteins, we will take advantage of in-vitro co-culture experiments involving HPV protein expressing keratinocytes, fibroblasts and other immune cells (including myeloid cells), to determine if one of the HPV proteins might be directly causing

these effects or if this is the result of an interplay between inflammation and other cell types in the skin. It will also be interesting to perform a more thorough characterization of the major myeloid cell population taking advantage of -omics platforms, similar to what I already did with neutrophils. These results might help the identification of targetable pathways that could be used to eliminate these suppressive cells or to disable their suppressive activity. In parallel, we will keep testing strategies to deplete myeloid cells. Given the poor results obtained with treatments involving single agents or limited combinations of a few, we plan on employing more complex approaches. The data that I collected so far has given us a broad perspective into how the different treatments work in the HPV+ mice. By taking advantage of this newly acquired knowledge, we want to rationally design strategies involving multiple and carefully-timed treatments aimed at different factors and cell populations simultaneously, with the goal of hitting myeloid cells and their detrimental activity in the GEMM.

However, given the widespread expression of the HPV proteins in the keratinocytes of all the skin surfaces, the suppressed phenotype of HPV+ mice might be too severe, and even the most carefully evaluated combinatorial treatment is not guaranteed to work. For this reason, we are also envisioning some alternative strategies to better assess the in-vivo role of myeloid cells.

First of all, we have preliminary data suggesting that HPV- littermates transplanted with SC1 (an HPV+ skin SCC-derived cell line) cells have a systemic increase in myeloid cells in the spleen that, although quite variable, was similar to what I observed in HPV+ mice (Fig. 2A, C, E and G). However, this increase was not as marked in the lymph nodes (Fig. 2B, D, F, and H). This indicates that the SC1 tumor can cause changes in myeloid cells in HPV- mice that resembles the ones measured in HPV+ transgenic mice, although more tests will be required to assess if these cells also gained immunosuppressive functions. As the anti-Ly6G treatment showed that depleting strategies can be used more effectively in HPV- mice, we plan on testing this and other similar approaches in SC1 transplanted HPV- mice. I believe that the use of this model could potentially represent an ideal compromise that will allow us to obtain relevant data on how the elimination of myeloid cells could impact the anti-tumor response. Alternatively, transplanting the HPV+ skin into HPV- mice could represent an additional model. The problem of rejection might not present itself in this setting, as it has been shown that the immune system does not attack the E7-expressing skin upon transplantation (259).

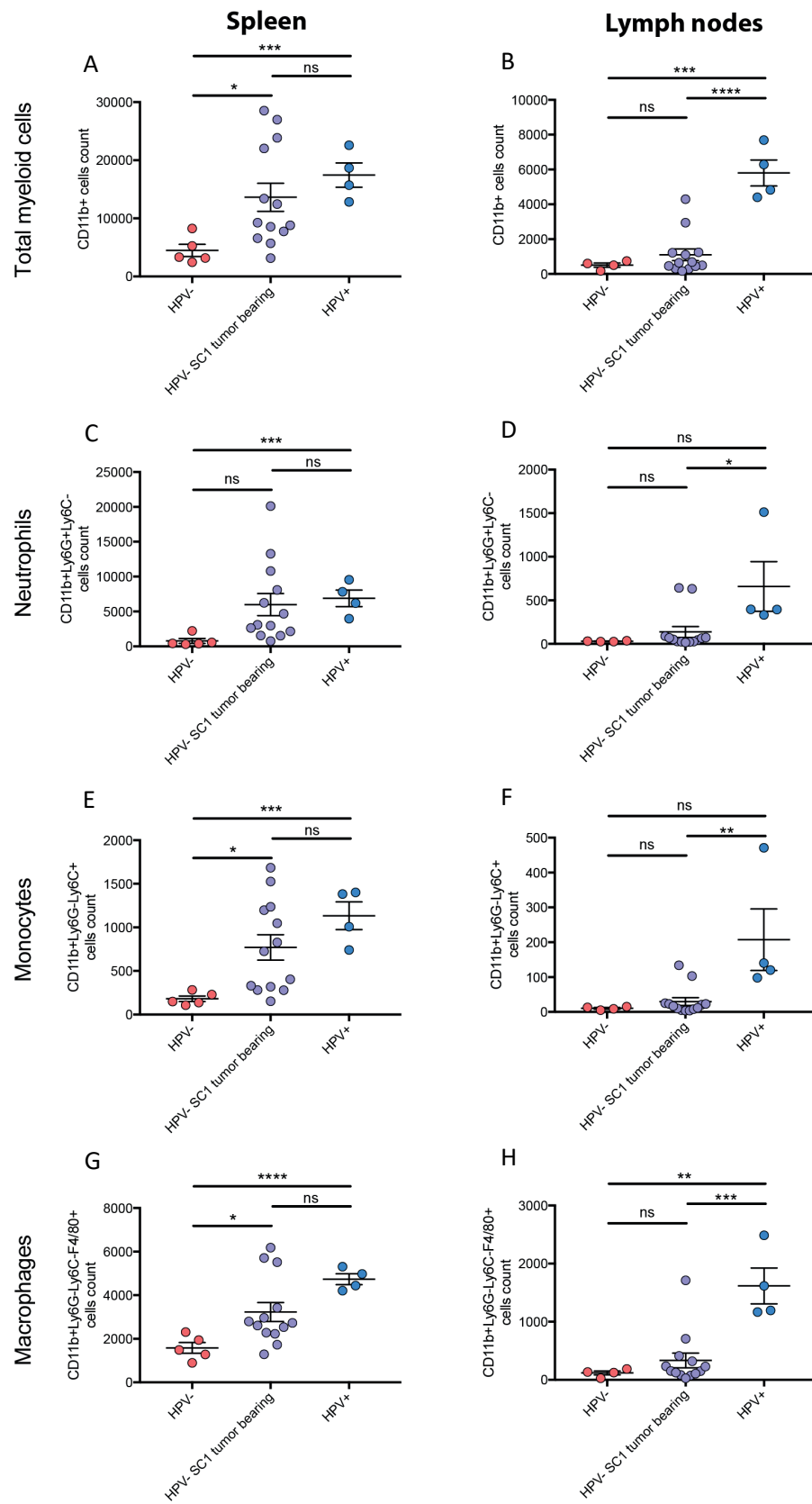


Figure 2. Flow cytometry analyses of myeloid cells in lymph nodes and spleen of SC1 tumor-bearing mice. Flow cytometry analyses of (A, B) CD11b+ total myeloid cells, (C, D) CD11b+Ly6G+Ly6C- neutrophils, (E, F) CD11b+Ly6G-Ly6C+ monocytes, (G, H) CD11b+Ly6G-Ly6C-F4/80+ macrophages cells in the lymph nodes or spleen. Statistics: * $p < 0.05$; ** $p < 0.01$; *** $p < 0.001$; **** $p < 0.0001$; n.s. = not significant.

The second strategy that is already under development by others in the lab revolves around the development of a novel mouse model of HPV-driven cancer. Following the successful establishment of a lentiviral transfer-based GBM model in the lab (unpublished results), we are pursuing the idea of delivering the HPV proteins (E6 and E7 only at the beginning, and later potentially all the others) by a lentiviral vector (or another mean of gene transfer) locally in the skin and/or in the cervix of the mice. Of course, many pitfalls might impair the success of this approach, like the low transfection rate of keratinocytes, the possible limited growth potential of the modified cells, or the generation of an immune response against the transgenes. However, should this approach lead to the localized development of HPV+ squamous cells carcinomas, it could represent a very relevant model in which to study immunotherapy. We believe that the more localized and confined expression of HPV-related genes will better mimic the situation in patients and might still lead to the development of features similar to the ones of HPV+ mice (and of patients) but that the potential immunosuppressed phenotype could be somehow less severe, allowing in-vivo targeting.

A third strategy, by contrast, involves the replacement of the bone marrow of HPV+ mice, with bone marrow cells engineered to express the Herpes simplex virus thymidine kinase or the diphtheria toxin receptor genes under the control of the CD11b or lysozyme promoter aiming to delete the myeloid cells more directly. Of course, this approach is also not guaranteed to work, as certain myeloid cells could be resistant or come back very fast after treatment with ganciclovir or diphtheria toxin. Additionally, the body might even generate neutralizing antibodies against the treatment. However, we hope that this system could provide a more robust way of depleting myeloid cells that could potentially still be combined with other treatments.

Finally, another promising approach that could also be combined with the above ones, is splenectomy. In fact, it has been demonstrated that the spleen acts as a reservoir of myeloid cells and that its removal helps to improve anti-tumor responses in mice (158). We believe that

removing this organ might lower the overall numbers of myeloid cells thereby making it easier to target them.

In conclusion, our future lines of research will be primarily focused on studying the balance between the anti-tumor immune response and the evasive cancer cells, thoroughly characterizing the mechanisms implicated in the defense of HPV+ tumors from immune destruction. I believe that these results will be of considerable interest for the field of tumor immunology, and will make a significant contribution to the advancement of the war on cancer.

Appendix

Abbreviations

HPV: Human papillomavirus
NP: Nanoparticles
SLP: Synthetic long peptide
TME: Tumor microenvironment
MDSC: Myeloid derived suppressor cell
GEMM: Genetically engineered mouse model
E7LP: E7 long peptide
NP-E7LP: NP-conjugated E7 long peptide
Free E7LP: Non-conjugated (free) E7 long peptide
HPV+ (referred to a mouse): FVB K14HPV16 H2b mouse
HPV- (referred to a mouse): FVB H2b (WT) mouse
DNA: Deoxyribonucleic acid
SCC: Squamous cell carcinoma
CIN: Cervical intraepithelial neoplasia
TLR: Toll like receptor
TAA: Tumor-associated antigen
PD1: Programmed cell-death protein 1
PD-L1: Programmed death-ligand 1
CTLA4: Cytotoxic T-lymphocyte-associated protein 4
DC: Dendritic cell
IFN γ : Interferon gamma
TNF α : Tumor necrosis factor alpha
GZB: Granzyme B
Lm: *Lysteria monocytogenes*
APC: Antigen presenting cell
EGFR: Epidermal growth factor receptor
VEGFA: Vascular endothelial growth factor A
G-CSF: Granulocyte colony-stimulating factor
GM-CSF: Granulocyte-macrophage colony-stimulating factor
M-CSF: Macrophage colony-stimulating factor
ACT: Adoptive cell transfer
CAR: Chimeric antigen receptor
ICD: Immunogenic cell death
Treg: T regulatory cell
CSF1: Colony stimulating factor 1
CSF1R: Colony stimulating factor 1 receptor
HLA: Human leucocyte antigen
PSMB: Proteasome subunit beta
TAP: Transporter associated with antigen processing
TAM: Tumor-associated macrophage
VIN: Vulvar intraepithelial neoplasia
MHC: Major histocompatibility complex

DAPI: 4',6-diamidino-2-phenylindole
 ICOS: Inducible T-cell costimulator
 MRC1: Mannose receptor C-type 1
 Luc: Luciferase
 DMSO: Dimethyl sulfoxide
 CTL: cytotoxic lymphocyte
 MPLA: Monophosphoryl Lipid A
 PBS: Phosphate-buffered saline
 FACS: *Fluorescence-activated cell sorting*
 IDO: Indoleamine 2,3-dioxygenase
 Arg1: Arginase 1
 iNOS: Inducible nitric oxide synthase
 VAX: Vaccine (often referring to: NP-E7LP + CpG formulation)
 COX2: Cyclooxygenase 2
 BMDC: Bone marrow dendritic cell
 LPS: lipopolysaccharide
 I.V.: intra-venous
 K14: Keratin 14
 CFSE: 5(6)-Carboxyfluorescein N-hydroxysuccinimidyl ester
 NAC: N-Acetyl-L-Cysteine
 NG: N^G-Monomethyl-L-arginine
 NW: N ω -Hydroxy-nor-L-arginine
 5FU: 5 fluorouracil

Gating strategies

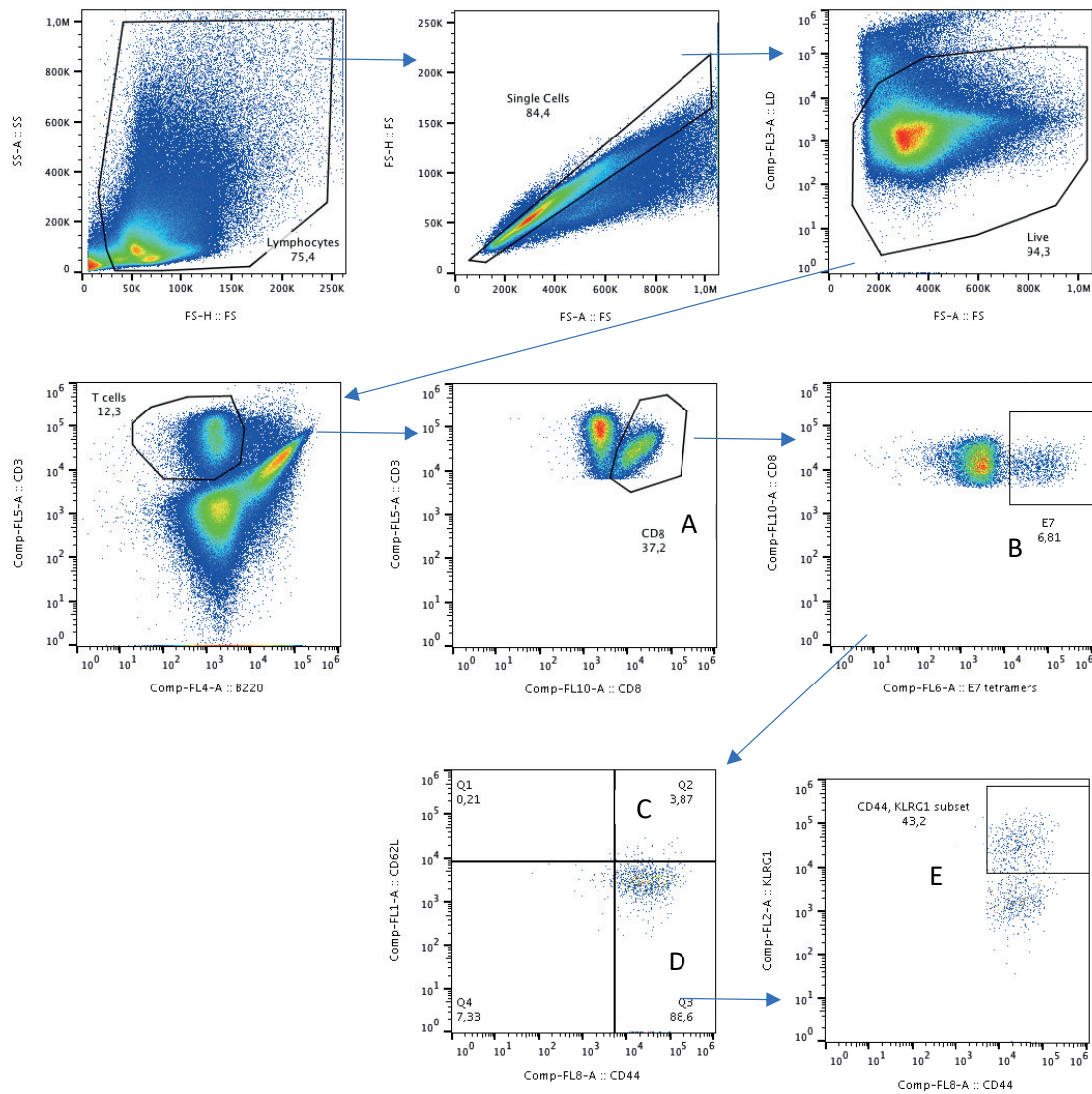


Figure 1. Gating strategy for CD8 T cells shown on splenocytes. (A) CD8 T cells, (B) E7 specific CD8 T cells, (C) CD62L+CD44+ E7 specific memory CD8 T cells, (D) CD62L-CD44+ E7 specific effector CD8 T cells and (E) CD62L-CD44+KLRG1+ E7 specific terminal effector CD8 T cells.

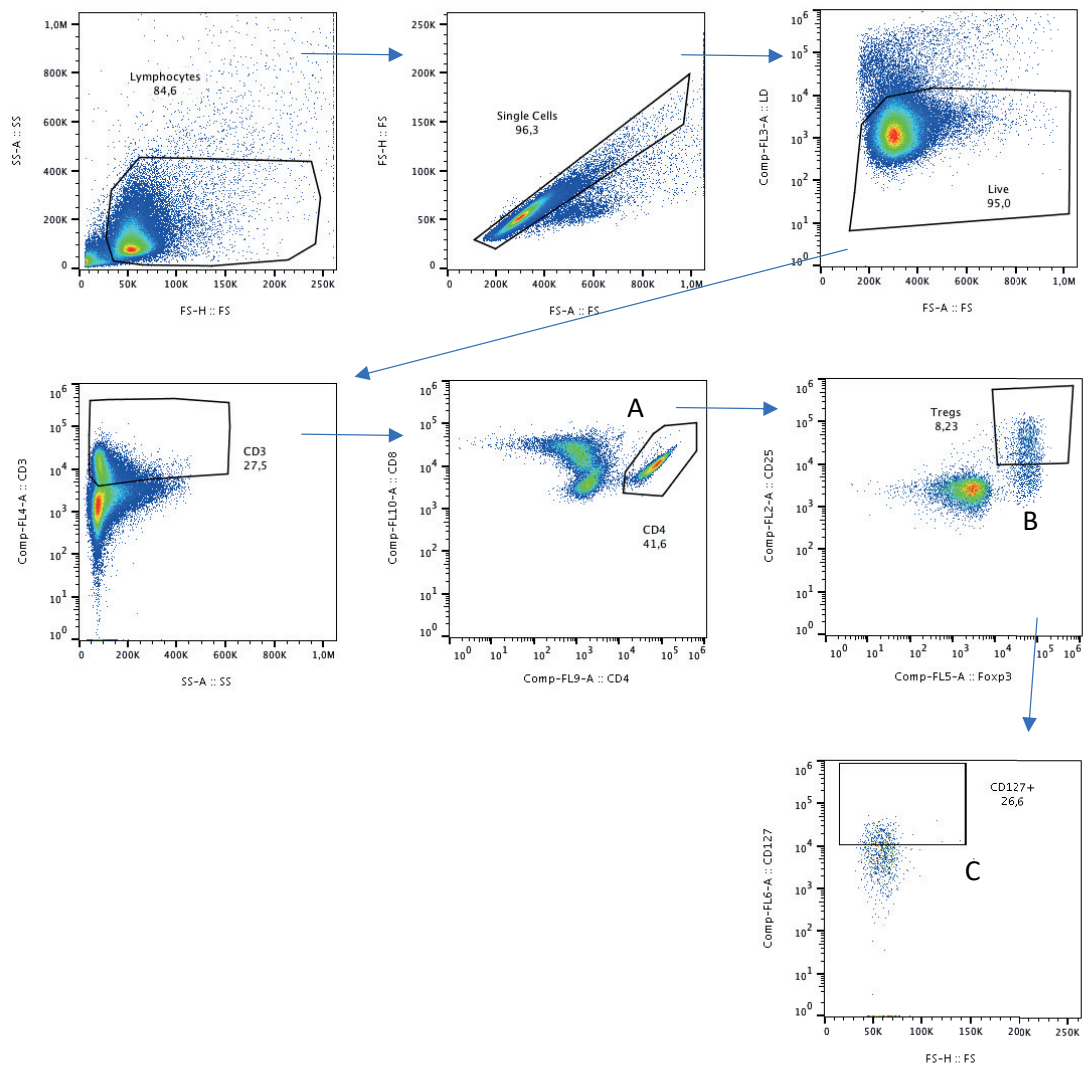


Figure 2. Gating strategy for CD4 T cells and T regulatory cells shown on splenocytes. (A) CD4 T cells, (B) Foxp3+CD25+ T regulatory cells and (C) CD127+ T regulatory cells.

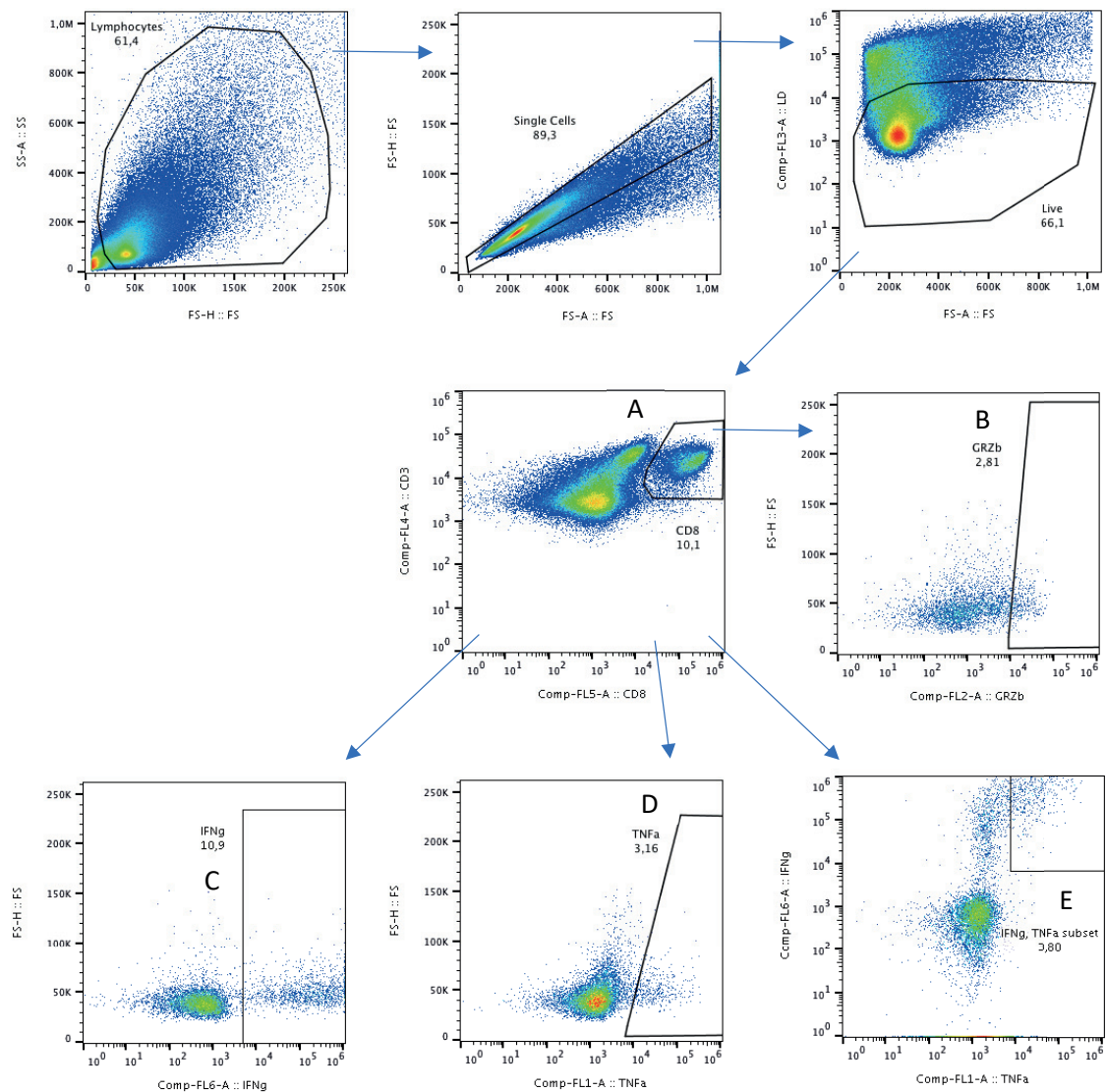


Figure 3. Gating strategy for cytokine production by CD8 T cells shown on splenocytes after re-stimulation with the E7 CD8 peptide. (A) CD8 T cells, (B) GZB+ CD8 T cells, (C) IFNγ+ CD8 T cells, (D) TNFα+ CD8 T cells and (E) IFNγ+TNFα+ CD8 T cells.

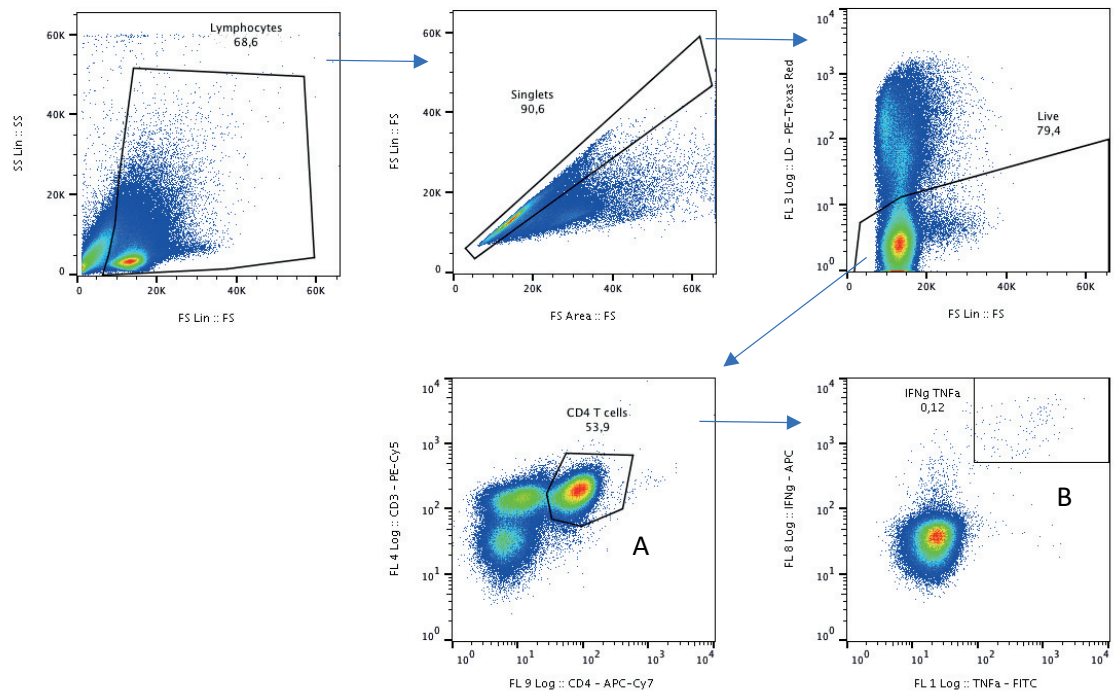


Figure 4. Gating strategy for cytokine production by CD4 T cells shown on splenocytes after re-stimulation with the full-lenght E7 protein. (A) CD4 T cell and (B) IFN γ +TNF α + CD4 T cells.

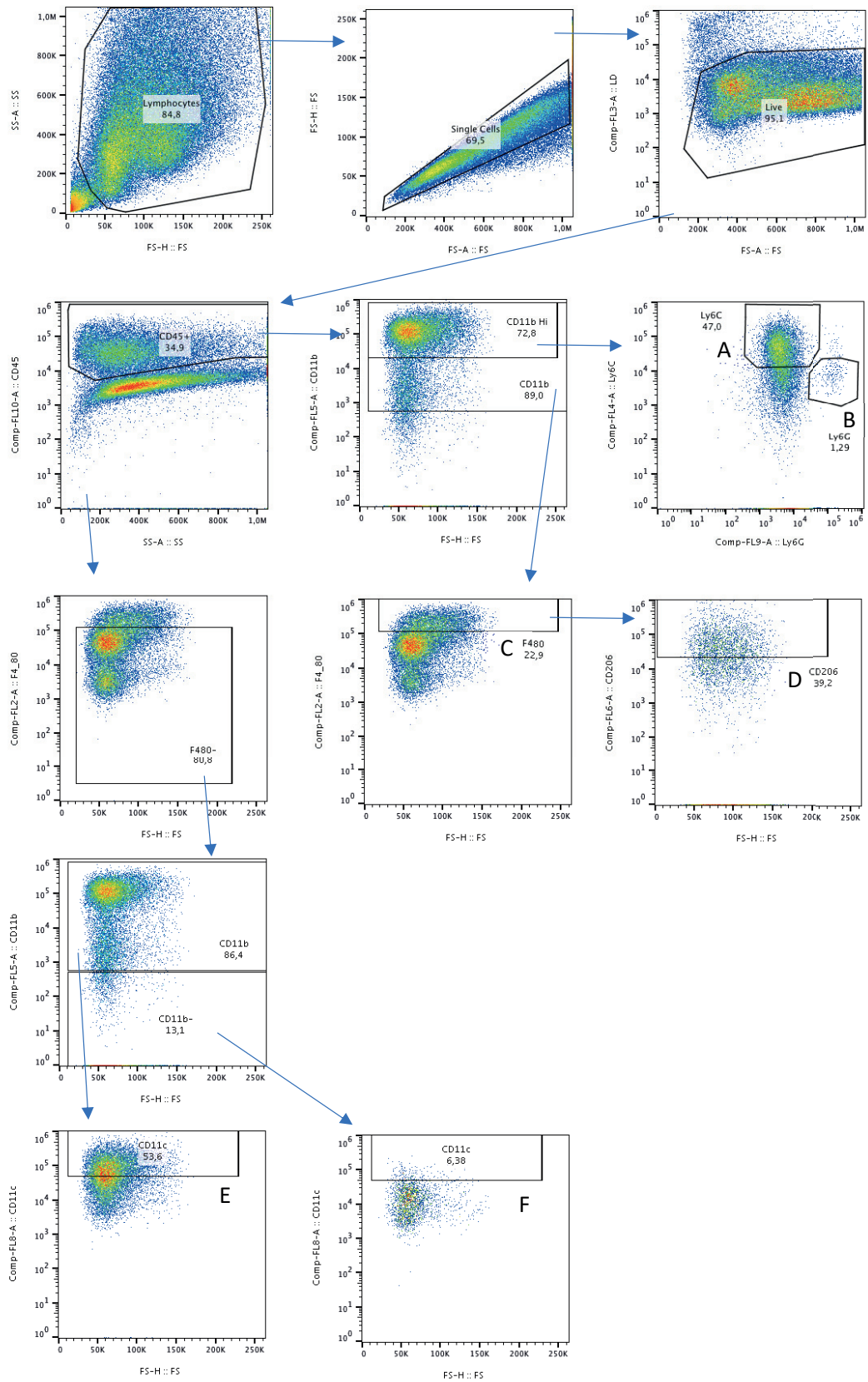


Figure 5. Gating strategy for innate immune cells shown on subcutaneous TC-1 tumor-derived cells. (A) CD11b^{hi}Ly6C⁺Ly6G⁻ cells, (B) CD11b^{hi}Ly6C⁻Ly6G⁺ cells, (C) CD11b⁺F4/80⁺ cells, (D) CD11b⁺F4/80⁺CD206⁺ cells, (E) F4/80⁻CD11b⁺CD11c⁺ cells and (F) F4/80⁻CD11b⁻CD11c⁺ cells.

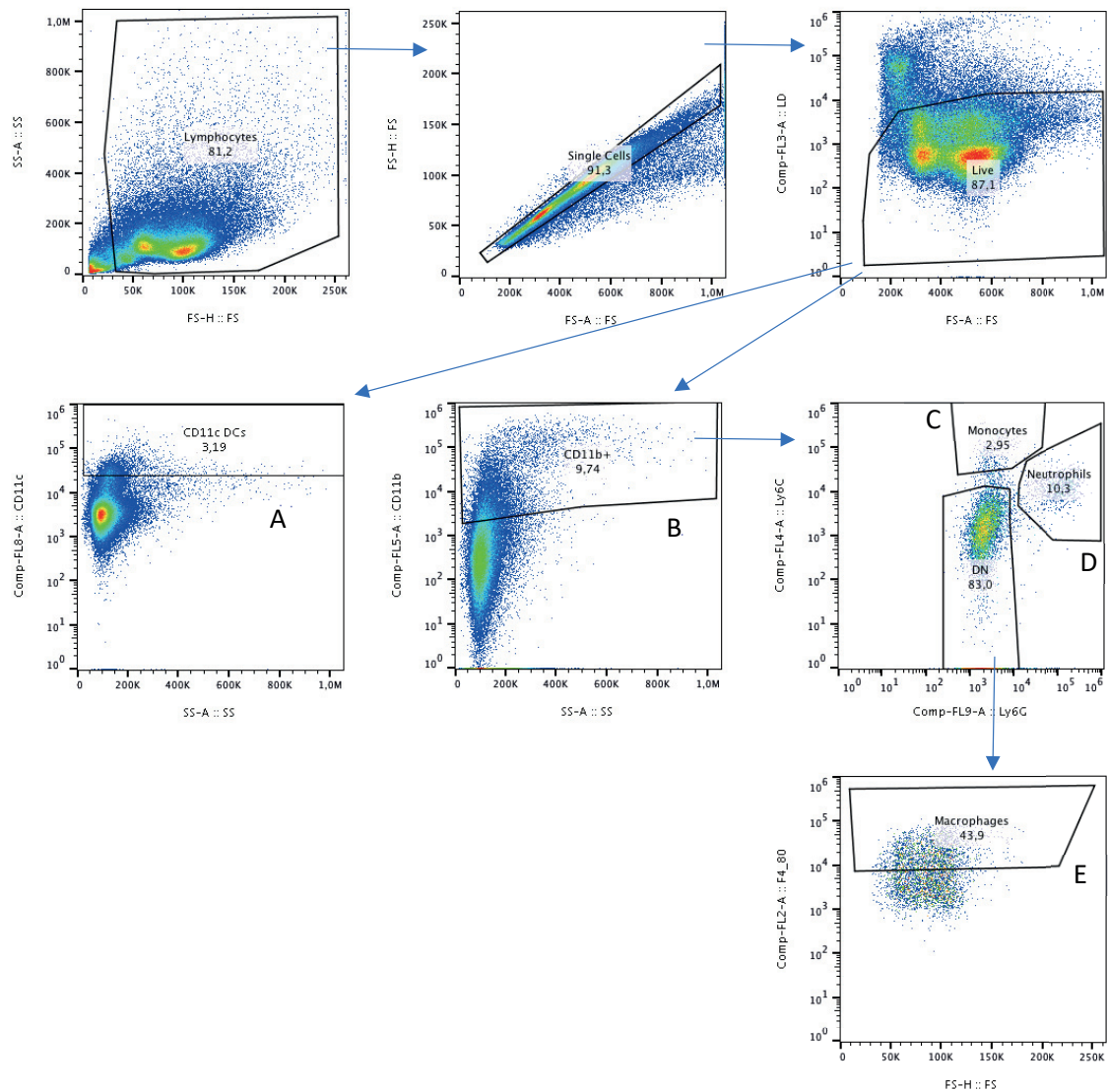


Figure 6. Gating strategy for MDSCs and macrophages shown on splenocytes. (A) CD11c+ cells, (B) CD11b+ cells, (C) CD11b+Ly6C+Ly6G- cells, (D) CD11b+Ly6C-Ly6G+ cells and (E) CD11b+Ly6C-Ly6G-F4/80+ cells.

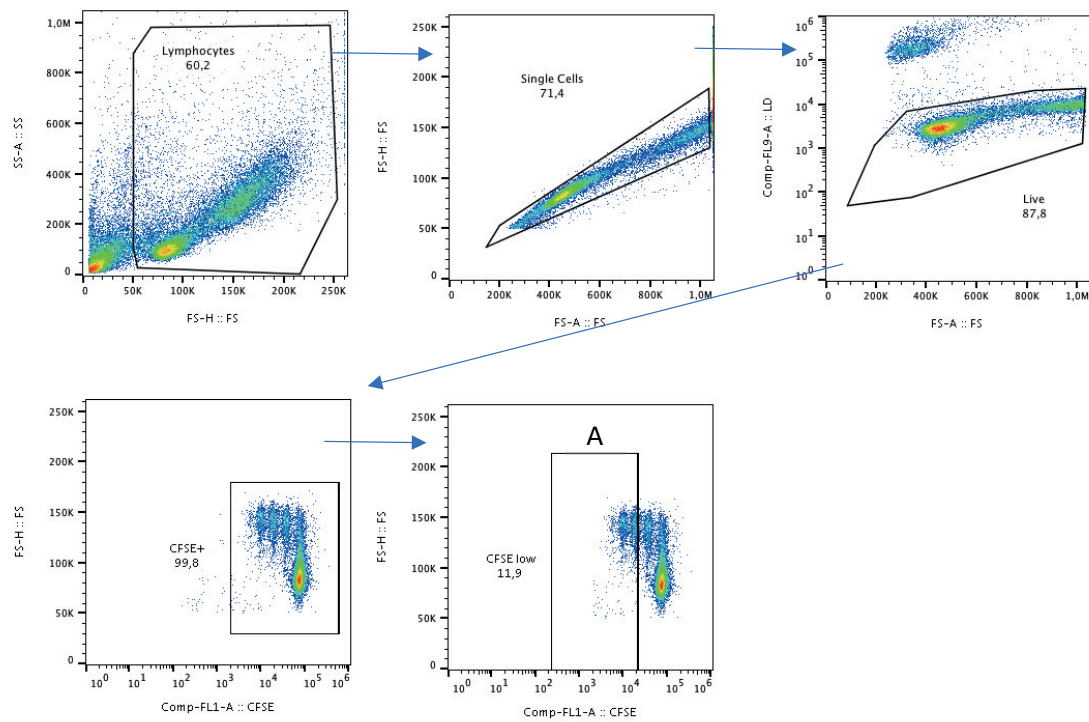


Figure 7. Gating strategy for CFSE low CD8 T cells after in-vitro proliferation. (A) CFSE low CD8 T cells.

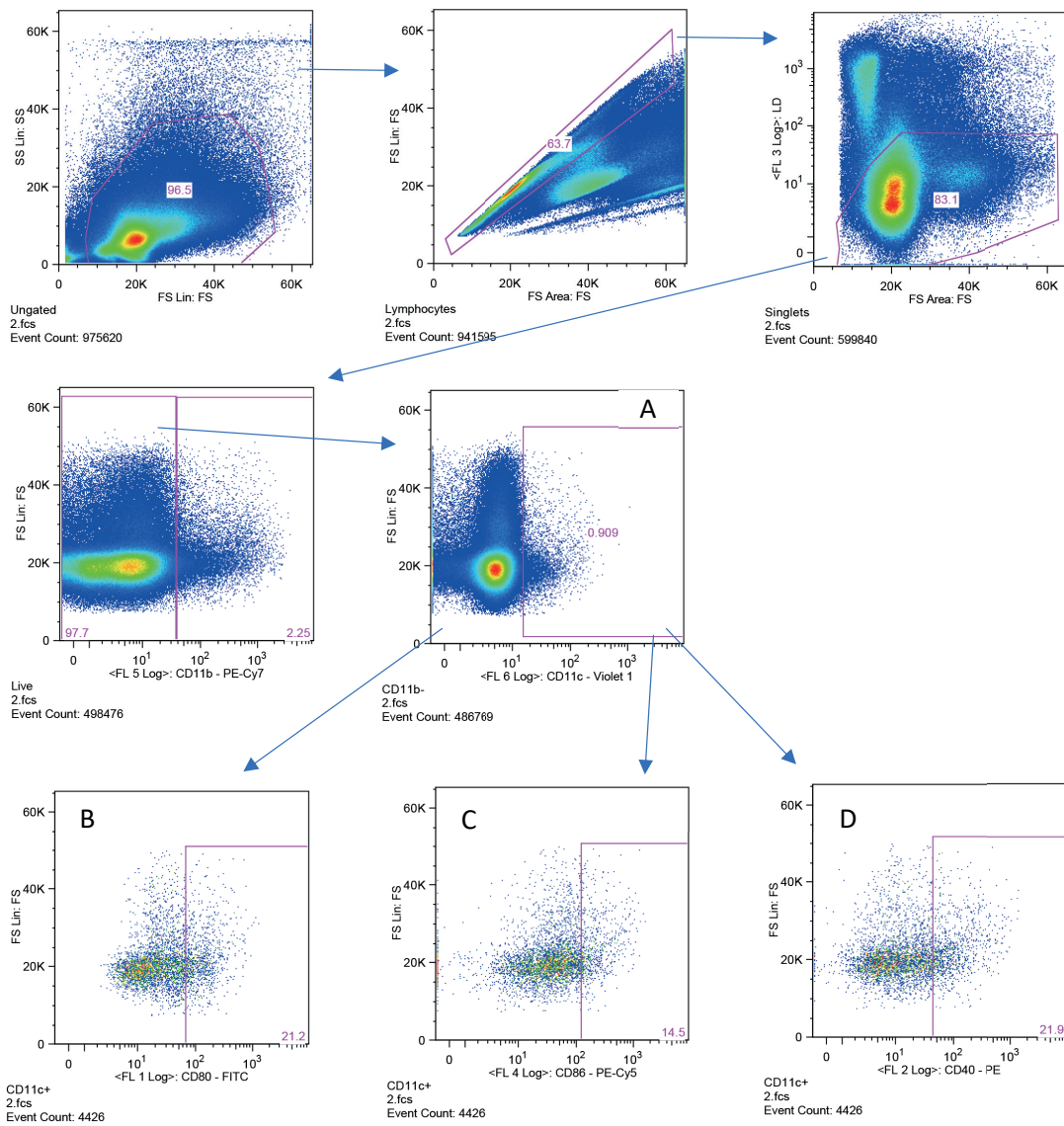


Figure 8. Gating strategy for endogenous DCs activation shown on lymph node cells. (A) CD11b-CD11c+ dendritic cells, (B, C, D) activation markers.

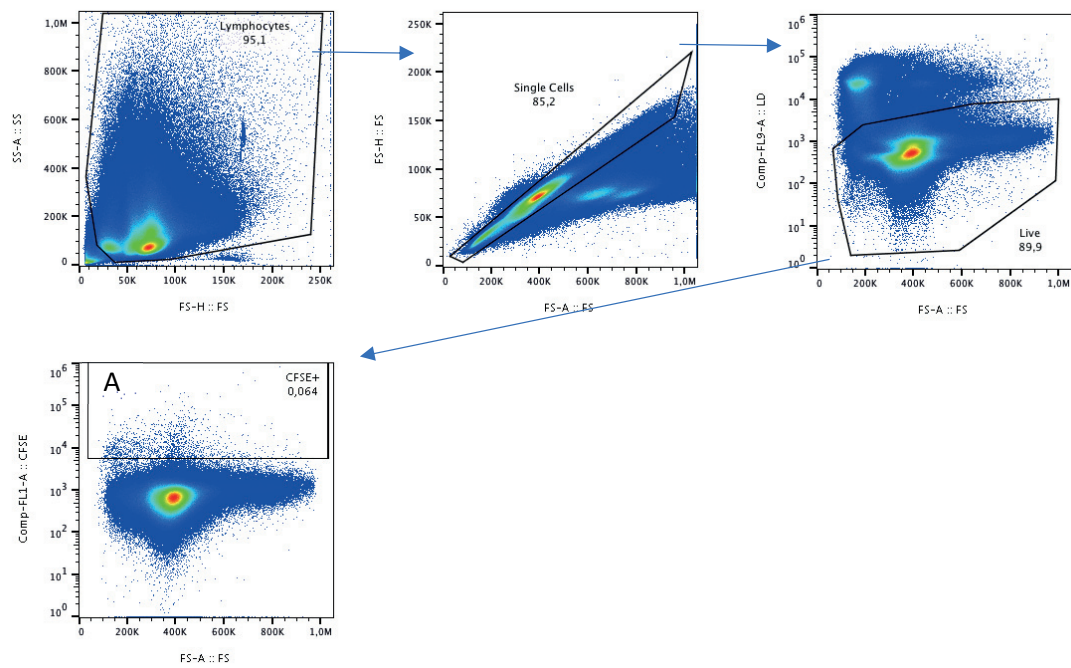


Figure 9. Gating strategy for CFSE-labeled BMDCs (DC-VAX) after in-vivo transfer shown on splenocytes. (A) CFSE+ transferred BMDCs.

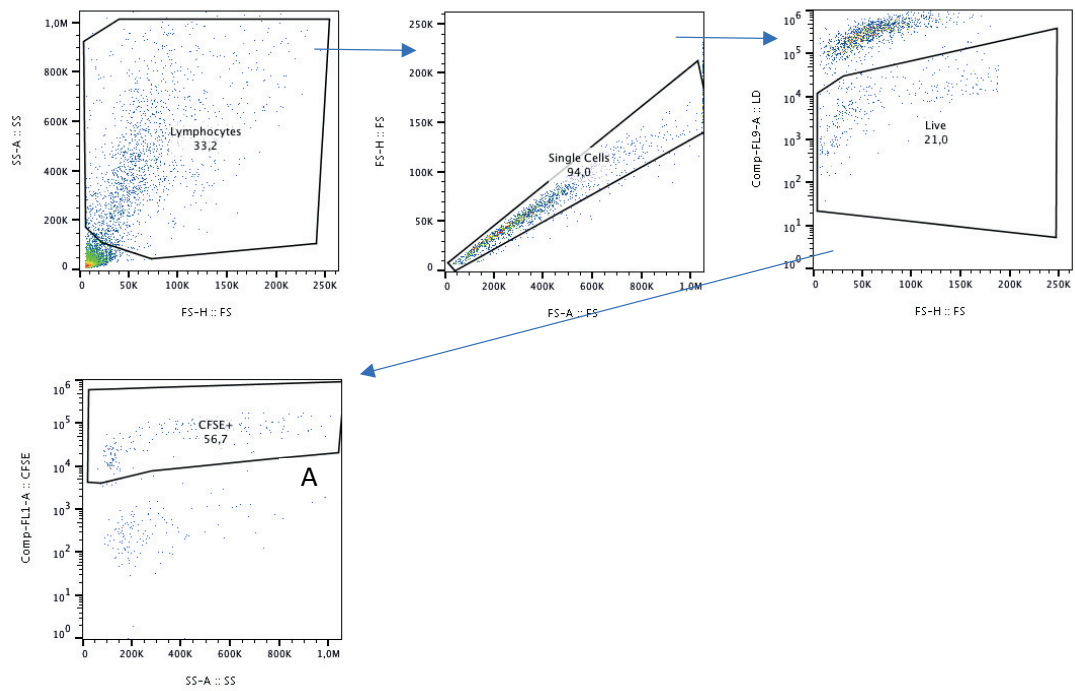


Figure 10. Gating strategy for CFSE-labeled BMDCs in in-vitro experiments. (A) CFSE+ BMDCs.

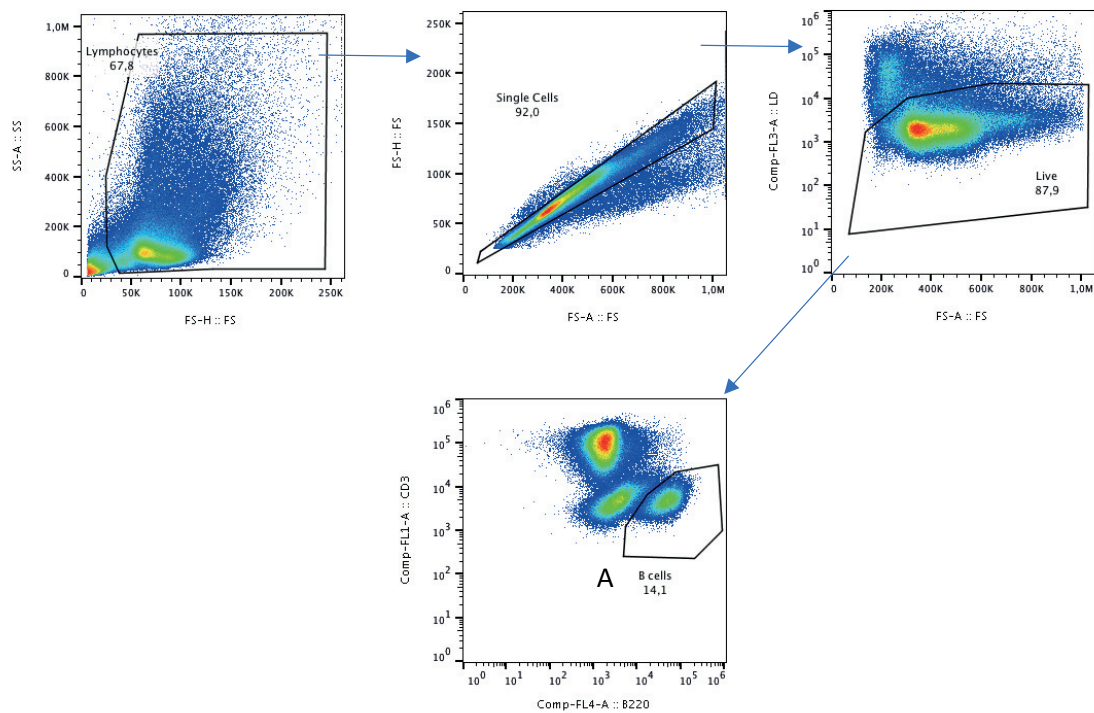


Figure 11. Gating strategy for B cells shown on splenocytes. (A) CD3-B220+ B cells.

Bibliography

1. Hanahan D, Weinberg RA (2000) The Hallmarks of Cancer. *Cell* 100(1):57–70.
2. Hanahan D, Weinberg RA (2011) Hallmarks of Cancer: The Next Generation. *Cell* 144(5):646–674.
3. Mueller MM, Fusenig NE (2004) Friends or foes - bipolar effects of the tumour stroma in cancer. *Nat Rev Cancer* 4(11):839–849.
4. Albini A, Sporn MB (2007) The tumour microenvironment as a target for chemoprevention. *Nat Rev Cancer* 7(2):139–147.
5. Chang Y, Moore PS, Weiss RA (2017) Human oncogenic viruses: nature and discovery. *Philos Trans R Soc Lond B Biol Sci* 372(1732). doi:10.1098/rstb.2016.0264.
6. Rowe M, Fitzsimmons L, Bell AI (2014) Epstein-Barr virus and Burkitt lymphoma. *Chin J Cancer* 33(12):609–619.
7. Durst M, Gissmann L, Ikenberg H, zur Hausen H (1983) A papillomavirus DNA from a cervical carcinoma and its prevalence in cancer biopsy samples from different geographic regions. *Proc Natl Acad Sci* 80(12):3812–3815.
8. Boshart M, et al. (1984) A new type of papillomavirus DNA, its presence in genital cancer biopsies and in cell lines derived from cervical cancer. *EMBO J* 3(5):1151–1157.
9. Bosch FX, Lorincz A, Muñoz N, Meijer CJLM, Shah KV (2002) The causal relation between human papillomavirus and cervical cancer. *J Clin Pathol* 55(4):244–265.
10. Giuliano AR, et al. (2015) EUROGIN 2014 roadmap: Differences in human papillomavirus infection natural history, transmission and human papillomavirus-related cancer incidence by gender and anatomic site of infection: EUROGIN 2014 roadmap. *Int J Cancer* 136(12):2752–2760.
11. Smola S (2017) Immunopathogenesis of HPV-Associated Cancers and Prospects for Immunotherapy. *Viruses* 9(9). doi:10.3390/v9090254.
12. de Villiers E-M (2013) Cross-roads in the classification of papillomaviruses. *Virology* 445(1–2):2–10.
13. Schiffman M, Castle PE, Jeronimo J, Rodriguez AC, Wacholder S (2007) Human papillomavirus and cervical cancer. *The Lancet* 370(9590):890–907.
14. de Sanjose S, et al. (2010) Human papillomavirus genotype attribution in invasive cervical cancer: a retrospective cross-sectional worldwide study. *Lancet Oncol* 11(11):1048–1056.
15. de Sanjosé S, et al. (2013) Worldwide human papillomavirus genotype attribution in over 2000 cases of intraepithelial and invasive lesions of the vulva. *Eur J Cancer* 49(16):3450–3461.
16. Ganguly N, Parihar SP (2009) Human papillomavirus E6 and E7 oncoproteins as risk factors for tumorigenesis. *J Biosci* 34(1):113–123.
17. Stubenrauch F, Laimins LA (1999) Human papillomavirus life cycle: active and latent phases. *Semin Cancer Biol* 9(6):379–386.
18. zur Hausen H (2002) Papillomaviruses and cancer: from basic studies to clinical application. *Nat Rev Cancer* 2(5):342–350.
19. de Sanjosé S, Brotons M, Pavón MA (2018) The natural history of human papillomavirus infection. *Best Pract Res Clin Obstet Gynaecol* 47:2–13.
20. Kanodia S, Fahey L, Kast WM (2007) Mechanisms Used by Human Papillomaviruses to Escape the Host Immune Response. *Curr Cancer Drug Targets* 7(1):79–89.

21. Scheffner M, Werness BA, Huibregtse JM, Levine AJ, Howley PM (1990) The E6 oncoprotein encoded by human papillomavirus types 16 and 18 promotes the degradation of p53. *Cell* 63(6):1129–1136.
22. Havre PA, Yuan J, Hedrick L, Cho KR, Glazer PM (1995) p53 inactivation by HPV16 E6 results in increased mutagenesis in human cells. *Cancer Res* 55(19):4420–4424.
23. Magal SS, et al. (2005) Downregulation of Bax mRNA expression and protein stability by the E6 protein of human papillomavirus 16. *J Gen Virol* 86(Pt 3):611–621.
24. Klingelhutz AJ, Foster SA, McDougall JK (1996) Telomerase activation by the E6 gene product of human papillomavirus type 16. *Nature* 380(6569):79–82.
25. Lee SS, Weiss RS, Javier RT (1997) Binding of human virus oncoproteins to hDlg/SAP97, a mammalian homolog of the Drosophila discs large tumor suppressor protein. *Proc Natl Acad Sci U S A* 94(13):6670–6675.
26. Watson RA, Thomas M, Banks L, Roberts S (2003) Activity of the human papillomavirus E6 PDZ-binding motif correlates with an enhanced morphological transformation of immortalized human keratinocytes. *J Cell Sci* 116(Pt 24):4925–4934.
27. Dyson N, Howley PM, Münger K, Harlow E (1989) The human papilloma virus-16 E7 oncoprotein is able to bind to the retinoblastoma gene product. *Science* 243(4893):934–937.
28. Dyson N (1998) The regulation of E2F by pRB-family proteins. *Genes Dev* 12(15):2245–2262.
29. Brehm A, et al. (1999) The E7 oncoprotein associates with Mi2 and histone deacetylase activity to promote cell growth. *EMBO J* 18(9):2449–2458.
30. Barnard P, McMillan NA (1999) The human papillomavirus E7 oncoprotein abrogates signaling mediated by interferon-alpha. *Virology* 259(2):305–313.
31. Um S-J, et al. (2002) Abrogation of IRF-1 response by high-risk HPV E7 protein in vivo. *Cancer Lett* 179(2):205–212.
32. Steinbach A, Riemer AB (2018) Immune evasion mechanisms of human papillomavirus: An update. *Int J Cancer* 142(2):224–229.
33. Finzer P, Aguilar-Lemarroy A, Rösl F (2002) The role of human papillomavirus oncoproteins E6 and E7 in apoptosis. *Cancer Lett* 188(1–2):15–24.
34. Serrano B, Brotons M, Bosch FX, Bruni L (2018) Epidemiology and burden of HPV-related disease. *Best Pract Res Clin Obstet Gynaecol* 47:14–26.
35. de Martel C, et al. (2012) Global burden of cancers attributable to infections in 2008: a review and synthetic analysis. *Lancet Oncol* 13(6):607–615.
36. de Martel C, Plummer M, Vignat J, Franceschi S (2017) Worldwide burden of cancer attributable to HPV by site, country and HPV type: Worldwide burden of cancer attributable to HPV. *Int J Cancer* 141(4):664–670.
37. Bruni L, et al. (2010) Cervical Human Papillomavirus Prevalence in 5 Continents: Meta-Analysis of 1 Million Women with Normal Cytological Findings. *J Infect Dis* 202(12):1789–1799.
38. Pisani P, Bray F, Parkin DM (2002) Estimates of the world-wide prevalence of cancer for 25 sites in the adult population. *Int J Cancer* 97(1):72–81.
39. Parkin DM, Bray F (2006) Chapter 2: The burden of HPV-related cancers. *Vaccine* 24 Suppl 3:S3/11–25.
40. Catarino R, Petignat P, Dongui G, Vassilakos P (2015) Cervical cancer screening in developing countries at a crossroad: Emerging technologies and policy choices. *World J Clin Oncol* 6(6):281–290.

41. Schiller JT, Castellsagué X, Garland SM (2012) A Review of Clinical Trials of Human Papillomavirus Prophylactic Vaccines. *Vaccine* 30:F123–F138.
42. Kim HJ, Kim H-J (2017) Current status and future prospects for human papillomavirus vaccines. *Arch Pharm Res* 40(9):1050–1063.
43. Schiller JT, Davies P (2004) Delivering on the promise: HPV vaccines and cervical cancer. *Nat Rev Microbiol* 2(4):343–347.
44. Winer RL, et al. (2011) Early Natural History of Incident, Type-Specific Human Papillomavirus Infections in Newly Sexually Active Young Women. *Cancer Epidemiol Biomarkers Prev* 20(4):699–707.
45. Rodriguez AC, et al. (2010) Longitudinal Study of Human Papillomavirus Persistence and Cervical Intraepithelial Neoplasia Grade 2/3: Critical Role of Duration of Infection. *JNCI J Natl Cancer Inst* 102(5):315–324.
46. Schiffman M, et al. (2016) Carcinogenic human papillomavirus infection. *Nat Rev Dis Primer* 2:16086.
47. Scott M, Stites DP, Moscicki AB (1999) Th1 cytokine patterns in cervical human papillomavirus infection. *Clin Diagn Lab Immunol* 6(5):751–755.
48. van der Burg SH, Melief CJ (2011) Therapeutic vaccination against human papilloma virus induced malignancies. *Curr Opin Immunol* 23(2):252–257.
49. Castle PE, et al. (2017) Treatment of cervical intraepithelial lesions. *Int J Gynecol Obstet* 138:20–25.
50. Schiffman M, Castle PE, Jeronimo J, Rodriguez AC, Wacholder S (2007) Human papillomavirus and cervical cancer. *Lancet Lond Engl* 370(9590):890–907.
51. Woodman CBJ, Collins SI, Young LS (2007) The natural history of cervical HPV infection: unresolved issues. *Nat Rev Cancer* 7(1):11–22.
52. Li H, Wu X, Cheng X (2016) Advances in diagnosis and treatment of metastatic cervical cancer. *J Gynecol Oncol* 27(4):e43.
53. Dobbs SP, et al. (2000) Does histological incomplete excision of cervical intraepithelial neoplasia following large loop excision of transformation zone increase recurrence rates? A six year cytological follow up. *BJOG Int J Obstet Gynaecol* 107(10):1298–1301.
54. Arbyn M, Paraskevaidis E, Martin-Hirsch P, Prendiville W, Dillner J (2005) Clinical utility of HPV-DNA detection: triage of minor cervical lesions, follow-up of women treated for high-grade CIN: an update of pooled evidence. *Gynecol Oncol* 99(3 Suppl 1):S7-11.
55. Scheurer ME, Tortolero-Luna G, Adler-Storthz K (2005) Human papillomavirus infection: biology, epidemiology, and prevention. *Int J Gynecol Cancer Off J Int Gynecol Cancer Soc* 15(5):727–746.
56. Gadducci A, Guerrieri ME (2017) Immune Checkpoint Inhibitors in Gynecological Cancers: Update of Literature and Perspectives of Clinical Research. *Anticancer Res* 37(11):5955–5965.
57. Monk BJ, et al. (2009) Phase III trial of four cisplatin-containing doublet combinations in stage IVB, recurrent, or persistent cervical carcinoma: a Gynecologic Oncology Group study. *J Clin Oncol Off J Am Soc Clin Oncol* 27(28):4649–4655.
58. Mellman I, Coukos G, Dranoff G (2011) Cancer immunotherapy comes of age. *Nature* 480(7378):480–489.
59. Galluzzi L, et al. (2014) Classification of current anticancer immunotherapies. *Oncotarget* 5(24). doi:10.18632/oncotarget.2998.
60. van Seters M, et al. (2008) Treatment of Vulvar Intraepithelial Neoplasia with Topical Imiquimod. *N Engl J Med* 358(14):1465–1473.

61. Terlou A, et al. (2010) Imiquimod-induced clearance of HPV is associated with normalization of immune cell counts in usual type vulvar intraepithelial neoplasia. *Int J Cancer* 127(12):2831–2840.
62. Couzin-Frankel J (2013) Breakthrough of the year 2013. Cancer immunotherapy. *Science* 342(6165):1432–1433.
63. Trimble CL, Frazer IH (2009) Development of therapeutic HPV vaccines. *Lancet Oncol* 10(10):975–980.
64. Ventriglia J, et al. (2017) Immunotherapy in ovarian, endometrial and cervical cancer: State of the art and future perspectives. *Cancer Treat Rev* 59:109–116.
65. Melief CJM, van der Burg SH (2008) Immunotherapy of established (pre)malignant disease by synthetic long peptide vaccines. *Nat Rev Cancer* 8(5):351–360.
66. Rice J, Ottensmeier CH, Stevenson FK (2008) DNA vaccines: precision tools for activating effective immunity against cancer. *Nat Rev Cancer* 8(2):108–120.
67. Khong H, Overwijk WW (2016) Adjuvants for peptide-based cancer vaccines. *J Immunother Cancer* 4(1). doi:10.1186/s40425-016-0160-y.
68. Palucka K, Banchereau J (2012) Cancer immunotherapy via dendritic cells. *Nat Rev Cancer* 12(4):265–277.
69. Banchereau J, Palucka AK (2005) Dendritic cells as therapeutic vaccines against cancer. *Nat Rev Immunol* 5(4):296–306.
70. Nemunaitis J (2005) Vaccines in cancer: GVAX, a GM-CSF gene vaccine. *Expert Rev Vaccines* 4(3):259–274.
71. Jia YY, et al. (2017) A Genetically Modified attenuated Listeria Vaccine Expressing HPV16 E7 Kill Tumor Cells in Direct and Antigen-Specific Manner. *Front Cell Infect Microbiol* 7:279.
72. Petit RG, Basu P (2013) ADXS11-001 immunotherapy targeting HPV-E7: updated survival and safety data from a phase 2 study in Indian women with recurrent/refractory cervical cancer. *J Immunother Cancer* 1(Suppl 1):P231.
73. Ma W, Melief CJ, van der Burg SH (2017) Control of immune escaped human papilloma virus is regained after therapeutic vaccination. *Curr Opin Virol* 23:16–22.
74. Welters MJP, et al. (2010) Success or failure of vaccination for HPV16-positive vulvar lesions correlates with kinetics and phenotype of induced T-cell responses. *Proc Natl Acad Sci* 107(26):11895–11899.
75. Kenter GG, et al. (2009) Vaccination against HPV-16 oncoproteins for vulvar intraepithelial neoplasia. *N Engl J Med* 361(19):1838–1847.
76. Kaplan-Lefko PJ, et al. (2010) Conatumumab, a fully human agonist antibody to death receptor 5, induces apoptosis via caspase activation in multiple tumor types. *Cancer Biol Ther* 9(8):618–631.
77. de La Motte Rouge T, et al. (2007) A novel epidermal growth factor receptor inhibitor promotes apoptosis in non-small cell lung cancer cells resistant to erlotinib. *Cancer Res* 67(13):6253–6262.
78. Kosits C, Callaghan M (2000) Rituximab: a new monoclonal antibody therapy for non-Hodgkin's lymphoma. *Oncol Nurs Forum* 27(1):51–59.
79. Motz GT, et al. (2014) Tumor endothelium FasL establishes a selective immune barrier promoting tolerance in tumors. *Nat Med* 20(6):607–615.
80. Ibrahim R, et al. (2006) Expression of FasL in squamous cell carcinomas of the cervix and cervical intraepithelial neoplasia and its role in tumor escape mechanism. *Cancer* 106(5):1065–1077.

81. Ferrara N, Hillan KJ, Gerber H-P, Novotny W (2004) Discovery and development of bevacizumab, an anti-VEGF antibody for treating cancer. *Nat Rev Drug Discov* 3(5):391–400.
82. Steiner M, Neri D (2011) Antibody-radionuclide conjugates for cancer therapy: historical considerations and new trends. *Clin Cancer Res Off J Am Assoc Cancer Res* 17(20):6406–6416.
83. Hubert P, Amigorena S (2012) Antibody-dependent cell cytotoxicity in monoclonal antibody-mediated tumor immunotherapy. *Oncoimmunology* 1(1):103–105.
84. Walter RB (2014) Biting back: BiTE antibodies as a promising therapy for acute myeloid leukemia. *Expert Rev Hematol* 7(3):317–319.
85. Dempke WCM, Fenchel K, Uciechowski P, Dale SP (2017) Second- and third-generation drugs for immuno-oncology treatment—The more the better? *Eur J Cancer* 74:55–72.
86. Swart M, Verbrugge I, Beltman JB (2016) Combination Approaches with Immune-Checkpoint Blockade in Cancer Therapy. *Front Oncol* 6:233.
87. Sun C, Mezzadra R, Schumacher TN (2018) Regulation and Function of the PD-L1 Checkpoint. *Immunity* 48(3):434–452.
88. Ribas A, Wolchok JD (2018) Cancer immunotherapy using checkpoint blockade. *Science* 359(6382):1350–1355.
89. Narazaki H, Zhu Y, Luo L, Zhu G, Chen L (2010) CD137 agonist antibody prevents cancer recurrence: contribution of CD137 on both hematopoietic and nonhematopoietic cells. *Blood* 115(10):1941–1948.
90. Vonderheide RH, Glennie MJ (2013) Agonistic CD40 antibodies and cancer therapy. *Clin Cancer Res Off J Am Assoc Cancer Res* 19(5):1035–1043.
91. Moran AE, Kovacsovics-Bankowski M, Weinberg AD (2013) The TNFRs OX40, 4-1BB, and CD40 as targets for cancer immunotherapy. *Curr Opin Immunol* 25(2):230–237.
92. Stevenson JP, et al. (2013) Immunological effects of the TGF β -blocking antibody GC1008 in malignant pleural mesothelioma patients. *Oncoimmunology* 2(8):e26218.
93. Wrzesinski SH, Wan YY, Flavell RA (2007) Transforming growth factor-beta and the immune response: implications for anticancer therapy. *Clin Cancer Res Off J Am Assoc Cancer Res* 13(18 Pt 1):5262–5270.
94. Vacchelli E, et al. (2012) Trial Watch: Immunostimulatory cytokines. *Oncoimmunology* 1(4):493–506.
95. Jiang T, Zhou C, Ren S (2016) Role of IL-2 in cancer immunotherapy. *Oncoimmunology* 5(6):e1163462.
96. Hodi FS, et al. (2014) Ipilimumab Plus Sargramostim vs Ipilimumab Alone for Treatment of Metastatic Melanoma: A Randomized Clinical Trial. *JAMA* 312(17):1744.
97. Maus MV, et al. (2014) Adoptive immunotherapy for cancer or viruses. *Annu Rev Immunol* 32:189–225.
98. Perica K, Varela JC, Oelke M, Schneck J (2015) Adoptive T cell immunotherapy for cancer. *Rambam Maimonides Med J* 6(1):e0004.
99. Buonaguro L, Petrizzo A, Tornesello ML, Buonaguro FM (2011) Translating tumor antigens into cancer vaccines. *Clin Vaccine Immunol CVI* 18(1):23–34.
100. Dotti G, Gottschalk S, Savoldo B, Brenner MK (2014) Design and development of therapies using chimeric antigen receptor-expressing T cells. *Immunol Rev* 257(1):107–126.
101. Galluzzi L, Lugli E (2013) Rejuvenated T cells attack old tumors. *Oncoimmunology* 2(2):e24103.
102. Mignot G, et al. (2008) The critical role of IL-15 in the antitumor effects mediated by the combination therapy imatinib and IL-2. *J Immunol Baltim Md 1950* 180(10):6477–6483.

103. Bracci L, Schiavoni G, Sistigu A, Belardelli F (2014) Immune-based mechanisms of cytotoxic chemotherapy: implications for the design of novel and rationale-based combined treatments against cancer. *Cell Death Differ* 21(1):15–25.
104. Kono K, Mimura K, Kiessling R (2013) Immunogenic tumor cell death induced by chemoradiotherapy: molecular mechanisms and a clinical translation. *Cell Death Dis* 4(6):e688–e688.
105. Kroemer G, Galluzzi L, Kepp O, Zitvogel L (2013) Immunogenic cell death in cancer therapy. *Annu Rev Immunol* 31:51–72.
106. Garg AD, et al. (2012) A novel pathway combining calreticulin exposure and ATP secretion in immunogenic cancer cell death. *EMBO J* 31(5):1062–1079.
107. Zhao J, et al. (2010) Selective depletion of CD4+CD25+Foxp3+ regulatory T cells by low-dose cyclophosphamide is explained by reduced intracellular ATP levels. *Cancer Res* 70(12):4850–4858.
108. Shang B, Liu Y, Jiang S, Liu Y (2015) Prognostic value of tumor-infiltrating FoxP3+ regulatory T cells in cancers: a systematic review and meta-analysis. *Sci Rep* 5(1). doi:10.1038/srep15179.
109. Vincent J, et al. (2010) 5-Fluorouracil Selectively Kills Tumor-Associated Myeloid-Derived Suppressor Cells Resulting in Enhanced T Cell-Dependent Antitumor Immunity. *Cancer Res* 70(8):3052–3061.
110. Suzuki E, Kapoor V, Jassar AS, Kaiser LR, Albelda SM (2005) Gemcitabine selectively eliminates splenic Gr-1+/CD11b+ myeloid suppressor cells in tumor-bearing animals and enhances antitumor immune activity. *Clin Cancer Res Off J Am Assoc Cancer Res* 11(18):6713–6721.
111. Welters MJ, et al. (2016) Vaccination during myeloid cell depletion by cancer chemotherapy fosters robust T cell responses. *Sci Transl Med* 8(334):334ra52.
112. Genard G, Lucas S, Michiels C (2017) Reprogramming of Tumor-Associated Macrophages with Anticancer Therapies: Radiotherapy versus Chemo- and Immunotherapies. *Front Immunol* 8:828.
113. Molinier-Frenkel V, Castellano F (2017) Immunosuppressive enzymes in the tumor microenvironment. *FEBS Lett* 591(19):3135–3157.
114. Allegranza MJ, Conejo-Garcia JR (2017) Targeted Therapy and Immunosuppression in the Tumor Microenvironment. *Trends Cancer* 3(1):19–27.
115. Mbongue JC, et al. (2015) The Role of Indoleamine 2, 3-Dioxygenase in Immune Suppression and Autoimmunity. *Vaccines* 3(3):703–729.
116. Routy J-P, Routy B, Graziani GM, Mehraj V (2016) The Kynurenine Pathway Is a Double-Edged Sword in Immune-Privileged Sites and in Cancer: Implications for Immunotherapy. *Int J Tryptophan Res IJTR* 9:67–77.
117. Ferns DM, et al. (2015) Indoleamine-2,3-dioxygenase (IDO) metabolic activity is detrimental for cervical cancer patient survival. *Oncoimmunology* 4(2):e981457.
118. Prendergast GC, Malachowski WP, DuHadaway JB, Muller AJ (2017) Discovery of IDO1 Inhibitors: From Bench to Bedside. *Cancer Res* 77(24):6795–6811.
119. Kadin ME, Vonderheid EC (2010) Targeted therapies: Denileukin diftitox—a step towards a “magic bullet” for CTCL. *Nat Rev Clin Oncol* 7(8):430–432.
120. Ghansah T (2012) A novel strategy for modulation of MDSC to enhance cancer immunotherapy. *Oncoimmunology* 1(6):984–985.
121. Iclozan C, Antonia S, Chiappori A, Chen D-T, Gabrilovich D (2013) Therapeutic regulation of myeloid-derived suppressor cells and immune response to cancer vaccine in patients with extensive stage small cell lung cancer. *Cancer Immunol Immunother CII* 62(5):909–918.

122. Strachan DC, et al. (2013) CSF1R inhibition delays cervical and mammary tumor growth in murine models by attenuating the turnover of tumor-associated macrophages and enhancing infiltration by CD8+ T cells. *Oncoimmunology* 2(12):e26968.
123. Russell SJ, Peng K-W, Bell JC (2012) Oncolytic virotherapy. *Nat Biotechnol* 30(7):658–670.
124. Ming Lim C, Stephenson R, Salazar AM, Ferris RL (2013) TLR3 agonists improve the immunostimulatory potential of cetuximab against EGFR+ head and neck cancer cells. *Oncoimmunology* 2(6):e24677.
125. Griffin H, et al. (2006) Inhibition of papillomavirus protein function in cervical cancer cells by intrabody targeting. *J Mol Biol* 355(3):360–378.
126. Song D, Li H, Li H, Dai J (2015) Effect of human papillomavirus infection on the immune system and its role in the course of cervical cancer. *Oncol Lett* 10(2):600–606.
127. Stanley MA (2012) Epithelial Cell Responses to Infection with Human Papillomavirus. *Clin Microbiol Rev* 25(2):215–222.
128. Fernandes JV, et al. (2015) Link between chronic inflammation and human papillomavirus-induced carcinogenesis (Review). *Oncol Lett* 9(3):1015–1026.
129. Bazzoni G, Dejana E (2002) Keratinocyte junctions and the epidermal barrier: how to make a skin-tight dress. *J Cell Biol* 156(6):947–949.
130. Pivarsci A, Kemény L, Dobozy A (2004) Innate immune functions of the keratinocytes. A review. *Acta Microbiol Immunol Hung* 51(3):303–310.
131. Burgers WA, et al. (2007) Viral oncoproteins target the DNA methyltransferases. *Oncogene* 26(11):1650–1655.
132. Cicchini L, et al. (2016) Suppression of Antitumor Immune Responses by Human Papillomavirus through Epigenetic Downregulation of CXCL14. *mBio* 7(3):e00270-16.
133. Laurson J, Khan S, Chung R, Cross K, Raj K (2010) Epigenetic repression of E-cadherin by human papillomavirus 16 E7 protein. *Carcinogenesis* 31(5):918–926.
134. Tindle RW (2002) Immune evasion in human papillomavirus-associated cervical cancer. *Nat Rev Cancer* 2(1):59–65.
135. Romani N, et al. (1989) Presentation of exogenous protein antigens by dendritic cells to T cell clones. Intact protein is presented best by immature, epidermal Langerhans cells. *J Exp Med* 169(3):1169–1178.
136. Pacini L, et al. (2015) Downregulation of Toll-Like Receptor 9 Expression by Beta Human Papillomavirus 38 and Implications for Cell Cycle Control. *J Virol* 89(22):11396–11405.
137. Kawai T, Akira S (2007) Antiviral signaling through pattern recognition receptors. *J Biochem (Tokyo)* 141(2):137–145.
138. Lau L, Gray EE, Brunette RL, Stetson DB (2015) DNA tumor virus oncogenes antagonize the cGAS-STING DNA-sensing pathway. *Science* 350(6260):568–571.
139. Grandvaux N, tenOever BR, Servant MJ, Hiscott J (2002) The interferon antiviral response: from viral invasion to evasion. *Curr Opin Infect Dis* 15(3):259–267.
140. Park JS, et al. (2000) Inactivation of interferon regulatory factor-1 tumor suppressor protein by HPV E7 oncoprotein. Implication for the E7-mediated immune evasion mechanism in cervical carcinogenesis. *J Biol Chem* 275(10):6764–6769.
141. Evans M, et al. (2001) Antigen processing defects in cervical carcinomas limit the presentation of a CTL epitope from human papillomavirus 16 E6. *J Immunol Baltim Md* 157(9):5420–5428.

142. Hasim A, et al. (2012) Post-Transcriptional and Epigenetic Regulation of Antigen Processing Machinery (APM) Components and HLA-I in Cervical Cancers from Uighur Women. *PLoS ONE* 7(9):e44952.
143. Steinbach A, et al. (2017) ERAP1 overexpression in HPV-induced malignancies: A possible novel immune evasion mechanism. *Oncoimmunology* 6(7):e1336594.
144. Georgopoulos NT, Proffitt JL, Blair GE (2000) Transcriptional regulation of the major histocompatibility complex (MHC) class I heavy chain, TAP1 and LMP2 genes by the human papillomavirus (HPV) type 6b, 16 and 18 E7 oncoproteins. *Oncogene* 19(42):4930–4935.
145. Iijima N, Goodwin EC, Dimaio D, Iwasaki A (2013) High-risk human papillomavirus E6 inhibits monocyte differentiation to Langerhans cells. *Virology* 444(1–2):257–262.
146. Strickler HD, et al. (2014) The Relation of Plasmacytoid Dendritic Cells (pDCs) and Regulatory T-Cells (Tregs) with HPV Persistence in HIV-Infected and HIV-Uninfected Women. *Viral Immunol* 27(1):20–25.
147. Kushwah R, Hu J (2011) Role of dendritic cells in the induction of regulatory T cells. *Cell Biosci* 1(1):20.
148. Berger A (2000) Science commentary: Th1 and Th2 responses: what are they? *BMJ* 321(7258):424–424.
149. Moerman-Herzog A, Nakagawa M (2015) Early Defensive Mechanisms against Human Papillomavirus Infection. *Clin Vaccine Immunol* 22(8):850–857.
150. Azar KK, et al. (2004) Increased secretion patterns of interleukin-10 and tumor necrosis factor-alpha in cervical squamous intraepithelial lesions. *Hum Pathol* 35(11):1376–1384.
151. Smith LK, et al. (2018) Interleukin-10 Directly Inhibits CD8 + T Cell Function by Enhancing N-Glycan Branching to Decrease Antigen Sensitivity. *Immunity* 48(2):299–312.e5.
152. Harizi H, Juzan M, Pitard V, Moreau J-F, Gualde N (2002) Cyclooxygenase-2-Issued Prostaglandin E2 Enhances the Production of Endogenous IL-10, Which Down-Regulates Dendritic Cell Functions. *J Immunol* 168(5):2255–2263.
153. Xu M, et al. (2017) Interactions between interleukin-6 and myeloid-derived suppressor cells drive the chemoresistant phenotype of hepatocellular cancer. *Exp Cell Res* 351(2):142–149.
154. Feng Q, et al. (2012) Th2 type inflammation promotes the gradual progression of HPV-infected cervical cells to cervical carcinoma. *Gynecol Oncol* 127(2):412–419.
155. Piersma SJ (2011) Immunosuppressive tumor microenvironment in cervical cancer patients. *Cancer Microenviron Off J Int Cancer Microenviron Soc* 4(3):361–375.
156. Lepique AP, Daghasanli KRP, Cuccovia IM, Villa LL (2009) HPV16 tumor associated macrophages suppress antitumor T cell responses. *Clin Cancer Res Off J Am Assoc Cancer Res* 15(13):4391–4400.
157. Molling JW, et al. (2007) CD4(+)CD25hi regulatory T-cell frequency correlates with persistence of human papillomavirus type 16 and T helper cell responses in patients with cervical intraepithelial neoplasia. *Int J Cancer* 121(8):1749–1755.
158. Kawano M, et al. (2015) The significance of G-CSF expression and myeloid-derived suppressor cells in the chemoresistance of uterine cervical cancer. *Sci Rep* 5:18217.
159. Jiang N, Tian Z, Tang J, Ou R, Xu Y (2015) Granulocyte Macrophage-Colony Stimulating Factor (GM-CSF) Downregulates the Expression of Protumor Factors Cyclooxygenase-2 and Inducible Nitric Oxide Synthase in a GM-CSF Receptor-Independent Manner in Cervical Cancer Cells. *Mediators Inflamm* 2015:1–10.
160. Wei LH, et al. (2001) Interleukin-6 in cervical cancer: the relationship with vascular endothelial growth factor. *Gynecol Oncol* 82(1):49–56.

161. Umansky V, Blattner C, Gebhardt C, Utikal J (2016) The Role of Myeloid-Derived Suppressor Cells (MDSC) in Cancer Progression. *Vaccines* 4(4). doi:10.3390/vaccines4040036.
162. Mabuchi S, et al. (2014) Uterine cervical cancer displaying tumor-related leukocytosis: a distinct clinical entity with radioresistant feature. *J Natl Cancer Inst* 106(7). doi:10.1093/jnci/dju147.
163. Alvarez KLF, et al. (2017) Local and systemic immunomodulatory mechanisms triggered by Human Papillomavirus transformed cells: a potential role for G-CSF and neutrophils. *Sci Rep* 7(1):9002.
164. Affara NI, et al. (2014) B cells regulate macrophage phenotype and response to chemotherapy in squamous carcinomas. *Cancer Cell* 25(6):809–821.
165. Walch-Rückheim B, et al. (2015) Stromal Fibroblasts Induce CCL20 through IL6/C/EBP β to Support the Recruitment of Th17 Cells during Cervical Cancer Progression. *Cancer Res* 75(24):5248–5259.
166. van Poelgeest MI, et al. (2013) HPV16 synthetic long peptide (HPV16-SLP) vaccination therapy of patients with advanced or recurrent HPV16-induced gynecological carcinoma, a phase II trial. *J Transl Med* 11(1):88.
167. Wu S-F, et al. (2012) Altered expression of survivin, Fas and FasL contributed to cervical cancer development and metastasis. *Eur Rev Med Pharmacol Sci* 16(15):2044–2050.
168. Reesink-Peters N, et al. (2005) Death receptors and ligands in cervical carcinogenesis: an immunohistochemical study. *Gynecol Oncol* 96(3):705–713.
169. Santos C, Vilanova M, Medeiros R, Gil da Costa RM (2017) HPV-transgenic mouse models: Tools for studying the cancer-associated immune response. *Virus Res* 235:49–57.
170. Buitrago-Pérez Á, et al. (2012) A Humanized Mouse Model of HPV-Associated Pathology Driven by E7 Expression. *PLoS ONE* 7(7):e41743.
171. Feltkamp MCW, et al. (1993) Vaccination with cytotoxic T lymphocyte epitope-containing peptide protects against a tumor induced by human papillomavirus type 16-transformed cells. *Eur J Immunol* 23(9):2242–2249.
172. van der Sluis TC, et al. (2015) Therapeutic Peptide Vaccine-Induced CD8 T Cells Strongly Modulate Intratumoral Macrophages Required for Tumor Regression. *Cancer Immunol Res* 3(9):1042–1051.
173. Domingos-Pereira S, et al. (2013) Intravaginal TLR agonists increase local vaccine-specific CD8 T cells and human papillomavirus-associated genital-tumor regression in mice. *Mucosal Immunol* 6(2):393–404.
174. Decrausaz L, et al. (2011) A novel mucosal orthotopic murine model of human papillomavirus-associated genital cancers. *Int J Cancer* 128(9):2105–2113.
175. Genter Williams SM, et al. (2005) Requirement of epidermal growth factor receptor for hyperplasia induced by E5, a high-risk human papillomavirus oncogene. *Cancer Res* 65(15):6534–6542.
176. Herber R, Liem A, Pitot H, Lambert PF (1996) Squamous epithelial hyperplasia and carcinoma in mice transgenic for the human papillomavirus type 16 E7 oncogene. *J Virol* 70(3):1873–1881.
177. Song S, Pitot HC, Lambert PF (1999) The human papillomavirus type 16 E6 gene alone is sufficient to induce carcinomas in transgenic animals. *J Virol* 73(7):5887–5893.
178. Arbeit JM, Howley PM, Hanahan D (1996) Chronic estrogen-induced cervical and vaginal squamous carcinogenesis in human papillomavirus type 16 transgenic mice. *Proc Natl Acad Sci U S A* 93(7):2930–2935.

179. Smith-McCune K, Zhu YH, Hanahan D, Arbeit J (1997) Cross-species comparison of angiogenesis during the premalignant stages of squamous carcinogenesis in the human cervix and K14-HPV16 transgenic mice. *Cancer Res* 57(7):1294–1300.
180. Elson DA, et al. (2000) Sensitivity of the cervical transformation zone to estrogen-induced squamous carcinogenesis. *Cancer Res* 60(5):1267–1275.
181. Daniel D, et al. (2005) CD4⁺ T Cell-Mediated Antigen-Specific Immunotherapy in a Mouse Model of Cervical Cancer. *Cancer Res* 65(5):2018–2025.
182. Pere H, et al. (2011) A CCR4 antagonist combined with vaccines induces antigen-specific CD8⁺ T cells and tumor immunity against self antigens. *Blood* 118(18):4853–4862.
183. Lin Y-H, et al. (2018) Integration of Oncogenes via Sleeping Beauty as a Mouse Model of HPV16+ Oral Tumors and Immunologic Control. *Cancer Immunol Res*. doi:10.1158/2326-6066.CIR-16-0358.
184. Brown SD, et al. (2014) Neo-antigens predicted by tumor genome meta-analysis correlate with increased patient survival. *Genome Res* 24(5):743–750.
185. Comber JD, Philip R (2014) MHC class I antigen presentation and implications for developing a new generation of therapeutic vaccines. *Ther Adv Vaccines* 2(3):77–89.
186. van Poelgeest MIE, et al. (2016) Vaccination against Oncoproteins of HPV16 for Noninvasive Vulvar/Vaginal Lesions: Lesion Clearance Is Related to the Strength of the T-Cell Response. *Clin Cancer Res* 22(10):2342–2350.
187. Rosalia RA, et al. (2013) Dendritic cells process synthetic long peptides better than whole protein, improving antigen presentation and T-cell activation: Antigen processing. *Eur J Immunol* 43(10):2554–2565.
188. Bijker MS, et al. (2008) Superior induction of anti-tumor CTL immunity by extended peptide vaccines involves prolonged, DC-focused antigen presentation. *Eur J Immunol* 38(4):1033–1042.
189. de Vos van Steenwijk PJ, et al. (2014) The long-term immune response after HPV16 peptide vaccination in women with low-grade pre-malignant disorders of the uterine cervix: a placebo-controlled phase II study. *Cancer Immunol Immunother* 63(2):147–160.
190. Jordanova ES, et al. (2008) Human Leukocyte Antigen Class I, MHC Class I Chain-Related Molecule A, and CD8⁺/Regulatory T-Cell Ratio: Which Variable Determines Survival of Cervical Cancer Patients? *Clin Cancer Res* 14(7):2028–2035.
191. Welters MJP, et al. (2008) Induction of Tumor-Specific CD4⁺ and CD8⁺ T-Cell Immunity in Cervical Cancer Patients by a Human Papillomavirus Type 16 E6 and E7 Long Peptides Vaccine. *Clin Cancer Res* 14(1):178–187.
192. Facciabene A, Motz GT, Coukos G (2012) T-Regulatory Cells: Key Players in Tumor Immune Escape and Angiogenesis. *Cancer Res* 72(9):2162–2171.
193. Liu Z, Kim JH, Falo LD, You Z (2009) Tumor Regulatory T Cells Potently Abrogate Antitumor Immunity. *J Immunol* 182(10):6160–6167.
194. Jeanbart L, et al. (2014) Enhancing Efficacy of Anticancer Vaccines by Targeted Delivery to Tumor-Draining Lymph Nodes. *Cancer Immunol Res* 2(5):436–447.
195. Nembrini C, et al. (2011) Nanoparticle conjugation of antigen enhances cytotoxic T-cell responses in pulmonary vaccination. *Proc Natl Acad Sci* 108(44):E989–E997.
196. Liu H, et al. (2014) Structure-based programming of lymph-node targeting in molecular vaccines. *Nature* 507(7493):519–522.
197. Jeanbart L, Swartz MA (2015) Engineering opportunities in cancer immunotherapy. *Proc Natl Acad Sci U S A* 112(47):14467–14472.

198. Bookstaver ML, Tsai SJ, Bromberg JS, Jewell CM (2017) Improving Vaccine and Immunotherapy Design Using Biomaterials. *Trends Immunol.* doi:10.1016/j.it.2017.10.002.
199. Hirose S, Kourtis IC, van der Vlies AJ, Hubbell JA, Swartz MA (2010) Antigen delivery to dendritic cells by poly(propylene sulfide) nanoparticles with disulfide conjugated peptides: Cross-presentation and T cell activation. *Vaccine* 28(50):7897–7906.
200. Reddy ST, Rehor A, Schmoekel HG, Hubbell JA, Swartz MA (2006) In vivo targeting of dendritic cells in lymph nodes with poly(propylene sulfide) nanoparticles. *J Controlled Release* 112(1):26–34.
201. Rincon-Restrepo M, et al. (2017) Vaccine nanocarriers: Coupling intracellular pathways and cellular biodistribution to control CD4 vs CD8 T cell responses. *Biomaterials* 132:48–58.
202. Ji H, et al. (1998) Antigen-specific immunotherapy for murine lung metastatic tumors expressing human papillomavirus type 16 E7 oncoprotein. *Int J Cancer* 78(1):41–45.
203. de Vos van Steenwijk PJ, et al. (2012) A placebo-controlled randomized HPV16 synthetic long-peptide vaccination study in women with high-grade cervical squamous intraepithelial lesions. *Cancer Immunol Immunother* 61(9):1485–1492.
204. Bartkowiak T, et al. (2015) Unique potential of 4-1BB agonist antibody to promote durable regression of HPV+ tumors when combined with an E6/E7 peptide vaccine. *Proc Natl Acad Sci U S A* 112(38):E5290-5299.
205. Chen Z, et al. (2014) Episomal expression of truncated listeriolysin O in LmddA-LLO-E7 vaccine enhances antitumor efficacy by preferentially inducing expansions of CD4+FoxP3- and CD8+ T cells. *Cancer Immunol Res* 2(9):911–922.
206. Crosbie EJ, Einstein MH, Franceschi S, Kitchener HC (2013) Human papillomavirus and cervical cancer. *The Lancet* 382(9895):889–899.
207. D’Souza G, Dempsey A (2011) The role of HPV in head and neck cancer and review of the HPV vaccine. *Prev Med* 53:S5–S11.
208. Alkatout I, et al. (2015) Vulvar cancer: epidemiology, clinical presentation, and management options. *Int J Womens Health*:305.
209. Wakeham K, Kavanagh K (2014) The Burden of HPV-Associated Anogenital Cancers. *Curr Oncol Rep* 16(9). doi:10.1007/s11912-014-0402-4.
210. Trosman SJ, et al. (2015) Effect of human papillomavirus on patterns of distant metastatic failure in oropharyngeal squamous cell carcinoma treated with chemoradiotherapy. *JAMA Otolaryngol-- Head Neck Surg* 141(5):457–462.
211. Faraji F, Eisele DW, Fakhry C (2017) Emerging insights into recurrent and metastatic human papillomavirus-related oropharyngeal squamous cell carcinoma: Recurrent and Metastatic HPV-Related OPC. *Laryngoscope Investig Otolaryngol* 2(1):10–18.
212. Lin K-Y, et al. (1996) Treatment of established tumors with a novel vaccine that enhances major histocompatibility class II presentation of tumor antigen. *Cancer Res* 56(1):21–26.
213. Mittal D, Gubin MM, Schreiber RD, Smyth MJ (2014) New insights into cancer immunoediting and its three component phases—elimination, equilibrium and escape. *Curr Opin Immunol* 27:16–25.
214. Baer C, et al. (2016) Suppression of microRNA activity amplifies IFN- γ -induced macrophage activation and promotes anti-tumour immunity. *Nat Cell Biol.* doi:10.1038/ncb3371.
215. Juneja VR, et al. (2017) PD-L1 on tumor cells is sufficient for immune evasion in immunogenic tumors and inhibits CD8 T cell cytotoxicity. *J Exp Med* 214(4):895–904.
216. Chen DS, Mellman I (2013) Oncology meets immunology: the cancer-immunity cycle. *Immunity* 39(1):1–10.

217. Rahimian S, et al. (2015) Polymeric nanoparticles for co-delivery of synthetic long peptide antigen and poly IC as therapeutic cancer vaccine formulation. *J Controlled Release* 203:16–22.
218. Varypataki EM, Benne N, Bouwstra J, Jiskoot W, Ossendorp F (2017) Efficient Eradication of Established Tumors in Mice with Cationic Liposome-Based Synthetic Long-Peptide Vaccines. *Cancer Immunol Res* 5(3):222–233.
219. Moynihan KD, et al. (2016) Eradication of large established tumors in mice by combination immunotherapy that engages innate and adaptive immune responses. *Nat Med* 22(12):1402–1410.
220. Goldinger SM, et al. (2012) Nano-particle vaccination combined with TLR-7 and -9 ligands triggers memory and effector CD8⁺ T-cell responses in melanoma patients: Cellular immune response. *Eur J Immunol* 42(11):3049–3061.
221. Li AW, et al. (2018) A facile approach to enhance antigen response for personalized cancer vaccination. *Nat Mater*. doi:10.1038/s41563-018-0028-2.
222. Ott PA, et al. (2017) An immunogenic personal neoantigen vaccine for patients with melanoma. *Nature* 547(7662):217–221.
223. Kamala T (2007) Hock immunization: A humane alternative to mouse footpad injections. *J Immunol Methods* 328(1–2):204–214.
224. Arbeit JM, Münger K, Howley PM, Hanahan D (1994) Progressive squamous epithelial neoplasia in K14-human papillomavirus type 16 transgenic mice. *J Virol* 68(7):4358–4368.
225. van der Vlies AJ, O’Neil CP, Hasegawa U, Hammond N, Hubbell JA (2010) Synthesis of Pyridyl Disulfide-Functionalized Nanoparticles for Conjugating Thiol-Containing Small Molecules, Peptides, and Proteins. *Bioconjug Chem* 21(4):653–662.
226. Thomas SN, Vokali E, Lund AW, Hubbell JA, Swartz MA (2014) Targeting the tumor-draining lymph node with adjuvanted nanoparticles reshapes the anti-tumor immune response. *Biomaterials* 35(2):814–824.
227. Ballester M, et al. (2011) Nanoparticle conjugation and pulmonary delivery enhance the protective efficacy of Ag85B and CpG against tuberculosis. *Vaccine* 29(40):6959–6966.
228. Kobayashi A, Weinberg V, Darragh T, Smith-McCune K (2008) Evolving immunosuppressive microenvironment during human cervical carcinogenesis. *Mucosal Immunol* 1(5):412–420.
229. Schmalzer M, et al. (2015) IL-7R signaling in regulatory T cells maintains peripheral and allograft tolerance in mice. *Proc Natl Acad Sci U S A* 112(43):13330–13335.
230. Yang W, Song Y, Lu Y-L, Sun J-Z, Wang H-W (2013) Increased expression of programmed death (PD)-1 and its ligand PD-L1 correlates with impaired cell-mediated immunity in high-risk human papillomavirus-related cervical intraepithelial neoplasia. *Immunology* 139(4):513–522.
231. Jing W, Gershan JA, Johnson BD (2009) Depletion of CD4 T cells enhances immunotherapy for neuroblastoma after syngeneic HSCT but compromises development of antitumor immune memory. *Blood* 113(18):4449–4457.
232. Shen Y-C, et al. (2018) Combining intratumoral Treg depletion with androgen deprivation therapy (ADT): preclinical activity in the Myc-CaP model. *Prostate Cancer Prostatic Dis* 21(1):113–125.
233. Bronte V, et al. (2016) Recommendations for myeloid-derived suppressor cell nomenclature and characterization standards. *Nat Commun* 7:12150.
234. Corzo CA, et al. (2009) Mechanism regulating reactive oxygen species in tumor-induced myeloid-derived suppressor cells. *J Immunol Baltim Md 1950* 182(9):5693–5701.

235. Dilek N, Vuillefroy de Silly R, Blancho G, Vanhove B (2012) Myeloid-derived suppressor cells: mechanisms of action and recent advances in their role in transplant tolerance. *Front Immunol* 3:208.
236. Bruhn KW, Dekitani K, Nielsen TB, Pantapalangkoor P, Spellberg B (2016) Ly6G-mediated depletion of neutrophils is dependent on macrophages. *Results Immunol* 6:5–7.
237. Kaneda MM, et al. (2016) PI3K γ is a molecular switch that controls immune suppression. *Nature* 539(7629):437–442.
238. Serafini P, et al. (2006) Phosphodiesterase-5 inhibition augments endogenous antitumor immunity by reducing myeloid-derived suppressor cell function. *J Exp Med* 203(12):2691–2702.
239. Andreu P, et al. (2010) FcR γ activation regulates inflammation-associated squamous carcinogenesis. *Cancer Cell* 17(2):121–134.
240. Cuenca AG, et al. (2011) A paradoxical role for myeloid-derived suppressor cells in sepsis and trauma. *Mol Med Camb Mass* 17(3–4):281–292.
241. Perfilyeva YV, et al. (2017) Expansion of CD11b+Ly6G^{high} and CD11b+CD49d⁺ myeloid cells with suppressive potential in mice with chronic inflammation and light-at-night-induced circadian disruption. *Inflamm Res Off J Eur Histamine Res Soc AI* 66(8):711–724.
242. Wang D, DuBois RN (2015) Immunosuppression associated with chronic inflammation in the tumor microenvironment. *Carcinogenesis* 36(10):1085–1093.
243. Kanterman J, Sade-Feldman M, Baniyash M (2012) New insights into chronic inflammation-induced immunosuppression. *Semin Cancer Biol* 22(4):307–318.
244. Erez N, Truitt M, Olson P, Arron ST, Hanahan D (2010) Cancer-Associated Fibroblasts Are Activated in Incipient Neoplasia to Orchestrate Tumor-Promoting Inflammation in an NF-kappaB-Dependent Manner. *Cancer Cell* 17(2):135–147.
245. Miao J, et al. (2017) Prostaglandin E2 and PD-1 mediated inhibition of antitumor CTL responses in the human tumor microenvironment. *Oncotarget* 8(52):89802–89810.
246. Obermajer N, Muthuswamy R, Lesnock J, Edwards RP, Kalinski P (2011) Positive feedback between PGE2 and COX2 redirects the differentiation of human dendritic cells toward stable myeloid-derived suppressor cells. *Blood* 118(20):5498–5505.
247. Amann R, Peskar BA (2002) Anti-inflammatory effects of aspirin and sodium salicylate. *Eur J Pharmacol* 447(1):1–9.
248. Coutinho AE, Chapman KE (2011) The anti-inflammatory and immunosuppressive effects of glucocorticoids, recent developments and mechanistic insights. *Mol Cell Endocrinol* 335(1):2–13.
249. Engblom C, Pfirschke C, Pittet MJ (2016) The role of myeloid cells in cancer therapies. *Nat Rev Cancer* 16(7):447–462.
250. Toor SM, et al. (2017) Myeloid cells in circulation and tumor microenvironment of breast cancer patients. *Cancer Immunol Immunother CII* 66(6):753–764.
251. Kumar V, Patel S, Tcyganov E, Gabrilovich DI (2016) The Nature of Myeloid-Derived Suppressor Cells in the Tumor Microenvironment. *Trends Immunol* 37(3):208–220.
252. Pawel Kalinski, Natasa Obermajer, Robert Edwards, Inge-Marie Svane and Morten Hansen Exhaustion of Human Dendritic Cells Results in a Switch from the IL-15R/IL-15- to IL-2R/IL-2-driven Expansion of Antigen-specific CD8⁺ T Cells. *J Immunol* May 1, 2016.
253. Casbon A-J, et al. (2015) Invasive breast cancer reprograms early myeloid differentiation in the bone marrow to generate immunosuppressive neutrophils. *Proc Natl Acad Sci U S A* 112(6):E566–575.

254. Diaz-Montero CM, et al. (2009) Increased circulating myeloid-derived suppressor cells correlate with clinical cancer stage, metastatic tumor burden, and doxorubicin-cyclophosphamide chemotherapy. *Cancer Immunol Immunother CII* 58(1):49–59.
255. Klemm F, Joyce JA (2015) Microenvironmental regulation of therapeutic response in cancer. *Trends Cell Biol* 25(4):198–213.
256. Joyce JA, Fearon DT (2015) T cell exclusion, immune privilege, and the tumor microenvironment. *Science* 348(6230):74–80.
257. Newburger PE, Dale DC (2013) Evaluation and management of patients with isolated neutropenia. *Semin Hematol* 50(3):198–206.
258. Kleinovink JW, et al. (2016) Combination of Photodynamic Therapy and Specific Immunotherapy Efficiently Eradicates Established Tumors. *Clin Cancer Res* 22(6):1459–1468.
259. Dunn LA, et al. (1997) Presentation of the HPV16E7 protein by skin grafts is insufficient to allow graft rejection in an E7-primed animal. *Virology* 235(1):94–103.

Curriculum Vitae

GABRIELE GALLIVERTI

Date of birth: 30/09/1987

Nationality: Italian

Address: Avenue De Sévelin 13E, 1004, Lausanne, Switzerland (CH)

Phone: +41 78 965 75 79

Email: gabriele.galliverti@gmail.com

Work experience

2013-2018

PhD Student in Bioengineering and Biotechnology at EPFL (Lausanne, Switzerland), Laboratory of Prof Melody Swartz and Laboratory of Prof. Douglas Hanahan

Projects:

- Develop novel therapeutic vaccination approaches for cervical and other HPV-related cancers
- Study the immunosuppressive barriers that impair the efficacy of immunotherapy against cervical and other HPV-related cancers

2011-2013

Undergraduate student and research fellow at the San Raffaele Institute (Milan, Italy), Laboratory of Matteo Iannaccone (Dynamics of immune responses lab)

Projects:

- Characterize the activity of bisphosphonate as novel adjuvant for B cell vaccines
- Study antiviral immune responses in the lymph nodes

Education

**Master degree in Medical, Cellular and Molecular Biotechnology
Vita-Salute San Raffaele University (Milan, Italy)**

Final score: 110/110 cum laude

Thesis title: Bisphosphonate have a TLR- and inflammasome- independent adjuvant activity for B cell responses

Bachelor degree in Molecular Biotechnology

University of Milan Bicocca (Milan, Italy)

Final score: 102/110

Thesis title: Controllo dell'omeostasi delle cellule T regolatorie da parte delle cellule dendritiche.
(Homeostatic control of T regulatory cells by dendritic cells)

High school diploma in Information technology and programming languages

ITIS C. Facchinetti (Busto Arsizio, Italy)

Skills

Personal skills: proficient organization and planning, presentation of data and concepts, critical evaluation of results, scientific writing (in English and Italian).

Languages spoken: Italian (mother tongue), English (fluent), French (basic reading and understanding of spoken language)

Computer skills: proficient use of Microsoft office, Adobe Illustrator, GraphPad Prism, FlowJo and Fiji (ImageJ). Basic understanding of programming languages (C++, SQL, HTML, PHP, Basic).

Driving licence: B (for cars)

Publications

Nanoparticle conjugation of human papillomavirus 16 E7-long peptides enhances therapeutic vaccination efficacy against well-established solid tumors in mice.

Galliverti G, Tichet M, Domingos-Pereira S, Hauert S, Nardelli-Haeffliger D, Swartz MA, Hanahan D, Wullschlegel S.

Under review.

Matrix-binding checkpoint immunotherapies enhance antitumor efficacy and reduce adverse events.

Ishihara J, Fukunaga K, Ishihara A, Larsson HM, Potin L, Hosseinchi P, **Galliverti G**, Swartz MA, Hubbell JA.

Sci Transl Med. 2017 Nov 8.

Advances in pancreatic islet monolayer culture on glass surfaces enable super-resolution microscopy and insights into beta cell ciliogenesis and proliferation.

Phelps EA, Cianciaruso C, Santo-Domingo J, Pasquier M, **Galliverti G**, Piemonti L, Berishvili E, Burri O, Wiederkehr A, Hubbell JA, Baekkeskov S.
Sci Rep. 2017 Apr 12.

Bisphosphonates target B cells to enhance humoral immune responses.

Tonti E, Jiménez de Oya N, **Galliverti G**, Moseman EA, Di Lucia P, Amabile A, Sammiceli S, De Giovanni M, Sironi L, Chevrier N, Sitia G, Gennari L, Guidotti LG, von Andrian UH, Iannacone M.
Cell Rep. 2013 Oct 31.